

# **Non-Catalytic and Catalytic Routes for Biodiesel Production**

**A Thesis Submitted**

In partial fulfillment of the requirements

for the Degree of

**DOCTOR OF PHILOSOPHY**

by

Zakir Hussain

PCH14-001



to the

**Department of Chemical Engineering**

**Rajiv Gandhi Institute of Petroleum Technology, Jais (Amethi)**

**December 2018**

## Thesis Approval

Thesis entitled as '**Non-Catalytic and Catalytic Routes for Biodiesel Production**' by Zakir Hussain (PCH14-001) is approved for the degree of Doctor of Philosophy.

Examiners

---

---

---

Supervisor

---

Chairman

---

Date:

Place:

## Candidate Declaration

I, hereby certify that the presented thesis entitled as “**Non-Catalytic and Catalytic Routes for Biodiesel Production**” is an authentic record of original research work carried out by me in Green Separation and Bio-Fuel Laboratory at Department of Chemical Engineering, RGIPT, Jais under the supervision of **Dr. Rakesh Kumar**. I further certify that the entire work contained in the thesis was not submitted to any other institute in India or abroad for the award of any degree or diploma.

Date:

Place:

Zakir Hussain

Enrollment No. PCH14-001

Green Separation and Bio-Fuel Lab

Department of Chemical Engineering

RGIPT, Jais (Amethi)

E-mail:- (1) zhussain@rgipt.ac.in

(2) zakirchem806@gmail.com

**RAJIV GANDHI INSTITUTE OF PETROLEUM TECHNOLOGY,**

**Jais, Amethi**

**CERTIFICATE OF COURSE WORK**

This is to certify that Mr. Zakir Hussain a Ph.D. candidate with roll no.-PCH14-001 successfully completed all the required courses and passed the comprehensive examination.

The details of the coursework done are given below;

<b>S.no.</b>	<b>course code</b>	<b>course name</b>	<b>course credits</b>
1	CHE504	Advance Thermodynamics	4
2	OE423	Fluidization Engineering & New Separation Processes	4
3	*CHE601A	Fundamentals of Chemical Engineering-1	9
4	*CHE613A	Chemical Reaction Engineering	9

\*Coursework is done at Indian Institute of Technology (IIT), Kanpur.

RGIPT

Registrar (Academic)

Dated:

## **CERTIFICATE**

This is to certify that the work incorporated in this Ph.D. thesis entitled as “**Non-Catalytic and Catalytic Routes for Biodiesel Production**”, submitted by **Mr. Zakir Hussain**, to the Department of Chemical Engineering at Rajiv Gandhi Institute of Petroleum Technology (Jais), in fulfillment of the requirements for the award of the degree of Doctor of philosophy, embodies original research work under my supervision. I further certify that this work has not been submitted elsewhere for any other degree or diploma.

Dr. Rakesh Kumar

Assistant Professor,

Department of Chemical Engineering

RGIPT, JAIS,

UTTAR PRADESH, INDIA

E-mail:- rkumar@rgipt.ac.in

Tel.:- +91-9450352043

**Dedicated**

*To*

*My Family*

## Synopsis

---

**Name:** Mr. Zakir Hussain

**Roll No.:** PCH14-001

**Degree for which thesis submitted:** Ph.D.

**Department:** Chemical Engineering

**Thesis title:** Non-Catalytic and Catalytic Routes for Biodiesel Production

**Name of thesis supervisor:** Dr. Rakesh Kumar

**Month and year of thesis submission:** December 2018

---

The fossil fuels such as coal, oil and natural gas are considered as primary source of energy throughout the world. Rapid exhaustion of fossil fuels and the environmental concerns due to their usage evoked the search for many promising alternative green energy sources like biofuels. Exploration and exploitation of various alternative energy sources have gained huge attention over the past few decades. Among the portfolio of biofuels, biodiesel is considered to be the best alternative fuel because of its high net energy returns (~90%). Biodiesel has been accepted worldwide as a green fuel and considered as an alternative to the diesel fuel. Federal and state governments are framing policies to widen the use of biodiesel due to its eco-friendly nature. Biodiesel is considered a renewable fuel, which produces lesser greenhouse emissions and has superior lubricating properties. It is intrinsically free of sulfur compared to petroleum-based diesel.

Biodiesel is an alkyl ester of long chain fatty acids derived from the reaction between vegetable oil and alcohol. Industrial scale biodiesel is produced using base-catalyzed transesterification of vegetable oil and alcohol. This process is limited by low mutual solubility between oil and alcohol phases. These phases are non-homogeneous or immiscible

in each other limiting the mass transfer through interphase. This raises the need for phase transfer catalytic process involving the formation of an intermediate complex which can solubilize the organic and inorganic phases.

Also, commercialization of biodiesel on large scale is limited due to the high cost of biodiesel production. The high cost of production using current technology is due to its requirement of high-quality feedstock and also its intolerance to impurities (free fatty acids and water) present in the low-quality feedstock. The common feedstock for biodiesel production involves pure fatty acids (oleic and palmitic acids), edible oils (palm, soybean, and sunflower) and non-edible oils (waste vegetable, Karanja, Jatropha and palm fatty acid distillates). Pure fatty acids are costlier compared to edible oils which in turn costlier than non-edible oils. Moreover, large-scale usage of edible oils for fuel may elevate the food versus fuel crisis. Therefore, non-edible and waste vegetable oils are the highly preferred feedstock's to lower the biodiesel production cost. However, non-edible oils contain a high amount of free fatty acids than edible oils. The free fatty acid (FFA) present in oils reacts with the alkali to form soap which results in the difficult product purification and low biodiesel yield. Therefore, it is essential to limit the FFA content present in feed oil prior to the base-catalyzed transesterification reaction and a certain reaction criterion needs to be adopted based on FFA content. Principally, a single-step (transesterification) process or a two-step (esterification followed by transesterification) process is generally used to produce high-quality biodiesel. The criteria required to use a single-step base-catalyzed transesterification process is high-quality vegetable oil (<3 wt. % FFA). However, for oils containing FFA >3 wt. %, a two-step process is generally preferred. This raises the need for the esterification process.

Concentrated sulfuric acid in a homogeneous form is used as a catalyst for esterification of non-edible oils having high FFA content. However, homogeneous acid imposes severe

environmental issues, corrosion problems, and usually nonrecyclable. Moreover, biodiesel produced using homogeneous catalysts also generates a substantial amount of water effluents together with the significant loss of biodiesel during the washing process.

The use of non-edible and waste vegetable oils can lower the cost of biodiesel production to a substantial extent. However, the disadvantage of lower solubility between reactants and also environmental hazards involved in the conventional process can be mitigated using an efficient catalyst. The current research work has been devoted to developing an economical and environmental friendly biodiesel process. The detailed work done in the current thesis has been described below;

## **1. Effect of Quaternary Ammonium Salt Addition to Conventional Biodiesel Production Process**

Transesterification of vegetable oils using a conventional homogeneous catalyst like KOH and NaOH is prone to water and FFA content. Moreover, this process is limited by the low mutual solubility of reactants (oil and alcohol). Tetramethylammonium bromide (TMAB) is a hygroscopic salt which is widely used as phase transfer catalyst. In the system consisting of two mutually-insoluble phases, either liquid-liquid or solid-liquid the distinct attribute of the phase-transfer catalytic process is that it forms an intermediate complex. This intermediate complex is mostly soluble in organic compounds to transfer inorganic ions into the organic phase. Since, transesterification is a base-catalyzed process and is also associated with a nucleophilic attack mechanism, using the TMAB can enhance the process and dampens the technical disadvantages in the conventional biodiesel production process. Therefore, the effect of TMAB addition on biodiesel yield, the molar ratio of methanol to oil requirement and washability characteristics of crude biodiesel was studied. The reaction between waste vegetable oil and methanol was carried out in a batch reactor at 65 °C using various molar ratios of oil to methanol (3:1 to 9:1). Further, the effect of various dosage of TMAB addition

to the reaction was studied. Results show that there is a strong influence of TMAB on the methanol requirement during the reaction and also on the washability characteristics of the produced biodiesel. It was observed that TMAB decreases the amount of methanol required for the reaction. Moreover, the addition of TMAB enhanced the washability of the final biodiesel by forming less foam. The less foam formation was due to the suppression of saponification. The addition of TMAB also lowered the wash water requirement during the purification process.

## **2. Esterification of Free Fatty Acids: Experiments, Kinetic Modeling, Simulation and Optimization**

The development of the process which can mitigate the drawbacks of catalytic esterification and handles high free fatty acid containing oils is the highly focused area in biodiesel production. In view of attaining the cleaner biodiesel production, the present research efforts are focused on studying the methyl esterification of FFA present in Karanja oil non-catalytically in a batch reactor. Kinetics of the reaction was modeled as the pseudo first order in the forward direction and second order bimolecular type in the backward direction to deduce kinetic parameters. The obtained parameters were used to simulate the process in Aspen Plus. Experimental results show that 96% conversion of FFA can be achieved at 220 °C and 1:6 (w/v) oil to methanol ratio. The calculated activation energy and rate constant are 48.53 kJ/mol and  $0.641 \text{ min}^{-1}$ , respectively for the forward reaction and 18.74 kJ/mol and  $4.18\text{E}^{-4} \text{ (g)/(mgKOH.min)}$  respectively, for the backward reaction. Simulation results showed a little higher conversion (99.85%) of oleic acid compared to the experimentally observed conversion (96%) at similar reaction conditions. The optimal process parameters were estimated using sensitivity analysis of Aspen Plus along with heat integration.

### 3. Synthesis and Characterization of Novel Corncob-Based Solid Acid Catalyst for Biodiesel Production

In order to mitigate the drawbacks associated with homogeneous esterification process, highly efficient solid acid catalysts based on corncob were synthesized in the present work. The effect of catalyst impregnation, carbonation, as well as sulfonation was evaluated for esterification of oleic acid with methanol. The synthesized catalysts were characterized using various techniques such as Fourier Transform Infrared Spectra (FTIR), BET surface area, and X-Ray Diffraction (XRD). The acid densities of the catalysts were estimated using the titrimetric method. FTIR analysis of the catalyst indicates the presence of multiple functional groups. Specific surface areas of the phosphoric acid impregnated catalyst and the final sulfonated catalyst was found to be 1268 m<sup>2</sup>/g and 641 m<sup>2</sup>/g, respectively. The maximum acid density of the synthesized catalyst was obtained as 5.56 mmol/g catalyst. The highest conversion of oleic acid (~94.4%) was achieved with a catalyst designated as  $I_{R=1}^{t=5} - C_{T=723}^{t=8} - S_{T=393}^{t=15}$  (H<sub>3</sub>PO<sub>4</sub> impregnation ratio = 1 and time = 5 h, carbonization temperature = 723 K and time = 8 h, sulfonation temperature = 393 K and time = 15 h). Further, the performance of the catalyst was also evaluated for esterification of Fatty acids (FA: oleic acid and palmitic acid) and the free fatty acids present in Karanja oil, at various reaction conditions. The effect of reaction variables such as time (1-5 h), temperature (328-343 K), the molar ratio of reactants (1:5-1:30) and the catalyst loading (5-20 wt. %) was studied in detail. The synthesized catalyst showed ~90% conversion of FA/FFA within 2 h at a mild temperature of 338 K using a molar ratio of 1:10 (fatty acid to methanol)/1:20 (Karanja oil to methanol), 10 wt. % catalyst. Finally, the reusability test of the catalyst revealed that it could be used for 20 times in a batch reactor to give ~90% conversion of the oleic acid.

#### 4. Kinetic Modelling and Simulation of Novel Corncob-Based Catalytic Biodiesel Process

In the current work, a sulfonic group-functionalized porous carbonaceous catalyst based on corncob ( $I_{R=1}^{t=5} - C_{T=723}^{t=8} - S_{T=393}^{t=15}$ ) was used for esterification of oleic acid. Langmuir-Hinshelwood–Hougen-Watson (LHHW) kinetic model was used to correlate the experimental data. The correlation coefficient ( $R^2$ ) obtained for all the kinetic parameters was close to 1, suggesting a very good statistical consistency of the experimental data fitting. The adsorption equilibrium constant for oleic acid ( $K_O$ ) was found in the range of 25.850 to 3.250 for a temperature range from 333.15 to 343.15 K. This value was much higher than other adsorption equilibrium constants for methanol ( $K_M$ ), methyl oleate ( $K_F$ ) and water ( $K_W$ ), indicating a strong affinity of oleic acid to the catalyst surface. Moreover, the adsorption affinity of oleic acid on the catalyst surface was approximately 325 times higher than that of methanol. The calculated activation energies and frequency factors were found to be 63.861 kJ/mol and  $4.105E^8$  m<sup>3</sup>/mol.kg<sub>cat</sub>.sec, respectively for the forward reaction and 746.138 kJ/mol and  $7.1581E^4$  m<sup>3</sup>/mol.kg<sub>cat</sub>.sec, respectively, for the backward reaction. The obtained kinetic parameters were incorporated in the Aspen Plus simulator (ver. 8.6) to simulate the continuous biodiesel production process. The simulation result showed 98.84% oleic acid conversion which was close to the experimentally observed conversion (98.9%).

## Acknowledgments

I express my deep sense of gratitude to my institution, “**Rajiv Gandhi Institute of Petroleum Technology**”, which has provided me an opportunity to fulfill my thesis requirement for the award of “**Doctor of Philosophy**” which is my long cherished dream. The teaching assistantship, research infrastructure, learned faculty and the pleasant family accommodation of my institution is very helpful in fulfilling the research assignments.

It is my privilege to express my deepest and sincere gratitude towards my guide and a role model **Dr. Rakesh Kumar** for his able guidance and immense faith in me throughout my research journey. His quest for perfection, untiring help, and constructive criticism made my research interesting and enjoyable. The countless and valuable discussions provided by him during manuscript preparations made me a better researcher. Other than the research, he also taught me the lessons to lead a meaningful life with good grace. I feel from the deepest of my heart that the time spent with him during my doctoral studies will help me to be a better person both personally and professionally in all my future endeavors.

I am grateful to **Professor Jai Prakash Gupta**, former director of RGIPT, **Professor Prashant Kumar Bhattacharya**, Hon'ble director of RGIPT, **Assoc. Professor's Uma Prasanna Ojha** (Associate Dean of Academic Affairs), **Alok Kumar Singh** (Associate Dean of Student Affairs) and **Marriyappan Sivagnanam Balathanigaimani** (Head of the Engineering Sciences Division) of RGIPT whose immense achievements and awards motivate me to be a person with a great passion. I also thank them for providing the necessary research infrastructure.

It gives me immense pleasure to express my gratitude to **Associate Professor's Amit Ranjan, and Abhay Kumar Choubey** and **Assistant Professor Venkata Subbarayudu Sistla** of RGIPT who provided a highly appreciable moral support during my studies.

It is a pleasure to express my deep sense of gratitude and indebtedness to the entire **faculty** of the Department of Chemical Engineering at **RGIPT** and **Indian Institute of Technology, Kanpur**, especially **Professor's R. P. Chhabra and Deepak Kunzru** for teaching me the courses while at **IITK** and also for their valuable guidance, encouragement and support, who have directly or indirectly had a hand in the successful completion of my thesis.

The help provided by **Professor Deepa Meghavathu** of Andhra University, Visakhapatnam is greatly acknowledged.

I feel extremely lucky for being a part of **Green Separations and Bio-fuel Lab** and I would like to thank all the lab members (**Mr. Mohammad Belal Haider, Ms. Divyam Jha, Ms. Komal Shukla, and Mr. Mata Mani Tripathi**) and colleagues (Mr. Bijoy Kumar Purohit) for creating and maintaining such a friendly environment. The support provided by all the **staff members** of RGIPT especially Mr. Raghunath Bhattacharya (former deputy registrar), Mr. Arun Kumar Singh (secretary to the Director), Mr. Jitendra Prasad, Mr. Rakesh Singh, Mr. Sudhir Arora, Mr. Tej Prakah Joshi, Ms. Preeti Singh, Mr. Arun Kumar Singh (JTS), Mr. Ashok Mourya, Mr. Anil Verma, Mr. Ashwini Kumar Choudhary and Mr. Amit Bhajpai is greatly acknowledged.

Most of all, I would like to thank **my family** for their help and support in various ways throughout my Ph.D. journey and making this memory as an unforgettable one.

**December, 2018**

**Zakir Hussain**

## Contents

Synopsis .....	vii
Acknowledgments .....	xiii
List of Publications from Thesis.....	xviii
List of Other Publications .....	xix
List of Conferences .....	xx
List of Abbreviations .....	xxiv
List of Notations .....	xxvi
List of Tables .....	xxviii
List of Figures .....	xxix
<b>1.</b> Introduction and Literature Review.....	1
1.1 Energy sources and demand .....	1
1.2 Biodiesel: A green energy fuel .....	2
1.3 Feedstock for biodiesel production .....	3
1.4 Conventional base-catalyzed transesterification process .....	5
1.5 Phase transfer catalysis .....	10
1.6 Conventional acid catalyzed esterification process .....	12
1.7 Non-catalytic process for biodiesel production.....	14
1.8 Heterogeneous catalytic process for biodiesel .....	15
1.9 Scope of present work .....	18
<b>2.</b> Effect of Quaternary Ammonium Salt Addition to Conventional Biodiesel Production Process.....	24
2.1 Experimental Details .....	24
2.1.1 Materials used.....	24
2.1.2 Experimental setup .....	25
2.1.3 Experimental procedure.....	26
2.1.4 Ester purification .....	27
2.1.5 Analysis of biodiesel samples .....	28
2.2 Results and Discussions.....	30
2.2.1 Composition of feed oil .....	30

2.2.2 Effect of reaction parameters on biodiesel yield.....	31
2.2.3 Effect of methanol to oil molar ratio on biodiesel properties .....	33
2.2.4 Effect of the TMAB addition on biodiesel production .....	34
<b>3.</b> Esterification of Free Fatty Acids: Experiments, Kinetic Modeling, Simulation and Optimization .....	48
3.1 Experimental Details .....	48
3.1.1 Materials used.....	48
3.1.2 Sample analysis .....	48
3.1.3 Experimental setup .....	49
3.1.4 Experimental procedure.....	50
3.2 Results and Discussions.....	51
3.2.1 Feasibility of reaction at reactor conditions/Phase equilibrium.....	51
3.2.2 Effect of agitation speed.....	52
3.2.3 Effect of reaction time and temperature .....	54
3.2.4 Effect of oil to methanol (w/v) ratio.....	55
3.2.5 Equilibrium constant and kinetic modeling .....	56
3.2.6 Effect of temperature on reaction rate constant .....	66
3.2.7 Effect of temperature on the equilibrium constant.....	67
3.2.8 Process modeling and simulation .....	69
<b>4.</b> Synthesis and Characterization of Novel Corncob-Based Solid Acid Catalyst for Biodiesel Production .....	76
4.1 Experimental Details .....	76
4.1.1 Materials used.....	76
4.1.2 Catalyst synthesis .....	76
4.1.3 Catalyst characterization .....	78
4.1.4 Esterification reaction.....	79
4.2 Results and Discussions.....	81
4.2.1 FT-IR analysis of the catalyst.....	81
4.2.2 BET analysis of the catalyst .....	83
4.2.3 XRD analysis of the catalyst .....	91
4.2.4 Effect of catalyst synthesis parameters .....	92

4.2.5 Esterification of oleic and palmitic acid.....	100
4.2.6 Esterification of FFA in Karanja oil.....	106
4.2.7 Reusability of the catalyst .....	111
4.2.8 Leaching test of the catalyst .....	115
4.2.9 Comparison of corncob catalyst with literature .....	115
<b>5.</b> Kinetic Modeling and Simulation of Novel Corncob-Based Catalytic Biodiesel Process .....	122
5.1 Kinetics of the oleic acid esterification .....	122
5.2 Effect of temperature on rate constants and adsorption constants .....	129
5.3 Effect of temperature on the reaction equilibrium constant .....	131
5.4 Process modeling and simulation .....	133
5.4.1 Process flow diagram .....	133
5.4.2 Process simulation .....	135
<b>6.</b> Conclusions and Future Recommendations .....	140
6.1 Conclusions.....	140
6.1.1 Effect of TMAB Addition on Conventional Process .....	140
6.1.2 Esterification of Free Fatty Acids .....	140
6.1.3 Synthesis and Characterization of Corncob-Based Solid Acid Catalyst .....	141
6.1.4 Kinetic Modeling and Simulation of Corncob-Based Catalytic Process .....	142
6.2 Recommendations.....	143
References.....	144
Appendix.....	171

## List of Publications from Thesis

1. **Zakir Hussain**, Deepa Meghavathu, Rakesh Kumar. “Effect of Quaternary Ammonium Salt Addition to Conventional Biodiesel Production”. **International Journal of Engineering & Technology**. 7 (4.5) (2018) 220-223.
2. **Zakir Hussain**, Belal Haider and Rakesh Kumar. “Production of Biodiesel with and without Catalytic Booster”. **Materials Today: Proceedings**. 3:10 (2016) 4115-4120.
3. **Zakir Hussain** and Rakesh Kumar. Non-Catalytic Esterification of Free Fatty Acids in Karanja Oil: Experiments, Kinetic Modeling, Simulation & Optimization. **International Journal of Green Energy**. 15:11 (2018) 629-640.
4. **Zakir Hussain** and Rakesh Kumar. “Kinetics & Simulation of Non-Catalytic Esterification”. **Materials Today: Proceedings**. 5:9 (2018) 18275-18284.
5. **Zakir Hussain** and Rakesh Kumar. Synthesis and Characterization of Novel Corncob-Based Solid Acid Catalyst for Biodiesel Production. **Industrial & Engineering Chemistry Research**. 57:34 (2018) 11645-11657.
6. **Zakir Hussain** and Rakesh Kumar. “Esterification of Free Fatty Acids in Karanja Oil using Novel Corncob-Derived Solid Acid Catalyst”. **Materials Today: Proceedings**. 5:9 (2018) 18033-18039.
7. **Zakir Hussain** and Rakesh Kumar. Kinetic Modelling and Simulation of Novel Corncob-Based Catalytic Biodiesel Process. **Chemical Engineering Research and Design** (under review)

## List of Other Publications

8. Belal Haider, **Zakir Hussain** and Rakesh Kumar. “CO<sub>2</sub> Absorption and Kinetic Study in Ionic Liquid Amine Blends”. *Journal of Molecular Liquids*. 224 (2016) 1025-1031.
9. B. Balraj, **Zakir Hussain and** Rakesh Kumar. “Effect of Carbon & Nitrogen Sources on Escherichia Coli Bacteria in Removing Dyes”. *Materials Today: Proceedings*. 3:10 (2016) 4023-4028.
10. **Zakir Hussain** and Rakesh Kumar. Synthesis and Characterization of a Novel Coconut-Based Solid Acid Catalyst for Biodiesel Production (**In Preparation for Industrial & Engineering Chemistry Research special Issue**).

## List of Conferences

1. **Zakir Hussain** and Rakesh Kumar. Synthesis and Characterization of a Novel Coconut-Based Solid Acid Catalyst for Biodiesel Production. **4<sup>th</sup> North American Symposium on Chemical Reaction Engineering to be held at Houston (USA)** on 10-13, March 2019. (Accepted)
2. **Zakir Hussain** and Rakesh Kumar. A Novel Corncob-Based Catalytic Biodiesel Production Process: Kinetic Modelling and Simulation. **2<sup>nd</sup> International Conference on New Frontiers in Chemical, Energy and Environmental Engineering** to be held at NIT Warangal on 11-12 March 2019. (Accepted)
3. **Zakir Hussain**, Md. Belal Haider and Rakesh Kumar. Synthesis, Characterization, Kinetic modeling and Simulation of a Biodiesel Production Process using Novel Corncob-Based Catalyst. **Joint Symposium of American Chemical Society and Indian Academy of Sciences** held at **BHU** on 1st November 2018.
4. **Zakir Hussain**, Rakesh Kumar. Biodiesel production using agricultural waste derived solid acid catalyst. **2018 American Oil Chemists' Society (AOCS) Annual Meeting & Expo.** 6-9<sup>th</sup> May 2018. Minnesota, USA. (Accepted)
5. **Zakir Hussain**, Rakesh Kumar. Transesterification of waste vegetable oil using spent FCC catalyst-Based solid base catalyst. **2018 AOCS Annual Meeting & Expo.** 6-9<sup>th</sup> May 2018. Minnesota, USA. (Accepted)
6. **Zakir Hussain**, Rakesh Kumar. Biodiesel production from neem oil using novel corncob derived solid acid catalyst. *11<sup>th</sup> International Symposium on Fuels & Lubricants.* 15-17<sup>th</sup> April 2018. Taj Vivanta **IOCL-R&D Centre**, Indian Oil Corporation Limited. (Accepted)

7. **Zakir Hussain**, Rakesh Kumar. “Dynamic biodiesel product pricing model: case study, process simulation, energy & cost analysis”. *11<sup>th</sup> International Symposium on Fuels & Lubricants*. 15-17<sup>th</sup> April 2018. **IOCL-R&D Centre**, Indian Oil Corporation Limited.  
(Accepted)
8. **Zakir Hussain**, Rakesh Kumar. Transesterification of waste vegetable oil using spent fluid catalytic cracking catalyst-based solid catalyst. *Research Scholars Day (RSD-2018)*. 17-18<sup>th</sup> Mar. 2018. **RGIPT**.
9. **Zakir Hussain**, Rakesh Kumar. “Kinetics & simulation of non-catalytic esterification”. *International conference on material processing & characterization (ICMPC-2018)*. 16-18<sup>th</sup> March 2018. **GRIET, Hyderabad**.
10. **Zakir Hussain**, Rakesh Kumar. “Esterification of Free Fatty Acids in Karanja oil using novel corncob-derived solid acid catalyst”. *International Conference on Material Processing & Characterization (ICMPC-2018)*.
11. **Zakir Hussain**, Rakesh Kumar, Deepa Meghavathu. “Glimpses of dynamic biodiesel product pricing model”. *International Conference on Recent Trends in Engineering & Sciences (ICRTES-2018)*. 20-21<sup>th</sup> Feb.2018. **Hotel Keys**, Visakhapatnam.
12. **Zakir Hussain**, Deepa Meghavathu, Rakesh Kumar. “Kinetics & thermodynamics of adsorption process using spent-FCC catalyst”. *ICRTES-2018*.
13. **Zakir Hussain**, Deepa Meghavathu, Rakesh Kumar. “Effect of quaternary ammonium salt addition to conventional biodiesel production”. *ICRTES-2018*.
14. **Zakir Hussain**, Rakesh Kumar. “A model framework to make biodiesel as sustainable alternative fuel: Towards a dynamic biodiesel product pricing approach”. *8<sup>th</sup> World Petro Coal Congress*. 15-17<sup>th</sup> February 2018. **NDDC-Convection Centre, Parliament Street**, New Delhi.

15. **Zakir Hussain**, Rakesh Kumar. “Perspectives towards dynamic biodiesel product pricing model through case study, process simulation, energy & cost analysis”. *1<sup>st</sup> International Conference on Emerging Challenges and Opportunities in Energy Sector*. 9-10<sup>th</sup> February 2018. **RGIPT**, Jais.
16. Deepa Meghavathu, P Suman; V Sridevi, **Zakir Hussain**. “Desalination studies on two single sloped solar stills with heat absorbing materials as coating material on Aluminium basin”. *International Conference on Advances in Chemical Engineering*. 18-20<sup>th</sup> January 2018. **Government Engineering College**, Thrissur, Kerala.
17. **Zakir Hussain**, Belal Haider, Rakesh Kumar. “Non-catalytic esterification of free fatty acids in Karanja oil: Experiments, kinetics modeling, simulation and optimization”. *Research Scholars Day*. **RGIPT**, Jais.
18. Komal Shukla, **Zakir Hussain**, Belal Haider, Rakesh Kumar. “Study of heterogeneous catalyst for biodiesel production: A comprehensive review”. *Research Scholars Day*. **RGIPT**, Jais.
19. **Zakir Hussain**, Belal Haider, Rakesh Kumar. “Production of biodiesel with and without a catalytic booster”. *International Conference on Materials Research & Applications (ICMRA)*. 11-13 March 2016. **CMR Technical Campus**, Hyderabad.
20. Bandary Balraj, **Zakir Hussain**, Rakesh Kumar. “Effect of carbon & nitrogen sources on Escherichia coli bacteria in removing dyes”. *ICMRA-2016*.
21. **Zakir Hussain**, Belal Haider, Rakesh Kumar. “Production biodiesel with and without catalytic booster”. *International Conference on Advances in Bioprocess Engineering and Technology (ICABET)*. 20-22 January 2016. **Heritage Institute of Technology**, Kolkata.
22. Bandary Balraj, **Zakir Hussain**, Pulipati King. “Effect of carbon & nitrogen sources on Escherichia coli bacteria in removing dyes”. *ICABET-2016*.

23. Belal Haider, **Zakir Hussain**, Rakesh Kumar. “Experimental study of ionic liquid blends. *Chemference-2015:6<sup>th</sup> National level annual research symposium of chemical engineering Research scholars*. 5-6<sup>th</sup> December 2015. **IIT Hyderabad**.
24. **Zakir Hussain**, Belal Haider, Rakesh Kumar. “Production and analysis of vegetable oil based biodiesel using KOH and NaOH as a catalyst”. *International Conference on New Frontiers in Chemical, Energy and Environmental Engineering (INCEEE)*. 20-21<sup>st</sup> March 2015. **NIT Warangal**. Page-95.
25. Belal Haider, **Zakir Hussain**, Rakesh Kumar. “CO<sub>2</sub> Capture by Ionic Liquid blends”. *INCEEE-2015*. Page-382. ISBN: 978-81-928314-1-1.
26. Belal Haider, **Zakir Hussain**, Rakesh Kumar. “CO<sub>2</sub> Capture by Ionic Liquid blends”. *Outstanding Young Chemical Engineers*. 14-15<sup>th</sup> March 2015. **D.J Sanghvi College of Engineering**, Mumbai.

## List of Abbreviations

ASTM = American Society of Testing and Materials

EN = European Norms

FAME = Fatty Acid Methyl Ester

FFA = Free Fatty Acid

PTC = Phase Transfer Catalyst

TMA = Tetramethylammonium

TMAB = Tetramethylammonium Bromide

SAC = Solid Acid Catalyst

WVO = Waste Vegetable Oil

LHHW = Langmuir-Hinshelwood-Hougen-Watson

MSTFA = N-methyl-N-trifluoroacetamide

GC = Gas Chromatograph

IS = Internal Standard

IS1 = Internal Standard 1

IS2 = Internal Standard 2

GC-FID = Gas Chromatograph with Flame Ionization Detector

CP= Cloud Point

PP = Pour Point

CFPP = Cold Filter Plugging Point

B = Base Catalyst

DMSO = Dimethyl sulfoxide

DMF = Dimethylformamide

EOS = Equation of State

BET = Brunauer-Emmett-Teller

BJH = Berrer, Joyner and Halenda

FTIR = Fourier-Transform Infrared

XRD = X-ray Diffraction

IUPAC = International Union of Pure and Applied Chemistry

PFD = Process Flow Diagram

TG = Triglyceride

DG = Diglyceride

MG = Monoglyceride

G = Glyceride

BD = Biodiesel

NRTL = Non-Random Two Liquid

## List of Notations

$Q^+$  = cation of phase transfer catalyst

$X^-$  = anion of phase transfer catalyst

$V$  = volume of standard potassium hydroxide used, ml

$N$  = normality of standard potassium hydroxide solution

$W$  = weight of the oil sample, gram

$f$  = volumetric filling fraction

$T_c$  = critical temperature, °C

$P_c$  = critical pressure, bar

$K$  = equilibrium constant

$K_c$  = equilibrium constant based on concentration

$K_\gamma$  = equilibrium constant based on the activity coefficient

$Q_i$  = activity of species 'i'

$\gamma_i$  = activity coefficient of species 'i'

$\nu_i$  = stoichiometric coefficient of species 'i'

$M$  = methanol

$ME$  or  $F$  = methyl Ester or fatty acid methyl ester

$k_f$  = forward reaction rate constant

$k_f'$  = forward reaction rate constant associated with pseudo-first-order kinetics

$k_r$  = backward reaction rate constant

$k_{-f}$  = backward reaction rate constant

$C_{FFA_0}$  and  $C_{FFA}$  = initial concentration and concentration of free fatty acids respectively

$AV_0$  and  $AV_P$  = initial acid value and final product acid value respectively

$X$  and  $X_e$  = conversion and equilibrium conversion respectively

$T$  = reaction temperature, °C or K

$P$  = pressure, bar

$t$  = time, h

$w$  = catalyst loading with respect to oil/fatty acids, wt. %

I = impregnation

$I_R$  = impregnation ratio

$I_t$  = impregnation time, h

C = carbonization

$C_T$  = carbonization temperature, K

$C_t$  = carbonization time, h

S = sulfonation

$S_T$  = sulfonation temperature, K

$S_t$  = sulfonation time, h

O = oleic acid

W = water

$C_{O_0}$  and  $C_O$  = initial concentration and concentration of oleic acid respectively

$C_{M_0}$  and  $C_M$  = initial concentration and concentration of methanol respectively

$C_F$  and  $C_W$  = concentrations of fatty acid methyl ester and water respectively

$C_V$  = concentration of vacant site on the catalyst surface

$K_O$  = adsorption equilibrium constant for oleic acid,  $m^3/mol$

$K_M$  = adsorption equilibrium constant for methanol,  $m^3/mol$

$K_F$  = adsorption equilibrium constant for fatty acid methyl ester,  $m^3/mol$

$K_W$  = adsorption equilibrium constant for water,  $m^3/mol$

R = molar ratio of oil to methanol

m = molar ratio of methanol to oil

$\Delta E$ ,  $\Delta H$ ,  $\Delta G$ , and  $\Delta S$  = change in internal energy (kJ/mol), change in enthalpy (kJ/mol), change in Gibbs free energy (kJ/mol) and change in entropy (kJ/mol K) respectively

$V_R$  = volume of the reactor,  $m^3$

$Q_R$  = reactor heat duty, kW

$Q_H$  = heat exchanger heat duty, kW

$Q_C$  = condenser heat duty, kW

$Q_{Re}$  = reboiler heat duty, kW

$Q_F$  = flash column heat duty, kW

## List of Tables

Table 2.1:- Fatty Acid Composition of Waste Vegetable Oil.....	30
Table 2.2:- Composition and Properties of Biodiesel Samples Catalyzed by KOH.....	44
Table 2.3:- Composition and Properties of Biodiesel Samples Catalyzed by KOH.....	46
Table 2.4:- Comparison of Synthesized Biodiesel with Standards.....	47
Table 3.1:- Physico-Chemical Properties of Karanja Oil .....	49
Table 3.2:- Kinetic Models .....	62
Table 3.3:- Calculated Reaction Parameters .....	65
Table 3.4: Calculated Arrhenius and Thermodynamic Parameters .....	67
Table 3.5:- Stream results of the simulated flow sheet.....	73
Table 4.1:- Acid Densities and Surface Area of I-C-corn cob at Various Carbonization Temperatures.....	87
Table 4.2:- Acid Densities of the Synthesized Catalyst.....	88
Table 4.3:- Textural Properties of the Synthesized Catalyst.....	90
Table 4.4:- Acid Densities of the Spent Catalysts Washed with n-Hexane.....	113
Table 4.5:- Acid Densities of the Spent Catalysts Washed with Methanol and Ethanol.....	114
Table 4.6:- Comparison of Present (I-C-S-corn cob) Catalyst Performance with Other Catalysts for Oleic Acid Esterification .....	118
Table 4.7:- Comparison of Present Catalyst (I-C-S-corn cob) Performance with Other Catalysts for Reduction of FFA .....	121
Table 5.1:- Estimated Kinetic and Arrhenius Parameters.....	128
Table 5.2:- Estimated equilibrium and van't Hoff parameters .....	132
Table 5.3:- DSTWU Results for Each Distillation Column .....	138
Table 5.4:- Stream Results of the Simulated Flow Sheet .....	139

## List of Figures

Figure 1.1:- World energy consumption. ....	2
Figure 1.2:- Transesterification reaction mechanism (A to E). ....	7
Figure 1.3:- Hydrolysis reaction of triglyceride (A to C). ....	9
Figure 1.4:- Saponification reaction of free fatty acids. ....	10
Figure 1.5:- Esterification reaction mechanism (A to D). ....	13
Figure 1.6:- Graphical abstract for the effect of quaternary ammonium salt addition to conventional biodiesel production. ....	19
Figure 1.7:- Graphical abstract for esterification of free fatty acids in Karanja oil: experiments, kinetic modeling, simulation and optimization. ....	20
Figure 1.8:- Graphical abstract for the synthesis and characterization of a novel corncob-based solid acid catalyst for biodiesel production. ....	21
Figure 1.9:- Graphical abstract for kinetic modeling and simulation of the novel corncob-based catalytic biodiesel process. ....	22
Figure 2.1:- Waste vegetable oil. ....	24
Figure 2.2:- Schematic of the experimental setup. ....	25
Figure 2.3:- Separation of biodiesel and glycerin as separate layers. ....	27
Figure 2.4:- Purification of biodiesel layer. ....	27
Figure 2.5:- Effect of catalyst loading on yield at various molar ratios of methanol to oil. ....	31
Figure 2.6:- Effect of catalyst loading on yield at various molar ratios of methanol to oil. ....	32
Figure 2.7:- Effect of methanol to oil molar ratio on yield. ....	33
Figure 2.8:- Effect of TMAB on biodiesel yield at various molar ratios of oil to methanol. ...	36
Figure 2.9:- Effect of TMAB on biodiesel yield at various molar ratios of oil to methanol. ...	37
Figure 2.10:- Mechanism of phase transfer catalysis. ....	37

Figure 2.11:- Washability of biodiesel (A) without TMAB (B) with TMAB. ....	41
Figure 3.1:- Schematic of the experimental setup. ....	50
Figure 3.2:- Effect of agitation speed on conversion at 220 °C, 10 bar and 1:6 oil to methanol ratio (w/v).....	53
Figure 3.3:- Effect of temperature on conversion at 1:6 oil to methanol ratio (w/v).....	54
Figure 3.4:- Effect of oil/methanol ratio on conversion at 220 °C temperature. ....	56
Figure 3.5:- Validation of the kinetic model.....	64
Figure 3.6:- Experimental and model predicted conversion at various temperatures.....	64
Figure 3.7:- Arrhenius plot. ....	66
Figure 3.8:- Van't Hoff plot.....	68
Figure 3.9:- Comparison of experimental and model predicted conversions. ....	68
Figure 3.10:- Flow diagram of the esterification process. ....	69
Figure 3.11:- Effect of operating pressure of flash column on methanol mole flow in E-106. ....	75
Figure 3.12:- Effect of operating pressure of flash column on triolein and methyl-oleate mole flows in E-106.....	75
Figure 4.1:- Transformation of corncob to the sulfonated catalyst.....	77
Figure 4.2:- Schematic of the experimental setup. ....	80
Figure 4.3:- FTIR spectra of the corncob, carbonized-corncob ( $C_T = 723\text{ K} - C_t = 8.5\text{ h}$ ), impregnated and carbonized-corncob ( $I_R = 1 - I_T = 5\text{ h} - C_t = 8.5\text{ h} - C_T = 723\text{ K}$ ), impregnated, carbonized and sulfonated-corncob catalyst ( $I_R = 1 - I_T = 5\text{ h} - C_t = 8.5\text{ h} - C_T = 723\text{ K} - S_T = 393\text{ K} - S_t = 16\text{ h}$ ). ....	82
Figure 4.4:- The N <sub>2</sub> adsorption-desorption isotherm of corncob (precursor). ....	84
Figure 4.5:- The N <sub>2</sub> adsorption-desorption isotherm of C-corncob ( $C_T = 723\text{ K} - C_t = 8\text{ h}$ ). ..	84

Figure 4.6:- The N <sub>2</sub> adsorption-desorption isotherm of I-C-corncob (I <sub>R</sub> = 1 - I <sub>T</sub> = 5 h - C <sub>t</sub> = 8 h - C <sub>T</sub> = 523 K).....	85
Figure 4.7:- The N <sub>2</sub> adsorption-desorption isotherms of I-C-corncob (I <sub>R</sub> = 1 - I <sub>T</sub> = 5 h - C <sub>t</sub> = 8 h - C <sub>T</sub> = 623 K).....	85
Figure 4.8:- The N <sub>2</sub> adsorption-desorption isotherm of I-C-corncob (I <sub>R</sub> = 1 - I <sub>T</sub> = 5 h - C <sub>t</sub> = 8 h - C <sub>T</sub> = 673 K).....	86
Figure 4.9:- The N <sub>2</sub> adsorption-desorption isotherm of I-C-corncob (I <sub>R</sub> = 1 - I <sub>T</sub> = 5 h - C <sub>t</sub> = 8 h - C <sub>T</sub> = 723 K).....	86
Figure 4.10:- The N <sub>2</sub> adsorption-desorption isotherms of I-C-corncob (I <sub>R</sub> = 1 - I <sub>T</sub> = 5 h - C <sub>t</sub> = 8 h - C <sub>T</sub> = 773 K).....	87
Figure 4.11:- The N <sub>2</sub> adsorption-desorption isotherms of I-C-S-corncob catalyst (I <sub>R</sub> = 1 - I <sub>T</sub> = 5 h - C <sub>t</sub> = 8 h - C <sub>T</sub> = 723 K - S <sub>T</sub> = 393 K - S <sub>t</sub> = 16 h).....	89
Figure 4.12:- XRD patterns of the impregnated and carbonized-corncob (I <sub>R</sub> = 1 - I <sub>T</sub> = 5 h - C <sub>t</sub> = 8.5 h - C <sub>T</sub> = 723 K), impregnated, carbonized and sulfonated-corncob catalyst (I <sub>R</sub> = 1 - I <sub>T</sub> = 5 h - C <sub>t</sub> = 8.5 h - C <sub>T</sub> = 723 K - S <sub>T</sub> = 393 K - S <sub>t</sub> = 16 h).....	92
Figure 4.13:- Effect of H <sub>3</sub> PO <sub>4</sub> impregnation ratio on conversion of oleic acid (I <sub>t</sub> = 10 h - C <sub>t</sub> = 10 h - C <sub>T</sub> = 673 K - S <sub>T</sub> = 393 K - S <sub>t</sub> = 16 h).....	94
Figure 4.14:- Effect of H <sub>3</sub> PO <sub>4</sub> impregnation time on oleic acid conversion (I <sub>R</sub> = 1 - C <sub>t</sub> = 10 h - C <sub>T</sub> = 673 K - S <sub>T</sub> = 393 K - S <sub>t</sub> = 16 h).....	95
Figure 4.15:- Effect of carbonization temperature on oleic acid conversion (I <sub>R</sub> = 1 - I <sub>t</sub> = 5 h - C <sub>t</sub> = 10 h - S <sub>T</sub> = 393 K - S <sub>t</sub> = 16 h).....	96
Figure 4.16:- Effect of carbonization time on oleic acid conversion (I <sub>R</sub> = 1 - I <sub>t</sub> = 5 h - C <sub>T</sub> = 723 K - S <sub>T</sub> = 393 K - S <sub>t</sub> = 16 h).....	98
Figure 4.17:- Effect of sulfonation temperature on oleic acid conversion (I <sub>R</sub> = 1 - I <sub>t</sub> = 5 h - C <sub>t</sub> = 8.5 h - C <sub>T</sub> = 723 K - S <sub>t</sub> = 16 h).....	99

Figure 4.18:- Effect of sulfonation time on-oleic acid conversion ( $I_R = 1$ - $I_t = 5$ h - $C_t = 8.5$ h - $C_T = 723$ K - $S_T = 393$ K).....	100
Figure 4.19:- Effect of reaction temperature at various intervals on oleic acid conversion ( $R = 1:9$ and $w = 8$ wt. %). ....	101
Figure 4.20:- Effect of reaction temperature at various intervals on palmitic acid conversion ( $R = 1:9$ and $w = 8$ wt. %). ....	102
Figure 4.21:- Effect of oleic acid to methanol ratio on oleic acid conversion ( $w = 8$ wt. % and $T = 338$ K). ....	103
Figure 4.22:- Effect of palmitic acid to methanol ratio on palmitic acid conversion ( $w = 8$ wt. % and $T = 338$ K). ....	104
Figure 4.23:- Effect of catalyst loading (wt. %) on oleic acid conversion ( $R = 1:10$ and $T = 338$ K). ....	105
Figure 4.24:- Effect of catalyst loading (wt. %) on palmitic acid conversion ( $R = 1:10$ and $T = 338$ K). ....	106
Figure 4.25:- Effect of reaction temperature on Karanja oil free fatty acid conversion ( $R = 1:10$ and $w = 10$ wt. %). ....	108
Figure 4.26:- Effect of Karanja oil to methanol ratio on free fatty acid conversion ( $w = 10$ wt. % and $T = 338$ K). ....	109
Figure 4.27:- Effect of catalyst loading on Karanja oil free fatty acid conversion ( $R = 1:20$ and $T = 338$ K). ....	110
Figure 4.28:- Catalyst reusability for oleic acid conversion ( $R = 1:10$ , $T = 338$ K and $t = 4$ h in each cycle). ....	111
Figure 5.1:- Relationship between initial rates ( $r_o$ ) and the molar ratio of methanol to oleic acid ( $m$ ) at various temperatures. ....	127
Figure 5.2:- Arrhenius plot for frequency factor. ....	130

Figure 5.3:- Arrhenius plot for adsorption parameters. ....	130
Figure 5.4:- Experimental and model predicted conversions of oleic acid.....	131
Figure 5.5:- Van't Hoff plot for the esterification process. ....	133
Figure 5.6:- Simulated Process flow sheet of the biodiesel production process.....	134

## Introduction and Literature Review

### 1.1 Energy sources and demand

Energy sources are broadly categorized into two groups [1]:

- i. Renewable energy
- ii. Non-renewable energy

Renewable energy is the source which can be easily replenished like biomass from plants, solar energy from the sun, hydropower from flowing water, wind energy from flowing air, geothermal energy from the heat inside the earth.

Non-renewable energy is the source which cannot be easily replenished like fossil energy (coal, natural gas, petroleum products, and hydrocarbon gas liquids) and nuclear energy. Energy plays a pivotal role in our survival and there are many efforts around the world towards conserving energy by using less of an energy service. Energy consumption is increasing day by day resulting in more demand for fossil fuels and simultaneously, depleting fossil fuels alarms us to look for their alternative replacement. Today, all the energy sources are in great demand due to the industrial advancement through which countries are prospering economically. According to the Energy Information Administration (United States), the total world energy consumption was 406 quadrillions British thermal units (BTU) in 2000 and by 2035, the energy demand is projected to increase by 769.8 quadrillions BTU(Figure 1.1) [2]. In accordance with Figure 1.1, there is an approximately 47.25% increase in energy demand between 2000 and 2035. A large portion of energy demand is met using the combustion of fossil fuels which are the main source of energy [3]. However, rapid

exhaustion of fossil fuels and the environmental concerns due to their usage evoked the search for many promising alternative green energy sources like biofuels [4]. The contribution from all the alternative resources is very important because of the aforementioned concerns with mainstream fossil fuels, and therefore biofuels can be one of the major contributors.

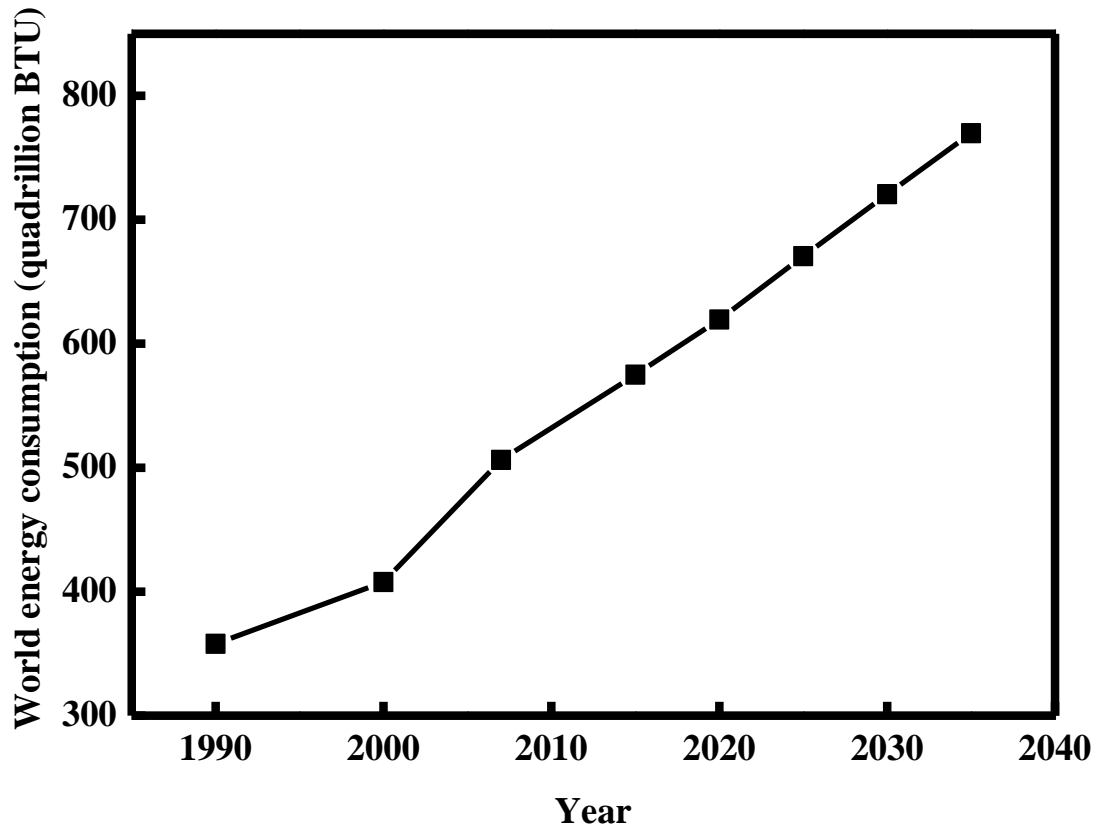


Figure 1.1:- World energy consumption [2].

## 1.2 Biodiesel: A green energy fuel

Diesel fuel is considered to be an impactful fuel in the industrial economy and plays a major part in the transportation sector whose demand for fuel is increasing exponentially. The intensity of this fuel consumption is directly proportional to the development of the society [5,6]. Indeed various technological advancements and socio-economic growth were made by many countries due to the use of energy generated from the combustion of fossil fuels [6,7].

However, combustion of fossils simultaneously created many environmental issues, which threatens the sustainability of our ecosystem [8]. The inevitably high demand for diesel fuel in the industrialized world and pollution problems caused by its widespread use, compelling for a sustainable and renewable energy source with a lesser impact on the environment [9,10]. Therefore, biodiesel which possesses renewable and eco-friendly characteristics was developed as a fuel to replace a fossil-derived diesel fuel [11-15].

Biodiesel is a fuel comprised of monoalkyl esters of long chain fatty acids. Biodiesel derived from vegetable oils or animal fats should meet the required standards set by the American Society of Testing and Materials (ASTM D-6751) or European Norms (EN-14214) [16]. Biodiesel or fatty acid methyl ester (FAME) is a green fuel with eco-friendly benefits and recognized as the replacement to the fossil-derived diesel fuel [3,17]. Although there is a minor power loss due to the combustion of diesel blended with biodiesel, reportedly this blend reduces the emission of particulate matter, carbon monoxide, and greenhouse gases to a substantial extent [18–22]. Among the portfolio of biofuels, biodiesel is considered to be the best alternative fuel because of its high net energy returns ( ~90%) more than the energy invested to produce it [23]. Considering the eco-friendly nature of biodiesel such as its biodegradability, lesser greenhouse emissions, superior lubricating properties and intrinsically free of sulfur compared to diesel, federal and state governments are framing policies to widen its use [24,25].

### **1.3 Feedstock for biodiesel production**

Biodiesel is typically made by reacting triglyceride (ester of three fatty acids and glycerol molecule) present in vegetable oils with alcohol. High-quality biodiesel can also be produced by reacting pure fatty acids like oleic, palmitic, linoleic etc. with alcohol [26-28]. However, most often vegetable oils whose composition has a complex blend of various fatty acids are the preferred source to produce biodiesel due to its low cost compared to pure fatty acids.

Vegetable oils are often classified as edible and non-edible based on their composition, source, and application. Edible oils like soybean, sunflower and palm are widely used to produce high-quality biodiesel. However, large-scale usage of edible oils for fuel may elevate the food versus fuel crisis [29]. Also, the use of edible oils in biodiesel production increases the cost of biodiesel which limits its commercialization. Waste vegetable oils and non-edible oils like Karanja, Jatropha, date seed, castor, rubber seed, mahua, some non-traditional seeds, and algae oils are preferred sources for biodiesel production [30-42]. In general, non-edible and waste vegetable oils contain a high amount of FFA's and water but, later have an advantage of no gum content in the oil. Thus, waste vegetable and non-edible oils are low quality and low-cost oils and using these oils in biodiesel production lowers the cost of biodiesel to a substantial extent [43,44]. Therefore, non-edible oils or waste vegetable oils are the highly preferred feedstock's to produce biodiesel.

Transesterification or esterification reaction between vegetable oil and alcohol is used to produce biodiesel. Principally, a single-step (transesterification) process or a two-step (esterification followed by transesterification) process is generally used to produce high-quality biodiesel [45]. The criteria required to use a single-step base-catalyzed transesterification process is high-quality vegetable oil whose FFA content is <3 wt. % [46,47]. However, for oils whose FFA content is >3 wt. %, a two-step process is generally preferred over the single-step process [48]. In a two-step process, there are two approaches to produce high-quality biodiesel [49]. In the first approach, FFA's in vegetable oil undergo esterification first followed by transesterification of triglycerides present in the esterified oil to give biodiesel [50]. In the second approach, triglycerides in vegetable oil undergo hydrolysis first to produce fatty acids. Then the resulting fatty acids undergo esterification to give biodiesel [51]. The former approach is suitable only when FFA is slightly higher than the limit specified for the usage of base-catalyzed transesterification process. The latter

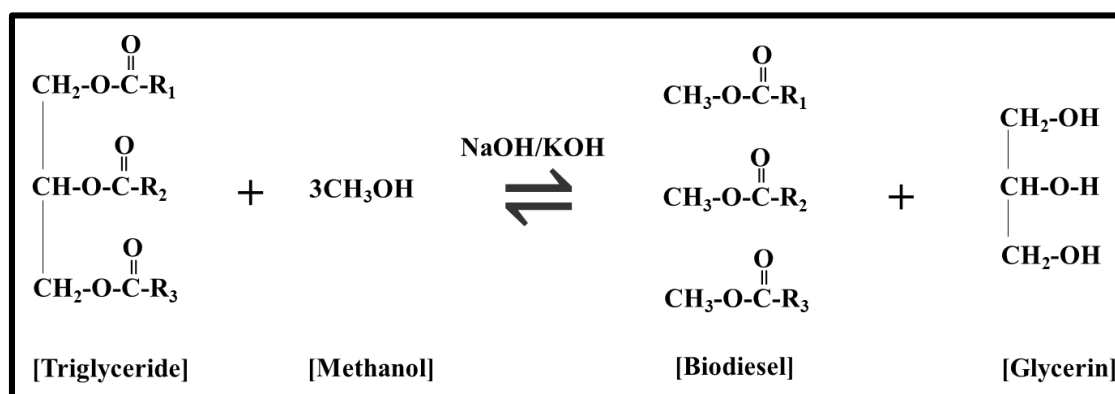
approach is especially beneficial when using oils containing high amounts of FFA like palm fatty acid distillates, Karanja oil and Jatropha oil to produce biodiesel. Apparently, in both the approaches esterification is a crucial processing step for biodiesel production.

#### 1.4 Conventional base-catalyzed transesterification process

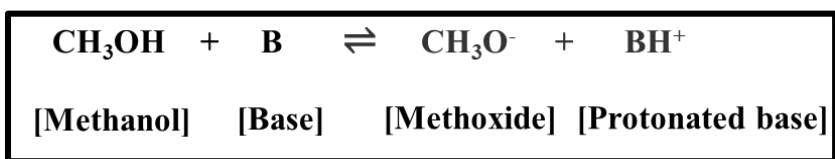
There are many types of catalysts used in biodiesel production like alkali, acid, and enzyme [49,51,52]. Among those the alkali-catalyzed transesterification (Figure 1.2) is most widely used because it gives high yield at mild reaction conditions [53,54]. The overall transesterification reaction in which one mole of triglyceride reacts with 3 moles of methanol to give 3 moles of fatty acid methyl ester or biodiesel and 1 mole of glycerol has been shown in Figure 1.2A. Transesterification mechanism involves the formation of alkoxide and protonated base by mixing alcohol with a base catalyst (Figure 1.2B). The formed alkoxide initiates the nucleophilic attack on the triglyceride molecule and on exchanging ions they form one molecule of biodiesel and diglyceride respectively (Figure 1.2C) [55,56]. Similarly, the same approach is followed in converting diglyceride to mono-glycerides (Figure 1.2D) and subsequently monoglyceride to biodiesel and glycerol molecules (Figure 1.2E).

##### Main reactions:

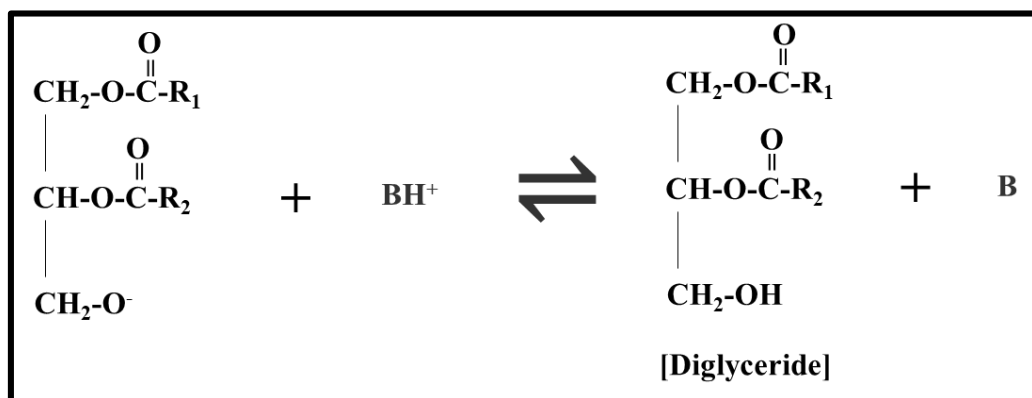
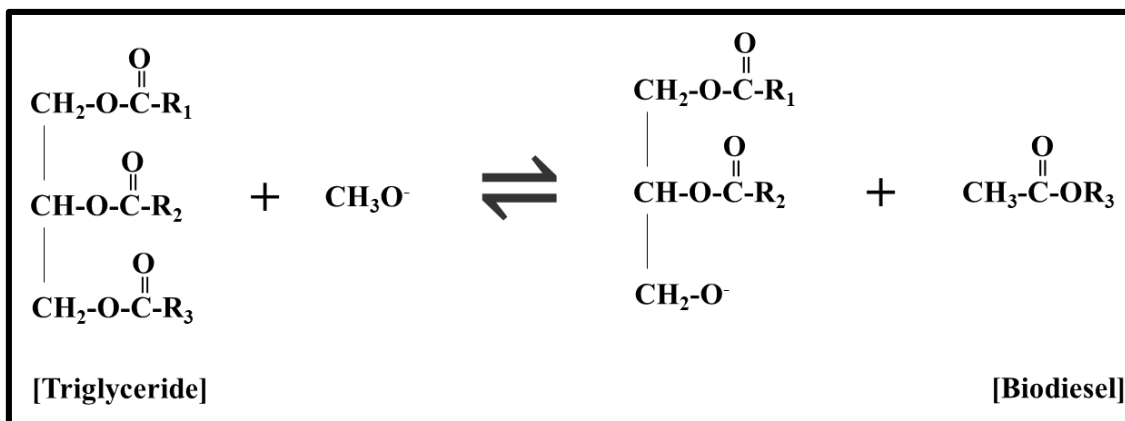
###### (A) Overall reaction



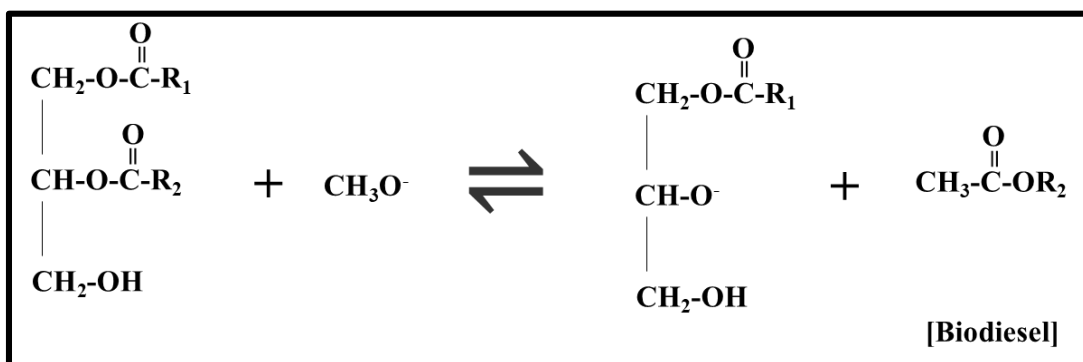
**(B) Formation of methoxide and protonated base catalyst**

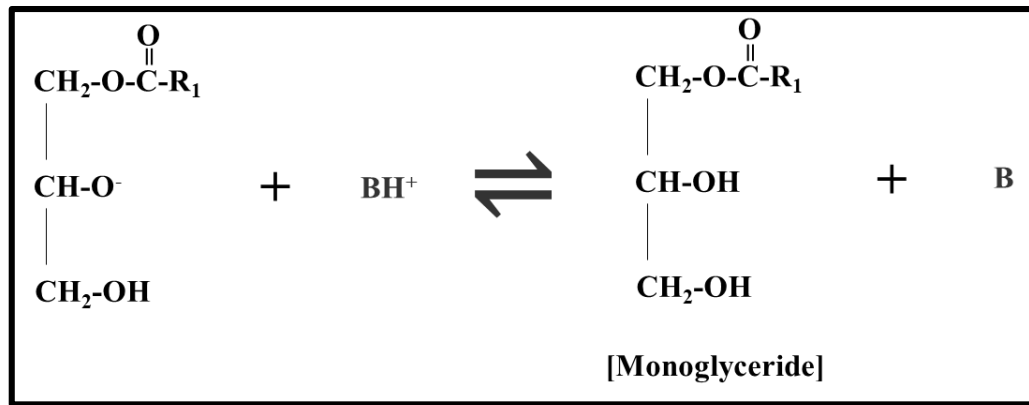


**(C) Nucleophilic attack of methoxide on triglyceride to form biodiesel and diglyceride**



**(D) Nucleophilic attack of the second molecule of methoxide on diglyceride**





(E) Nucleophilic attack of the third molecule of methoxide on monoglyceride

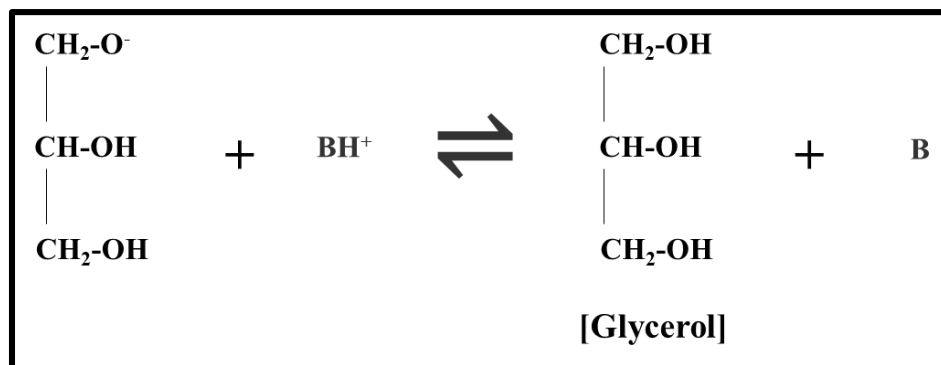
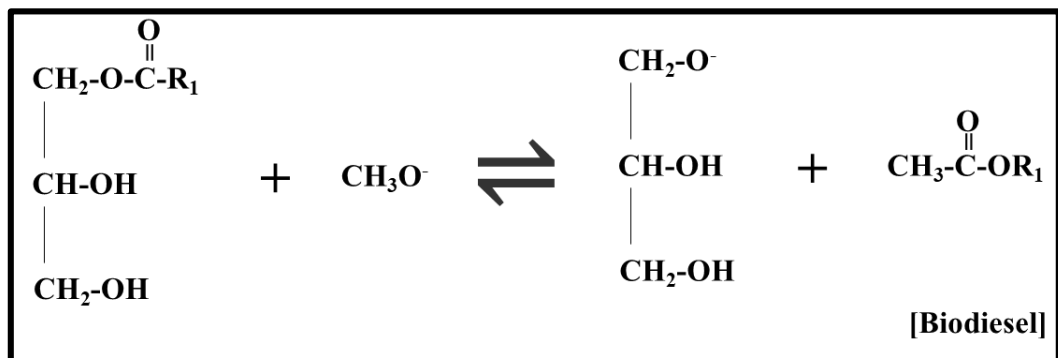


Figure 1.2:- Transesterification reaction mechanism (A to E).

Conventional single-step base (KOH and NaOH) catalyzed transesterification process is used to produce biodiesel on a commercial scale [36]. However, this process is limited by interphase mass transfer and sensitivity to feedstock;

**(i) Interphase mass transfer**

The mass transfer between oil and methanol phases plays a critical role during the transesterification reaction [57-59]. Since oil (nonpolar) and alcohol (polar) are two

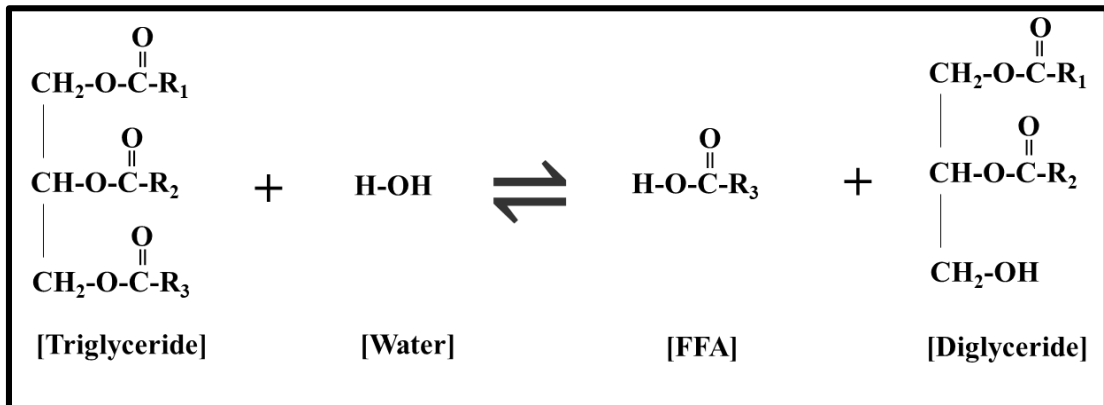
dissimilar species they suffer from limited solubility in each other [60–63]. Moreover, Boocock et al.[64–66] confirmed that the base-catalyzed reaction between vegetable oil and methanol is not a homogeneous reaction. Due to this non-homogeneity, base-catalyzed transesterification reaction was characterized to be associated with very slow reaction rates at the initial and final reaction stages [57,60,67]. The slow reaction rates during the initial stage of the reaction are due to the immiscibility of the reactants. At the final stage of the reaction glycerol being a polar compound formed during the reaction extracts the catalyst, which remains separated from reactants resulting in slow reaction rates. These slow reaction rates at initial and final stage of the reaction result in the reaction to be slow or would stop the reaction without complete conversion of reactants [60]. Therefore, the mass transfer resistance between phases limits the conventional base-catalyzed transesterification process.

#### **(ii) Sensitivity to feedstock**

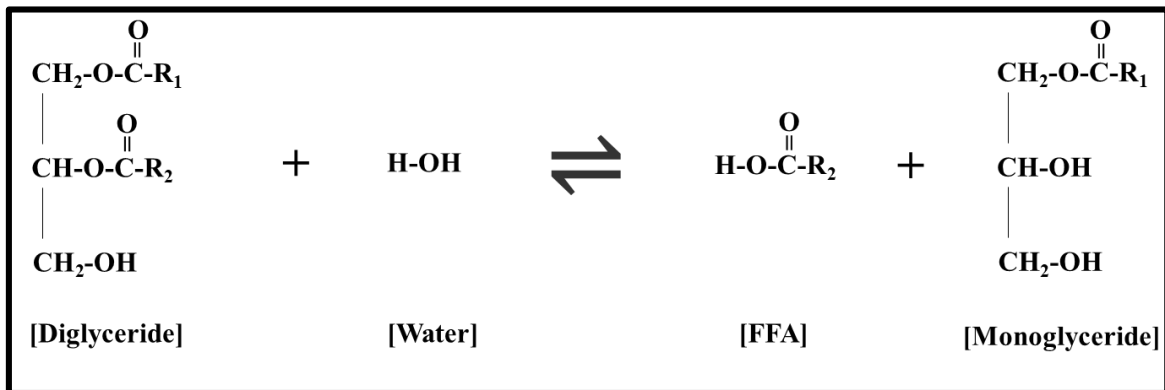
Using waste vegetable and non-edible oils for biodiesel production can lower the cost of biodiesel. However, the presence of water and FFA in the oil is counterproductive to the biodiesel production through single-step base-catalyzed transesterification route. The presence of water fragments the triglycerides to diglyceride (Figure 1.3A), diglyceride to monoglyceride (Figure 1.3B) and monoglyceride to glycerol (Figure 1.3C), and a molecule of free fatty acid (FFA) in each step as shown in Figure 1.3. Consequently, the FFA reacts with the base catalyst and form soaps by saponification as shown in Figure 1.4 which counters the transesterification and complicates the product purification [30,68].

**Side reactions:**

**(A) Triglyceride fragment to free fatty acid and diglyceride**



**(B) Diglyceride fragment to free fatty acid and monoglyceride**



**(C) Monoglyceride fragment to free fatty acid and glycerol**

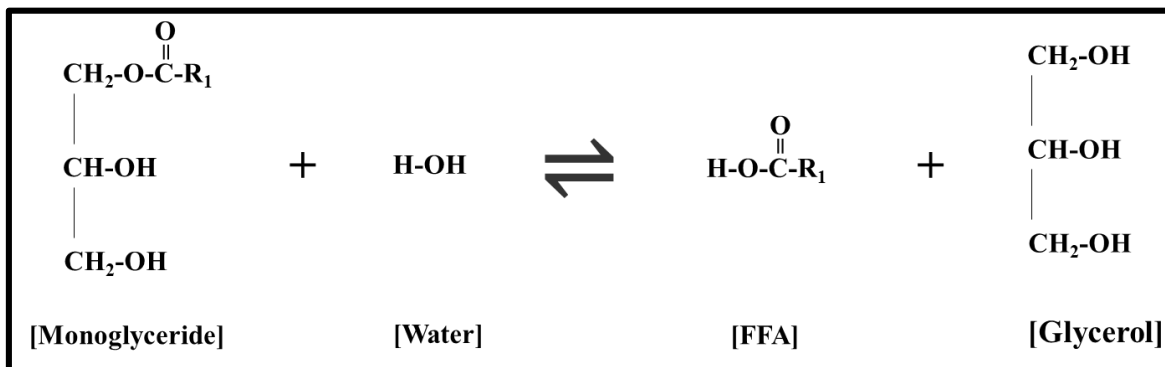


**Figure 1.3:-** Hydrolysis reaction of triglyceride (A to C).

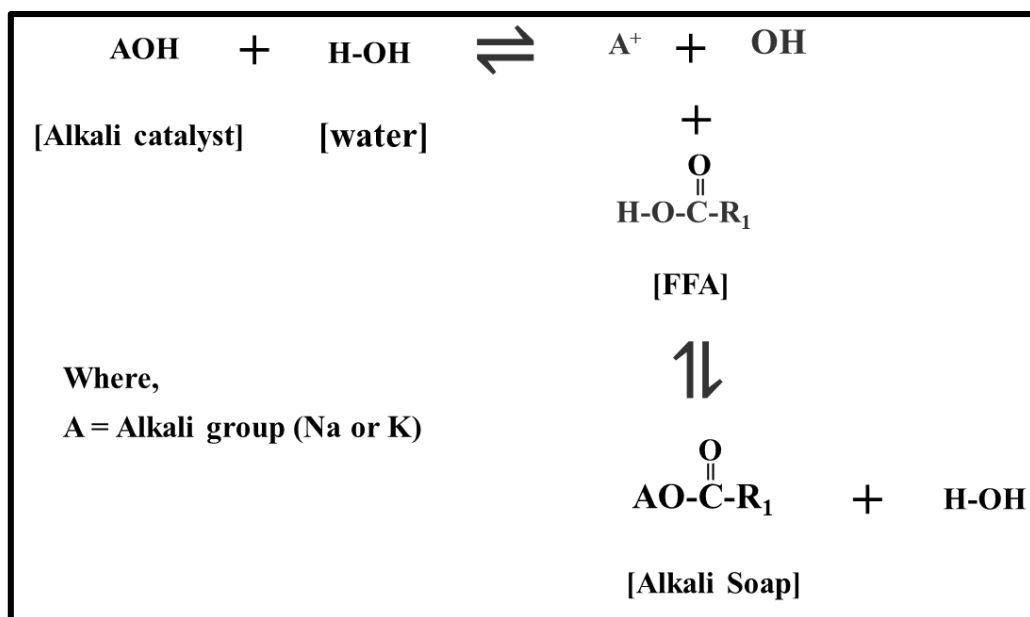


**Figure 1.4:-** Saponification reaction of free fatty acids.

Since transesterification reaction is the main reaction mechanism in forming biodiesel, hydrolysis of triglycerides and saponification of FFA's are considered as side reactions [69,70]. Moreover, the formation of soaps during transesterification not only hinders the reaction progress but also increases the loss of produced biodiesel to byproduct phase (glycerol) during washing [71]. This result in a higher water requirement for washing crude biodiesel during purification which indeed increases the cost of biodiesel production [68]. Therefore, the sensitivity to impurities in feedstock limits the use of a single-step base-catalyzed transesterification process. The limitations of using single-step base-catalyzed transesterification process (interphase mass transfer and sensitivity to feedstock) could be overcome using phase transfer catalyst as transesterification process enhancer.

### 1.5 Phase transfer catalysis

Phase transfer catalysis is a process which facilitates the interphase mass transfer of species present in two immiscible phases to accelerate the reaction [58]. The chemical compound which is involved in this process is referred to as phase transfer catalyst (PTC). Most of the

reactions occurring in conventional, homogeneous conditions require each of the dissimilar species (organic and inorganic) to be soluble during the reaction and the efficacy of the process largely depends on their mutual solubility's [58,72]. In sparingly soluble reactants the reaction rates will be very low. These disadvantages in direct organic synthesis reaction raise the need for phase transfer catalytic processes [57]. During phase transfer catalysis, PTC forms a complex with the reactant in phase A and this complex diffuse into phase B to react with the reactant in that phase. After the reaction, PTC diffuses back to the phase A and promotes the process further. Since the vegetable oil and methanol are mutually insoluble and form distinct phases, the concentration of two reactants in any single phase will be very low for good reaction rates. Moreover, transesterification using base-catalyst requires strict anhydrous conditions [30] and whose reaction rates are frequently considered to be controlled by diffusion and characterized by a slow reaction rate [57,73]. There are several ways to overcome this mass transfer limitation and enhance the contact between two phases such as; the use of large excess alcohol, mechanical mixing, using polar aprotic solvents or inert co-solvent, ultrasonic and hydrodynamic cavitation, supercritical conditions [17,74–84]. However, these techniques are associated with one or more drawbacks like the high cost of solvent or require a very excessive amount of solvents, the high cost of operations, generation of huge amounts of effluents and higher capital costs [57,67,73,85,86]. It was evident that eliminating the mass transfer limitations using either co-solvent (which forms pseudo-homogeneous phase) or catalyst-free processes (conducted at high temperature and pressure), faster transesterification rates could be achieved [64–66,87]. So, phase transfer catalysis is also a promising technique which can be explored to enhance the reaction rates between reactants forming two immiscible phases. There are many types of PTC's such as onium salts (quaternary ammonium, sulfonium, phosphonium or arsonium salts), crown ether groups and cryptates [58]. Among those quaternary ammonium salts are most widely used because of

less interference of their ions in reactions [58,88] and also they are much cheaper than other PTC's [82,89]. Tetramethylammonium (TMA) cations are a type of quaternary ammonium salts known to possess phase transfer catalytic properties and they are positively charged simplest quaternary ammonium cations with four methyl groups attached to the central nitrogen atom. They are often associated with some anion groups such as bromide, chloride, iodide, and hydroxide. Previous studies used PTC's (such as cetyltrimethylammonium bromide, tetrabutylammonium hydroxide, tetrabutylammonium acetate, tetrabutylammonium nitrate, benzyltrimethylammonium hydroxide, tetrabutylammonium hydrogen sulphate, 18-crown-6 ether, and choline hydroxide) as a process enhancer for conventional base-catalyzed transesterification process [60–62,67]. Tetramethylammonium hydroxide was also used as a phase transfer catalyst in biodiesel synthesis [86]. However, tetramethylammonium bromide (TMAB) was never used for this purpose.

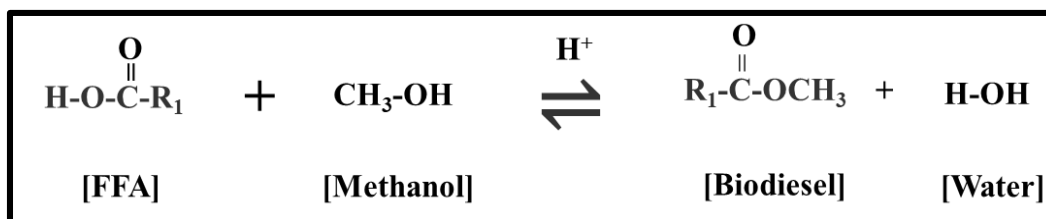
## **1.6 Conventional acid catalyzed esterification process**

Since single-step base-catalyzed transesterification is sensitive to FFA in feedstock and therefore, it is essential to limit the FFA in feed oil prior to transesterification reaction [90,91]. Several pretreatment techniques such as esterification, distillation, and neutralization are employed to lower the FFA content in the feed oil. Among all these techniques, the esterification process is found to be the most efficient in reducing the FFA content of feed oil [45,92,93].

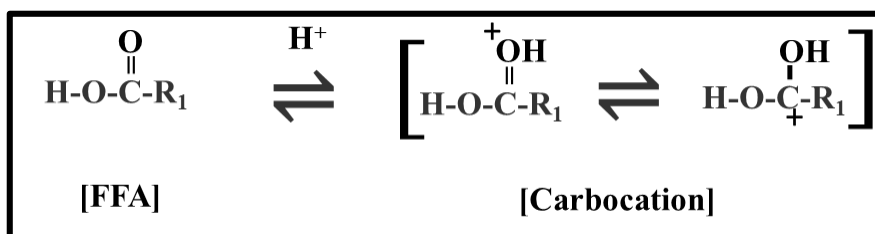
Esterification is a reversible reaction in which equimolar quantities of FFA and alcohol react to produce the equimolar amount of alkyl ester and water in the presence or absence of the acid catalyst [50,94] as shown in Figure 1.5A. Esterification mechanism involves the protonation of the carboxylic group to give carbocation (Figure 1.5B). Then the methanol initiates the nucleophilic attack on the carbocation as soon as it is formed and results in a

tetrahedral intermediate (Figure 1.5C). Finally, the formed tetrahedral intermediate results in the biodiesel and water with a series of protonation and deprotonation steps (Figure 1.5D).

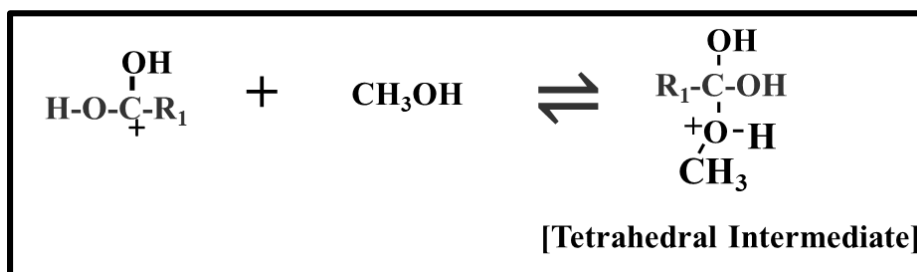
**(A) Overall reaction**



**(B) Protonation of carboxylic group of FFA to form a carbocation**



**(C) Nucleophilic attack of methanol on carbocation**



**(D) Formation of biodiesel**

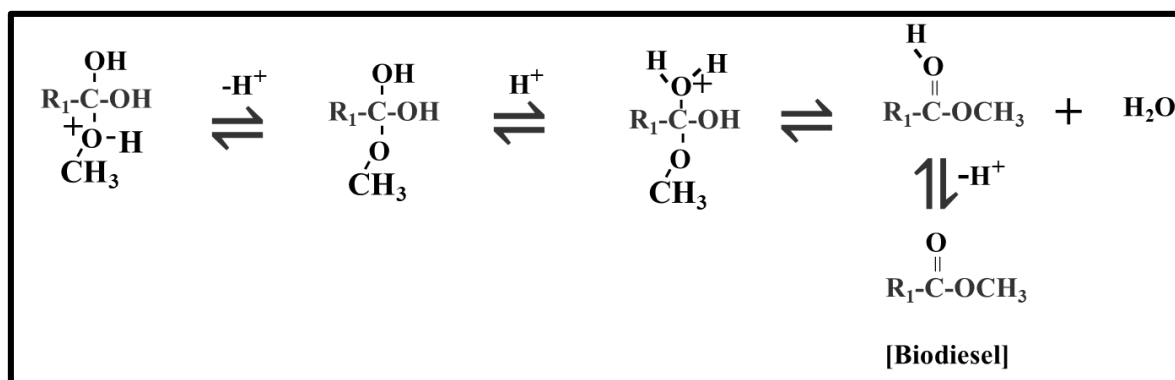


**Figure 1.5:- Esterification reaction mechanism (A to D).**

The acid catalyzed esterification process is suitable to produce biodiesel using non-edible oils having high FFA content [35,95]. Moreover, it has the ability to catalyze both esterification and transesterification simultaneously [96]. Conventionally, concentrated sulfuric acid in a homogeneous form is used as a catalyst in the esterification. However, homogeneous acid imposes severe environmental issues, corrosion problems, and usually nonrecyclable [97]. Moreover, biodiesel produced using homogeneous catalysts also generates a substantial amount of water effluents together with the significant loss of biodiesel during the washing process [98]. In order to curb these disadvantages, a non-catalytic esterification route and heterogeneous catalytic processes were explored.

### **1.7 Non-catalytic process for biodiesel production**

The problems associated with homogeneous catalysts are corrosion of the equipment, difficulty in product separation, non-recovery and non-reusability of the catalyst and large volumes of unprocessed effluents. In order to mitigate these drawbacks with a homogeneous catalyst, the non-catalytic process is highly focused areas in biodiesel production. Many studies have explored the non-catalytic supercritical processes to overcome the limitation of the catalytic processes and have shown significantly higher yield (~97%) of biodiesel in a very short period of time [54,99-104]. But, the severe conditions employed in the supercritical processes demand higher capital cost as well as operating cost which limits their commercialization [85]. Some studies even proved the thermal degradation of esters at supercritical synthesis condition [105,106]. The non-catalytic subcritical esterification process mitigated the above-stated drawbacks and produced an ester yield and conversion nearly equal to that produced in other processes. For example, the product yield of ~ 94% was achieved by Minami and Sake [107] at 270 °C and 200 bar using 1:0.9 rapeseed oil to methanol ratio (v/v). Melo Junior et al. [108] observed C18 fatty acids conversion of 60% non-catalytically in a short period of time (60min) under microwave irradiation. In 5 h

reaction time at 1:4 Jatropha oil to methanol ratio (w/v), 190 °C and 27.1 bars, ~95% conversion was reported by Rani et al. [109]. Cho et al. [110] achieved a desirable final product acid value of fewer than 0.5 mg KOH/g using palm fatty acid distillate and methanol in 3 h at 290 °C and 8.5 bar. Pinnarat and Savage [28] investigations revealed that the noncatalytic esterification can be carried out smoothly even at subcritical conditions and also reported the feasibility of subcritical esterification process in tolerating moderate content of water in the feed oil. It was also reported that the presence of a moderate amount of water even enhances the effectiveness of subcritical esterification process [85]. Simulation study carried out by Haas et al. [111], West, Posarac, and Ellis [112] and Lee, Posarac, and Ellis [113] in Aspen HYSYS demonstrated the continuous biodiesel production processes using edible oils and assessed the technical and economic feasibility. In view of this, there is a lag in kinetic modeling and process simulation studies of non-catalytic esterification process.

## **1.8 Heterogeneous catalytic process for biodiesel**

Solid catalyst is the catalyst in a solid form that does not dissolve in the reaction media. Usually, they are present in the different phase compared to the reactants, due to this reason they are often used in heterogeneous catalysis and referred to as heterogeneous catalysts. Industrially solid catalysts are preferred more due to their capability to be easily separable and reusable. Use of non-edible and waste vegetable oils for the biodiesel production can lower the cost of the process to a substantial extent [114-116]. However, the environmental hazards involved in the conventional production process can only be mitigated using a sustainable and efficient catalyst. Therefore, to avoid problems with homogeneous catalysts, its counterpart; heterogeneous catalysts was explored in the biodiesel production.

The solid base catalysts used in the biodiesel production are very sensitive towards FFA and water content present in the feed [97,117-121]. However, solid acid catalysts are found tolerant towards the low-quality feedstock [49,122,123]. Also, their application in biodiesel

production eliminates equipment corrosion, lowers water effluents, dampens the toxicity as well as facilitates the catalyst separation and offers the advantage of reusability [124–128]. Therefore, the heterogeneous solid acid catalyst was explored to produce biodiesel.

Solid acid catalyst (SAC) is particularly important when oils containing higher amounts of FFA employed as a feedstock for biodiesel production. There were several SAC's such as niobic acid, amberlyst, protonated-Nafion and sulfated zirconia investigated in the past for biodiesel production [129-132]. However, these catalysts remain associated with one or more disadvantages like low acid density, small pore size, low porosity, fast deactivation, poor tolerance towards the water, poor stability and the high cost of synthesis [133]. Moreover, they are usually hydrophilic and their activity decreases due to the water produced during the esterification reaction. For example, due to the low protonic acid density in the case of zeolites and niobic acid, these catalysts readily lose their activity in the presence of water. Although higher amounts of sulfonic ( $\text{SO}_3\text{H}$ ) groups are present on Nafions, their catalytic activity is very much lower than the concentrated sulfuric acid [26,133]. Due to these disadvantages research efforts are focused on the low-cost catalysts, which offers environmentally benign and economically feasible biodiesel production process.

The cost of catalyst will also have enough impact on the total production cost of biodiesel [47,134,135]. Carbon-based SAC derived from sugars (glucose and sucrose) [52,136-138], and polysaccharides (starch and cellulose) [139] showed high potential for esterification. However, due to the higher cost of glucose and starch and various other prolific applications, attention was diverted towards the cheaper and environmentally benign waste biomass-derived catalysts. Besides, some research groups have also proved the potential of various waste natural resources such as coconut shell, bamboo, and bagasse towards esterification of high FFA containing oils [133,140-142]. However, a search for many waste biomass resources and their transformation to value-added products are still in progress[143,144].

Corn is the most widely cultivated crop in India and many other parts of the world. In India, it is the third largest crop grown after wheat and rice. Production of corn in India remains mostly dominated by Andhra Pradesh and Karnataka and accounts for ~38% of total agricultural production [145]. After separating the grains from the corn, the corncob remains generally left as agricultural waste and then subjected to incineration for being worthless. There are studies devoted to various applications of corncob as an adsorbent [146–149]. However, very limited literature is available on corncob as catalyst support [150,151]. Researchers in the past have shown that the phosphoric acid impregnation on organic waste followed by incomplete carbonization (below 773 K) yield a highly porous carbon material [152]. Also, sulfonation of these carbons produces carbon-based SAC containing polycyclic aromatic carbon sheets with acidic groups on the surface [153,154]. Therefore, corncob was chosen to synthesize SAC and used for biodiesel production.

There is very limited literature available on simulation of the heterogeneously catalyzed biodiesel production process. Haas et al. [111] developed a versatile Aspen Plus process simulation model to estimate biodiesel production costs which allow the user to determine the effect of changing unit operations, material flows, and raw material costs on the process economics. However, the model was limited to a traditional alkali-catalyzed production method. Zhang and coworkers [155] developed an HYSYS based process simulation model to assess the technological feasibility of four biodiesel plant configurations. The configurations are a homogeneous alkali-catalyzed pure vegetable oil process; a two-step process to treat waste vegetable oil (WVO); a single-step homogeneous acid-catalyzed process to treat WVO, and a homogeneous acid-catalyzed process using hexane extraction to purify the biodiesel. The same Zhang et al. [156] group extended the study by conducting an economic analysis of these four designs and revealed that one step acid-catalyzed process was the most economically attractive among all the designs. West et al. [112] developed a

series of process simulation models in HYSYS using the traditional homogeneous processes as base cases and compared with simulations of the heterogeneous acid-catalyzed process and the supercritical process. It was found that the heterogeneous acid-catalyzed process was the most economically advantageous, and is the only one process to yield a positive rate of return. Another study carried out by West et al. [157] simulated the biodiesel production process using a heterogeneous catalyst ( $\text{SO}_4/\text{ZrO}_2$ ). However, they used the stoichiometric reactor in their model due to the nonavailability of kinetic data.

## **1.9 Scope of present work**

In view of the above-reviewed literature and discussion, it can be asserted that the conventional base-catalyzed transesterification process is limited by low mutual solubility of reactants and also it is a feedstock sensitive process. The catalyst cannot be recovered due to the reaction in a homogeneous phase and also consumes a huge amount of water resulting in a large volume of unprocessed effluents. Similarly, the conventional esterification process using concentrated sulfuric acid in a homogeneous form is also associated with various drawbacks like longer reaction time, require elevated reaction conditions, equipment corrosion and discharge of the huge amount of effluents. Therefore, due to the high cost of feedstock, disadvantages of using low-quality feedstock and environmental hazards associated with the conventional biodiesel production processes, biodiesel has not been commercialized globally.

In this thesis, we have used waste vegetable oil as a feedstock for biodiesel production and a tetramethylammonium bromide (a phase transfer catalyst) was added to enhance the conventional transesterification process. Then the esterification of Karanja oil with high free fatty acid content was carried out using a non-catalytic route whose kinetics was modeled and the process was simulated using Aspen Plus. Moreover, a corncob-based solid acid catalyst was synthesized for biodiesel production and used for esterification of oleic acid, palmitic

acids and free fatty acids present in Karanja oil. Finally, the kinetics of the biodiesel production process was modeled using Langmuir-Hinshelwood-Hougen-Watson (LHHW) kinetic model and the process was simulated in Aspen Plus.

Chapter 2 focuses on the base-catalyzed batch scale production of biodiesel using waste vegetable oil and methanol as feedstocks, NaOH and KOH as a catalyst and tetramethylammonium bromide as the process enhancer (or booster). The effect of oil to methanol molar ratio and effect of TMAB addition on the transesterification reaction for biodiesel production was studied in detail. The graphical abstract of the study was presented in Figure 1.6.

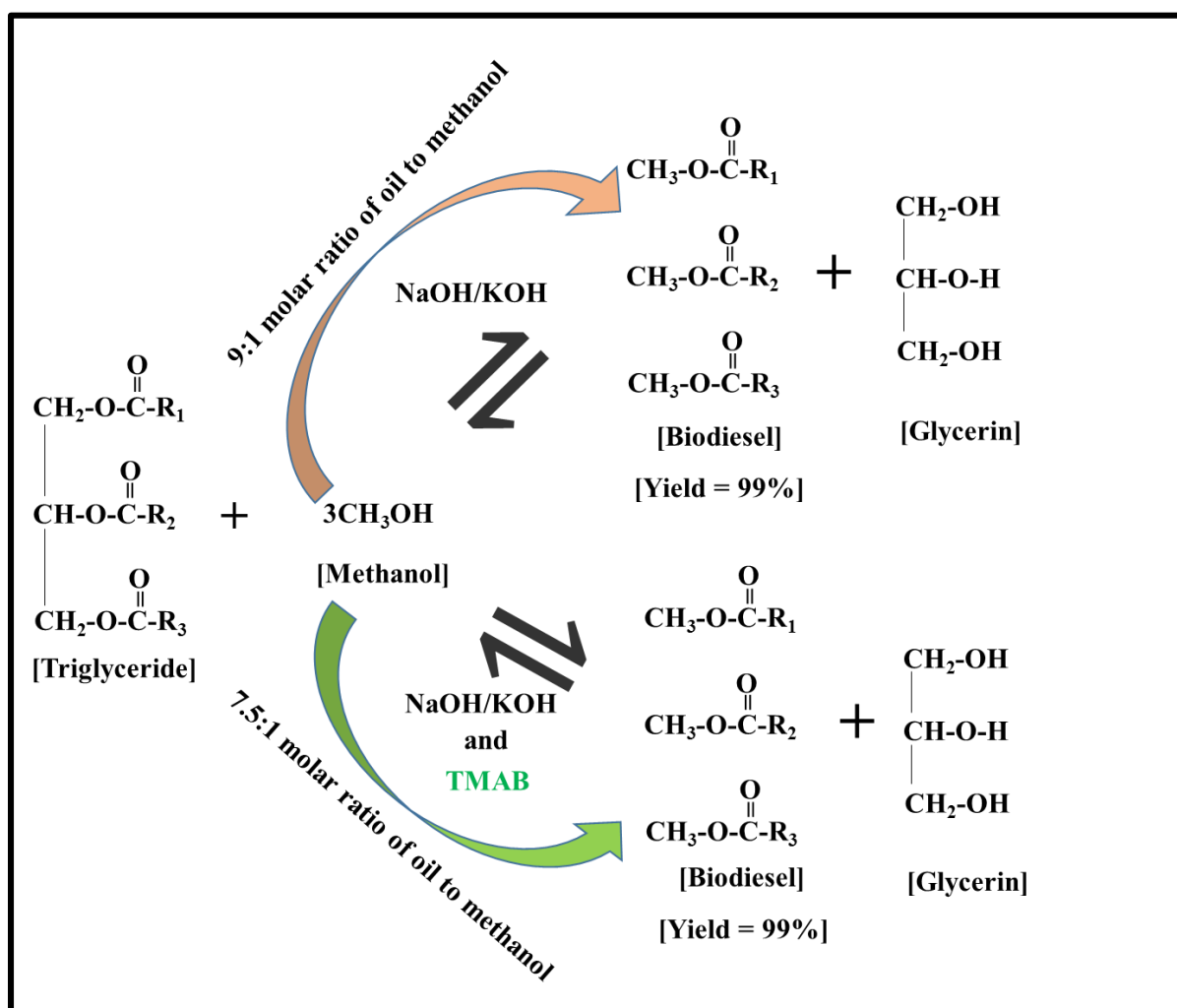


**Figure 1.6:-** Graphical abstract for the effect of quaternary ammonium salt addition to conventional biodiesel production.

In chapter 3, the effect of esterification process variables such as speed of stirring, reaction time, temperature and ratio of oil to methanol was investigated non-catalytically in a batch experiment. Then the experimental data were modeled to determine the kinetic parameters. The obtained kinetic parameters were used to simulate the process in Aspen Plus. Further, the sensitivity analysis was carried out to obtain the optimal process parameters along with heat integration. The graphical abstract of the work is shown in Figure 1.7.

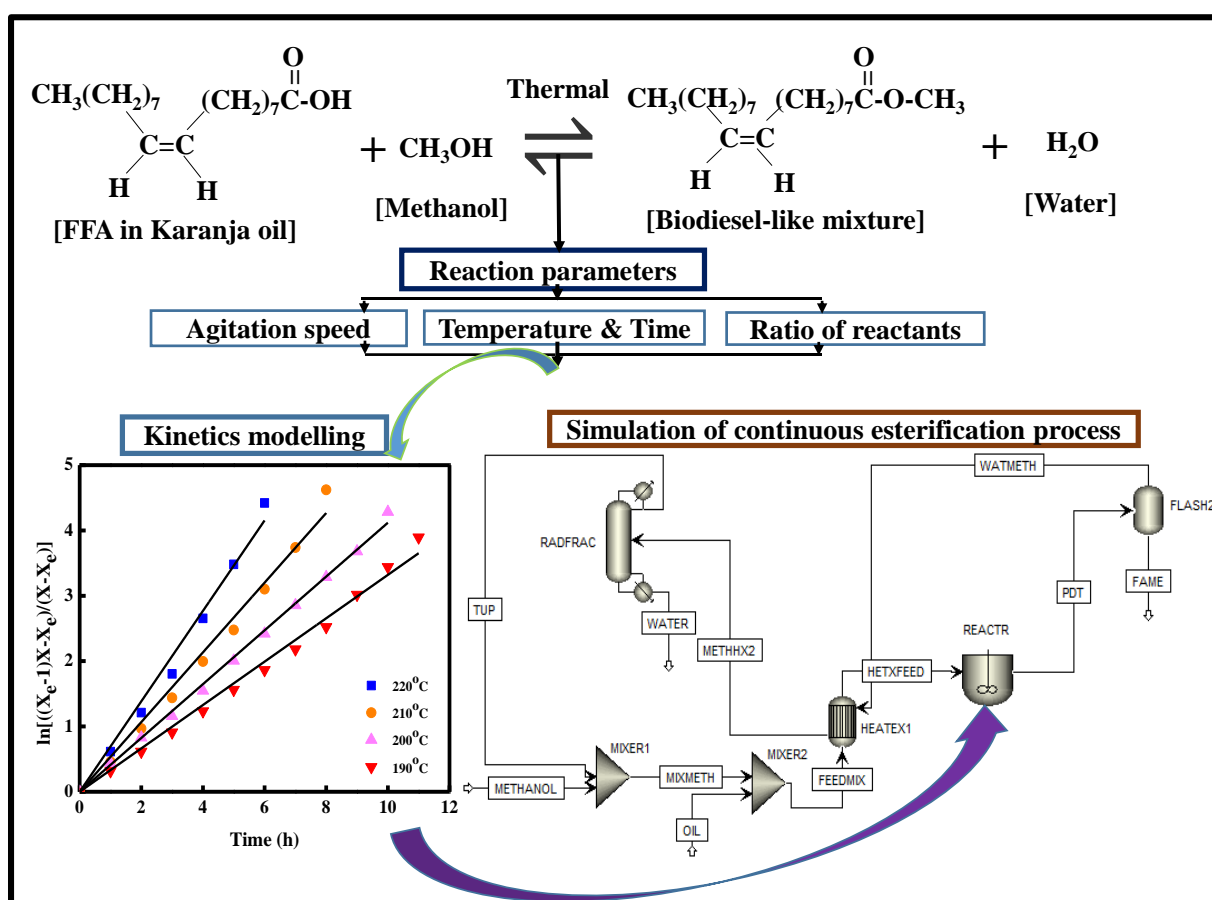


**Figure 1.7:-** Graphical abstract for esterification of free fatty acids in Karanja oil: experiments, kinetic modeling, simulation and optimization.

Chapter 4 presents the synthesis and characterization of corncob-based solid acid catalysts by impregnating phosphoric acid followed by carbonation, and sulfonation of corncob. The synthesized catalysts were characterized to find the surface functional groups, structure, acid

density, surface area, and pore volume. The effect of impregnation ratio and time, the carbonization temperature and time and the sulfonation temperature and time on esterification of oleic acid were studied. Moreover, the performance of the catalyst in esterifying fatty acids (oleic acid and palmitic acid) and free fatty acids present in Karanja oil at various reaction conditions were also studied. Further, the effect of washing solvents on catalyst regeneration and reusability of the catalyst in oleic acid esterification was also evaluated. Furthermore, the performance of the present corncob catalyst with other potential catalysts reported in the literature for biodiesel production was assessed and discussed. The graphical abstract was presented in Figure 1.8.

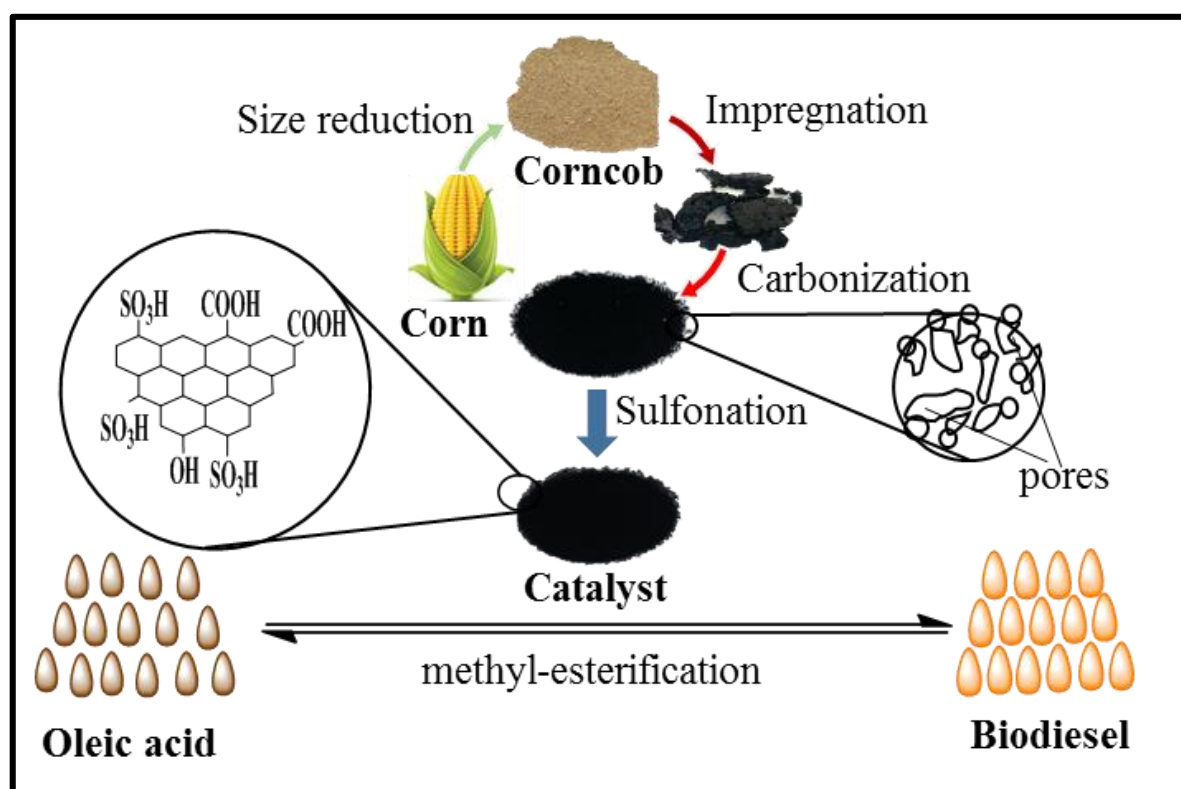


**Figure 1.8:-** Graphical abstract for the synthesis and characterization of a novel corncob-based solid acid catalyst for biodiesel production.

In chapter 5, a sulfonic group-functionalized porous carbonaceous catalyst based on corncob ( $I_{R=1}^{t=5} - C_{T=723}^{t=8} - S_{T=393}^{t=15}$ ) was used for esterification of oleic acid. Langmuir-

Hinshelwood–Hougen-Watson kinetic model was used to correlate the experimental data as shown in the graphical abstract (Figure 1.9).

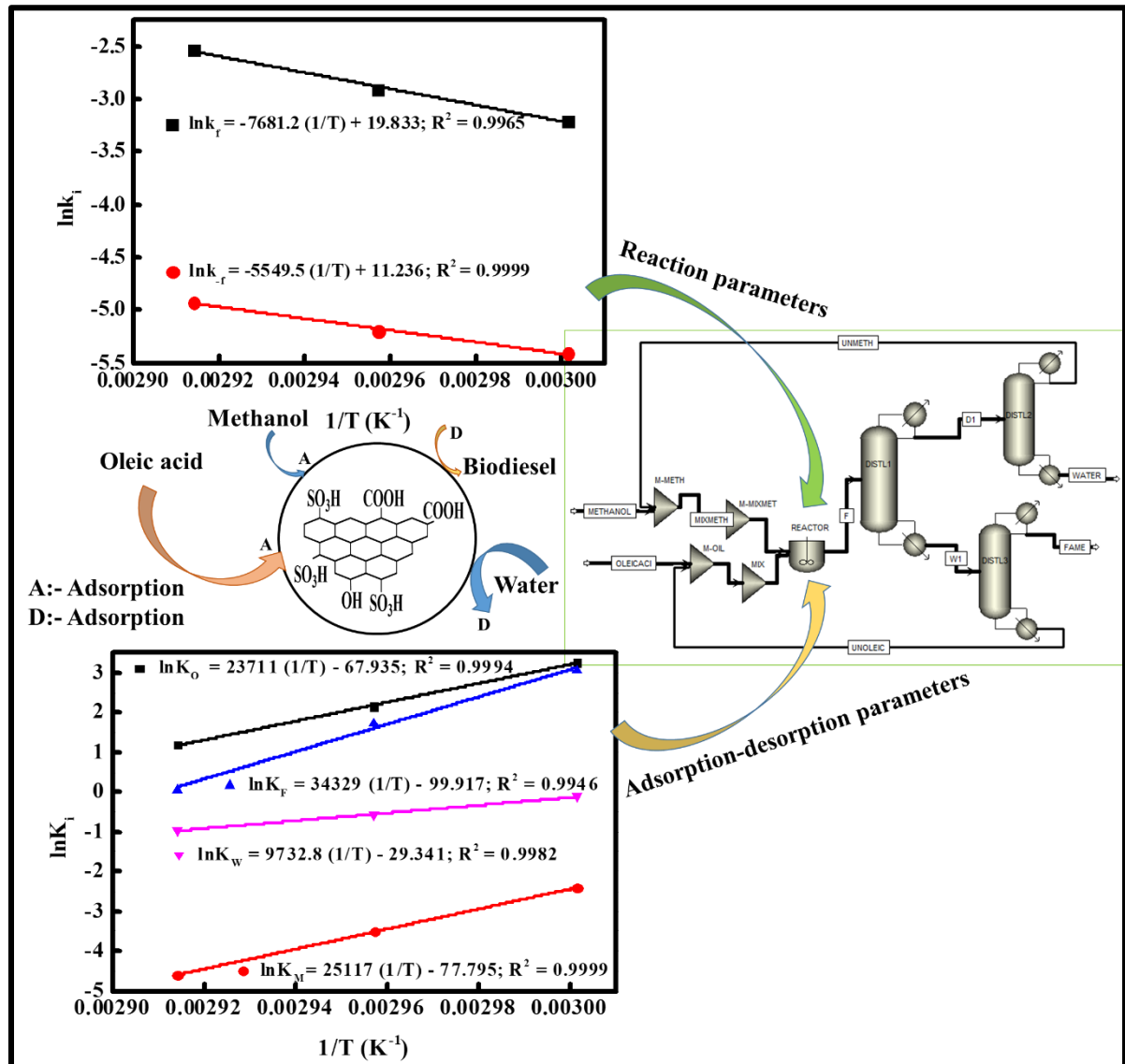


**Figure 1.9:-** Graphical abstract for kinetic modeling and simulation of the novel corn-cob-based catalytic biodiesel process.

The data presented in chapter-4 for oleic acid esterification was used for modeling. First, the forward reaction parameter ( $k_f$ ) and adsorption parameters ( $K_o$  and  $K_M$ ) were found from the initial reaction rates. Then the obtained parameters were used to deduce other parameters using nonlinear regression. All the parameters were fitted in the linear form of the Arrhenius

equation to obtain activation energies and frequency factors of each parameter in the form of slope and intercept, respectively. Finally, these slope and intercept values were incorporated in Aspen Plus to simulate the continuous biodiesel production process.

# Effect of Quaternary Ammonium Salt Addition to Conventional Biodiesel Production Process

## 2.1 Experimental Details

### 2.1.1 Materials used

Waste vegetable oil (WVO) was collected from the selected households and it was dark brown in color containing food contaminants as shown in Figure 2.1.



**Figure 2.1:-** Waste vegetable oil.

The other chemicals such as methanol, sodium hydroxide, potassium hydroxide, glacial acetic acid, hexane, diethyl ether, potassium permanganate, chloroform, iodine monochloride, potassium iodide, sodium thiosulphate, ethanol, hydrochloric acid, phenolphthalein indicator and tetramethylammonium bromide (TMAB) were purchased from Fluka chemicals and were used without further purification. The analytical standards such as; caprylic, decanoic, lauric, myristic, palmitic, palmitoleic, stearic, oleic, linoleic, linolenic, arachidic, behenic, and lignoceric acids; Internal standards: butanetriol, tricaprins; reference standards: mono-olein, di-olein, and triolein; derivatizer: N- methyl-N-trifluoroacetamide (MSTFA) of Sigma-

Aldrich were used for chromatographic analysis. All the standards are used with pyridine solvent. The instrument grade helium, hydrogen, and zero-air were supplied by Sigma-gases and services, New Delhi, India.

### 2.1.2 Experimental setup

The experimental setup shown in Figure 2.2 is divided into two zones namely the reactor zone and the heating zone. Three necked round bottom glass flask of 2 L capacity was used for transesterification reaction. A double coiled reflux condenser was fitted to a neck of the glass flask to condense methanol vapor formed during the reaction.

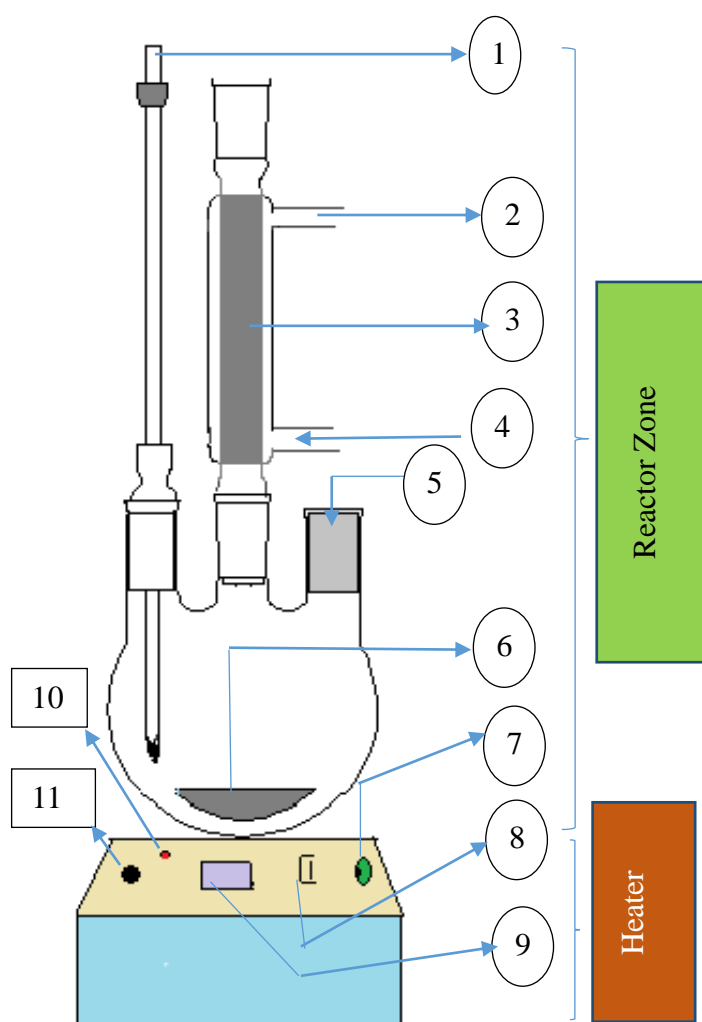


**Figure 2.2:-** Schematic of the experimental setup.

## **Nomenclature:**

### **Reactor Zone**

- 1) Thermometer
- 2) Cooling water Outlet
- 3) Double coiled reflux condenser
- 4) Cooling water Inlet
- 5) Feed Inlet
- 6) Magnetic stirrer

### **Heater Zone**

- 7) Speed controller
- 8) Power switch Cold
- 9) Digital speed indicator
- 10) Power on/off indicator
- 11) Temperature controller

Cooling water was circulated through the coil of the reflux condenser. A thermometer having a temperature range of 0-200 °C was inserted into the second neck of the flask to measure the temperature of the reaction mixture. A plate heater with a magnetic stirrer was used for heating and uniform stirring of the mixture in the flask. Waste vegetable oil, methanol, and other chemicals were transferred into the flask through the third neck, at the beginning of each experiment using a glass funnel and were closed with a rubber stopper during the reaction. A constant reaction temperature of 65 °C was maintained for each experimental run.

### **2.1.3 Experimental procedure**

The contaminants in waste vegetable oil were removed by screening with fiber cloth placed on a Buchner funnel and then the moisture was removed by heating at 120 °C for 45 minutes with stirring continuously. Experiments were conducted at various methanol to oil molar ratios (3:1, 6:1, 7.5:1, and 9:1) using KOH and NaOH as a catalyst. The KOH and NaOH amounts were varied in the range of 0.25 to 2 wt. % with respect to waste vegetable oil. The reaction temperature and stirring speed were held constant at 65 °C and 500 rpm respectively. Another set of transesterification experiments were performed using various dosages of Tetramethylammonium bromide (TMAB: 0.2-1.0 gram) to study the effect of TMAB on the transesterification process.

After completion of the reaction (90 min), the batch was poured into the separating funnel and left for 24h for phase separation by gravity settling. On cooling and separation, the

formation of two layers (top: ester and bottom: glycerin) was observed as shown in Figure 2.3. Glycerin formed was separated from the ester layer and the ester layer was further subjected to purification.



**Figure 2.3:-** Separation of biodiesel and glycerin as separate layers.

#### **2.1.4 Ester purification**

The ester layer was subjected to remove the catalyst (KOH/NaOH/TMAB) and excess methanol. The catalyst present in the ester layer was removed by adding a small amount of glacial acetic acid to neutralize the ester followed by washing with hot distilled water (at 60 °C) as shown in Figure 2.4.



**Figure 2.4:-** Purification of biodiesel layer.

Then the obtained pure ester was heated at 120 °C for 10 minutes to remove any moisture present and the samples and thereafter stored for analysis using a gas chromatograph (GC).

### **2.1.5 Analysis of biodiesel samples**

The GC analysis of biodiesel was carried out following the method of ASTM D6584-08 which require a five-level calibration curve at five different known amounts of standards [158]. The internal standards (IS) like butanetriol (IS1) for glycerin identification and tricaprin (IS2) along with the calibration standards like monoolein, diolein and triolein were used for individual glycerides quantification.

Before analysis, derivatization of the standard and samples were carried out using MSTFA. The derivatization reaction involves the replacement of active hydrogen of the hydroxyl group by the trimethylsilyl-group. Usually, samples and standards having molecules like monoglycerides (MG), diglycerides (DG), triglycerides (TG), and glycerin are derivatized to reduce their polarity and improve the thermal stability of these molecules. After derivatization, the hexane was added to each vial containing samples and standards, and the vial was capped and shaken vigorously. A 1 µL of the derivatized sample from vial was injected through the injector of a gas chromatograph equipped with a flame ionization detector (GC-FID). The Perkin Elmer GC-FID (model: Clarus-580) and the Zebron capillary column (30m x 0.25 mm x 0.25 µm) was used for analysis. Helium was used as a carrier gas with the flow of H<sub>2</sub> and zero-air maintained at 45 mL/ min and 450 mL/min respectively.

The oven of GC was programmed as per the following conditions:

Oven program initial temperature was maintained at 50 °C with a first hold time of 1 minute against ramp-1 at 15 °C/min. Then the temperature was increased to 180 °C with the second hold time of zero min against ramp-2 at 7 °C/min. Further, the temperature was set to increase up to 230 °C with a third hold time of zero min, against ramp-3 at 10 °C/min.

Finally, the oven program temperature was set at 370 °C with a hold time of 5 min and allowed for equilibrating.

Each analyte was identified using their retention times (in minutes) of reference standards and are given according to their appearance of a peak in ascending order of the chromatogram as follows:

Glycerin (5.379); Butanetriol (6.259); Total monoglycerides (17.872); Tricaprin (19.903); Diglyceride (21.653); Triglyceride (25.013).

A calibration curve was generated to identify the unknown amount of analyte in the produced biodiesel. Reference standards at five different amounts are taken to ensure a linear relationship between FID response (Area) and the weight percentage of the analyte. The regression values ( $R^2$ ) obtained for the calibration plots are 0.9963 for total monoglycerides, 0.9991 for total diglycerides, 0.9963 for total triglycerides and 0.9991 for glycerin. The calibration curve for each analyte demonstrated a good fit with an  $R^2$  value greater than 0.99. The total chrome workstation software was used to find the chromatograph area generated in the analysis. The experiments were replicated four times and the average yield of the biodiesel was calculated using Equation 2.1 [86,159].

$$Yield, \% = \frac{FAME\ output\ (weight)}{Oil\ input\ (weight)} \quad 2.1$$

The kinematic viscosity, density and flash point are the major criteria that define the suitability of biodiesel in internal combustion engines. Also, cloud point, pour point and cold filter plugging point is the cold temperature properties of biodiesel which plays major defining criteria for cold temperature operation of biodiesel. Therefore, the obtained biodiesel was analyzed for various properties using standard methods such as kinematic viscosity (Saybolt viscometer), density (ASTM D4052), flash point (ASTM D93: closed cup), cloud point (ASTM D2500), pour point (ASTM D97) and cold filter plugging point (ASTM

D6371) [160,161]. All these tests were carried out in triplicate and average values were reported.

## 2.2 Results and Discussions

### 2.2.1 Composition of feed oil

Estimating the composition of feed oil is very important as the biodiesel fuel properties are influenced by the composition and structure of the FAME [162–164]. The composition of the waste vegetable oil used in the present study was given in Table 2.1 which contains a total of 49.531 wt. % of saturated fatty acids.

**Table 2.1:-** Fatty Acid Composition of Waste Vegetable Oil

S. no.	Fatty Acid	% mass
1	Caprylic (C8:0)	0.024
2	Capric (C10:0)-	0.016
3	Lauric (C12:0)-	0.216
4	Myristic (C14:0)-	0.794
5	Palmitic (C16:0)-	44.1
6	Palmitoleic (C16:1)	0.208
7	Stearic (C18:0)-	4.121
8	Oleic (C18:1)-	39
9	Linoleic (C18:2)-	10.52
10	Linolenic (C18:3)-	0.132
11	Arachidic (C20:0)-	0.146
12	Behenic (C22:0)-	0.060
13	Lignoceric (C24:0)-	0.054
14	Others	0.61

Therefore, the biodiesel produced from this oil will have high oxidation stability due to the presence of a high amount of saturated fatty acids which offers resistance to auto-oxidation [165]. The WVO has the acid value of 1.8 mg KOH/g oil, the moisture content of 2.3 wt. % (from Dean and Stark), a specific gravity of 0.923 and viscosity of 38.7 c.St. The viscosity of waste vegetable oil is very high and needs to be lowered in order to get a viscosity in the range of diesel fuels used in the internal combustion engines. As the present feedstock contains <3 wt. % FFA, it is suitable to produce the biodiesel directly using transesterification.

### 2.2.2 Effect of reaction parameters on biodiesel yield

In accordance with Figure 2.5, increasing the KOH loading from 0.25 to 0.5 wt. % increases the yield from 95.32 to ~99% in the case of 9:1 oil to methanol molar ratio. However, an increase in the catalyst loading beyond 0.5 wt. % results in the gradual decline in the biodiesel yield.

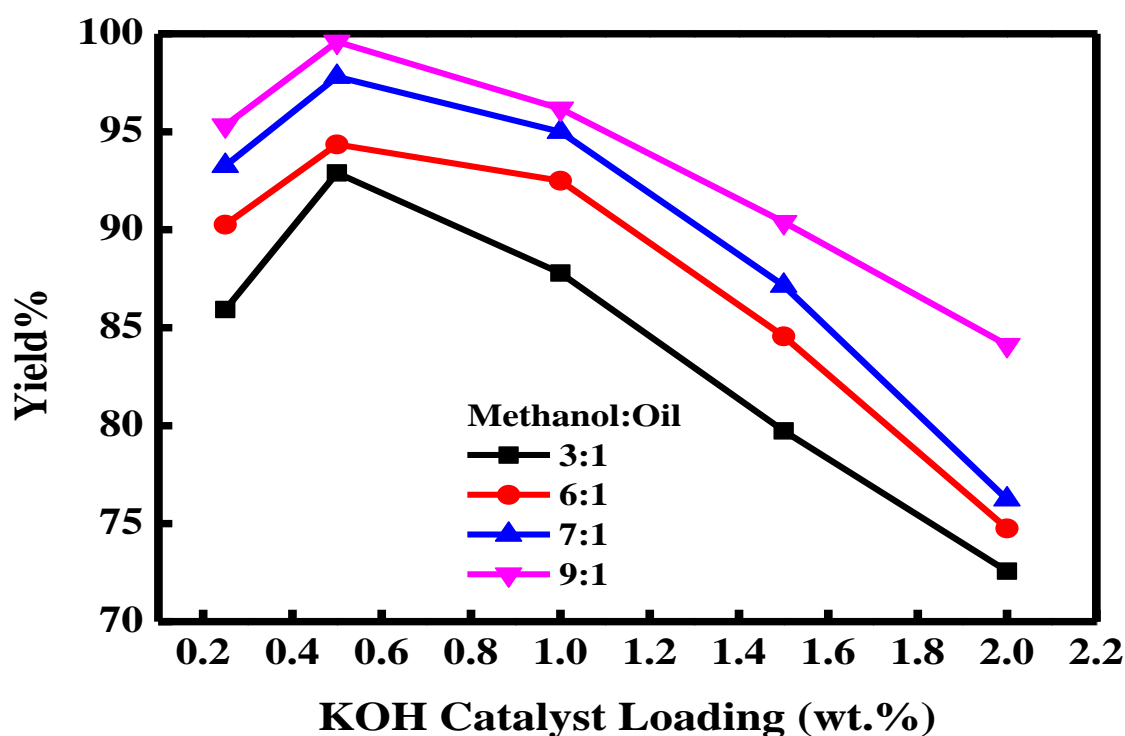


**Figure 2.5:-** Effect of catalyst loading on yield at various molar ratios of methanol to oil.

Similarly, in the case of NaOH, the maximum yield of ~99% was observed at NaOH loading of 1 wt. % and beyond 1 wt. % NaOH loading the yield is declining as shown in Figure 2.6. The decrease in yield can be ascribed to the formation of potassium or sodium soaps utilizing the excess amount of alkali towards saponification [159,166].

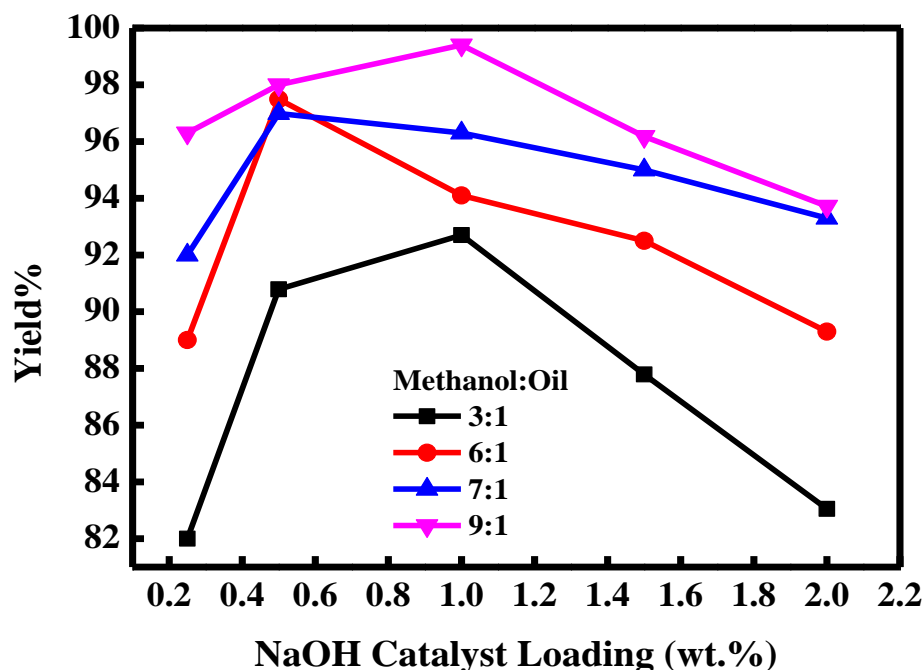


**Figure 2.6:-** Effect of catalyst loading on yield at various molar ratios of methanol to oil.

The effect of methanol to oil molar ratio on the biodiesel yield was studied in the range of 3:1 to 9:1. It was found that increasing the molar ratio up to 9:1 favorably increases the yield as shown in Figure 2.7. Since oil is the limiting reactant, providing the methanol in excess shifts the equilibrium towards higher product formation which increases the percentage yield. Further increasing the ratio beyond 9:1 there was a considerable decrease in the yield. It is due to the fact that the presence of excessive methanol dilutes the concentration of the catalyst in the total reaction mixture and decreasing the probability of contact between reactants and the catalyst. Similar trends were observed in the case of Leung & Guo [167] and Zhang et.al. [156]. Therefore, the optimum methanol to oil molar ratio was found to be 9:1.

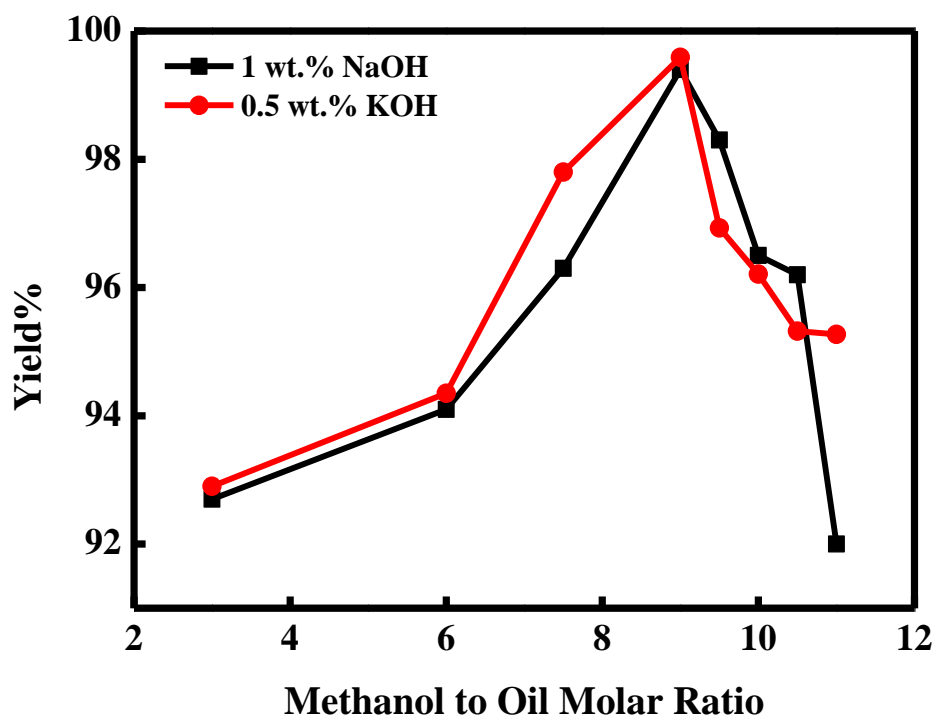


**Figure 2.7:-** Effect of methanol to oil molar ratio on yield.

### 2.2.3 Effect of methanol to oil molar ratio on biodiesel properties

On one hand, the higher viscosity of the fuel can result in poor vaporization, poor fuel atomization, and blocks the filter during the flow of fuel from fuel storage tank to the combustion chamber of the engine. On the other hand, lower viscosity of fuels may results in wear in injection pump and pump leakages. Therefore, the kinematic viscosity of the synthesized biodiesel has to comply with the standards. Biodiesel kinematic viscosity was found to vary with a molar ratio of methanol to oil as well as with the type of catalyst used. It was observed that, increasing the molar ratio of methanol to oil from 3:1 to 9:1 decreases the viscosity from 4.5 to 3.8 c.St in the case of KOH and from 4.8 to 4.2 c.St in the case of NaOH catalyst, respectively. The viscosity of the obtained biodiesel in the range of 3.4-4.5 c.St is close to the viscosity of mineral diesel (2-4.5 c.St) which indicates that it can be used in the diesel engine without modifications.

Flashpoint is the important property of fuel, describing the minimum temperature at which

the fuel catches the fire. According to safety norms, it is mandatory to specify the flashpoint for every fuel. Flashpoint was found to vary considerably with methanol to oil molar ratio from 173 °C (3:1 methanol/oil) to 160 °C (9:1 methanol/oil) for KOH catalyzed samples and from 180 °C (3:1 methanol/oil) to 174 °C (9:1 methanol/oil) for NaOH catalyzed samples. It was observed that increasing the molar ratio of methanol to oil, decreases the flash point of the produced biodiesel. The obtained biodiesel flash point was found within the standards and also higher than the flash point of the mineral diesel. Therefore, the transportation and storage of biodiesel are safer than the petro-diesel. The obtained flashpoints are also consistent with the flashpoints of other biodiesels derived from palm and Pongamia oils [33].

The cold flow properties of the biodiesel such as cloud point, pour point and cold filter plugging point was evaluated. The cloud point (CP) of the obtained fuel represents the temperature at which the wax formation takes place (hazy cloud as an indicator) and can clog the fuel filter as well as flow lines. The pour point (PP) of the fuel indicates the temperature below which the liquid ceases its flow characteristics. The cold filter plugging point (CFPP) is the temperature at which the components of the fuel form crystals or gels. The CP, PP, and CFPP of obtained biodiesel samples were found to be  $9.2 \pm 1$ ,  $7.6 \pm 3$  °C and  $4.2 \pm 5$  °C, respectively and showed the negligible change with a change in methanol to oil molar ratio. The obtained biodiesel may work below the temperature of 9.2 °C (CP) but it definitely cannot work below 7.6 °C (PP). These values are consistent with the available literature [33].

#### **2.2.4 Effect of the TMAB addition on biodiesel production**

Tetramethylammonium bromide is a hygroscopic salt which is widely used as the phase transfer catalyst [168]. In the system consisting of two mutually-insoluble phases, either liquid-liquid or solid-liquid the distinct attribute of the phase-transfer catalytic process is that it forms an intermediate complex. This intermediate complex is mostly soluble in organic compounds to transfer inorganic ions into the organic phase. Such techniques are notably

useful in base-catalyzed reactions and nucleophilic displacements. Industrial processes widely adopt these techniques due to their faster, cleaner reactions and greatly simplified ramp-up which do not necessitate the strict anhydrous conditions. Since, transesterification is a base-catalyzed process and is also associated with a nucleophilic attack mechanism, using the TMAB can enhance the process and dampens the technical disadvantages associated with the conventional biodiesel production process. Therefore, the effect of TMAB addition on biodiesel yield, the molar ratio of methanol to oil requirement and washability characteristics of crude biodiesel was studied.

The effect of TMAB addition to conventional transesterification process at the optimized catalyst loading of 1 wt. % NaOH and 0.5 wt. % KOH was studied. It was observed that there was a very little increase in the biodiesel yield and a substantial decrease in the methanol requirement when TMAB was added to the reaction as shown in Figures 2.8 and 2.9. The values of yield at 7.5:1 and 9:1 molar ratios of methanol to oil are almost similar suggesting methanol to oil molar ratio of 7.5:1 is enough when TMAB was incorporated in the biodiesel production process. Similar observations were also revealed in the available literature [60,61]. In the conventional production of biodiesel, the base catalyst (B) first mixes with methanol to give methoxide ( $\text{CH}_3\text{O}^-$ ) and protonated base ( $\text{BH}^+$ ). Then the methoxide initiates a nucleophilic attack on triglyceride resulting in the formation of FAME. Compared to methoxide, the formed intermediate complex when TMAB was used will have higher solubility with the vegetable oil. This might be the reason behind the decrease in methanol requirement. Also, FAME formation is the organic synthesis reactions, the use of TMAB might dissolve each ionic and valence species, thereby effectively increase the basic strength and nucleophilicity of the anions. This can be postulated by the fact that decreasing ion-pairing and removing the associating impact of a hydroxylic solvent naturally increases the base strength and nucleophilicity of anions [169]. A similar phenomenon can also be

observed using dipolar, aprotic solvents like dimethyl sulfoxide (DMSO) [170] or dimethylformamide (DMF) [47]. However, these solvents are not readily separable from the reaction product [58]. Their separation might require a lengthy workup like;

- (i) Washing with a larger volume of water.
- (ii) Distillation of the solvent followed by product filtration, centrifugation, and further washing.
- (iii) Multiple extractions with a unique water-immiscible solvent, washing with water followed by evaporation of the extraction solvent.

Such procedures are time-consuming, volume-inefficient and generate large volumes of effluent containing solvent mixtures that are tough to recycle. Therefore, the TMAB being a phase transfer catalyst which poses a distinct mechanism and can catalyze the reactions in a simpler approach can be used to enhance the conventional transesterification process. The proposed mechanism when TMAB was used as a phase transfer catalyst is shown in Figure 2.10.

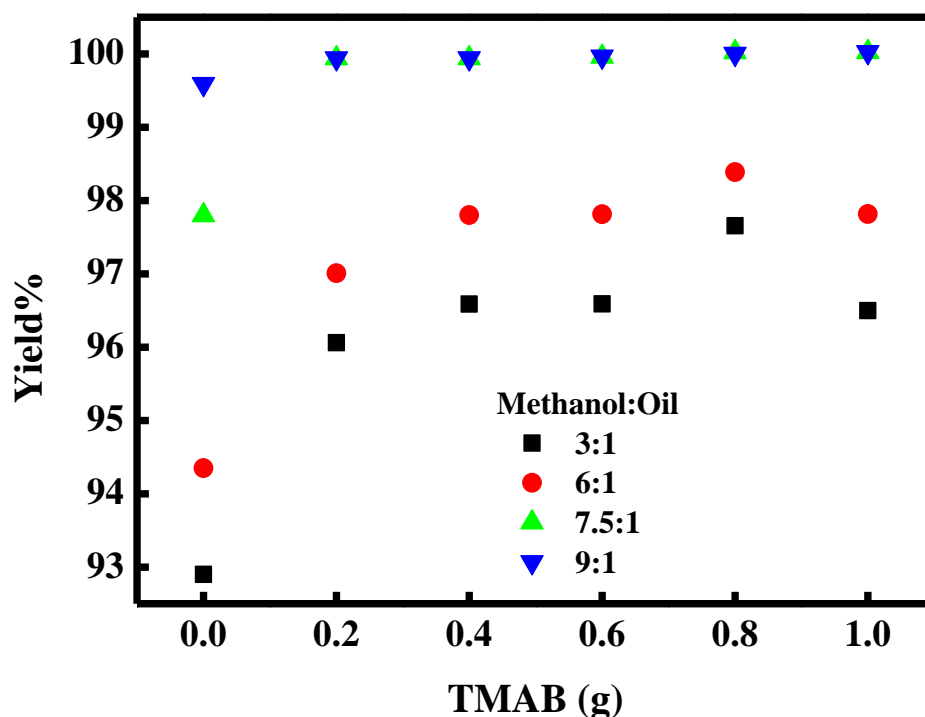


**Figure 2.8:-** Effect of TMAB on biodiesel yield at various molar ratios of oil to methanol.

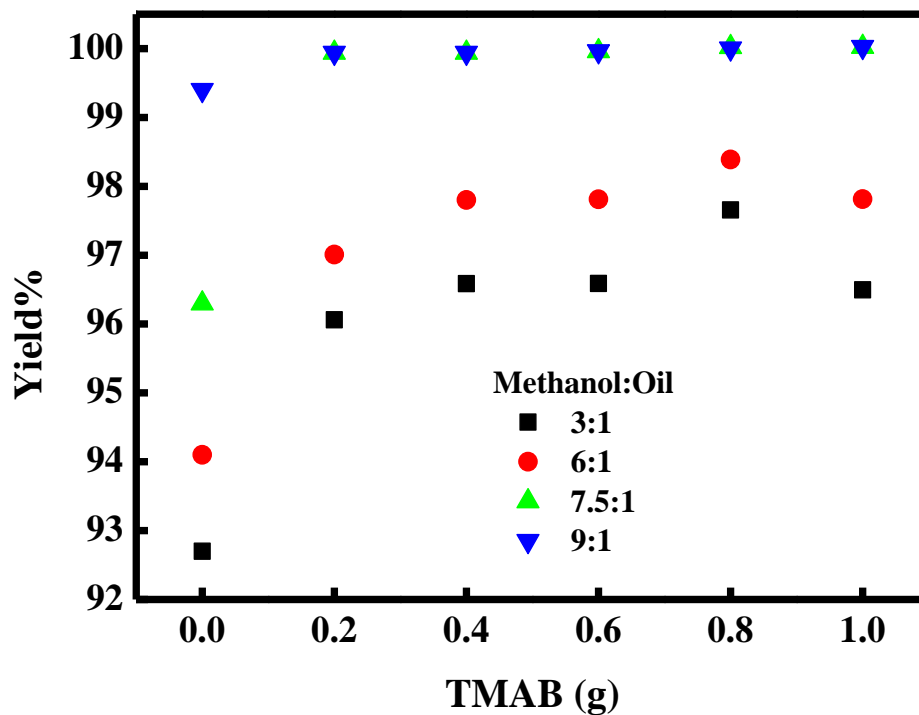


Figure 2.9:- Effect of TMAB on biodiesel yield at various molar ratios of oil to methanol.

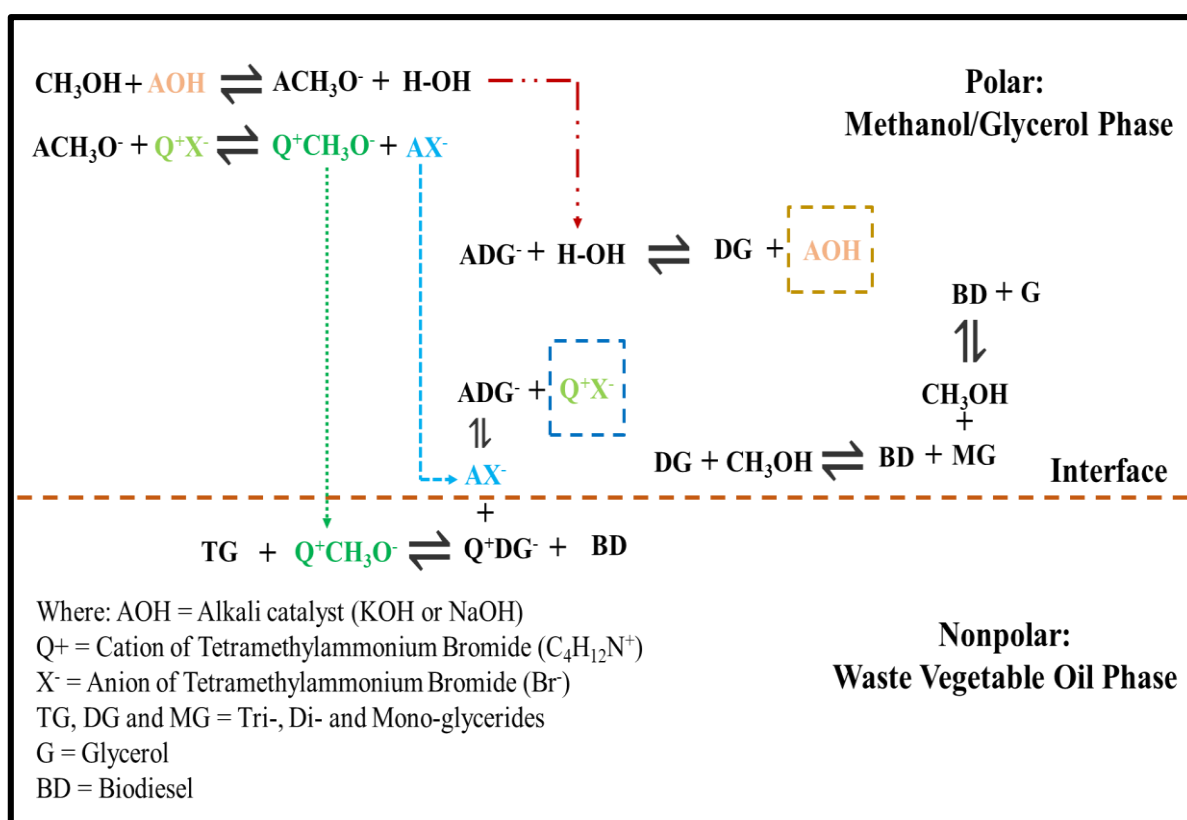
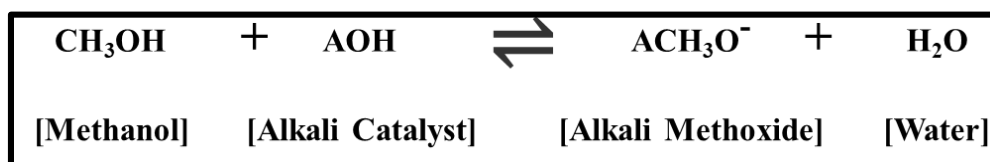


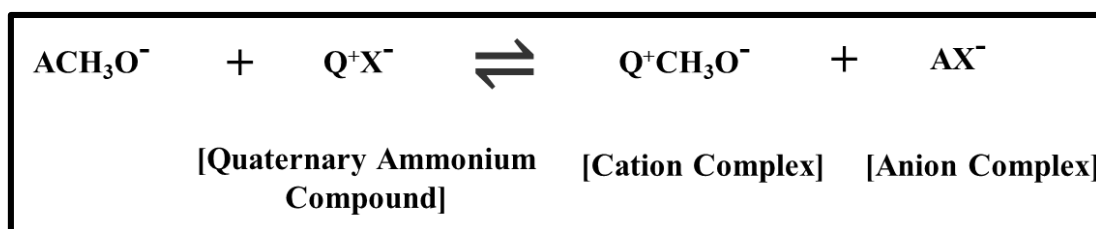
Figure 2.10:- Mechanism of phase transfer catalysis.

The quaternary ammonium salt (TMAB) is composed of cation (which is usually referred to as  $Q^+ = (CH_3)_4N^+$ ) and anion (which is usually referred to as  $X^- = Br^-$ ). First, methanol combines with alkali catalyst to dissociate into alkali methoxide and water (A). Then the alkali methoxide ( $ACH_3O^-$ ) complexes with the cation of TMAB as shown in (B).

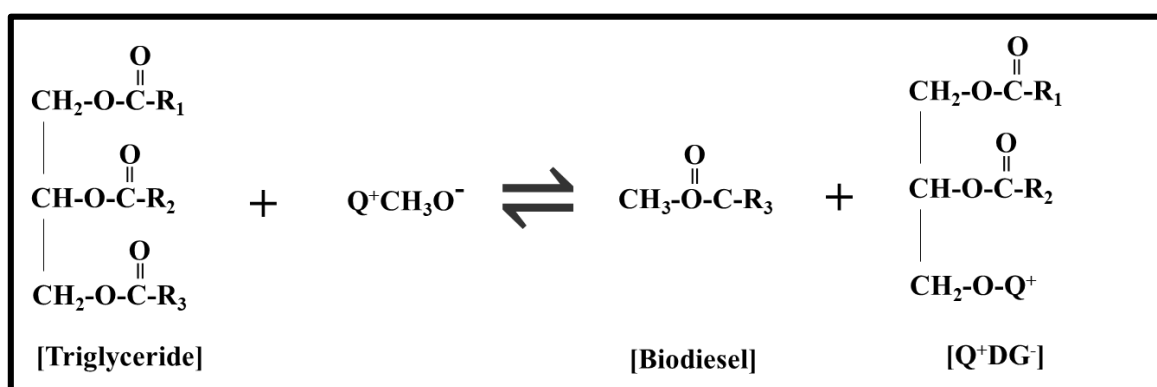
**(A) Formation of alkali-methoxide**



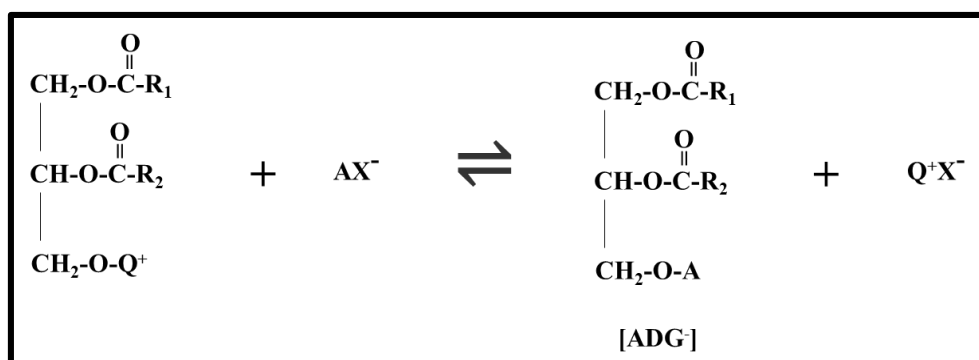
**(B) Formation of cation and alkali oxide complex**



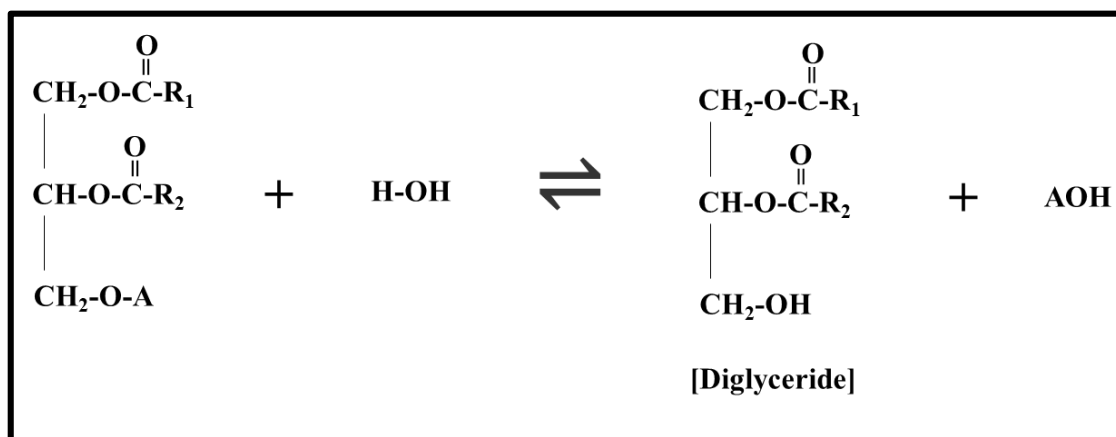
**(C) Nucleophilic attack of cation-complex on triglyceride to give biodiesel**



**(D) Realignment of quaternary ammonium compound**

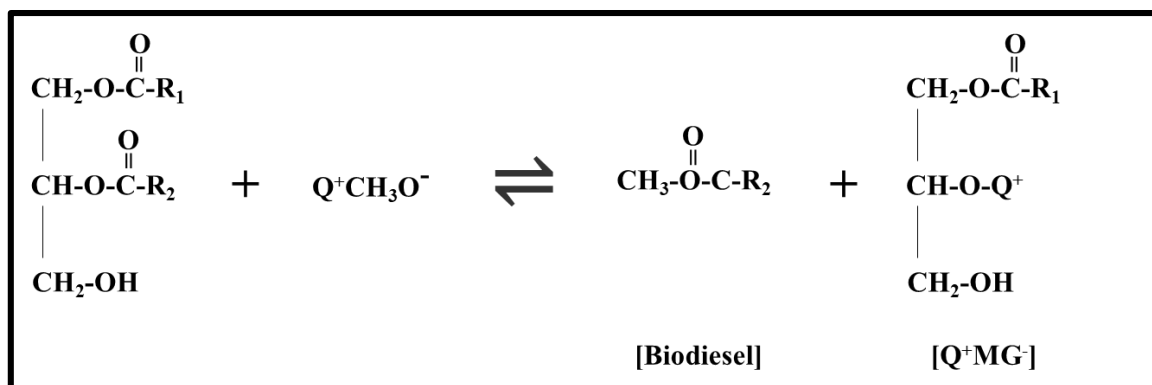


**(E) Realignment of an alkali catalyst**

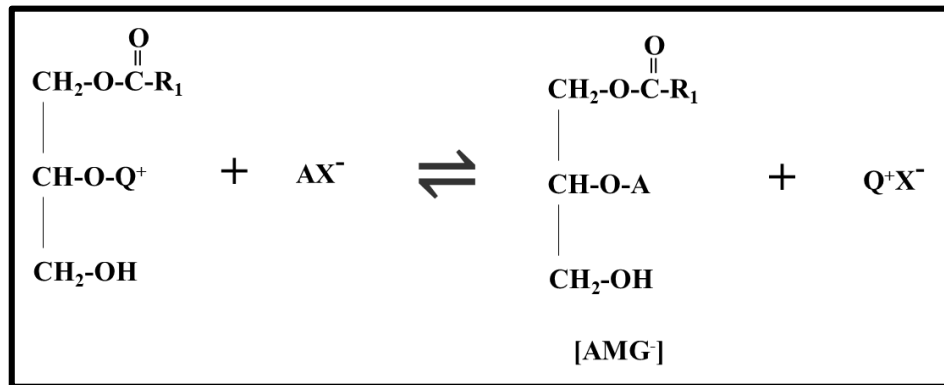


The formed cation-complex dissolves more easily in the oil phase and initiates a nucleophilic attack on triglyceride to form biodiesel and a diglyceride complex with the cation of quaternary ammonium compound as given in (C). In subsequent steps, the complex of the anion with diglyceride ( $\text{Q}^+\text{DG}^-$ ) realigns to quaternary ammonium compound and alkali catalyst with a release of diglyceride molecule as shown in (D) and (E). This completes one cycle of the phase transfer catalysis to produce one molecule of biodiesel and diglyceride each. Similarly, the cycle repeats for diglyceride and monoglyceride to produce biodiesel and glycerol as shown from (F) to (K). In a phase transfer catalysis, the ability of PTC compound to form a complex is a key which enhances the reaction between reactants in two immiscible phases. Consequently, the transesterification assisted by TMAB completes with a little higher yield of biodiesel and at lower methanol to oil molar ratio.

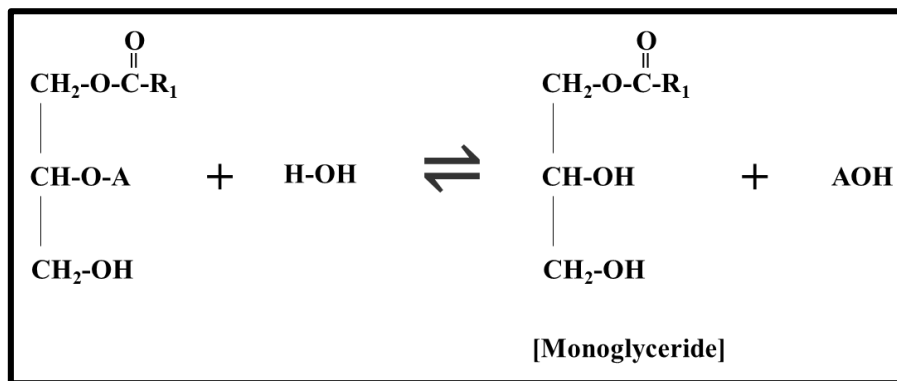
**(F) Nucleophilic attack of cation complex on diglyceride to give biodiesel**



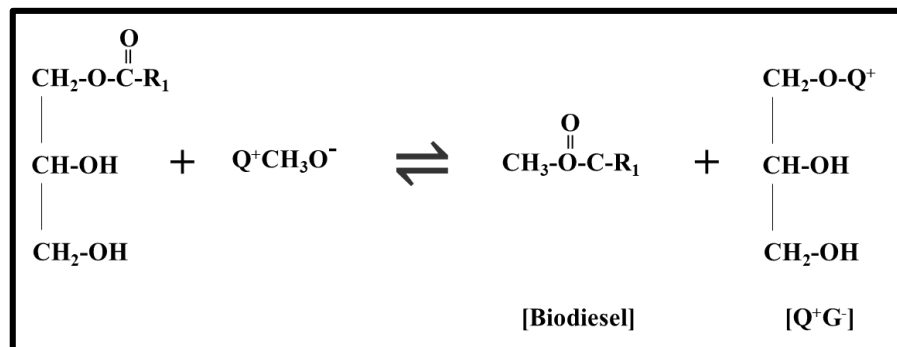
**(G) Realignment of quaternary ammonium compound**



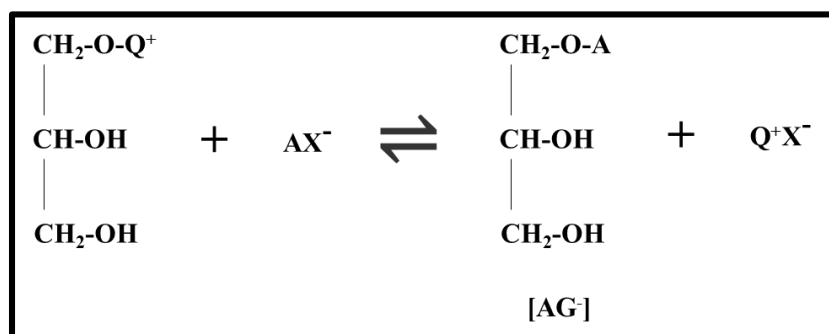
**(H) Realignment of an alkali catalyst**



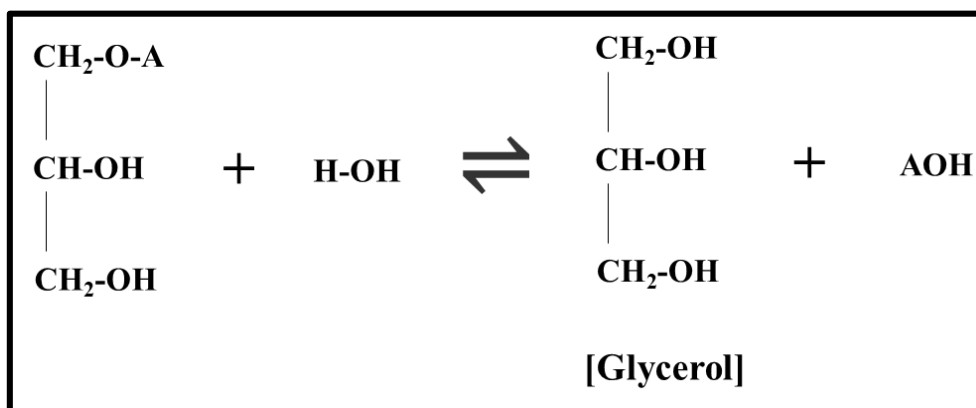
**(I) Nucleophilic attack of cation complex on monoglyceride to give biodiesel**



**(J) Realignment of quaternary ammonium compound**



**(K) Realignment of an alkali catalyst**



In accordance with Figure 2.11, it was observed that during washing of biodiesel synthesized in presence of TMAB, a very less amount of water was required (reduced nearly half of the volume). For example, to wash a biodiesel sample synthesized in a conventional route, approximately a 10 L water was required. Whereas, to wash biodiesel sample synthesized in the presence of TMAB, wash water of only 5 L was required.

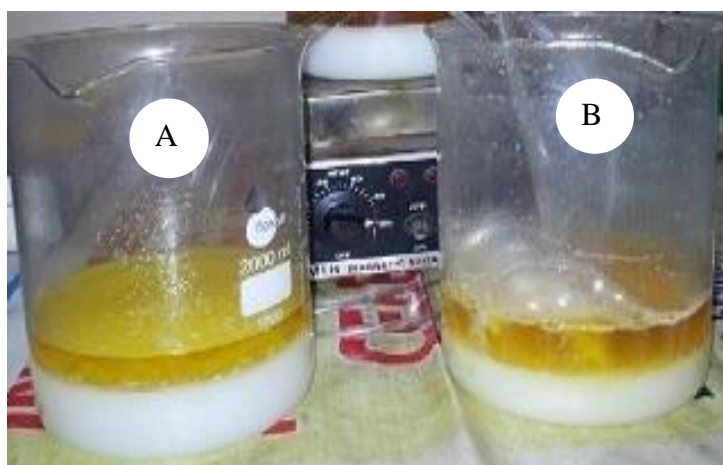


**Figure 2.11:-** Washability of biodiesel (A) without TMAB (B) with TMAB.

Unlike washing the biodiesel synthesized using KOH or NaOH alone (conventional process), washing biodiesel samples (assisted by TMAB) enhanced the overall reaction and also washing. Moreover, there was no disturbance in settling was also observed. The reason behind this positive outcome is due to the fact that TMAB being the hygroscopic quaternary

ammonium salt which can assimilate the water content (including bound) during the reaction. Since alkali-catalyzed transesterification reaction is greatly affected by the presence of water which makes the reaction partially shift towards saponification [68]. Therefore, adding TMAB to the process suppresses and diminishes the soap formation. Diminishing the soap formation can be directly related to the less water requirement for washing. Thus, the crude biodiesel can be handled easily making the overall process relatively more economical than the existing commercial process.

The TMAB used here adds the advantage of easy separation of the products rather than lengthy workup as in the case of DMSO or DMF solvents. It also offers an advantage of comparatively less expensive than most dipolar aprotic solvents [58,82,89]. The use of TMAB is recommended in order to make the process economically and technically feasible. Therefore, the water content prone-conventional process can be made simple by just conducting the reaction in the presence of TMAB. The work carried out by Qi et.al. [171], using SO<sub>3</sub>H-functionalized quaternary ammonium ionic liquid as a catalyst to synthesize biodiesel from waste cooking oil reported 95% of biodiesel yield in 1h. They reported the optimum reaction conditions as methanol/oil/ionic liquid molar ratios as 10/1/0.063 and temperature = 120 °C. Since the boiling point of methanol is ~65 °C, operating the transesterification reaction above the boiling point of methanol is a difficult task. The TMAB used in the current work is a quaternary ammonium salt comparable to their reported ionic liquid gives a yield greater than 95% in 1.5 h under mild reaction conditions of 65 °C, 7.5:1 molar ratio of methanol to oil and 0.2 g TMAB. Therefore, use of TMAB offers the triple facet benefits like economical (less expensive), technically feasible (lesser water requirement for washing) and environmentally viable (lesser water effluent).

The glyceride compositions and properties of KOH and NaOH catalyzed biodiesel samples are presented in Tables 2.2 and 2.3, respectively. When biodiesel samples assisted by

TMAB was analyzed for flash and fire points, it was observed that there was a considerable effect of TMAB on these properties. The lower flash and fire point of the biodiesel was observed compared to the samples synthesized using a conventional process. However, these values are within the limits set for biodiesel standards. The CP, PP, and CFPP of obtained biodiesel samples were found to be  $7.2 \pm 1$  °C,  $4.8 \pm 3$  °C and  $2.9 \pm 5$  °C and showed the negligible change with a change in TMAB dosage. There was a considerable decrease in these temperatures (CP, PP, and CFPP) compared to the biodiesel samples synthesized by the conventional process. This creates an opportunity to produce biodiesel with enhanced cold flow properties using a booster, TMAB (for cold climate) and high cold flow properties without a booster (for hot climate). Therefore, the produced biodiesel may call as usage specific biodiesel with and without a catalytic booster. Although ASTM does not specify the value of cloud point required for the biodiesel, it is customer-friendly to specify the cold flow properties at which fuel form gels. Otherwise, there will be no idea where (at what temperature) the fuel will cease to flow or gets clogged and fail in the engine. In accordance with Table 2.4, the biodiesel synthesized in the current work complied with the standards set by ASTM D6751-12.

**Table 2.2:-** Composition and Properties of Biodiesel Samples Catalyzed by KOH

Methanol: Oil	TMAB (g)	Impurities composition (% mass)				Properties	
		TG	DG	MG	G	Flash point (°C)	Fire point (°C)
3:1	0	0.546	0.583	1.452	0.045	175	187
	0.2	0.543	0.589	1.456	0.045	175	187
	0.4	0.546	0.589	1.454	0.036	176	186
	0.6	0.545	0.586	1.454	0.029	176	186
	0.8	0.545	0.584	1.452	0.021	175	186
	1.0	0.545	0.584	1.452	0	175	186
6:1	0	0.459	0.428	1.256	0.046	175	186
	0.2	0.459	0.425	1.248	0.045	159	163
	0.4	0.445	0.425	1.248	0.041	159	164
	0.6	0.445	0.425	1.246	0.039	158	165
	0.8	0.446	0.425	1.246	0.026	159	165
	1.0	0.445	0.425	1.246	0	158	165

7.5:1	0	0.021	0.022	0.196	0.048	177	191
	0.2	0.015	0.025	0.012	0.048	129	137
	0.4	0.022	0.020	0.007	0.039	129	137
	0.6	0.019	0.032	0.013	0.038	129	137
	0.8	0.107	0.035	0.022	0.024	128	136
	1.0	0.073	0.020	0.004	0	128	136
9:1	0	0.011	0.014	0.177	0.052	179	194
	0.2	0.015	0.026	0.012	0.051	129	136
	0.4	0.025	0.020	0.007	0.049	129	136
	0.6	0.020	0.032	0.013	0.025	129	136
	0.8	0.110	0.036	0.022	0.013	129	136
	1.0	0.071	0.023	0.004	0	129	136

**Table 2.3:-** Composition and Properties of Biodiesel Samples Catalyzed by KOH

Methanol: Oil	TMAB (g)	Impurities composition (% mass)				Properties		
		TG	DG	MG	G	Flash point (°C)	Fire point (°C)	Density (g/cc)
7.5:1	0	0.0490	0.0562	0.2545	0.0293	175	187	0.8630
8:1	0	0.0372	0.0442	0.2125	0.0291	175	186	0.8628
8.5:1	0	0.0212	0.0225	0.1967	0.0290	177	191	0.8610
9:1	0	0.0115	0.0145	0.1776	0.0290	179	194	0.8600
7.5:1	0.2	0.0132	0.0250	0.0124	0.0139	129	137	0.8608
	0.4	0.0121	0.0103	0.0073	0	129	137	0.8608
	0.6	0.0121	0.0101	0.0037	0	129	137	0.8608
	0.8	0.0103	0.004	0.0049	0	128	136	0.8708
	1.0	0.1906	0.0201	0.1793	0	128	136	0.8708

**Table 2.4:-** Comparison of Synthesized Biodiesel with Standards

<b>S. no.</b>	<b>Properties</b>	<b>Biodiesel Standard [68]</b>	<b>Biodiesel (with TMAB)</b>	<b>Biodiesel (without TMAB)</b>
1	Kinematic viscosity at 40°C (c.St)	1.9 - 6.0	3.5	3.8
2	Flash point, (°C)	130	129	175
3	Fire point, (°C)	-	137	186
4	Acid value (mg KOH/g)	0.5 (max)	0.112	0.112
5	Density (g/cc)	0.860-0.900	0.8608	0.8628
6	Distillation Temperature (°C)	360 (max)	300	320
7	Free glycerin (% mass)	0.020	0	0.052

### Esterification of Free Fatty Acids: Experiments, Kinetic Modeling, Simulation and Optimization

#### 3.1 Experimental Details

##### 3.1.1 Materials used

Karanja oil of physicochemical properties given in Table-3.1 was purchased from Suyash herbs exports Pvt. Ltd. Gujarat, India. The entire analytical grade chemicals used in this work such as methanol, ethanol, potassium hydroxide pellets, and phenolphthalein powder were purchased from Sigma-Aldrich (India) Pvt. Ltd and used as obtained. Argon gas cylinder was purchased from sigma gases and services, New Delhi.

##### 3.1.2 Sample analysis

Acid value and FFA content of the Karanja oil were determined using the titrimetric method and estimated using Equations 3.1 and 3.2 as given below [172].

$$\text{Acid value} = \frac{56.1 \times V \times N}{W} \quad 3.1$$

$$\text{FFA as oleic acid} = \frac{28.2 \times V \times N}{W} \quad 3.2$$

Where,

$V$  is the volume of standard potassium hydroxide used, ml;

$N$  is the normality of standard potassium hydroxide solution;

$W$  is the weight of the sample, gram.

**Table 3.1:- Physico-Chemical Properties of Karanja Oil**

<b>Properties</b>		<b>Value</b>
Moisture (Dean and Stark method)		0.05%
Density @ 25 °C		0.93 g/cc
Viscosity @ 40 °C		40.07 c.St.
Color in inch cell on Lovibond scale		34.90
Impurities (insoluble in hexane)		0.43%
Acid value		62.80 mg KOH/g
<b>Fatty acid composition (wt. %)</b>	Palmitic acid	4.20
	Stearic acid	2.90
	Oleic acid	66.80
	Linoleic acid	17.60
	Arachidic acid	3.80
	Behenic acid	4.70

### 3.1.3 Experimental setup

The esterification reaction was conducted in an experimental setup as shown in Figure 3.1. The batch reactor having a capacity of 25 ml was made up of stainless steel and placed inside a jacketed vessel. The reactor was fitted with the pressure gauge for measuring the reactor pressure. A magnetic stirrer with the heater was used as a primary source for heating and mechanical agitation. There was a provision for the inert gas inlet to the reactor for maintaining the constant pressure. Also, the constant temperature inside the reactor was ensured using a chiller.

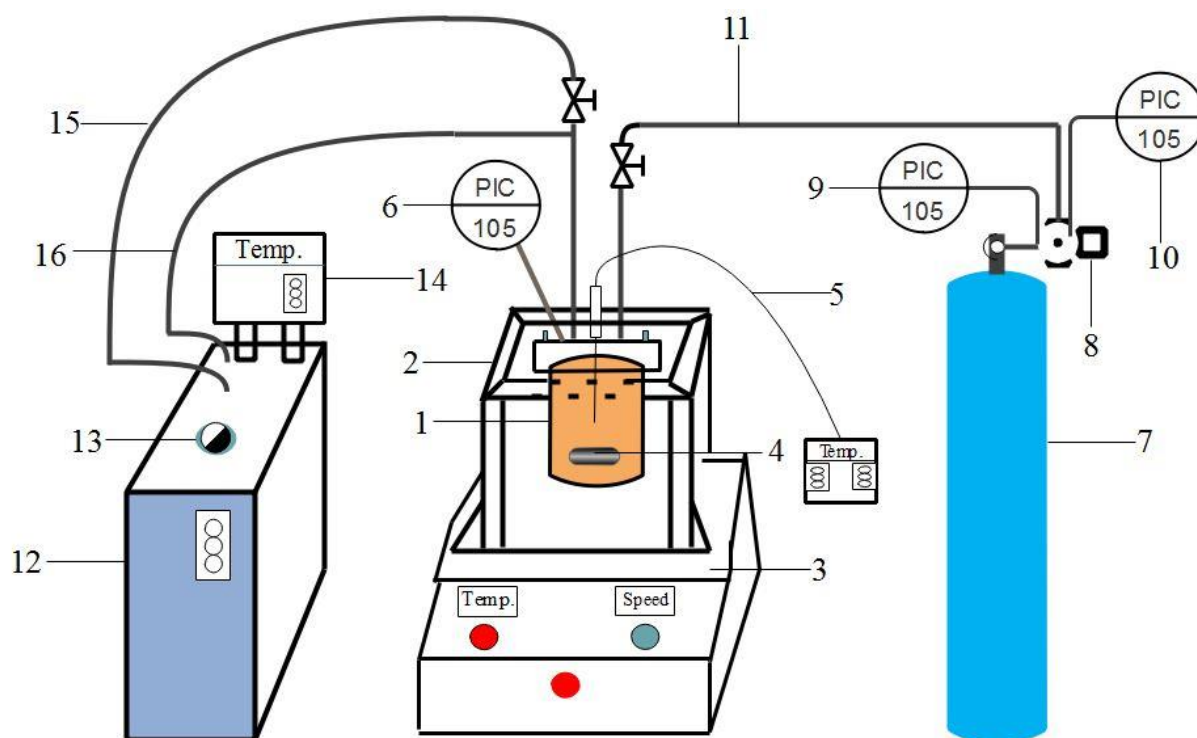


**Figure 3.1:-** Schematic of the experimental setup.

### **Nomenclature:**

1- Reactor; 2- Outer shell/Jacket to reactor; 3- Magnetic stirrer with heater; 4- Magnetic bar; 5-Digital thermometer; 6, 9, 10- Pressure gauges; 7- Argon gas cylinder; 8-Pressure regulator; 11-Gas inlet pipe to the reactor; 12-Chiller; 13-Chiller opening/knob for coolant feed; 14-Chilling temperature indicator or set point panel; 15-Coolant inlet pipe to the reactor; 16-Coolant outlet pipe to the reactor.

### **3.1.4 Experimental procedure**

The Karanja oil was washed thoroughly with hot deionized water (~80 °C) to remove soluble impurities present in the oil and then it was treated with silica gel to remove the water content. Further, the oil was heated at 105 °C for 1 h to remove the trace amount of water. Therefore, the water content present in the oil was assumed as negligible. In a typical run, the reactor was charged with ~4.34 g Karanja oil and ~17.36 ml methanol. These reactant

amounts were selected so as to meet the required criteria of volumetric filling fraction (ratio of the volume of reactants charged to the total reactor volume,  $f$ ). It controls the phases that co-exist at reaction conditions. Maintaining higher values of  $f$  under subcritical conditions leads to liquid phase reactions when the reaction is to be performed under inevitable subcritical conditions. Therefore, we have selected the values of  $f$  such that the reactants remain in the homogeneous phase.

After charging the reactants into the reactor, the top of the reactor was covered and fastened using bolts. It was then placed into the jacketed vessel and the whole assembly was kept on a magnetic stirrer equipped with a heater. The reaction temperature and agitation speed were varied with the help of magnetic stirrer and argon gas was supplied to maintain the desired pressure inside the reactor. The variables affecting the reaction such as agitation speed, temperature, reaction time, oil to methanol ratio were studied. The reaction was stopped at various time intervals and the reaction mass was analyzed to estimate the acid value. The conversion of the FFA was calculated using Equation 3.3 [96,140,173];

$$\text{Conversion (\%)} = \frac{(\text{Acid Value})_{t=0} - (\text{Acid Value})_{t=t}}{(\text{Acid Value})_{t=0}} \times 100 \quad 3.3$$

## 3.2 Results and Discussions

### 3.2.1 Feasibility of reaction at reactor conditions/Phase equilibrium

The reaction conditions employed to study the conversion of FFA are above the boiling point of methanol and also below its critical conditions ( $T_c = 239.35$  °C and  $P_c = 80.8$  bar). Therefore it is usually expected the presence of liquid and vapor phases. To maintain only one phase in the reactor the volumetric filling fraction (ratio of the volume of reactants charged to the total reactor volume,  $f$ ) is varied to study the phases coexisted at the reaction conditions. In addition to experimental runs, we also performed phase equilibrium calculations using Aspen Plus ver.8.6 software. ‘PRMHV2’ method which uses the Peng-

Robinson equation of state (EOS) with modified Huron-Vidal mixing rules were used to estimate thermodynamic properties of the present non-electrolytic system. 'Flash2' block was used to study the phase equilibrium of reactants. The input for the calculations was the composition of feed streams, temperature, and pressure or vapor fraction. This information will provide the result for reactor pressure, a fraction of coexisting phases when multiple phases were present or pressure at which the reactor must be maintained when a single phase is to exist. For instance, at a 1:5 ratio of oil to methanol, 220 °C and  $f = 0.88$  the calculated pressure is 56 bar. Aspen Plus reveals that, at these conditions, most of the reactants are in the liquid phase. Whereas, at a reaction temperature of 220 °C and  $f = 0.65$  the calculated pressure was 10 bar. According to aspen most of the reactants are in the vapor phase at these conditions. In the study carried out by Pinnarat and Savage [28], reported that, at 230 °C and  $f = 0.56$  the calculated pressure was 52 bar observing a single liquid phase, at 250 °C and  $f = 0.26$  the calculated pressure was 52.8 bar observing 50/50 liquid and vapor and at 250 °C with  $f = 0.04$ , mostly vapors are observed using oleic acid and ethanol as esterification reactants. In addition, they concluded that maintaining low and high values of  $f$  leads to gas and liquid phase systems respectively and concluded that supercritical conditions are not at all required to obtain the desirable esterification conversion. To evaluate the reaction progress and kinetics of the reaction, a single phase was ensured by choosing the reactor conditions in such a way that, at low temperatures, the higher volumetric filling fraction was maintained and at high temperatures lower oil to methanol ratios was maintained coveting subcritical conditions. Additionally, optimal agitation was ensured to suppress the heterogeneity of reactant mixture.

### **3.2.2 Effect of agitation speed**

To study the effect of agitation on the esterification reaction, the speed was varied from 500-700 rpm. The agitation speed has a strong influence on the conversion of the reaction as

shown in Figure 3.2. Due to the heterogeneous nature of the reactants (oil and methanol), conversion of FFA was increasing with increase in the agitation speed. It was observed that the conversion of FFA at 500 rpm are much lower than the conversions at 600 rpm. This behavior can be attributed to the fact that there exists mass transfer resistance at lower agitation speeds which becomes negligible at a higher speed of agitation [17]. This fact has been reported by various researchers and showed that the initial phase of the reaction as mass transfer controlled [174-178].

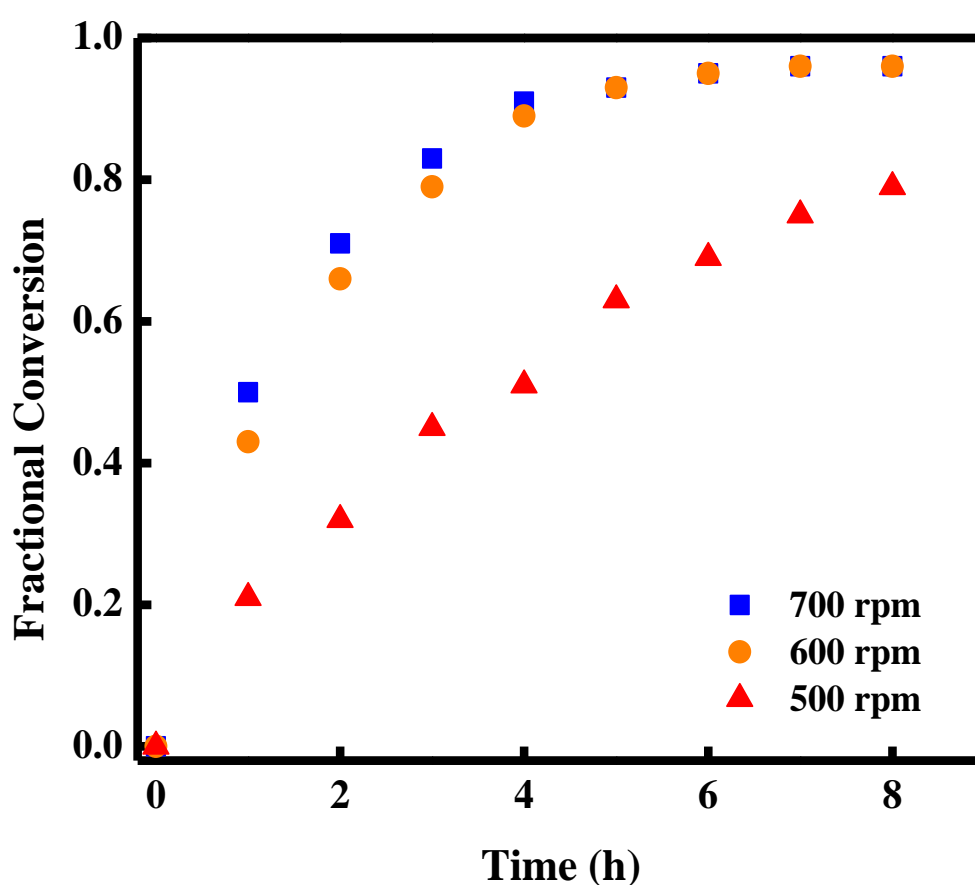


**Figure 3.2:-** Effect of agitation speed on conversion at 220 °C, 10 bar and 1:6 oil to methanol ratio (w/v).

In the mixing of two immiscible liquids such as oil and methanol there exist two distinct phases called dispersed and continuous phases. The main purpose of agitation is to completely incorporate the dispersed phase into the continuous phase by promoting good

contact between the phases so that the mass transfer rate increases by extending interfacial area between them. The speed at which the dispersed phase is completely incorporated into the continuous phase is termed as minimum agitation speed or critical speed [96]. The conversion values become almost equal on further increasing the agitation speed from 600 to 700 rpm. Therefore, 600 rpm was selected as the critical speed of agitation and used for all the experiments.

### 3.2.3 Effect of reaction time and temperature

The present study reveals the increasing trend of FFA conversion with time and reached 43% after 1 h of reaction time as shown in Figure 3.3.

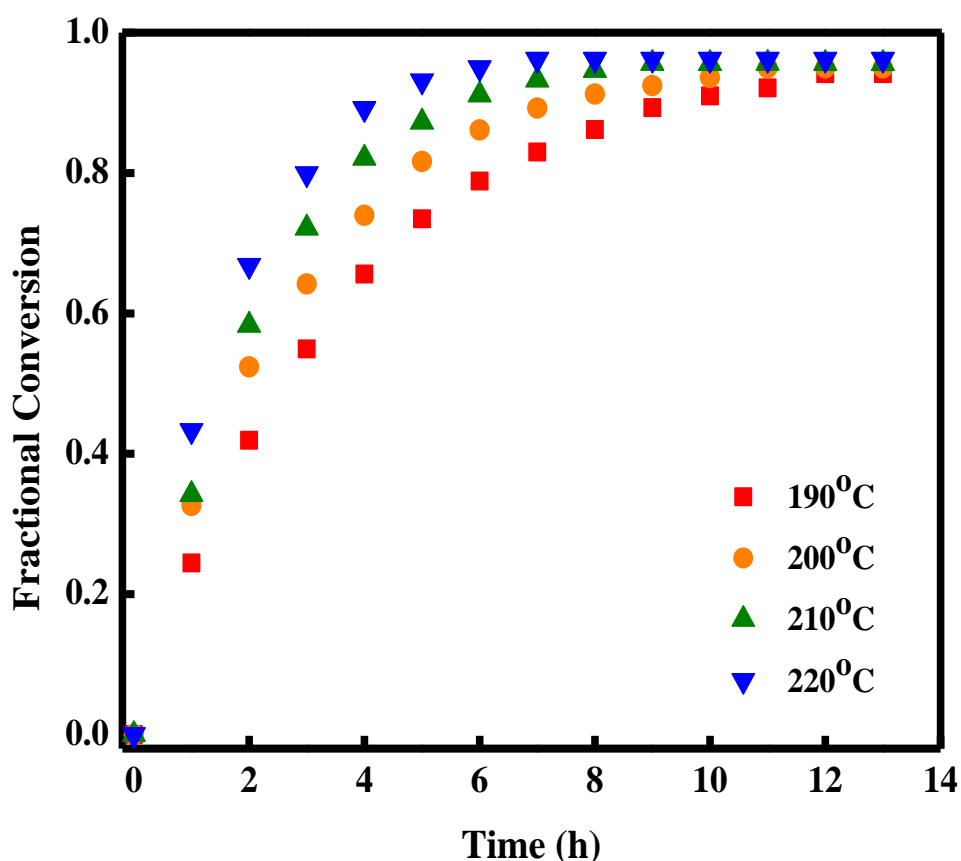


**Figure 3.3:-** Effect of temperature on conversion at 1:6 oil to methanol ratio (w/v).

Maximum conversion of 96% was observed in 7 h at 220 °C and 1:6 ratio of Karanja oil to methanol (w/v). The reaction approached the equilibrium condition after 7 h, therefore, no

change in conversion was observed. Due to the presence of a distinct layer between the oil and methanol, the reaction between them is not the spontaneous one. Therefore, a change in the reaction temperature may affect the reaction rate. To study the effect of temperature, it was varied in the range of 190 to 220 °C. The increase in temperature resulted in the higher conversion values from 82% at 190 °C to 96% at 220 °C as shown in Figure 3.3. This shows the endothermic nature of the reaction. These results are close to the results of 95.1% equilibrium conversion at 190 °C and 1:4 (w/v) Jatropha oil to methanol ratio in 5 h using batch reactor [109] and 99.85% conversion at 290 °C in 3 h reaction time when 2.4 g/min methanol was supplied to esterify 860 g of PFAD in a semi-batch reactor [110].

#### **3.2.4 Effect of oil to methanol (w/v) ratio**

The ratio of oil to methanol is an important parameter in both esterification and transesterification reactions. Esterification of FFA is the reversible reaction and oil to methanol ratio may have a strong influence on the ester formation. Methanol used in excess may help to shift the equilibrium towards product formation. To study its effect, we performed the experiments at three different oil/methanol ratios; 1:4, 1:5 and 1:6 as shown in Figure 3.4. It was observed that the increase in the oil to methanol ratio increases the conversion of FFA. For instance, at 1:4 ratio only 79% conversion was achieved as compared to 96% at 1:6 oil/methanol ratio (w/v). The conversion values for 1:5 ratios were found almost equal to the values at 1:6 ratios; therefore 1:5 (w/v) oil/methanol ratios was treated as optimal. This result was in good agreement with a similar study conducted for Jatropha oil [109] where optimum oil/methanol ratio was found to be 1:4 (w/v). The deviation in oil/methanol ratio may be attributed to higher acid value in the present study, 62.80 mg KOH/g Karanja oil than the acid value of 54.43 mg KOH/g Jatropha oil.

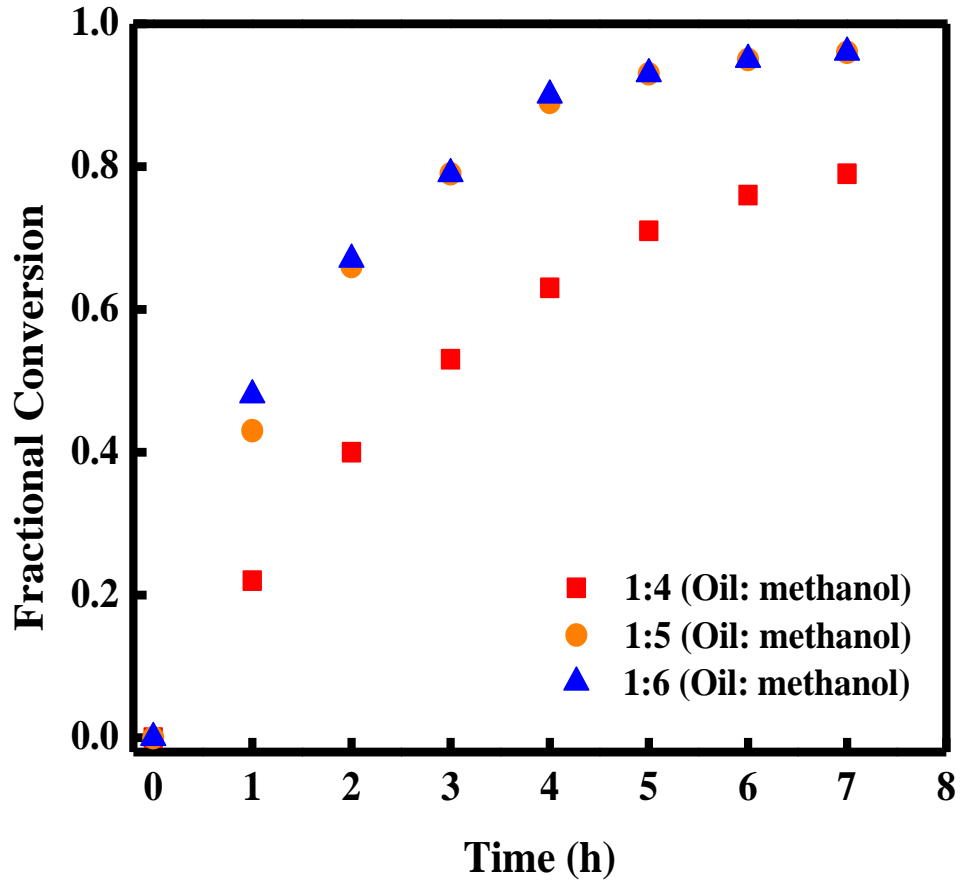


Figure 3.4:- Effect of oil/methanol ratio on conversion at 220 °C temperature.

### 3.2.5 Equilibrium constant and kinetic modeling

Equilibrium conditions are reached when the composition of the reaction mixture doesn't change further over a course of time. The composition of reactants and products at equilibrium are required to determine equilibrium constant experimentally. Principally rigorous thermodynamic methods based on activity coefficients are the correct method to determine the equilibrium constant as given in Equation 3.4.

$$K = \prod_i (a_i)^{\nu_i} = \frac{a_{ME} a_{H_2O}}{a_{FFA} a_M} = K_\gamma K_C \quad 3.4$$

where,  $a_i$  is the activity of species  $i$ ,  $K_\gamma = \prod_i (\gamma_i)^{\nu_i}$ , is the equilibrium constant based on activity coefficient,  $K_C = \prod_i (C_i)^{\nu_i}$  is the equilibrium constant based on concentration [179]. Activity-based treatment of equilibrium constant was used by many researchers [179–182] and

observed that the concentration based treatment of data fits better in the model [180,181,183]. For example, Keurentjes, Janssen, and Gorissen [181] used both activation-based and concentration-based approaches to study the kinetics of esterification of tartaric acid with ethanol and reported that both the approaches predict the kinetic parameters reasonably, but prediction with later perform better. Similarly in the case of esterification of acetic acid with methanol carried out by Ronnback et al. [180] showed no significant improvement in kinetic parameters estimation with the activation-based approach and concluded that the model fit is better when the concentration-based approach was applied. Additionally, Hassan and Vinjamur [183] carried out esterification of oleic acid as FFA's in sunflower oil and corroborated the observation of Keurentjes, Janssen, and Gorissen [181] and Ronnback et al. [180], that concentration-based approach in estimating equilibrium composition is reasonable. Moreover, studies carried out by Liu et al. [184] on liquid-liquid immiscibility of (i) oleic acid + methanol + water, (ii) methyl ester (ME) + methanol + water, (iii) oleic acid + methanol + oil, (iv) ME + methanol + oil systems, observed that the oil + oleic acid and methanol + oleic acid systems as completely miscible systems but, methanol + oil is partially miscible system. They observed that the miscibility (inter solubility) of oil and methanol increases with temperature and also with an increase in FFA or oleic acid content in the Jatropha oil. A single homogeneous phase was found when there is a 20 wt. % oleic acid content was present in Jatropha oil [183]. Similar solubility was found in the work of Batista et al. [185] using canola oil + oleic acid + methanol. This seems that the vegetable oil type has a little effect on mutual solubilities with methanol. In the present study, the content of FFA is 31.55 wt. % of Karanja oil and temperature is high enough. Together gaining confidence from the work of Vijaya Lakshmi, Venkateshwar, and Satyavathi [96], where they demonstrated the critical speed of agitation at which dispersed phase is completely incorporated into the continuous phase and used the concentration-based approach to study

the mixing regime of Karanja oil and methanol. Therefore, from the credence of above-reviewed literature, it is expected that there exists a single homogeneous phase in the reactor and we used the concentration-based approach to evaluate the kinetics of esterification of FFA in Karanja oil.

The esterification of FFA with methanol is represented by a reversible reaction as shown in Equation 3.5;



Where M is methanol; Me is methyl ester and H<sub>2</sub>O is water.

The rate of the above reaction is expressed as;

$$-r_{\text{FFA}} = -\frac{dC_{\text{FFA}}}{dt} = k_f C_{\text{FFA}} C_{\text{M}} - k_r C_{\text{Me}} C_{\text{H}_2\text{O}} \quad 3.6$$

Where,  $C_{\text{FFA}}$ ,  $C_{\text{M}}$ ,  $C_{\text{ME}}$  and  $C_{\text{H}_2\text{O}}$  are the concentrations of FFA, methanol, methyl ester, and water, respectively, in mg KOH/g oil;  $k_f$  and  $k_r$  are the reaction rate constants for the forward and backward reactions in  $\text{min}^{-1}$  and  $(\text{mg KOH h/g oil})^{-1}$ , respectively,.

Following assumptions were considered for simplifying the rate expression;

- i. Due to the presence of a mixing regime, only the presence of one phase is assumed.
- ii. Neglecting mass transfer effects, the reaction is assumed to be kinetically controlled.
- iii. Since methanol has been used in excess, therefore, forward reaction (esterification of FFA) was considered as pseudo-first-order and the backward reaction (hydrolysis of ester) was taken as a bimolecular second order.

Following expressions were obtained from material balance;

$$C_{\text{FFA}} = C_{\text{FFA}_0}(1 - X); \text{ and } C_{\text{Me}} = C_{\text{H}_2\text{O}} = C_{\text{FFA}_0} - C_{\text{FFA}} = C_{\text{FFA}_0}X$$

Where,  $C_{\text{FFA}_0}$  is the initial concentration of FFA

On applying assumptions and materials balance expressions in Equation 3.6 we get;

$$\begin{aligned} \Rightarrow -\frac{dC_{FFA}}{dt} &= k'_f C_{FFA} - k_r C_{Me} C_{H_2O} \\ C_{FFA_0} \frac{dX}{dt} &= k'_f C_{FFA_0} (1 - X) - k_r C_{FFA_0}^2 X^2 \\ \therefore \frac{dX}{dt} &= k'_f (1 - X) - k_r C_{FFA_0} X^2 \end{aligned} \quad 3.7$$

Also, we know that at equilibrium;

$$\frac{dX}{dt} = 0 \text{ and } X = X_e$$

Therefore Equation 3.7 becomes as;

$$\begin{aligned} 0 &= k'_f (1 - X_e) - k_r C_{FFA_0} X_e^2 \\ K &= \frac{1}{C_{FFA_0}} \frac{k'_f}{k_r} = \frac{X_e^2}{1 - X_e} \\ \therefore k_r &= \frac{k'_f}{C_{FFA_0}} \frac{1 - X_e}{X_e^2} \end{aligned} \quad 3.8$$

Where  $K$  and  $X_e$  are the equilibrium constant and equilibrium conversion respectively.

On substituting Equation 3.8 in equation 3.7 we get;

$$\frac{dX}{dt} = k'_f (1 - X) - \frac{k'_f}{C_{FFA_0}} \frac{1 - X_e}{X_e^2} C_{FFA_0} X^2$$

$$\frac{dX}{dt} = \frac{k'_f}{X_e^2} [X_e^2 - XX_e^2 - X^2 + X^2 X_e]$$

$$\int \frac{dX}{[X_e^2 - XX_e^2 - X^2 + X^2 X_e]} = \frac{k'_f}{X_e^2} \int dt$$

Integration of the above equation gives;

$$\ln \left[ \frac{(X_e - 1)X - X_e}{X - X_e} \right] = \frac{k'_f t}{X_e} (2 - X_e) \quad 3.9$$

Equation 3.9 can also be written in linear form  $y = mx$ .

Where,  $y = \ln \left[ \frac{(X_e - 1)X - X_e}{X - X_e} \right]$ ,  $x = t$  and slope,  $m = \frac{k'_f t}{X_e} (2 - X_e)$

Simplifying Equation 3.9 for conversion of FFA as a function of time, we get;

$$X = \frac{X_e \left[ \exp \left( \frac{k'_f t (2 - X_e)}{X_e} \right) - 1 \right]}{\exp \left( \frac{k'_f t (2 - X_e)}{X_e} \right) - (X_e - 1)} \quad 3.10$$

The kinetic model along with the reaction conditions proposed by various researchers for esterification of FFA has been summarized in Table 3.2. The current model shows relatively new treatment of reaction kinetics based on the assumptions which are associated with ultimate facts of the reaction. The experimental conversion versus time data at each temperature was plugged into the linear form of Equation 3.9 to evaluate  $x$  and  $y$  values. The obtained values were plotted for each temperature as shown in Figure 3.5. The proposed model fits experimental data very well at each temperature with  $R^2 = 0.98$ . Further, the slope of each straight line was used to calculate the forward reaction rate constant ( $k_f$ ). The calculated  $k_f$  values were used in Equation 3.8 to obtain the backward reaction rate constant. The obtained reaction parameters are presented in Table 3.3. Various researchers have used the trial and error method to calculate equilibrium conversion and rate constants in the case of limited experimental data and unavailability of experimental equilibrium conversion [28,103,109]. To check the model applicability for such conditions, conversion versus time data was regressed using the Levenberg-Marquardt algorithm. The regression of experimental data was carried out by providing initial guess values of unknown parameters  $X_e$  and  $k_f$  until Equation 3.10 fits well. The model predicts the conversion versus time profile closely

matching ( $R^2 = 0.99$ ) with experimental values at each temperature as shown in Figure 3.6. The parameters such as rate constants and equilibrium conversion obtained through trial and error method have been reported in Table 3.3. The parameters match well with the experimental equilibrium conversion as well as rate constant at each temperature.

**Table 3.2:- Kinetic Models**

Reference	Reactants	Reactor type and optimum conditions	Assumptions	Model equation
Present study	Karanja oil and methanol	Batch reactor T= 220°C; *Ratio = 1:5 (w/v) P = 10 bar; X <sub>e</sub> = 96.0% t = 7 h	1. Forward reaction is pseudo first order 2. Backward reaction is second order	$X = \frac{X_e \left[ \exp\left(\frac{k'_f t(2-X_e)}{X_e}\right) - 1 \right]}{\exp\left(\frac{k'_f t(2-X_e)}{X_e}\right) - (X_e - 1)}$
[110]	PFAD and methanol	Semi batch reactor T= 290°C; *Ratio= 1:1.58 (w/v) P = 8.5 bar; X <sub>e</sub> = 99.9% t = 3 h	1.A reversible reaction is neglected 2.The overall reaction follows first order	$\ln\left(\frac{C_{FA,t}}{C_{FA,0}}\right) = k'_f t$ Where C <sub>FA,t</sub> , C <sub>FA,0</sub> is fatty acid conc. at t = t and t = 0, respectively.
[109]	Jatropha oil and methanol	Batch reactor T= 190°C; *Ratio= 1:4 (w/v)	Both forward and backward reactions are considered as second	$X = \frac{X_e \left[ \exp\left(2k_1 C_{Ao} \left(\frac{1}{X_e} - 1\right) t\right) - 1 \right]}{\exp\left(2k_1 C_{Ao} \left(\frac{1}{X_e} - 1\right) t\right) - 2(X_e - 1)}$

		P= 27.1 bar; $X_e = 95.1\%$  t = 5 h	order	Where $C_{A0}$ is the initial acid value  $k_1$ is the forward reaction rate constant
[173]	Oleic acid and ethanol	Plug flow reactor  T = 300°C; Molar ratio = 1:6  P = 200 bar; $X_e = 88.0\%$  t = 0.33 h	No kinetic study	-

\*Ratio represents oil: methanol

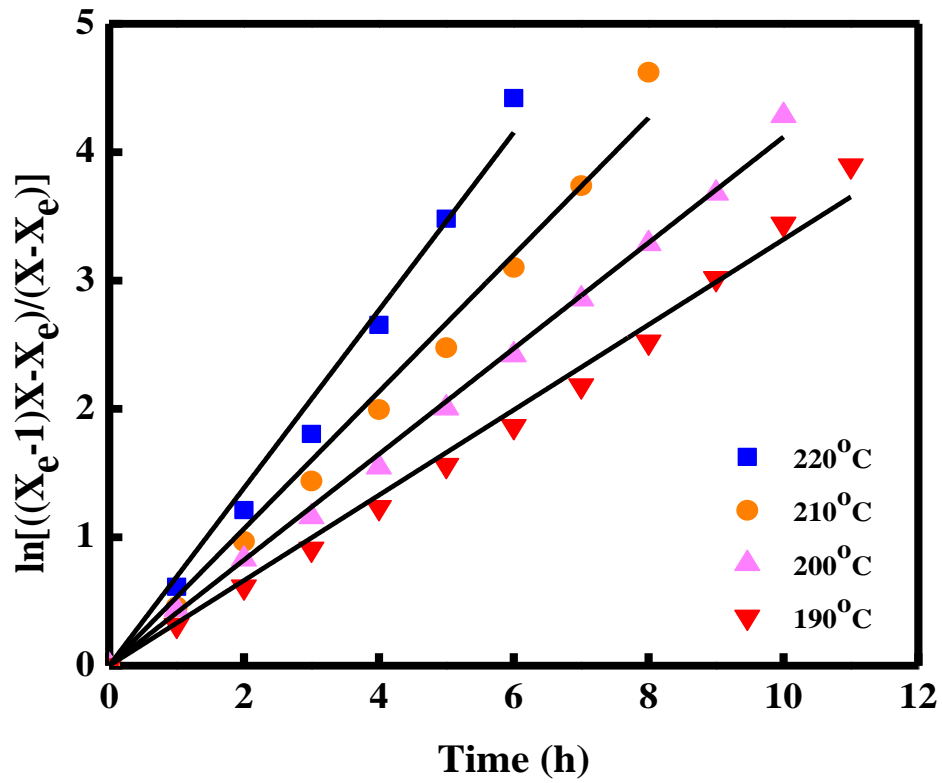


Figure 3.5:- Validation of the kinetic model.

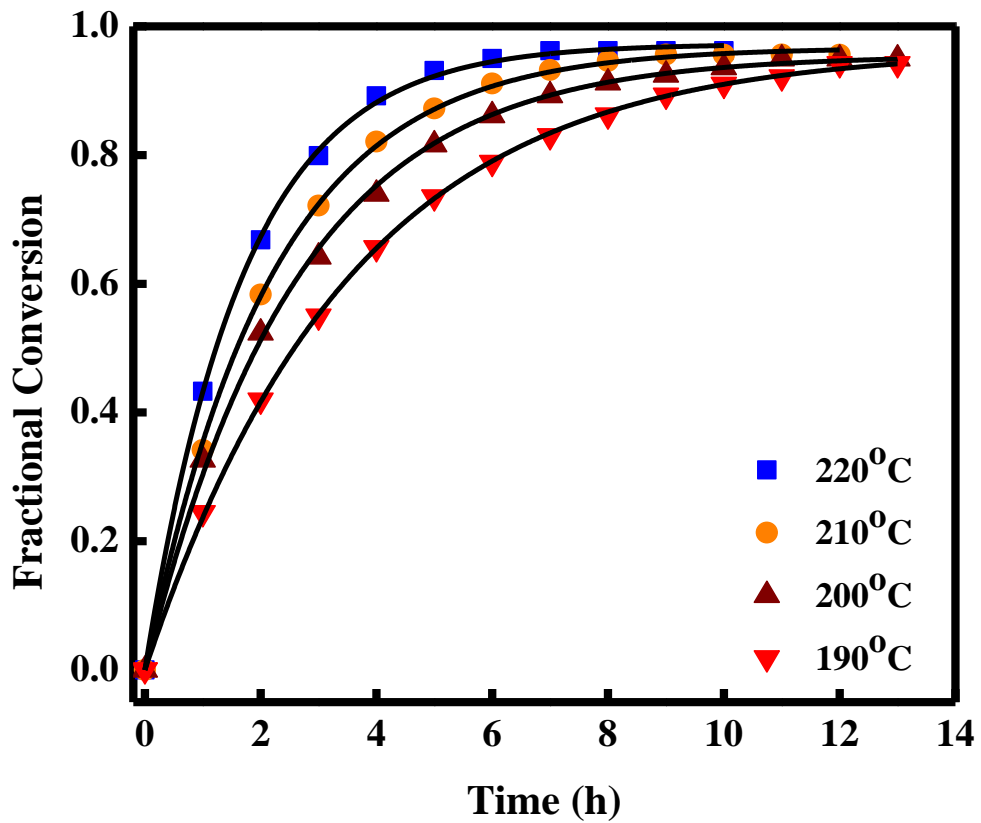


Figure 3.6:- Experimental and model predicted conversion at various temperatures.

**Table 3.3:-** Calculated Reaction Parameters

T °C	Experimental				Trial and error method			
	X <sub>e</sub>	k <sub>r</sub> ' (min <sup>-1</sup> )	k <sub>r</sub> (g/mgKOH min)	R <sup>2</sup>	X <sub>e</sub>	k <sub>r</sub> ' (min <sup>-1</sup> )	k <sub>r</sub> (g/mgKOH min)	R <sup>2</sup>
190	0.941	0.295	3.09E-4	0.991	0.964	0.291	1.79E-4	0.999
200	0.950	0.372	3.31E-4	0.997	0.955	0.368	2.89E-4	0.999
210	0.956	0.469	3.60E-4	0.995	0.966	0.461	2.67E-4	0.999
220	0.962	0.641	4.18E-4	0.987	0.972	0.638	3.01E-4	0.999

### 3.2.6 Effect of temperature on reaction rate constant

The effect of temperature on reaction rate constant was studied using the linear form of Arrhenius equation as given below;

$$\ln k = -\frac{\Delta E}{RT} + \ln k_0 \quad 3.11$$

$\ln k$  versus  $1/T$  data was plotted for both rate constants ( $k_f$ ,  $k_r$ ) as shown in Figure 3.7. Change in activation energy ( $\Delta E$ ) and frequency factor ( $k_0$ ) for the forward and backward reactions were evaluated from the slope and intercept of the straight lines, respectively and tabulated in Table 3.4.

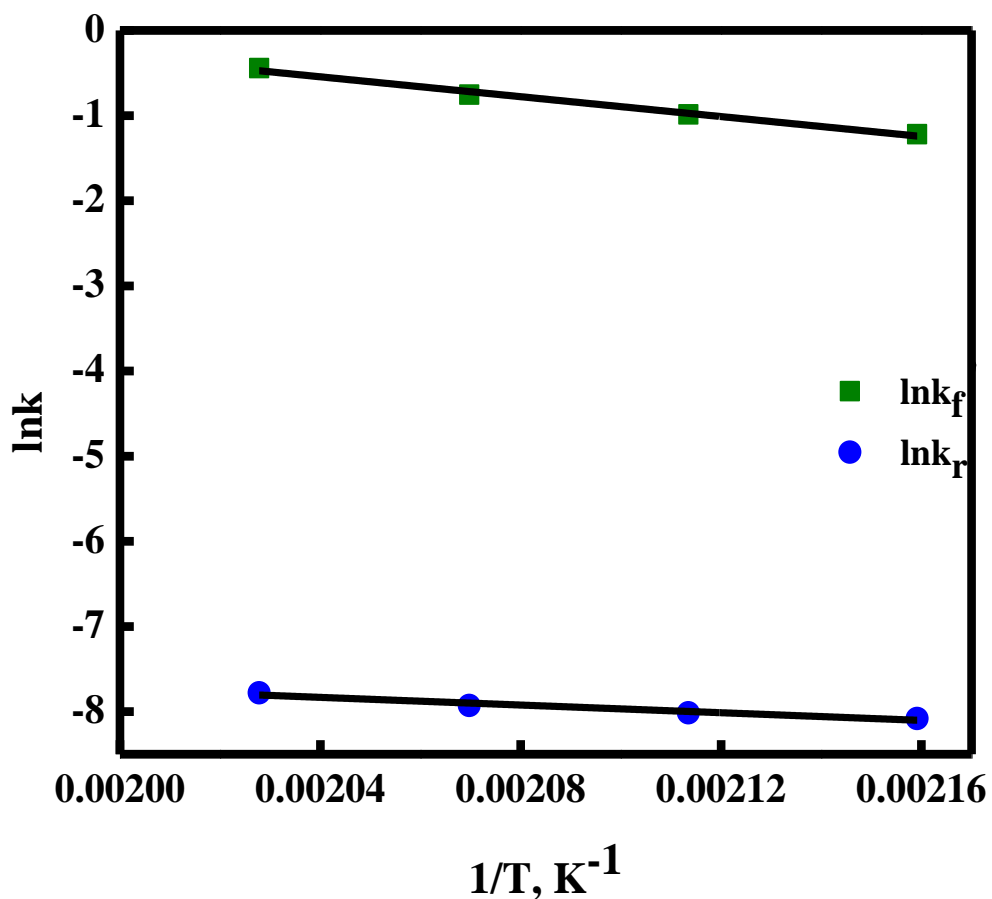


Figure 3.7:- Arrhenius plot.

**Table 3.4:** Calculated Arrhenius and Thermodynamic Parameters

Parameters	Forward reaction	Backward reaction
$k_o$	86249.54 (min <sup>-1</sup> )	0.04 (g/mg KOH min)
$\Delta E$ (KJ/mol)	48.53	18.74
$\Delta G$ (KJ/mol)	-26.42	-27.64
$\Delta H$ (KJ/mol)	29.79	
$\Delta S$ (kJ/mol °C)	0.12	

### 3.2.7 Effect of temperature on the equilibrium constant

The effect of temperature on the equilibrium constant was studied using the Van't Hoff equation. The  $\ln K$  versus the inverse of temperature data was fitted to a straight line as shown in Figure 3.8. The slope and intercept of the line were used to calculate the change in enthalpy ( $\Delta H$ ) and entropy ( $\Delta S$ ) of the reaction, respectively. The values of  $\Delta H$  and  $\Delta S$  obtained are +29.79 kJ/mol and +0.121 kJ/mol.K, respectively as given in Table 3.4. The positive sign of  $\Delta H$  indicates the endothermic nature of the reaction and  $+\Delta S$  shows the increased entropy of the system. To find whether the reaction is spontaneous or not, the Gibbs free energy was also calculated at each temperature using the following Equation 3.12;

$$\ln K = -\frac{\Delta H}{RT} + \frac{\Delta S}{R} \quad 3.12$$

The calculated Gibb's free energy change ( $\Delta G$ ) was found to be negative at each temperature as shown in Table 3.4. The large negative values of  $\Delta G$  along with  $+\Delta H$  and  $+\Delta S$  confirms that the reaction is spontaneous at high temperatures. Experimentally observed conversion values were plotted against the model predicted conversions to test the statistical significance of the data using Student's paired t-test. It can be seen from Figure 3.9 that the proposed model satisfactorily represents all the experimental data.

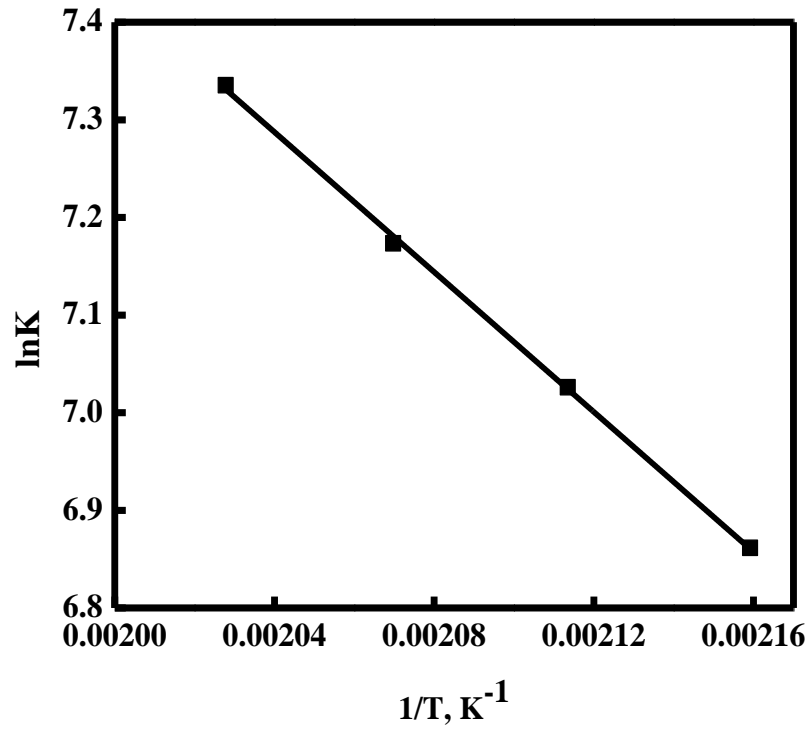


Figure 3.8:- Van't Hoff plot.

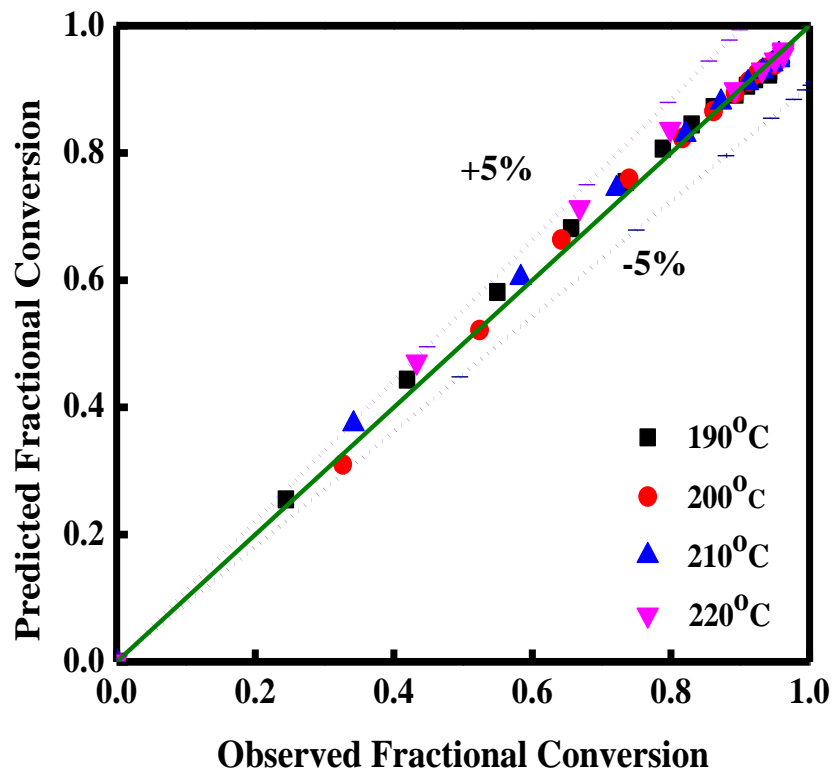


Figure 3.9:- Comparison of experimental and model predicted conversions.

### 3.2.8 Process modeling and simulation

#### 3.2.8.1 Modeling

Process modelling and simulation is known to provide valuable information about the operating conditions efficiently in a short period of time. In spite of the fact that there are some differences between real process and process simulation, yet, they are widely used to provide reliable information due to their extensive component library, comprehensive thermodynamic packages, and diverse computational methods [112]. The non-catalytic esterification process was modeled using Aspen Plus simulator (ver. 8.6). The complete flow sheet of the process is shown in Figure 3.10.

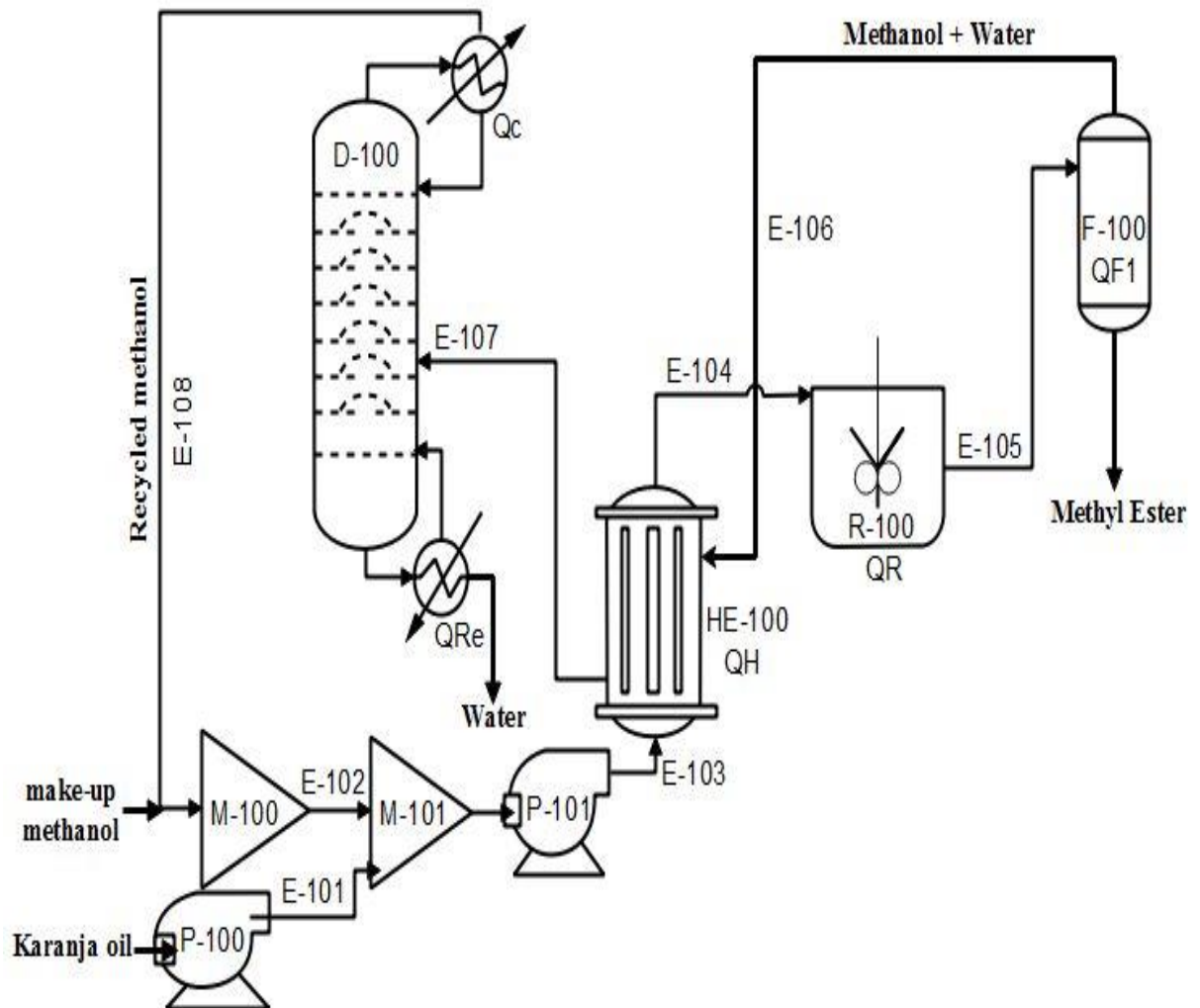


Figure 3.10:- Flow diagram of the esterification process.

### **Nomenclature:**

M-100, 101:- Feed mixers; P-100, 101:- Feed pumps; HE-100:- Heat exchanger; F-100:- Flash column; D-100:- Distillation column; R-100:- Continuous stirred tank reactor;  $Q_H$ :- Heat exchanger heat duty;  $Q_R$ :- Reactor duty;  $Q_{F1}$ :- Flash column duty;  $Q_C$ :- Condenser duty;  $Q_{Re}$ :- Reboiler duty.

Karanja oil was pumped using a feed pump (P-100) and resulting stream (E-101) was introduced into the feed mixer (M-101). The recycled methanol (E-108) was mixed with makeup methanol in a mixer (M-100) and resulting methanol stream (E-102) was sent to feed mixer (M-101). After mixing, reactants were pumped again using mixed feed pump (P-101) and resulting stream (E-103) was sent to a heat exchanger (HE-100) on the tube side. The heated feed from the heat exchanger (E-104) having zero vapor fraction enters the continuous stirred tank reactor (R-100), where the esterification reaction takes place. The product stream (E-105) of the reactor is passed through the flash column (F-100) where pure methyl ester was collected as a bottom product, and unreacted methanol, as well as water, was removed from the top as mixed stream (E-106). In order to utilize the heat of the mixed stream, it was passed through the shell side of the heat exchanger to heat the feed stream. Product stream resulting from the heat exchanger (E-107) was fed to the distillation column (D-100) in which pure methanol was recovered from the top and recycled (E-108) to the mixer (M-100). The by-product water was recovered from the bottom of the distillation column. The CSTR, flash column, distillation column shown in the flow sheet were modeled using RCSTR, FLASH-2 and RADFRAC subroutines of Aspen Plus software, respectively.

#### ***3.2.8.2 Simulation***

The simulation was carried out by importing the required databanks and specifying all the components present in the process. Activity coefficient based NRTL thermodynamic model was selected for estimation of properties as well as the calculation of phase equilibrium.

Triglycerides (TG) are assumed to be homogeneous and each TG composed of only one type of fatty acid radical. The flow rate of Karanja oil in feed stream (E-101) was selected to be 1050 kg/h with composition as given in Table 3.5. In order to lower the process complexity and also due to the high oleic acid composition in the present Karanja oil, the FFA was assumed entirely as oleic acid. Methanol was fed continuously to the reactor ( $4547.51 \text{ m}^3$ ) at the rate of 6300 l/h i.e. at 1:6 (w/v) ratio. The kinetic parameters obtained through experiment such as  $k_o = 86249.54 \text{ min}^{-1}$ ,  $\Delta E = 48.534 \text{ kJ/mol}$  for the forward reaction and  $k_o = 0.039 \text{ (g)/(mg KOH min)}$ ,  $\Delta E = 18.744 \text{ kJ/mol}$  for the backward reaction were used in RCSTR subroutine of the reactor model. Previously, West, Posarac, and Ellis [112] and West [186] have used CSTR for simulation of transesterification process at  $350 \text{ }^\circ\text{C}$  and 200 bar. The reaction product of oleic acid (FFA) and methanol were designated as methyl-oleate (methylo). After completion of the reaction, the product was separated using a flash drum. The temperature and pressure of the flash drum were maintained at  $220 \text{ }^\circ\text{C}$  and 10 bar, respectively. The pure product was collected from the bottom and water as well as methanol was collected from the top. Product recovery greater than 87% (ratio of molar flow rates of all the components excluding water and methanol in methyl ester stream to the molar flow rate of all the components including methanol and water in E-105 stream) was observed with the minor loss of methyl-oleate and triolein into the top product. The top product was then passed through the heat exchanger to recover heat followed by separation of water and recovery of methanol in a distillation column. Distillation column was modeled using rigorous Radfrac subroutine of the Aspen simulator. The required inputs for Radfrac were calculated first by DSTWU model. The molar flow rate, composition and stream conditions of E-107 were given as input to the DSTWU unit. The light key (methanol) and heavy key (water) recoveries were specified in DSTWU as 0.99 and 0.01, respectively. DSTWU simulation result shows that at a reflux ratio of 1.3, 23 stages are required to get the desired

product purity with 155.333 kmol/h distillate flow rate and suggested to locate the feed on the 20<sup>th</sup> stage. This information was used as input to the Radfrac and nearly pure (0.999) methanol was recovered. The recovered methanol was recycled back to the mixer-1 where it was mixed with the makeup methanol stream.

### ***3.2.8.3 Sensitivity analysis***

To study the effect of flash column pressure on product recovery, sensitivity analysis tool of Aspen Plus was used to determine the optimum pressure that would maximize the molar flow of all the components other than water and methanol in the ester stream. Sensitivity results show that when the flash column is operated at 2 bar, the maximum amount of methanol (156.87 kmol/h) and water (1.2430 kmol/h) are recovered in methanol + water (E-106) stream as shown in Figure 3.11. However, at this pressure, there was a considerable loss of triolein and methyl-oleate to E-106 stream as shown in Figure 3.12. When the flash column is operated at 10 bar pressure, a good esterified product recovery was observed at the expense of allowing the little amount of water (0.0065 kmol/h) and methanol (0.37 kmol/h) into the ester stream. Therefore, the flash column pressure was selected as 10 bar. A simulation result of the complete flow sheet was given in Table 5.5. The calculated heat duties of each unit are as follows:

Heat exchanger heat duty ( $Q_H$ ) = 26 kW; Reactor duty ( $Q_R$ ) = 2038 kW; Flash column duty ( $Q_{F1}$ ) = 0; Condenser duty ( $Q_C$ ) = -3481 kW; Reboiler duty ( $Q_{Re}$ ) = 1601 kW.

The simulation results showed the conversion of oleic acid to be 99.85% which was close to the experimental conversion (96.21%). The little deviation in the predicted conversion may be attributed to the fact that in simulation only oleic acid was used to represent FFA. However, in experiments, FFA was a complex blend of various fatty acids in Karanja oil.

**Table 3.5:-** Stream results of the simulated flow sheet

	<b>E-101</b>	<b>E-102</b>	<b>E-103</b>	<b>E-104</b>	<b>E-105</b>	<b>ME</b>	<b>E-106</b>	<b>E-107</b>	<b>E-108</b>	<b>Water</b>	<b>Make-up</b>	
T (°C)	25	63.89	59.72	64.52	220	220	220	210.5	64.54	75.67	25	
P (bar)	1	1	1	1	10	10	10	10	1	1	1	
Mass flow rate (kg/h)	1050	5067.07	6117.07	6117.07	6117.07	970.44	5146.63	5146.63	4976.96	169.67	90.11	
Molar flow rate (kmol/h)	2.02	158.14	160.16	160.16	160.16	2.13	158.03	158.03	155.33	2.70	2.81	
<b>Molar composition</b>	<b>OOO</b>	0.217	0	2.75E-3	2.75E-3	2.75E-3	0.179	3.53E-4	3.53E-4	0	0.020	0
	<b>O</b>	0.607	0	7.68E-3	7.68E-3	1.14E-5	7.87E-4	0	0	0	0	0
	<b>Methanol</b>	0	0.99	0.98	0.98	0.98	0.17	0.99	0.99	0.99	0.45	1

	<b>Water</b>	<b>0</b>	1.11E-4	1.09E-4	1.09E-4	7.78E-3	3.03E-3	7.85E-3	7.85E-3	1.13E-4	0.452	0
	<b>M-O</b>	0	0	0	0	7.67E-3	0.481	1.26E-3	1.26E-3	0	0.073	0
	<b>PPP</b>	0.028	0	3.58E-4	3.58E-4	3.58E-4	0.026	0	0	0	0	0
	<b>SSS</b>	0.017	0	2.24E-4	2.24E-4	2.24E-4	0.016	0	0	0	0	0
	<b>LLL</b>	0.108	0	1.38E-3	1.38E-3	1.38E-3	0.103	0	0	0	0	0
	<b>AAA</b>	0.020	0	2.57E-4	2.57E-4	2.57E-4	0.019	0	0	0	0	0

ME: Methyl Ester, OOO: triolein, O: oleic acid, M-O: methyl-oleate, PPP: tripalmitin, SSS: tristearin, LLL: trilenolein, AAA: triarachidic.

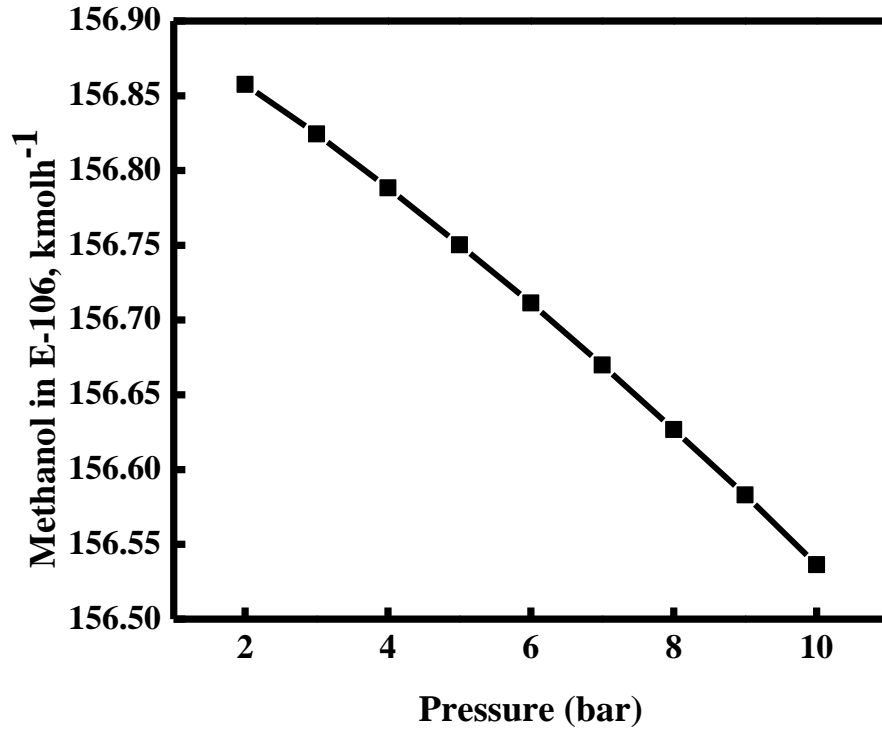


**Figure 3.11:-** Effect of operating pressure of flash column on methanol mole flow in E-106.

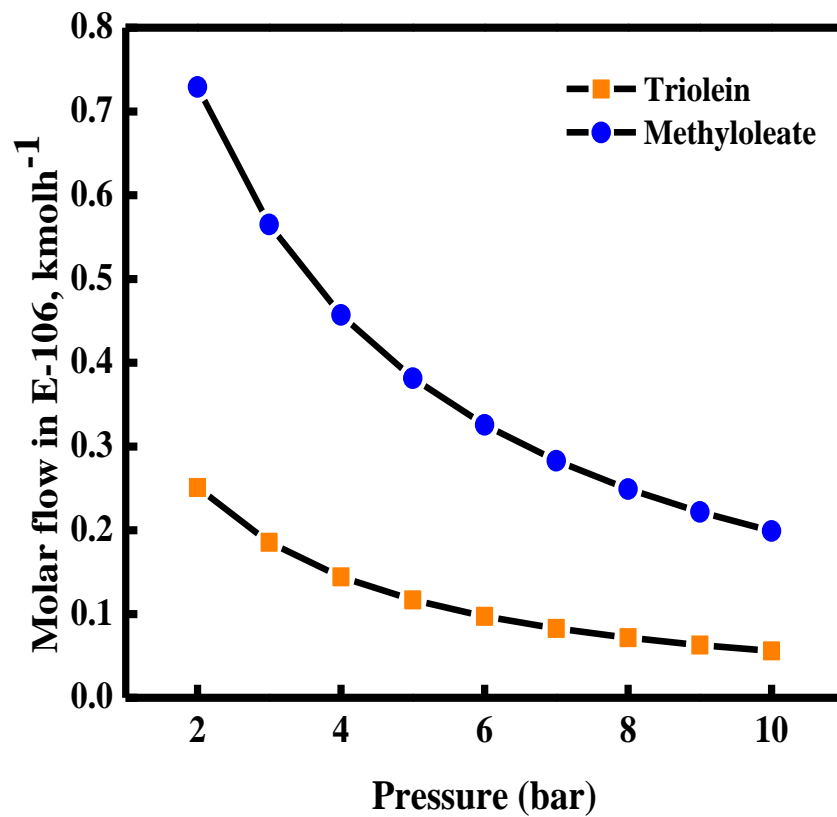


**Figure 3.12:-** Effect of operating pressure of flash column on triolein and methyl-oleate mole flows in E-106.

### Synthesis and Characterization of Novel Corncob-Based Solid

#### Acid Catalyst for Biodiesel Production

#### 4.1 Experimental Details

##### 4.1.1 Materials used

The fresh corn was purchased from a local market near RGIPT, Jais, Uttar Pradesh. All corncob used in the current study were collected from a single source to ensure sample uniformity. Methanol, ethanol, oleic acid, palmitic acid, phenolphthalein indicator, phosphoric acid, sulfuric acid, hydrochloric acid, barium chloride, sodium chloride, sodium bicarbonate, potassium hydroxide and Whatman filter paper (40  $\mu\text{m}$ ) were purchased from S. D. Fine-Chem. Limited, Kanpur. Karanja oil with physicochemical properties as given in Table 3.1 was obtained from Suyash Herbs Exports India Private Limited, Gujarat.

##### 4.1.2 Catalyst synthesis

###### 4.1.2.1 Size reduction

The fresh corn was made free from corn kernels by picking. The obtained corncob was washed with deionized water to remove surface impurities and dried under the sun for 48h. Then the dried corncob was ground using a grinder and sieved to get a powder having a size 0.149 mm- 0.2038 mm (100-72 mesh numbers).

###### 4.1.2.2 Impregnation

An accurately weighed 100 grams of corncob powder was impregnated with a 250 ml aqueous solution of phosphoric acid at a desired impregnation ratio (mass of dry  $\text{H}_3\text{PO}_4$ /mass of powdered corncob) between 0-1.25. Then the resulting mixture was kept at room

temperature for various intervals of time (5-20 h). Finally, the samples were dried in a hot air oven at 393 K for 12 h and called as I-corncob.

#### **4.1.2.3 Carbonization**

I-corncob samples were then subjected to carbonization in a muffle furnace at various temperatures (423-823 K) and time (0.5-10.5 h). The carbonized samples were extensively washed using 0.1 N HCl solution (at 373 K) for 1 h followed by washing with hot deionized water (above 353 K) until the filtrate was free from chloride ions. After washing, the samples were dried at 383 K for 1 h and designated as I-C-corncob.

#### **4.1.2.4 Sulfonation**

Sulfonation was carried out in a three-neck round bottom flask of 250 ml capacity. Argon gas was used to purge the flask initially and to support an inert atmosphere inside the reactants charged flask. In a typical synthesis, one gram of I-C-corncob sample was mixed with a 10 ml concentrated sulfuric acid and held at various temperatures (353-413 K) and time (12-19 h). After sulfonation, the excess amount of acid was diluted using deionized water. Then the obtained solid samples were washed thoroughly with hot deionized water to remove the sulfate ions attached to the surface. Finally, the solid catalysts were dried at 383 K for 1 h and designated as I-C-S-corncob. The transformation of corncob in each stage is shown in Figure 4.1.



**Figure 4.1:-** Transformation of corn cob to the sulfonated catalyst.

### **4.1.3 Catalyst characterization**

#### ***4.1.3.1 Analysis of functional groups***

Functional groups present on the surface of the catalyst were analyzed using Perkin Elmer: spectrometer-spectrum two. The FT-IR spectra of all the samples were obtained in the range of 500-4000  $\text{cm}^{-1}$  wave number.

#### ***4.1.3.2 Acid density of the catalysts***

The acid densities of the synthesized catalysts were estimated by titration method as given in the literature [187].  $\text{SO}_3\text{H}$  group density was determined by sonicating the mixture of 0.25 g catalyst in 30 ml of NaCl solution (0.05 mol/l) for 1 h in an ultrasonic bath at room temperature. After sonication, solids were separated using a centrifuge. Then the obtained solids were washed with deionized water keeping solids on Whatman filter paper (40  $\mu\text{m}$ ). The retentate obtained after centrifugation and the filtrate obtained after solids washing were mixed and titrated against 0.05 N NaOH solution using phenolphthalein as indicator. Similarly, the densities of other acidic functional groups were determined by sonicating a mixture of 0.5 g catalyst in 25 ml of 0.05 mol/l base (NaOH and  $\text{NaHCO}_3$  each) solution for 1 h. Then the mixture was left for acid-base reaction at room temperature for 24 h. The solid catalyst was separated using a centrifuge and washed using deionized water. Then a 50 ml of 0.05 N HCl solution was added to the filtrate. Finally, the excess HCl in the filtrate was quantified by anti-titration against 0.05 N NaOH solution using phenolphthalein as an indicator. The acidic densities were estimated based on the hypothesis that NaOH can neutralize all the acidic groups ( $\text{SO}_3\text{H} + \text{COOH} + \text{OH}$ ). Whereas,  $\text{NaHCO}_3$  only reacts with a carbonyl group (COOH) [188].

#### ***4.1.3.3 Analysis of catalyst structure***

The structure of the catalyst was determined using X-ray Diffraction (XRD) instrument of PANalytical, X'Pert PRO, Netherland, with the scanning range of  $2\theta$  from  $10^\circ$  to  $90^\circ$  with step size ( $2\theta$ ) of 0.017 and a scan step time of 50.16 s.

#### ***4.1.3.4 Analysis of the catalyst textural properties***

The textural properties such as total surface area, pore volume, and pore size distribution were estimated using  $N_2$  adsorption-desorption isotherm data which is obtained using a surface area analyzer (Micrometrics ASAP 2020 of JEOL make). Samples were degassed initially at 473 K for 24 h. Then the isotherms are generated by contacting the clean samples with liquid  $N_2$  at 77 K. The Brunauer-Emmett-Teller (BET) theory was used to calculate the surface area. The t-plot and Berrer, Joyner and Halenda (BJH) methods were used to evaluate the pore size distribution.

#### **4.1.4 Esterification reaction**

The esterification reaction between oleic acid and methanol was carried out in a three-neck round bottom flask of 250 ml capacity fitted with a Dean and Stark apparatus as shown in Figure 4.2. The reaction was carried out for 2 h at 338 K using 1:9 molar ratio of oleic acid to methanol. The amount of catalyst added during the reaction was 10 wt. % [weight of catalyst/ (weight of catalyst + weight of oleic acid)]. Heating and mechanical stirring (500 rpm) were provided using a hot-plate magnetic stirrer (IKA: C-MAG HS 7). After completion of the reaction, the reaction mass was withdrawn and filtered through Whatman filter paper (40 $\mu$ m) to recover the catalyst. Then the liquid phase was subjected to vacuum evaporation (at 150 mbar and 338 K) for 20 min in a rotary evaporator (Heidolph model:-Hei-VAP Precision) to eliminate methanol and water. Finally, the obtained product was analyzed for the acid value of unconverted FA's/FFA's. The acid value was estimated using the standard procedure and method available in the manual [172]. The conversion of the reaction was calculated using

the initial acid value of FA/FFA and the final acid value of the product using Equation-4.1 as given below;

$$\text{Fractional Conversion}(X) = \frac{(AV_o) - (AV_p)}{(AV_o)} \quad 4.1$$

Where  $AV_o$  and  $AV_p$  are the initial acid value and the final product acid value in mg.KOH/g.

Similarly, the effect of various reaction variables such as time, temperature, oil/methanol molar ratio and catalyst loading on the esterification of oleic acid, palmitic acid, and FFA's present in Karanja oil was also studied.

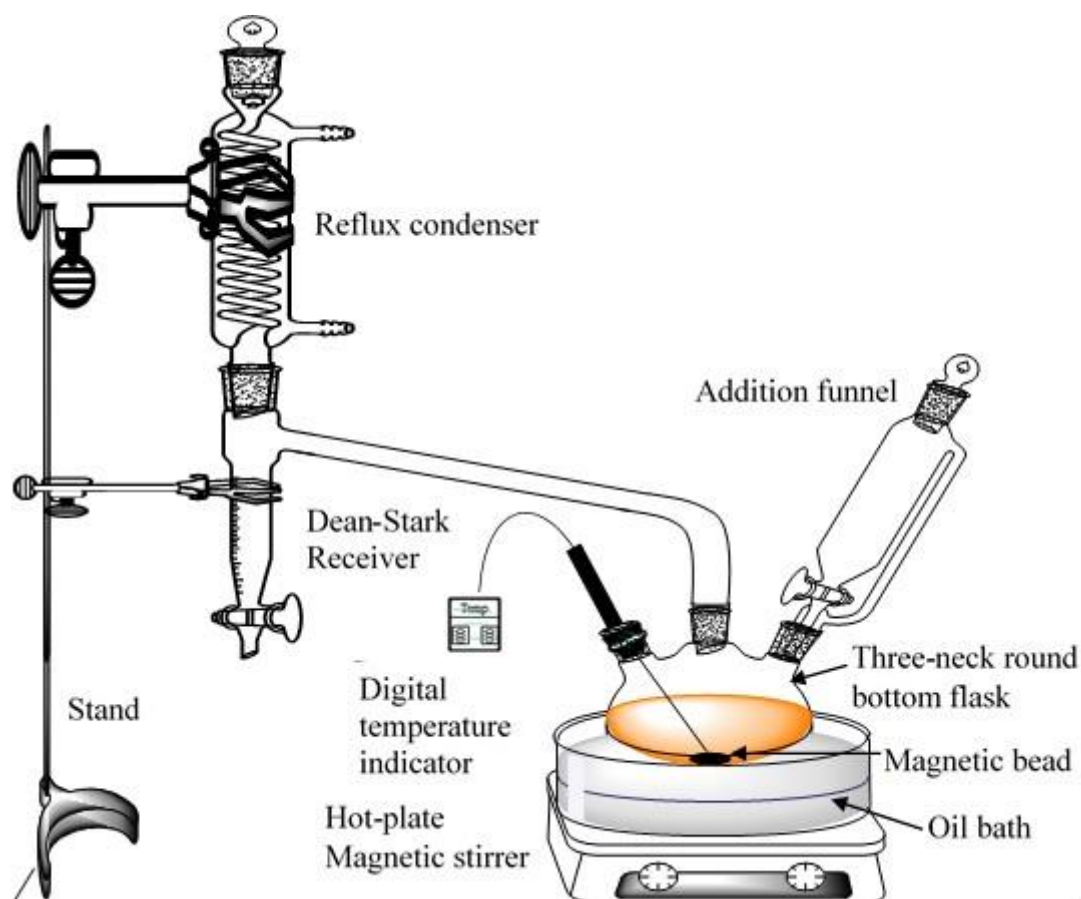


**Figure 4.2:-** Schematic of the experimental setup.

## 4.2 Results and Discussions

### 4.2.1 FT-IR analysis of the catalyst

Fourier transform infrared (FTIR) spectra showing the characteristics of surface functional groups present on the catalyst at various pretreatment stages was shown in Figure 4.3. FTIR spectra show the presence of multiple functional groups on the catalysts and these spectra are in good agreement with other catalysts from various lignocellulosic precursors [150–152,187,189]. The existing broad spectra in the region  $900\text{--}1300\text{ cm}^{-1}$  is due to the C-O stretching of acids, alcohols, ethers, phenols, and esters. More specifically, a small shoulder at  $1265\text{ cm}^{-1}$  in the spectra of I-C-corncob and I-C-S-corncob resembles the characteristics of phosphorous and phospho-carbonaceous compounds. The spectra of corncob showed a peak at  $1747\text{ cm}^{-1}$  which indicates the C=O stretching of the carbonyl group. This peak has enhanced substantially after activation of corncob using phosphoric acid. The relatively low intensity of this peak in the descending order; C-corncob > I-C-corncob > I-C-S-corncob compared to the corncob peak shows the C=O conjugation to the aromatic ring system. As a result, the small intensity of this peak anticipates having a low content of carboxylic acid compared to other oxygen groups on I-C-S-corncob. These results are in good agreement with the reported FTIR spectra of porous adsorbent derived from the corncob [152]. The band at  $1588\text{--}1600\text{ cm}^{-1}$  along with a peak at  $3000\text{ cm}^{-1}$  indicate the C=C stretching vibration of the polyaromatic ring [150,151,187] and show the multiple aromatic rings in the carbon structure [190]. IR spectra of corncob and C-corncob contain both aliphatic and aromatic hydrocarbons. The three peaks at  $2855$ ,  $2926$  and  $2981\text{ cm}^{-1}$  show aliphatic C-H stretching and the peak at  $890\text{ cm}^{-1}$  is due to aromatic C-H bending. However, only the spectra of I-C-corncob and I-C-S-corncob showed the peak at  $890\text{ cm}^{-1}$  due to aromatic C-H bending. Thus, the activation using phosphoric acid increases the aromaticity of the carbon materials [152]. The specific peak in the case of corncob at about  $3330\text{ cm}^{-1}$  is a characteristic of the hydroxyl

(OH) groups from carboxyl, alcohols or phenols. This peak becomes weaker in other cases which suggest that incomplete carbonization of carbon precursor results in lower hydroxyl groups [150]. The main changes in the catalyst observed after sulfonation is the peaks at 1030  $\text{cm}^{-1}$  and 1168  $\text{cm}^{-1}$  due to O=S=O symmetric and asymmetric stretching, respectively [55,150]. Moreover, the bands at 1215  $\text{cm}^{-1}$  (S=O) and 1030  $\text{cm}^{-1}$  (C-S) confirm the sulfonic group's presence [151].

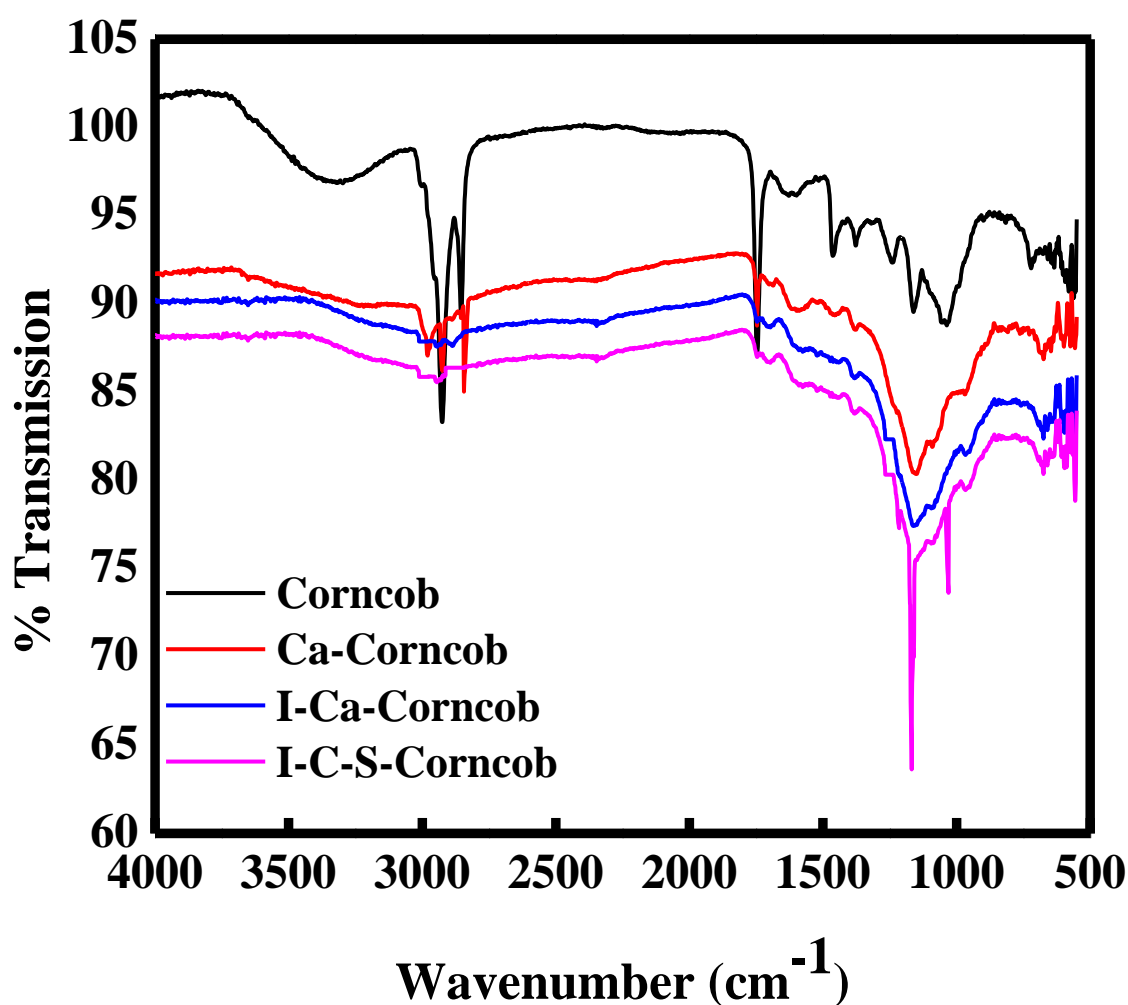


**Figure 4.3:-** FTIR spectra of the corncob, carbonized-corncob ( $C_T = 723 \text{ K} - C_t = 8.5 \text{ h}$ ), impregnated and carbonized-corncob ( $I_R = 1 - I_T = 5 \text{ h} - C_t = 8.5 \text{ h} - C_T = 723 \text{ K}$ ), impregnated, carbonized and sulfonated-corncob catalyst ( $I_R = 1 - I_T = 5 \text{ h} - C_t = 8.5 \text{ h} - C_T = 723 \text{ K} - S_T = 393 \text{ K} - S_t = 16 \text{ h}$ ).

## 4.2.2 BET analysis of the catalyst

### 4.2.2.1 Effect of carbonization temperature on surface area and acid densities

Most of the heterogeneous catalysts are porous solids. Their pore structures emerge from the preparation method [191,192]. The N<sub>2</sub> adsorption-desorption isotherms of corncob (precursor) and carbonized corncob (C-corncob) is shown in Figures 4.4 and 4.5, respectively. The BET surface area of the corncob and C-corncob is very low. Moreover, the isotherm of C-corncob is not overlapping with each other. It is due to the formation of narrow slit pores or bottle-shaped pores which are usually found in the microporous structures [193]. Microporous structures of the materials are particularly helpful in many applications involving the adsorption of molecules whose dimensions are less than 2 nm [146–149]. However, mesoporous structures are suitable for most catalytic applications [143,192,194] particularly, in the biodiesel production involving heavy molecules like triglycerides, oleic acid, and alkyl esters [121,194,195]. Therefore, the corncob was impregnated using H<sub>3</sub>PO<sub>4</sub> and carbonized to increase the surface area and pore volume.

The important factor that determines the catalytic performance of SO<sub>3</sub>H functionalized amorphous carbon catalysts is the carbonization temperature (C<sub>T</sub>) of the precursor material (corncob) [196]. Figures 4.6-4.10 show the N<sub>2</sub> adsorption-desorption isotherms of I-C-corncob carbonized at various temperatures. Table 4.1 lists the acid densities and surface areas of the impregnated corncob carbonized under various temperatures (523-773 K). At the C<sub>T</sub> of 523 and 623 K, the surface area observed was the lowest. Further increasing the C<sub>T</sub> from 623-723 K resulted in the increased surface area and the highest surface area of the catalyst (1268 m<sup>2</sup>/g) was found at the C<sub>T</sub> of 723 K. It can be attributed to the removal of a significant amount of volatile matters [197]. When the C<sub>T</sub> was raised beyond 723 K the surface area was drastically reduced from 1268 to 613 m<sup>2</sup>/g which can be ascribed to the collapse of smaller pores at higher temperature [198]. The catalyst carbonized at a

temperature of 723 K exhibited the highest total acid density (5.56 mmol/g catalyst) due to the highest surface area (1268 m<sup>2</sup>/g) as shown in Table 4.2.

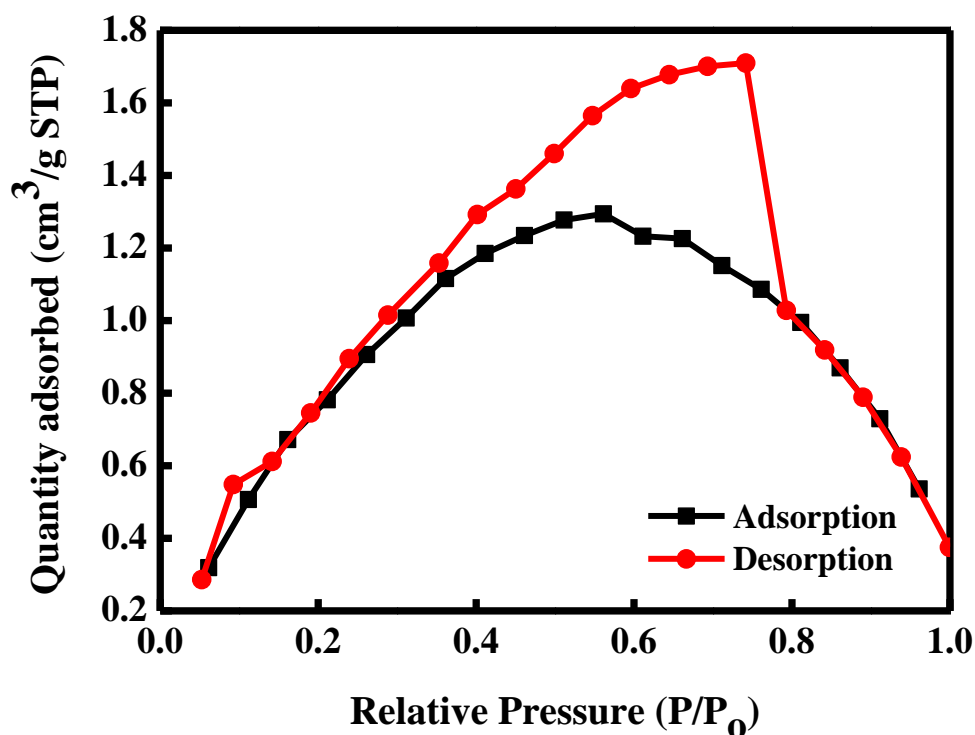


Figure 4.4:- The N<sub>2</sub> adsorption-desorption isotherm of corncob (precursor).

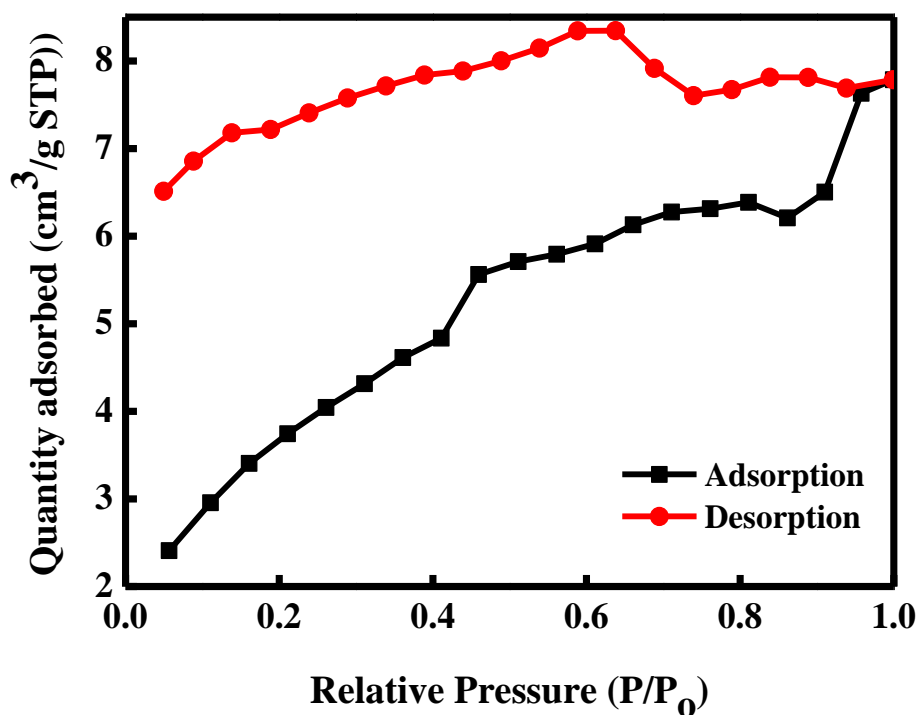
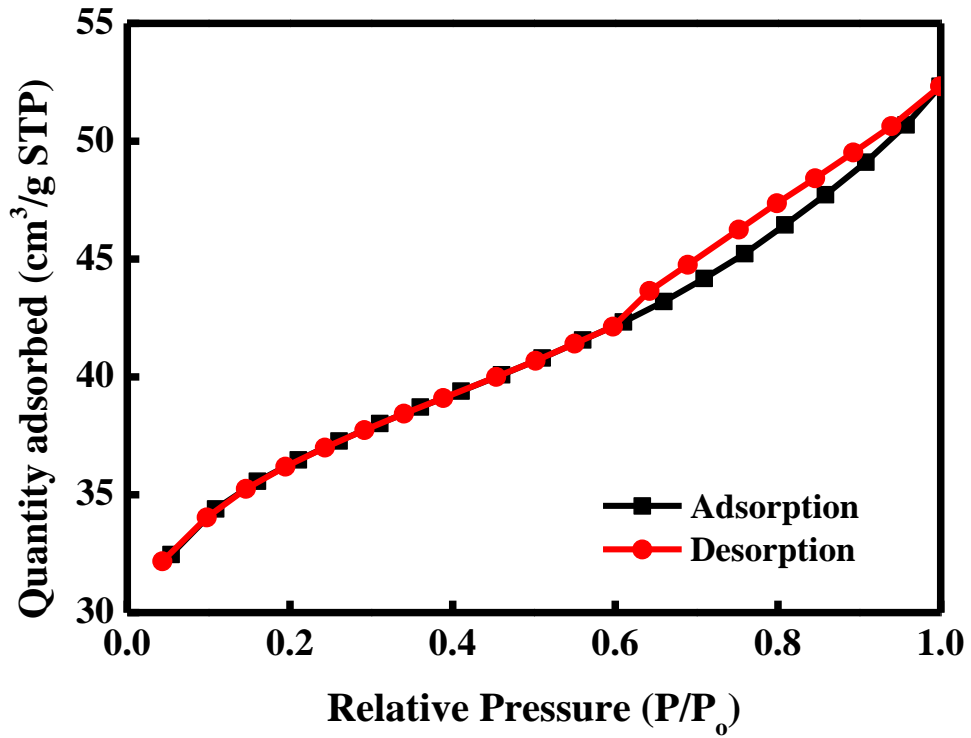
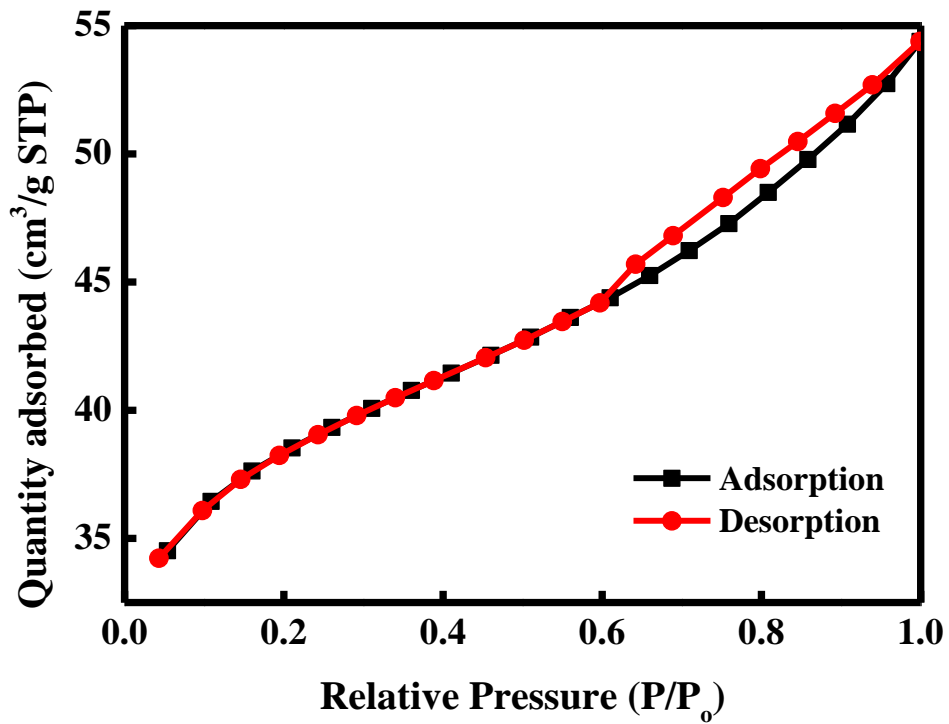


Figure 4.5:- The N<sub>2</sub> adsorption-desorption isotherm of C-corn cob (C<sub>T</sub> = 723 K - C<sub>t</sub> = 8 h).



**Figure 4.6:-** The N<sub>2</sub> adsorption-desorption isotherm of I-C-corncob ( $I_R = 1 - I_T = 5$  h -  $C_t = 8$  h -  $C_T = 523$  K).



**Figure 4.7:-** The N<sub>2</sub> adsorption-desorption isotherms of I-C-corncob ( $I_R = 1 - I_T = 5$  h -  $C_t = 8$  h -  $C_T = 623$  K).

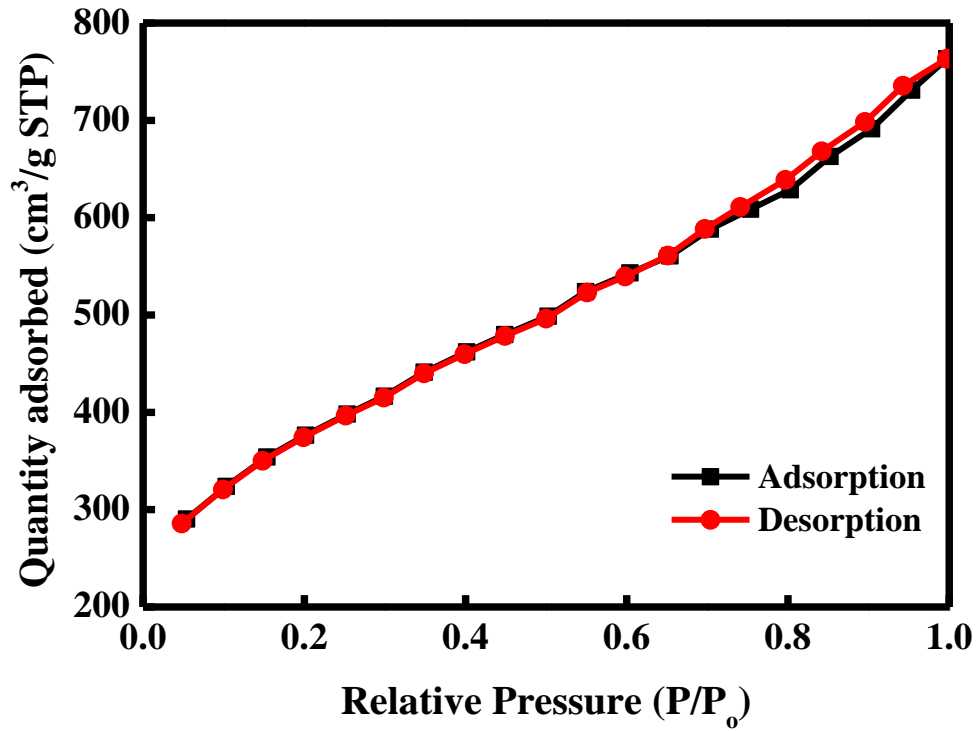


**Figure 4.8:-** The N<sub>2</sub> adsorption-desorption isotherm of I-C-corncob ( $I_R = 1 - I_T = 5$  h -  $C_t = 8$  h -  $C_T = 673$  K).

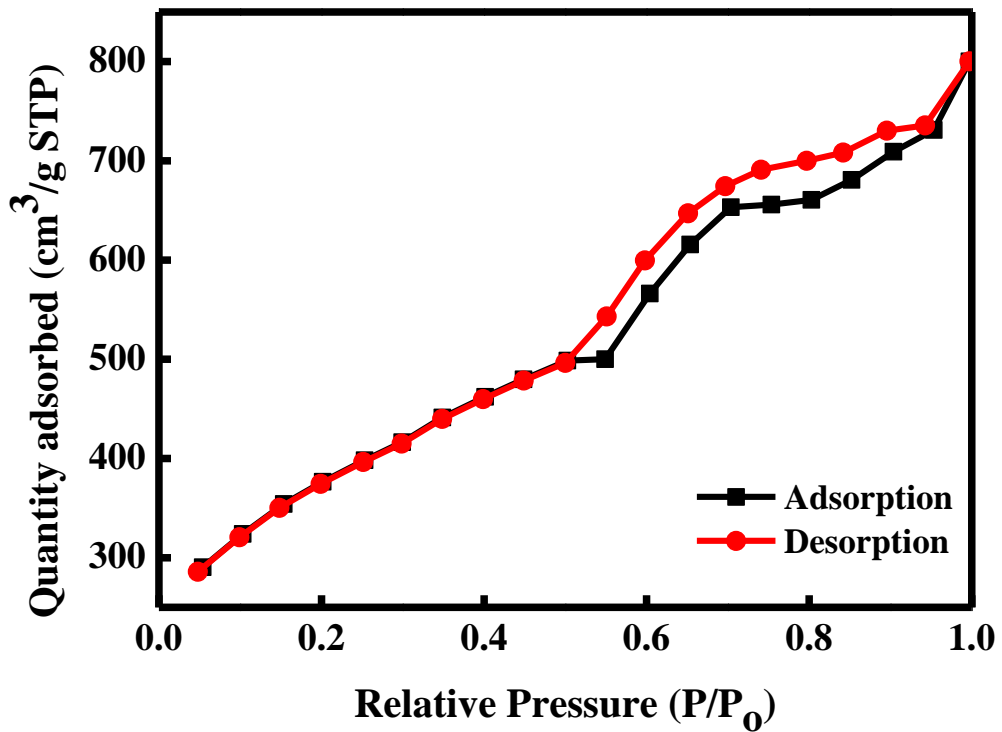


**Figure 4.9:-** The N<sub>2</sub> adsorption-desorption isotherm of I-C-corncob ( $I_R = 1 - I_T = 5$  h -  $C_t = 8$  h -  $C_T = 723$  K).

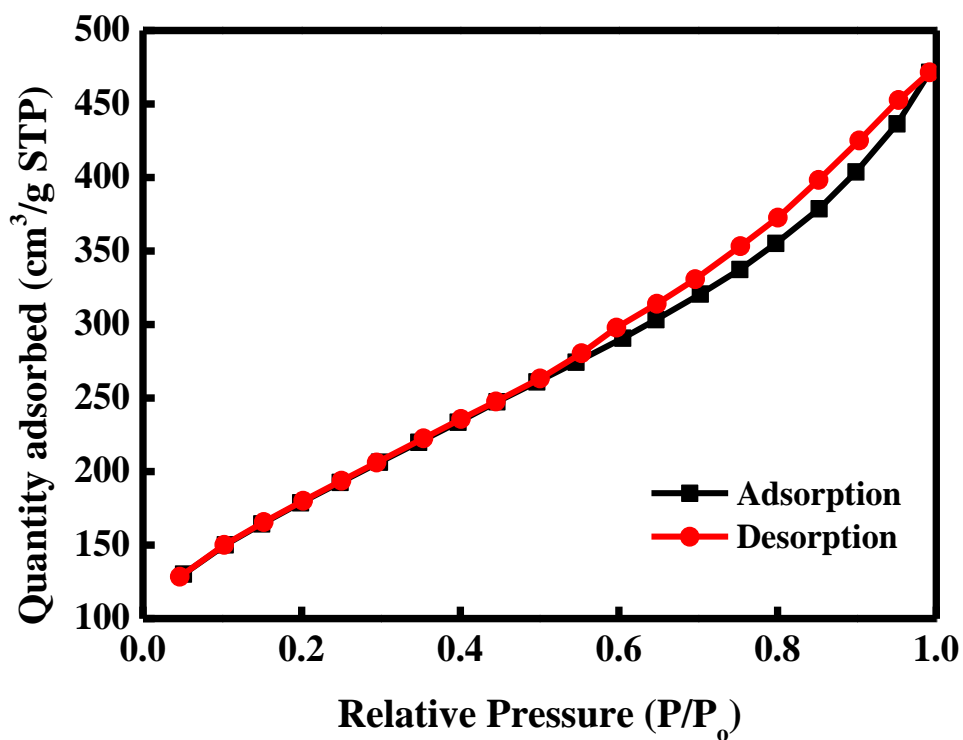


**Figure 4.10:-** The N<sub>2</sub> adsorption-desorption isotherms of I-C-corncob ( $I_R = 1 - I_T = 5$  h -  $C_t = 8$  h -  $C_T = 773$  K).

**Table 4.1:-** Acid Densities and Surface Area of I-C-corncob at Various Carbonization Temperatures

I-C-corncob	Acid densities (mmol/g catalyst)		Surface area, $S_{BET}$ (m <sup>2</sup> /g)
	COOH	OH	
$I_{R=1}^{t=5} - C_{T=523}^{t=8}$	2.05	1.25	113
$I_{R=1}^{t=5} - C_{T=623}^{t=8}$	1.96	1.16	116
$I_{R=1}^{t=5} - C_{T=673}^{t=8}$	1.88	0.26	1226
$I_{R=1}^{t=5} - C_{T=723}^{t=8}$	2.22	0.18	1268
$I_{R=1}^{t=5} - C_{T=773}^{t=8}$	1.06	0.52	613

**Table 4.2:-** Acid Densities of the Synthesized Catalyst

S.No.	I-C-S-corncob catalyst	Acid densities (mmol/g catalyst)			
		SO <sub>3</sub> H	COOH	OH	Total
1	$I_{R=0}^{t=0} - C_{T=723}^{t=8} - S_{T=393}^{t=15}$	0.16	0.38	0.19	0.73
2	$I_{R=0.5}^{t=5} - C_{T=723}^{t=8} - S_{T=393}^{t=15}$	1.73	1.06	0.56	3.35
3	$I_{R=1}^{t=5} - C_{T=723}^{t=8} - S_{T=393}^{t=15}$	3.16	2.22	0.18	5.56
4	$I_{R=1.25}^{t=5} - C_{T=723}^{t=8} - S_{T=393}^{t=15}$	1.02	3.78	0.21	5.01
5	$I_{R=1}^{t=1} - C_{T=723}^{t=8} - S_{T=393}^{t=15}$	0.89	0.46	0.19	1.54
6	$I_{R=1}^{t=10} - C_{T=723}^{t=8} - S_{T=393}^{t=15}$	0.96	1.88	0.19	3.03
7	$I_{R=1}^{t=5} - C_{T=523}^{t=8} - S_{T=393}^{t=15}$	1.62	2.07	1.24	4.93
8	$I_{R=1}^{t=5} - C_{T=623}^{t=8} - S_{T=393}^{t=15}$	1.86	1.99	1.14	4.99
9	$I_{R=1}^{t=5} - C_{T=673}^{t=8} - S_{T=393}^{t=15}$	2.93	1.88	0.27	5.08
10	$I_{R=1}^{t=5} - C_{T=773}^{t=8} - S_{T=393}^{t=15}$	0.59	1.06	0.63	2.28
11	$I_{R=1}^{t=5} - C_{T=723}^{t=7.5} - S_{T=393}^{t=15}$	2.68	1.84	0.18	4.70
12	$I_{R=1}^{t=5} - C_{T=723}^{t=8.5} - S_{T=393}^{t=15}$	2.96	1.86	0.22	5.04
13	$I_{R=1}^{t=5} - C_{T=723}^{t=8} - S_{T=383}^{t=15}$	2.65	1.82	0.21	4.68
14	$I_{R=1}^{t=5} - C_{T=723}^{t=8} - S_{T=403}^{t=15}$	0.98	1.78	0.14	2.90
15	$I_{R=1}^{t=5} - C_{T=723}^{t=8} - S_{T=393}^{t=13}$	1.63	1.88	0.25	3.76
16	$I_{R=1}^{t=5} - C_{T=723}^{t=8} - S_{T=393}^{t=16}$	1.89	1.87	0.26	4.02

Where subscript and superscript in ‘C’ and ‘S’ denotes temperature (K) and time (h) respectively; subscript and superscript in I denotes the impregnation ratio and time (h) respectively.

#### 4.2.2.2 Surface area and pore size distribution of catalysts prepared under optimum conditions

As per the International Union of Pure and Applied Chemistry (IUPAC) classification, the isotherms of both I-C-corncob carbonized at 723 K (Figure 4.9) and I-C-S-corncob (Figure 4.11) falls under type IV class with type H1 hysteresis [192,199]. A similar type of isotherms was observed in the phosphonic functional group-based mesoporous silica [193] and amino-functionalized mesoporous silica [200]. The isotherm, type IV is usually correlated with the materials whose geometry is of mesoporous and most catalysts belong to this category [192,194]. Moreover, the material is generally considered mesoporous when there is a non-overlapping adsorption-desorption curve (hysteresis) at high relative pressures [192].

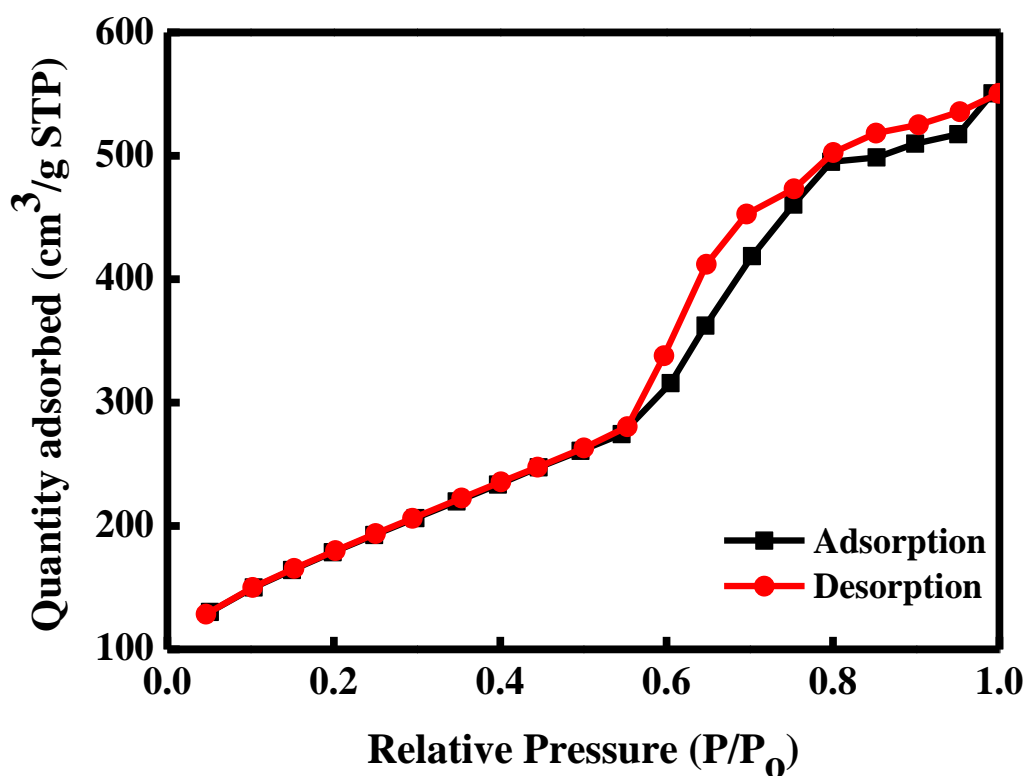


**Figure 4.11:-** The N<sub>2</sub> adsorption-desorption isotherms of I-C-S-corncob catalyst (I<sub>R</sub> = 1 - I<sub>T</sub> = 5 h - C<sub>t</sub> = 8 h - C<sub>T</sub> = 723 K - S<sub>T</sub> = 393 K - S<sub>t</sub> = 16 h).

There are three major groups of porous materials classified based on their size such as microporous (<2nm), mesoporous (2-50 nm) and macroporous (>50 nm) [192]. Mesoporous materials are particularly helpful in reactions involving heavy molecules like triglycerides (5.8 nm), glycerin (0.6 nm), and methyl-oleate (2.5 nm) [121,194,195]. The pore size of the catalysts must be larger than the molecular size of the reactant to make sure successful adsorption of the reactants on active sites. Table 4.3 shows the textural properties such as specific surface area, pore volume, average pore diameter and pore size distribution of the catalysts.

**Table 4.3:-** Textural Properties of the Synthesized Catalyst

Property		I-C-corncob	I-C-S-corncob
Surface area, $S_{BET}$ ( $m^2/g$ )		1268.00	641.60
Pore volume ( $cc/g$ )		1.184	7.312E-1
Average pore diameter ( $A^\circ$ )		3.73E+1	4.56E+1
Pore size distribution (%)	Microporous (<2 nm)	13.60	6.92
	Mesoporous (2-50 nm)	76.90	64.29
	Macroporous (>50 nm)	9.50	28.79

The pore diameter of the I-C-S-corncob is 4.56 nm which could allow the moderately bulk oleic acid molecule to get access to the active site easily during the reaction. Moreover, it also lowers the mass transfer resistance to the flow of reactants from the mouth of the pore to the active site and products from the active site to the surface of the pore [195,201]. Furthermore, when the size of the mesoporous material matches the reactant molecular dimension, the reactant will be deeply absorbed into the internal surface of mesoporous material than on the external surface [200]. The decrease in the specific surface area of the I-C-corncob (1268  $m^2/g$ ) after sulfonation; I-C-S-corncob (641  $m^2/g$ ) is due to loading of  $SO_3H$  groups on the

surface [187]. The specific surface area of I-C-corncob is 1268 m<sup>2</sup>/g, which is higher than that of C-corncob. It shows the effectiveness of the phosphoric acid as an activating agent and the addition of it leads to the form of a porous structure in the carbon [152,187]. Arancon et al. [151] prepared the SAC by sulfonating (sulfonation temperature = 423 K) the valorized corncob (carbonization temperature = 873 K) and obtained a microporous structure with the specific surface area of 120 m<sup>2</sup>/g. Therefore, the present catalyst showed the highest specific surface area (641 m<sup>2</sup>/g) with a coveted mesoporous geometry compared to the catalyst obtained by Arancon et al. [151].

#### **4.2.3 XRD analysis of the catalyst**

XRD spectra's of I-C-corncob and I-C-S-corncob from Figure 4.12 shows a broad diffraction peak in the range of  $2\theta = 15-35^\circ$ . This pattern ascribes to the amorphous carbon composed of polycyclic aromatic carbon sheets oriented in a very random fashion [150,151,202]. The weak band at  $2\theta = 40-50^\circ$  show the graphite plane in amorphous carbon [202]. After sulfonation, the amorphous carbon structure ( $2\theta = 15-35^\circ$ ) remained unaltered. Whereas, the weak diffraction band at  $2\theta = 40-50^\circ$  becomes more visible, suggesting further carbonization by sulfuric acid during sulfonation [133]. These results are consistent with the acid densities of catalysts observed at various sulfonation temperatures as presented in Table 4.2. For instance, at a sulfonation temperature of 383 K, the observed SO<sub>3</sub>H group density was 2.65 mmol/g catalyst. While under a sulfonation temperature of 403 K, the SO<sub>3</sub>H group density observed was only 0.96 mmol/g catalyst. However, when the sulfonation temperature was at its optimum (393 K) the observed SO<sub>3</sub>H density (3.16 mmol/g catalyst) and total density (5.56 mmol/g catalyst) was the highest. It suggests that increasing the sulfonation temperature beyond 393 K, further carbonization by H<sub>2</sub>SO<sub>4</sub> may be prevalent and causes hindrance in anchoring of SO<sub>3</sub>H groups to the surface [133,140,150]. Thus, this produces a rigid catalytic structure with lesser SO<sub>3</sub>H group density at 403 K.

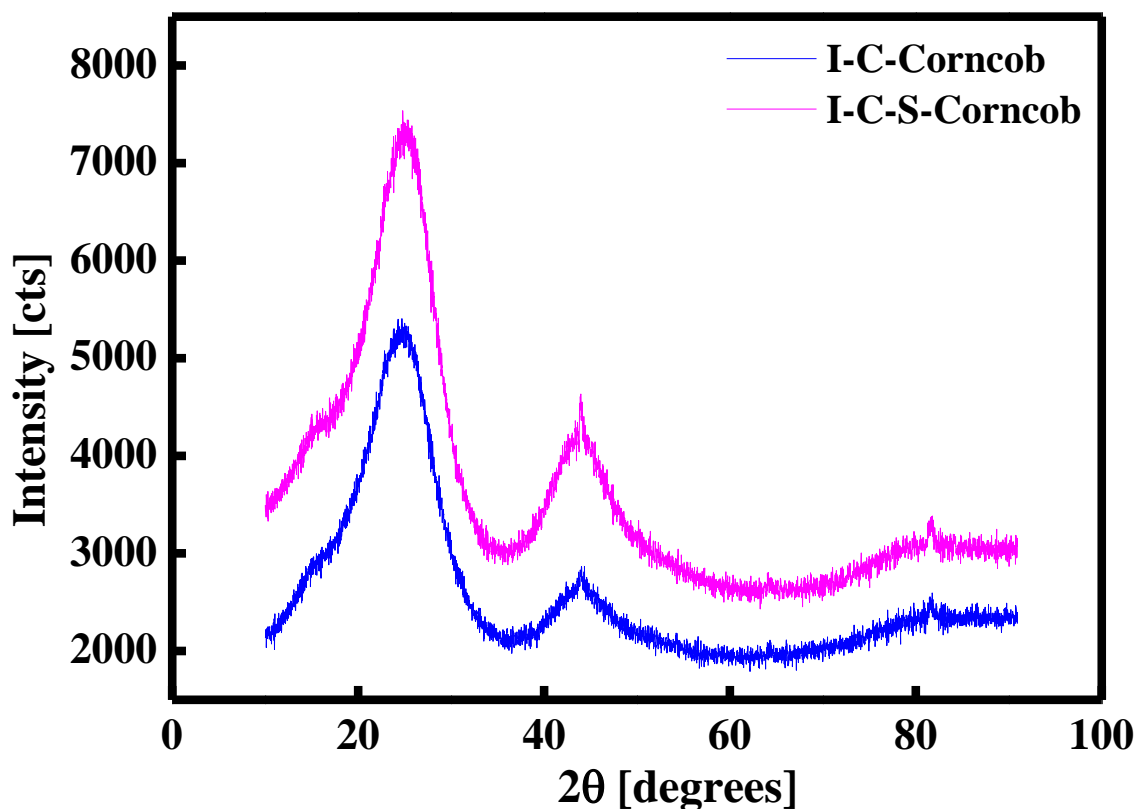


**Figure 4.12:-** XRD patterns of the impregnated and carbonized-corncob ( $I_R = 1$  -  $I_T = 5$  h -  $C_t = 8.5$  h -  $C_T = 723$  K), impregnated, carbonized and sulfonated-corncob catalyst ( $I_R = 1$  -  $I_T = 5$  h -  $C_t = 8.5$  h -  $C_T = 723$  K -  $S_T = 393$  K -  $S_t = 16$  h).

#### 4.2.4 Effect of catalyst synthesis parameters

The influence of catalyst synthesis parameters such as  $H_3PO_4$  impregnation ratio (0-1.25), impregnation time (1-20 h), carbonization temperature (423-823 K), carbonization time (0-10 h), sulfonation temperature (353-413 K) and sulfonation time (12-19 h) on catalytic activity was studied and the optimum synthesis parameters were determined.

##### 4.2.4.1 Effect of impregnation ratio

Impregnation ratio ( $I_R$ ) of an activating agent plays a major role in defining the efficiency of the activation process. Since, beyond a threshold value of  $I_R$ , the efficiency of the activation process reduces [203]. According to Figure 4.13, increasing the  $I_R$  from 0 to 1 increases the oleic acid conversion. At the  $I_R$  of 1, the highest conversion observed was 94.32 % and

further increasing the  $I_R$ , there was a marked decrease in the conversion observed. The possible reason behind this behavior is due to the bond cleavage and cross-linkage phenomenon ( $H_3PO_4$  acts as a catalyst) or insulating layer phenomenon ( $H_3PO_4$  acts as a catalyst poison) [152]. When the particles of corncob impregnated with the phosphoric acid solution, it acts as a catalyst with two positive sides and one negative side. The positive sides of the phosphoric acid promote bond cleavage and facilitate the cross-linkage of phosphates and polyphosphates via cyclization, condensation, and formation. It suggests that the more the amount of phosphoric acid added, the higher will be the number of polyphosphates formed. During washing and on separation, these phosphates and polyphosphates leave the porous cavities in the material. Subsequently, these pores are the assets to accommodate a large number of sulfonic acid groups. In the present case, this phenomenon was associated up to the  $I_R$  of 1, owing to the increase in oleic acid conversion. When the amount of phosphoric acid used is excess, the formed polyphosphates come in contact with each other resulting in thinning of the pore wall. Finally, they form an insulating layer over the corncob particles (catalyst poison) which decrease the surface area and results in lower acid density. It could be the reason behind the decrease in the oleic acid conversion beyond  $I_R$  of 1.0. This phenomenon is clear from the acid densities of the catalysts given in Table 4.2. For instance, the acid density of the synthesized catalyst showed an increase in total acid density from 3.35 to 5.56 mmol/g when  $I_R$  was increased from 0.5 to 1, respectively. Moreover, the catalyst obtained at  $I_R = 1$  contains the higher  $SO_3H$  group (3.16 mmol/g) density compared to this density at  $I_R = 0.5$  (1.73 mmol/g). However, increasing the  $I_R$  from 1 to 1.25 decreases the total acid density of the catalyst. Moreover, the acid density of  $SO_3H$  group reduced drastically from 3.15 mmol/g (at  $I_R = 1$ ) to 1.02 mmol/g (at  $I_R = 1.25$ ) compared to the decrease in total acid density from 5.56 mmol/g (at  $I_R = 1$ ) to 5.01 mmol/g (at  $I_R = 1.25$ ).

Therefore, due to the highest conversion and acid densities at  $I_R$  of 1, during the further experiments, this ratio was kept constant.

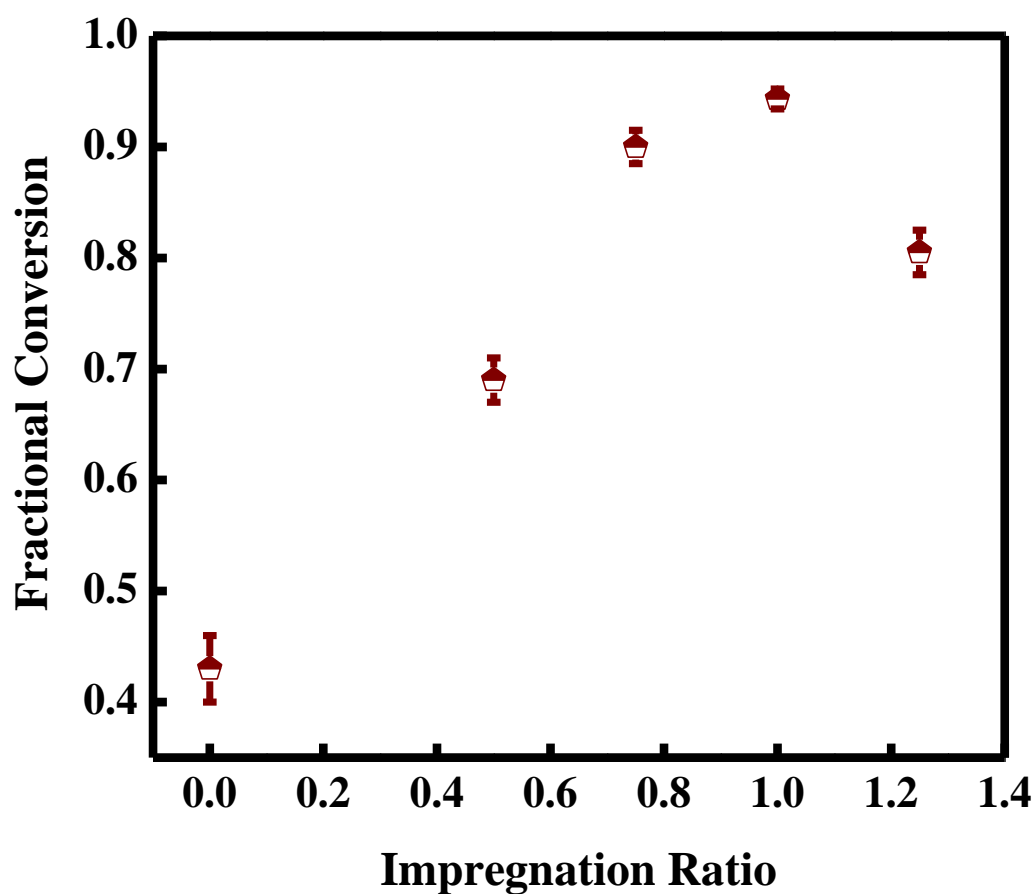


**Figure 4.13:-** Effect of  $H_3PO_4$  impregnation ratio on conversion of oleic acid ( $I_t = 10$  h -  $C_t = 10$  h -  $C_T = 673$  K -  $S_T = 393$  K -  $S_t = 16$  h).

#### 4.2.4.2 Effect of impregnation time

Time of impregnation also has a strong influence on the conversion and holds a similar effect as that of impregnation ratio. In accordance with Figure 4.14, there was an increase in oleic acid conversion from 28 to 94.4% with an increase in the impregnation time ( $I_t$ ) from 1 to 5 h, respectively. Increasing the  $I_t$  beyond 5 h does not affect the conversion. This behavior demonstrates that during the shorter  $I_t$  (1 h),  $H_3PO_4$  acts as an oxidation inhibitor for carbon oxidation. As the  $I_t$  increased to 5 h, the more amount of volatile compounds (tars) gets

detached from the surface resulting in higher amounts of polyphosphates formation [152]. Consequently, the activity of the catalyst was higher between 5 and 10 h of impregnation time. The decline in conversion at higher  $I_t$  is due to wall thinning and formation of an insulating layer over the corncob particles. On the basis of these observations, the impregnation ratio ( $I_R$ ) of 1 and impregnation time ( $I_t$ ) of 5 h was held constant for further studies.

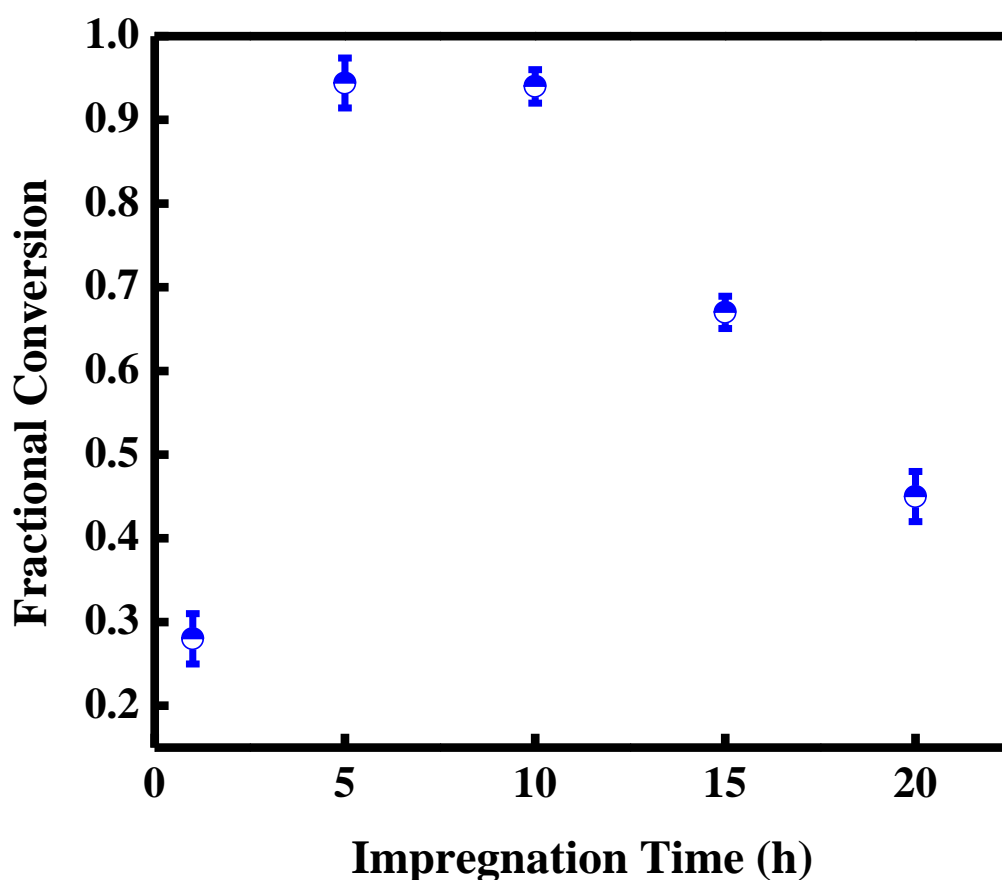


**Figure 4.14:-** Effect of  $H_3PO_4$  impregnation time on oleic acid conversion ( $I_R = 1 - C_t = 10$  h -  $C_T = 673$  K -  $S_T = 393$  K -  $S_t = 16$  h).

#### 4.2.4.3 Effect of carbonization temperature

The effect of  $C_T$  on the oleic acid conversion in the range of 423-823 K as shown in Figure 4.15 observed the highest catalytic activity with 94.2 % conversion at a  $C_T$  of 723 K. There was a higher impact of  $C_T$  on oleic acid conversion when  $C_T$  was above 723 K compared to

the  $C_T$  below 723 K. Almost there was a linear increase in the conversion upon increasing the  $C_T$  from 423-723 K. Moreover, there was no significant increase in the conversion observed with increasing  $C_T$  from 673-723 K. This behavior is due to the phenomenon that incomplete carbonization of organic wastes at lower temperatures leads to a less rigid structure with higher densities of highly hydrophilic -OH groups [133]. This phenomenon is clear from the acid densities of the catalysts given in Table 4.2. If the -OH group concentrations are high, the water (generated during esterification) adsorbs on the catalyst surface at faster rates than the more hydrophobic molecule like oleic acid [170]. It consecutively reduces the conversion to a significant extent.

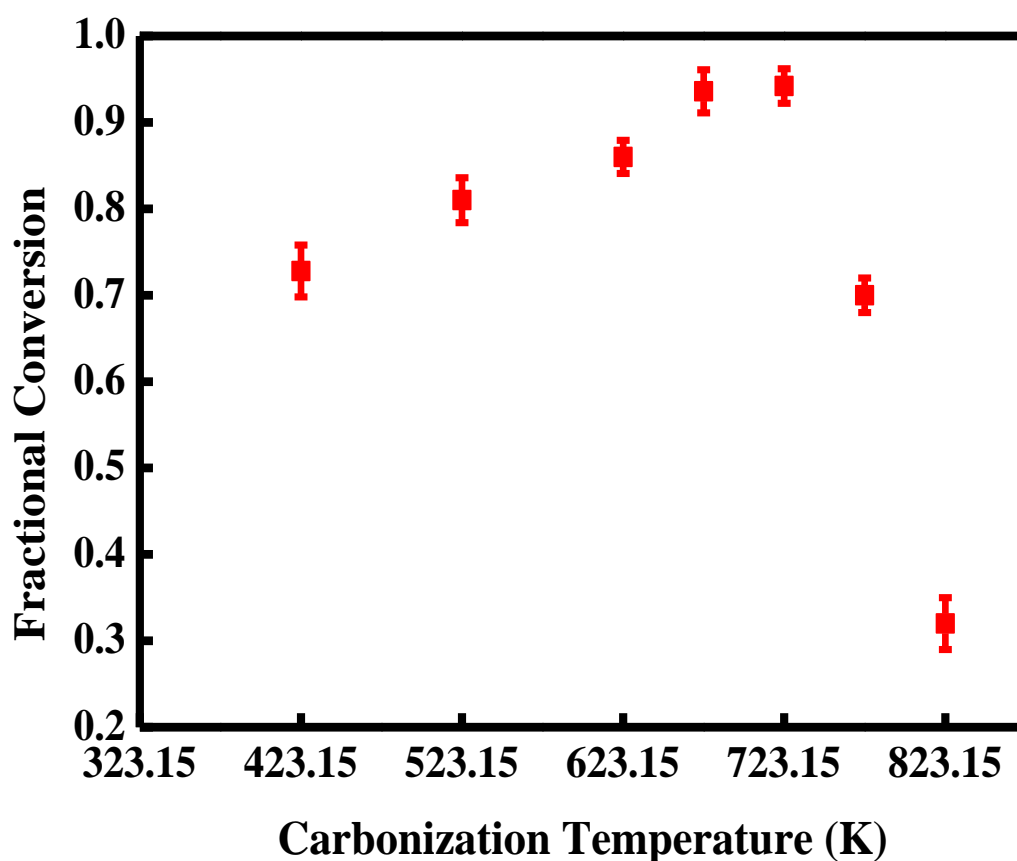


**Figure 4.15:-** Effect of carbonization temperature on oleic acid conversion ( $I_R = 1$  -  $I_t = 5$  h -  $C_t = 10$  h -  $S_T = 393$  K -  $S_t = 16$  h).

Thus, increase in  $\text{SO}_3\text{H}$  group and decrease in  $-\text{OH}$  group concentrations result in the higher conversion of oleic acid up to the  $C_T$  of 723 K. Further, increasing the  $C_T$  beyond 723 K, conversion reduces drastically. Therefore, in further experiments, 723 K has held constants. The reason behind the decrease in conversion at temperatures higher than 723 K is due to that impregnated corncob when heated at high temperatures forms a more rigid catalytic structure with lower  $\text{SO}_3\text{H}$  densities [133]. The similar trend was also observed in the available literature [133,140,202,204] and reported their optimum  $C_T$  in between 648-773 K. In a study conducted by Lou et al. [133], synthesized SAC based on bagasse and found optimum  $C_T$  as 648 K. Endut et al. [140] observed 773 K as optimum  $C_T$  for coconut shell-derived SAC. Also, Lokman et al. [202] found 673 K as optimum  $C_T$  for starch-derived SAC. Samori et al. [204] reported 693 K as optimum  $C_T$  for molasses-derived SAC.

#### ***4.2.4.4 Effect of carbonization time***

The effect of carbonization time ( $C_t$ ) on conversion of oleic acid shown in Figure 4.16 exhibits increasing conversion with  $C_t$ . Similar to the  $C_T$ , increasing the  $C_t$  from 1 to 8 h results in the higher conversion values. There was a sudden jump in reaction conversion while increasing the  $C_t$  from 6.5 to 7.5 h. The maximum of 94% conversion observed at a  $C_t$  of 8 h, after that, it remains almost constant. Therefore, 8 h  $C_t$  was considered optimum for catalyst synthesis. Carbonization at optimum temperature and time produces a robust catalyst with polycyclic aromatic rings which can accommodate a higher density of  $\text{SO}_3\text{H}$  groups [150]. The reason behind the increased conversion is due to this higher density of  $\text{SO}_3\text{H}$  groups. Some studies reported optimum  $C_t$  of 15 h for sulfonated carbon-based SAC derived from carbohydrates [136,139]. Whereas, in sulfonated carbon-based SAC derived from bagasse and coconut shell, the optimum  $C_t$  observed was 0.5 h and 4 h, respectively [133,140].

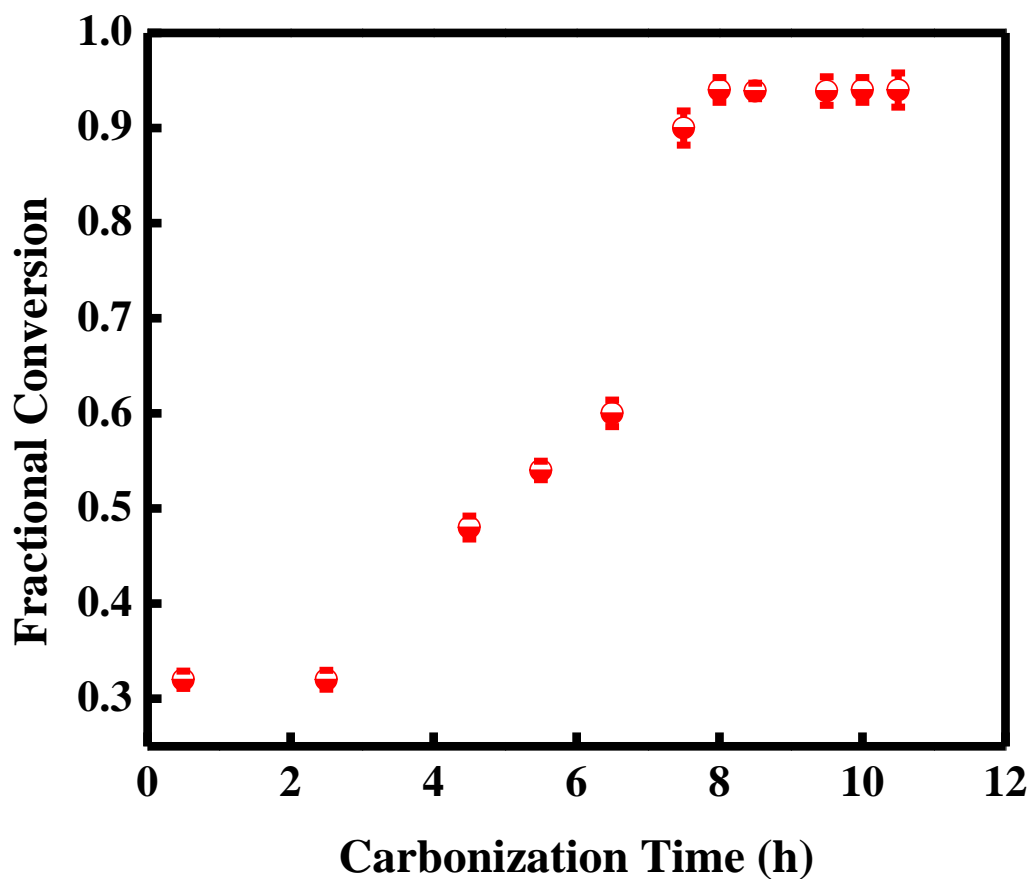


**Figure 4.16:-** Effect of carbonization time on oleic acid conversion ( $I_R = 1$  -  $I_t = 5$  h -  $C_T = 723$  K -  $S_T = 393$  K -  $S_t = 16$  h).

#### 4.2.4.5 Effect of sulfonation temperature

After carbonization, the synthesis parameters optimized were sulfonation temperature ( $S_T$ ) and sulfonation time ( $S_t$ ). Figure 4.17 shows the effect of  $S_T$  on oleic acid conversion. As the  $S_T$  increases, oleic acid conversion also increases leading to highest conversion at 393 K. The high conversion was due to the higher acid density of the catalyst at 393 K, as shown in Table 4.2. There was a sudden drop in the conversion value beyond  $S_T$  of 393 K. It is because, after carbonization at 723 K for 8 h, further carbonization using sulfuric acid at higher temperatures, produce a rigid catalytic structure with lesser  $SO_3H$  group density. The lower density of  $SO_3H$  group results in lesser active sites for the reaction. These observations are

consistent with the findings of various other researchers[133,140,150]. They have reported that lower  $S_T$  favors the anchoring of  $SO_3H$  groups on the catalyst surface.

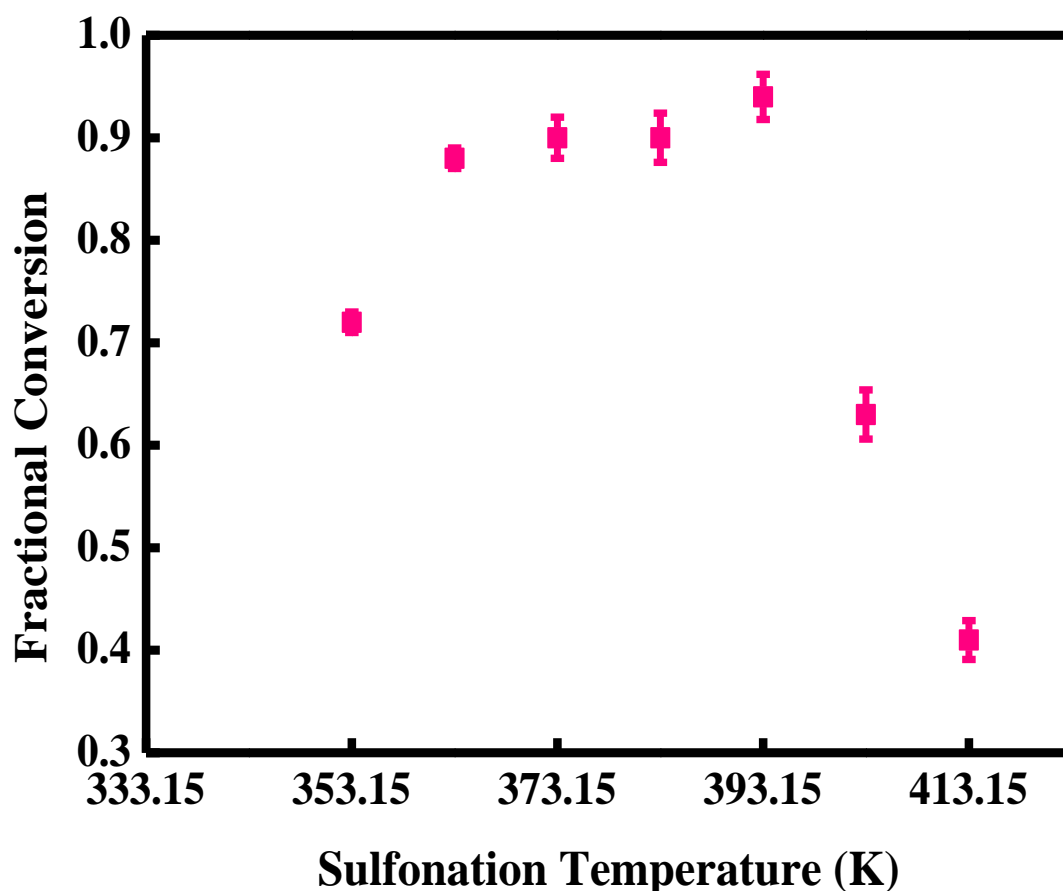


**Figure 4.17:-** Effect of sulfonation temperature on oleic acid conversion ( $I_R = 1$  -  $I_t = 5$  h -  $C_t = 8.5$  h -  $C_T = 723$  K -  $S_t = 16$  h).

#### 4.2.4.6 Effect of sulfonation time

There was an increase in oleic acid conversion observed with increasing sulfonation time ( $S_t$ ) from 12 to 15 h, as shown in Figure 4.18. It is due to the higher  $SO_3H$  density (5.56 mmol/g) of the catalyst obtained at 15 h  $S_t$ , as given in Table 4.2. Further, increasing the  $S_t$  decreased the oleic acid conversion. It is because of the carbon surface saturation at prolonged sulfonation time which causes hindrance in the anchoring of  $SO_3H$  groups [150]. The reported optimum  $S_t$  for bagasse, coconut shell, and corncob derived catalysts were 20, 15

and 10 h, respectively [133,140,150]. On the basis of the current results, a sulfonation time of 15 h was considered as optimum.

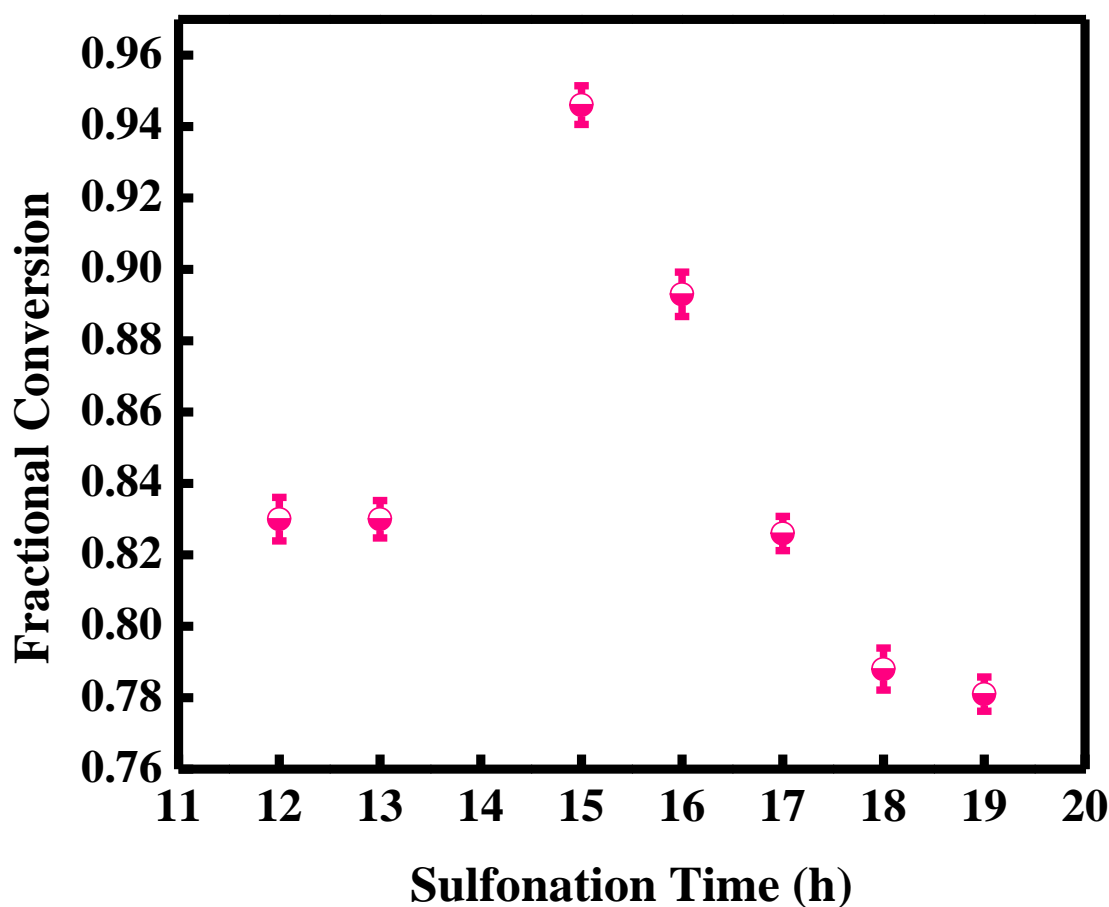


**Figure 4.18:-** Effect of sulfonation time on-oleic acid conversion ( $I_R = 1$  -  $I_t = 5$  h -  $C_t = 8.5$  h -  $C_T = 723$  K -  $S_T = 393$  K).

#### 4.2.5 Esterification of oleic and palmitic acid

To find the best-operating conditions of the esterification reaction, the reaction variables such as temperature ( $T = 328$ - $343$  K), time ( $t = 1$ - $4$  h), reactants molar ratio ( $R = 1$ : $7$ - $1$ : $10$ ), catalyst loading ( $w = 5$ - $20$  wt. %) and catalyst reusability (up to 20 runs) were further evaluated.

#### 4.2.5.1 Effect of reaction time and temperature

Experimental results show that conversions of both oleic acid and palmitic acid increase with an increase in the reaction temperature (Figures 4.19) and time (Figure 4.20). The highest conversion in case of oleic acid and palmitic acid was 96.5% and 97.5%, respectively observed within 4h at 338 K. There was a significant effect of temperature on the oleic acid and palmitic acid conversions. The oleic acid conversion increased two folds by increasing the reaction temperature from 328 to 333 K. The oleic acid conversion increased only 5% with an increase in the temperature from 333 to 338 K. The effect of temperature on conversion was insignificant beyond 338 K. In the case of palmitic acid, increasing the temperature from 333 to 338 K increases the conversion by only 10%. It is consistent with the reported literature [205]. The conversion observed at 338 K was highest in both the cases of oleic acid and palmitic acid. Therefore, 338 K was held constant in further study.

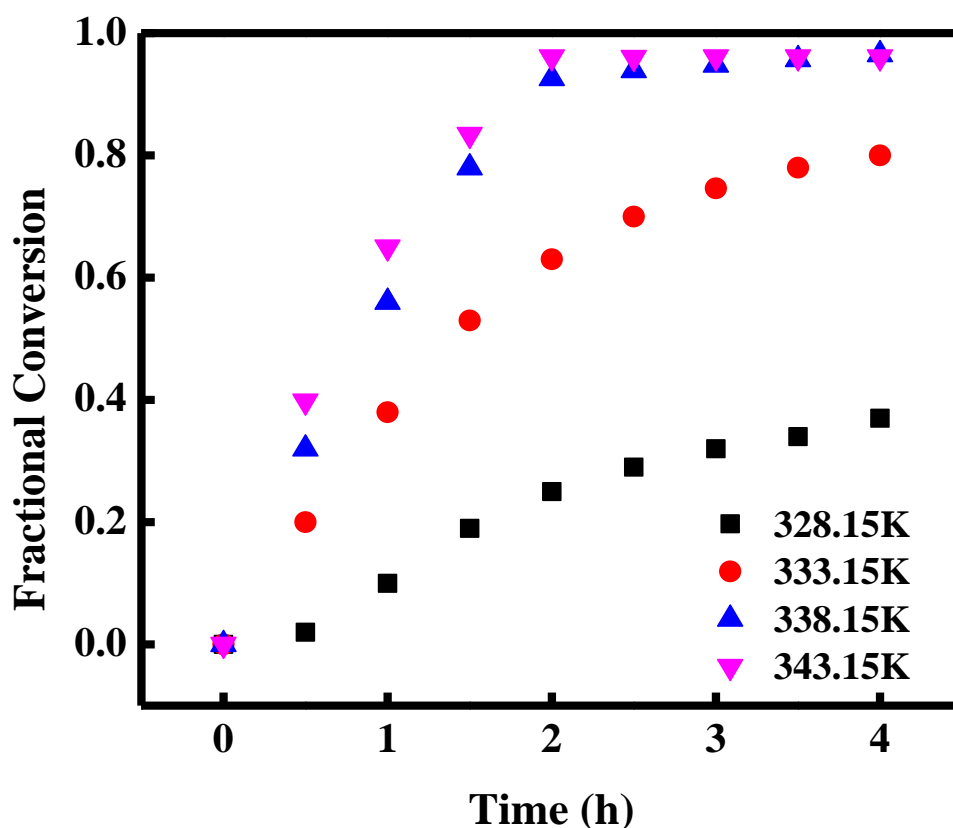


**Figure 4.19:-** Effect of reaction temperature at various intervals on oleic acid conversion (R = 1:9 and w = 8 wt. %).

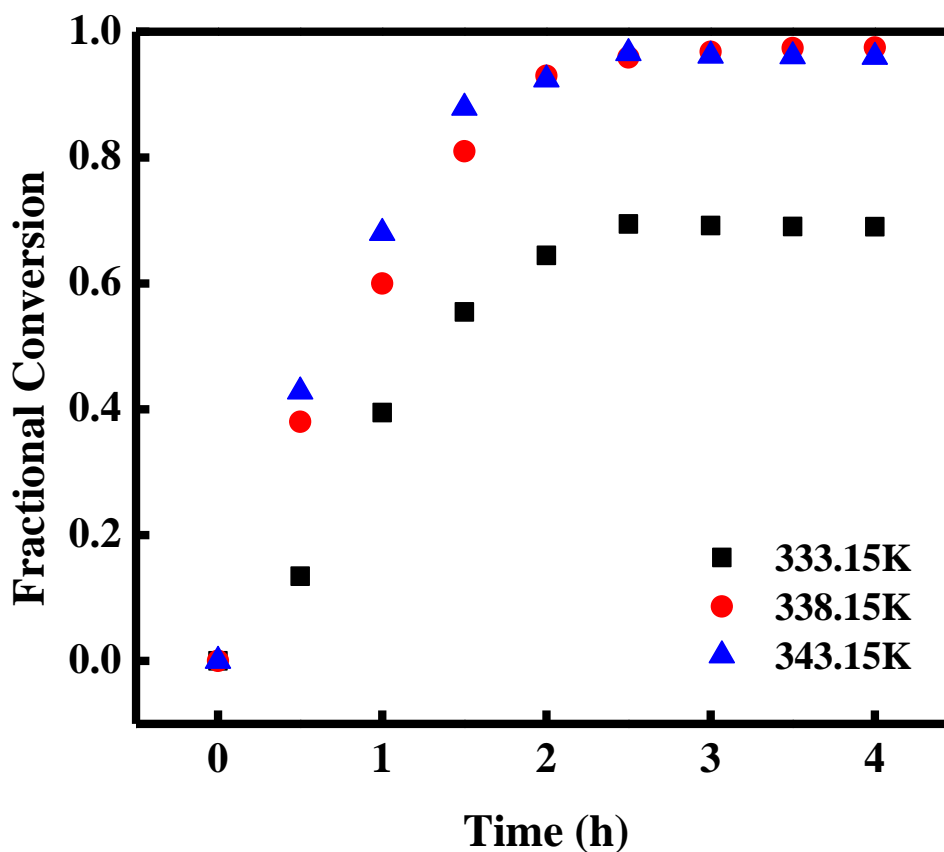


**Figure 4.20:-** Effect of reaction temperature at various intervals on palmitic acid conversion  
(R = 1:9 and w = 8 wt. %).

#### 4.2.5.2 Effect of reactants molar ratio

The molar ratio of fatty acid to methanol is an important factor which not only has a strong influence on fatty acids conversion but, also has a huge impact on the overall production cost. Stoichiometrically, esterification requires only 1:1 molar ratio of fatty acid to methanol. However, due to the reversible nature of the reaction; in practice higher than the stoichiometric ratio is used to drive the reaction towards product formation. Increase in the molar ratio of fatty acid to methanol from 1:7 to 1:10 increases the conversions of both oleic acid and palmitic acid as shown in Figures 4.21 and 4.22. For instance, at 1:7 molar ratio, the observed conversion was only 56.3 and 54.6% in the case of oleic acid and palmitic acid, respectively. However, increasing the ratio to 1:10, the conversions of both oleic and palmitic acid shoot-up to 98.9 and 99.6%, respectively. The progress of the reaction tends to be slower

by providing an insufficient amount of methanol as in the case of 1:7 and 1:8 and consecutively decreases the conversion. Also, the esterification reaction occurs as soon as the fatty acids (oleic/palmitic) chemisorbed on the active sites of the catalyst. Then the protonation of the carbonyl group of the fatty acid gives carbocation, which then reacts with methanol to form oleic/palmitic esters. The approach of methanol molecules towards carbocation enhances when methanol is present in an excess amount and results in the higher conversion of the reaction. However, a large excess of methanol floods the active sites of the catalyst before the chemisorption of fatty acids and hinders the protonation process [206]. Therefore, methanol usage in large excess results in the lower conversion of esterification reaction. The conversion observed was highest at 1:10 oil to methanol molar ratio, thus, this ratio was held constant in further study.

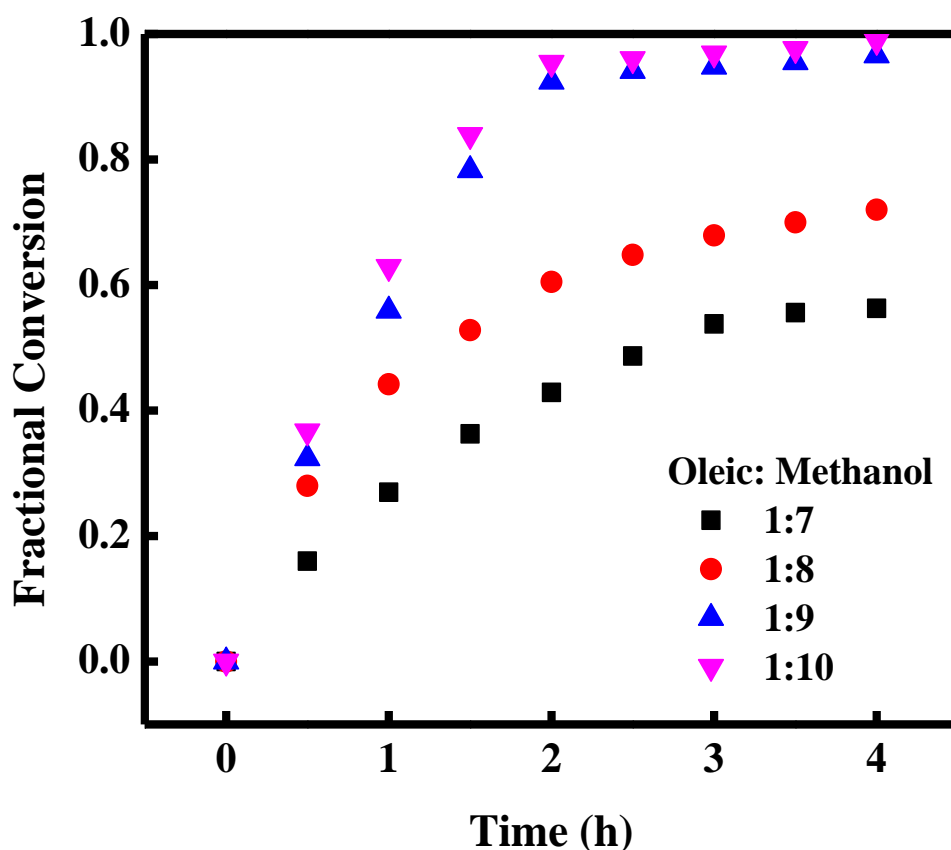


**Figure 4.21:-** Effect of oleic acid to methanol ratio on oleic acid conversion (w = 8 wt. % and T = 338 K).

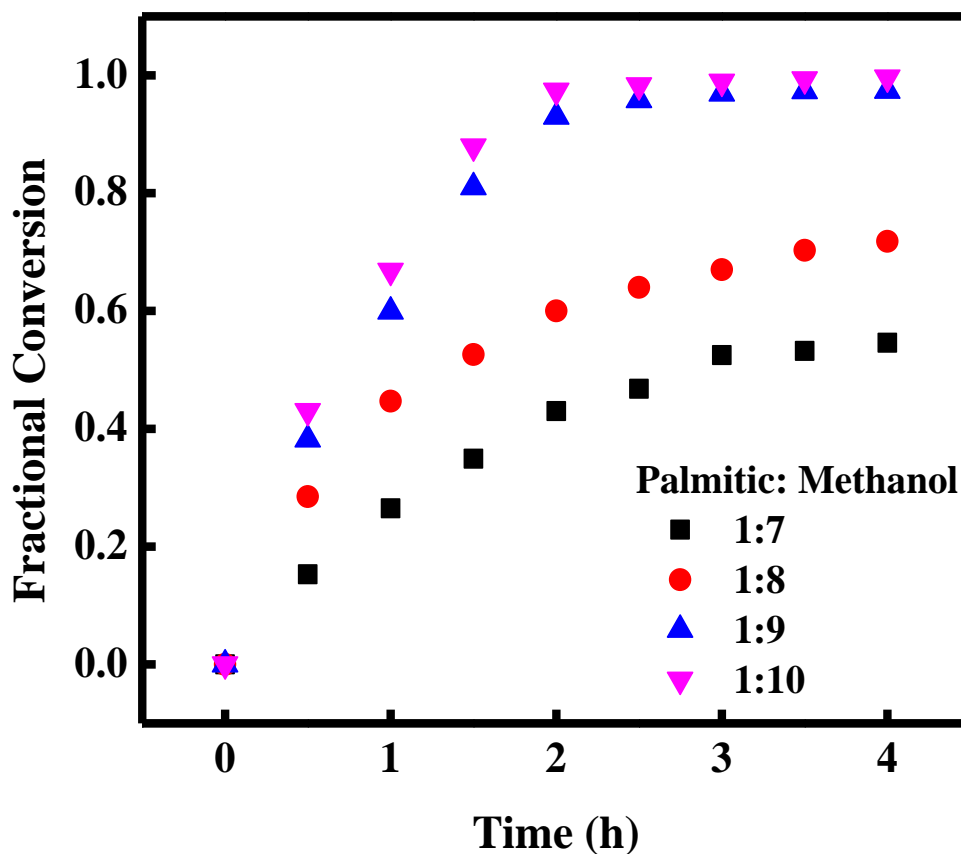


**Figure 4.22:-** Effect of palmitic acid to methanol ratio on palmitic acid conversion ( $w = 8$  wt. % and  $T = 338$  K).

#### 4.2.5.3 Effect of catalyst loading

The optimum catalyst amount required for the reaction evaluated by conducting a reaction using 1:10 molar ratio of fatty acid to methanol at 338 K shows the increasing trend of fatty acids conversion with catalyst loading. In accordance with Figures 4.23 and 4.24, an increase in the catalyst amount from 5 to 10 wt. % increases the conversion of oleic acid from 78.6 to 98.4% and palmitic acid from 78.3 to 98.5% respectively. However, increasing the catalyst loading beyond 10 wt. %, there was no significant increase in the conversion. The amount of solid catalyst determines the amount of surface area and the number of active sites available for the reaction. Increase in the amount of catalyst increases the conversion because of more active sites. It is the phenomenon observed only until a certain amount of catalyst loading.

Further increase in the catalyst amount remains conversion unaffected. For instance, when the catalyst amount provided during the reaction is less, a large number of reactants molecules stay in the pipeline to access the catalyst surface/active site to start the reaction. As a result, the conversion observed is lower due to the limited participation of reactants and lower reaction rates. On the other hand, when the added catalyst amount is higher, the amount of catalyst provided in excess will float around the reactants and reaction speed will not increase further. It will keep the conversion unaffected. However, when an amount of catalyst provided during the reaction is optimum, all the reactant molecules can have access to the catalyst surface which consequently increases the reaction rate and conversion due to the likely participation of all the reactant molecules. It is consistent with the reported literature [207]. Therefore, 10 wt. % catalyst was considered as optimum loading and used in further experiments.

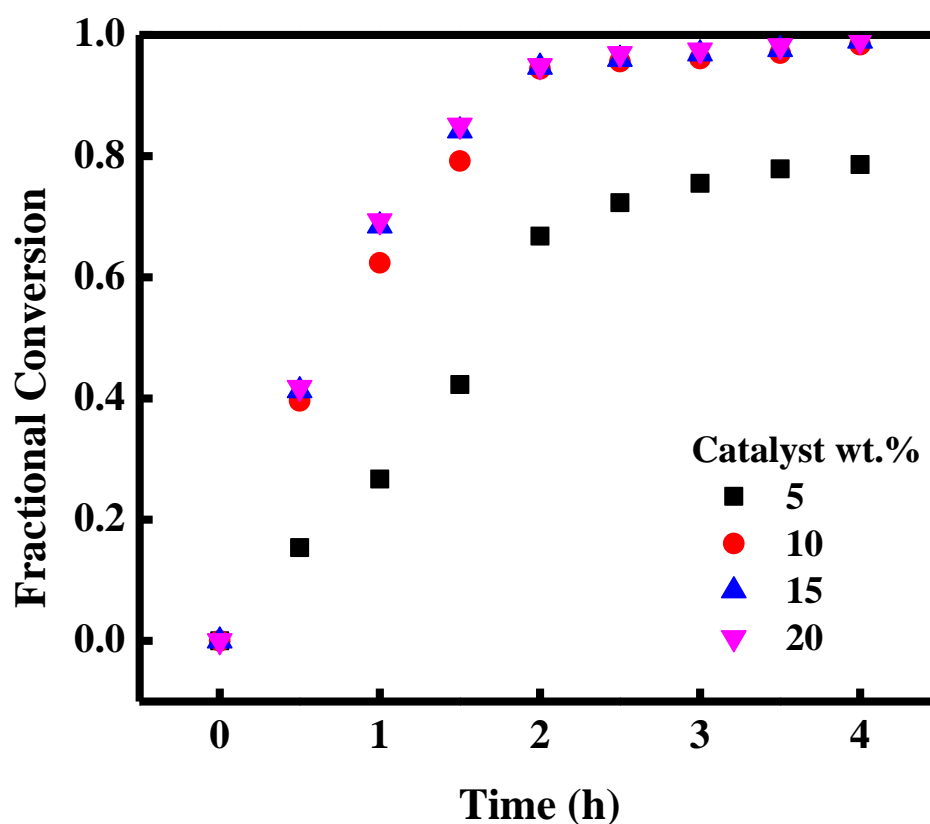


**Figure 4.23:-** Effect of catalyst loading (wt. %) on oleic acid conversion (R = 1:10 and T = 338 K).

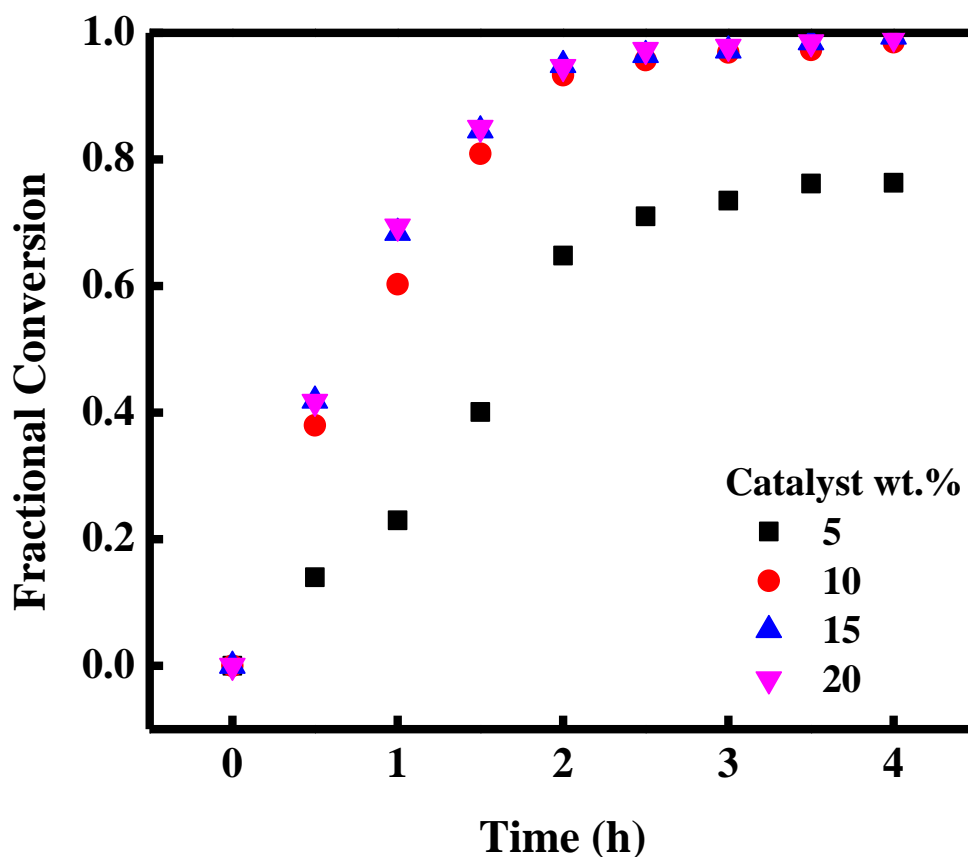


**Figure 4.24:-** Effect of catalyst loading (wt. %) on palmitic acid conversion (R = 1:10 and T = 338 K).

#### 4.2.6 Esterification of FFA in Karanja oil

Vegetable oils and animal fats are the aggregates composed of various types of homogeneous and non-homogeneous blends of fatty acids. Commercially, they are the preferred source to produce biodiesel on large scales due to their abundant availability at cheaper cost compared to individual fatty acids. Esterification of FFA in the feed oil is a significant reaction in the biodiesel production because of an amount of FFA greater than 3 wt. % renders the feed oil unsuitable for the transesterification process. Therefore, it is of great interest to lower the FFA content in the non-edible oil like Karanja oil which has a high amount of FFA's than edible oils. Further, this study extends towards esterification of FFA in Karanja oil.

#### ***4.2.6.1 Effect of reaction temperature and time***

The effect of temperature on the FFA conversion studied by conducting the reaction using a constant 1:10 molar ratio of Karanja oil to methanol and a catalyst loading of 10 wt. % shows an increasing trend of conversion with temperature and time. Increase in the reaction temperature from 328 to 343 K increases the FFA conversion from 39 to ~85%, respectively as shown in Figure 4.25. Increasing the reaction temperature from 338 K to 343 K there was a significant increase in the conversion observed up to 2 h reaction time. However, after 2 h, the conversion values at 338 K and 343 K became identical. The increasing conversion at 343 K is due to the transesterification of triglycerides in the Karanja oil [205]. To start the reaction in acid-catalyzed conditions both triglycerides (TG) and FFA require activation of their carboxylic/carbonyl groups by protonation [208]. Due to the bulkiness of TG molecules, as compared to FFA, the carbonyl group activation of TG requires higher reaction temperatures. The work carried out by Lou et al. [133], using sulfonated SAC derived from bagasse, reported transesterification of TG with simultaneous esterification of FFA at a reaction temperature of 353 K. They achieved a 90% yield due to the esterification along with 8.5% yield due to the transesterification. These findings corroborate with the study of Leung and Gua [167], who ascertained that temperatures higher than 323 K are beneficial to esterify high viscosity and high FFA containing oils like waste vegetable oils and non-edible oils. These findings are also supported by Guan et al. [209], who reported a 97.1% yield of fatty acid methyl ester in 2 h using dimethyl ether as a co-solvent at 353 K.

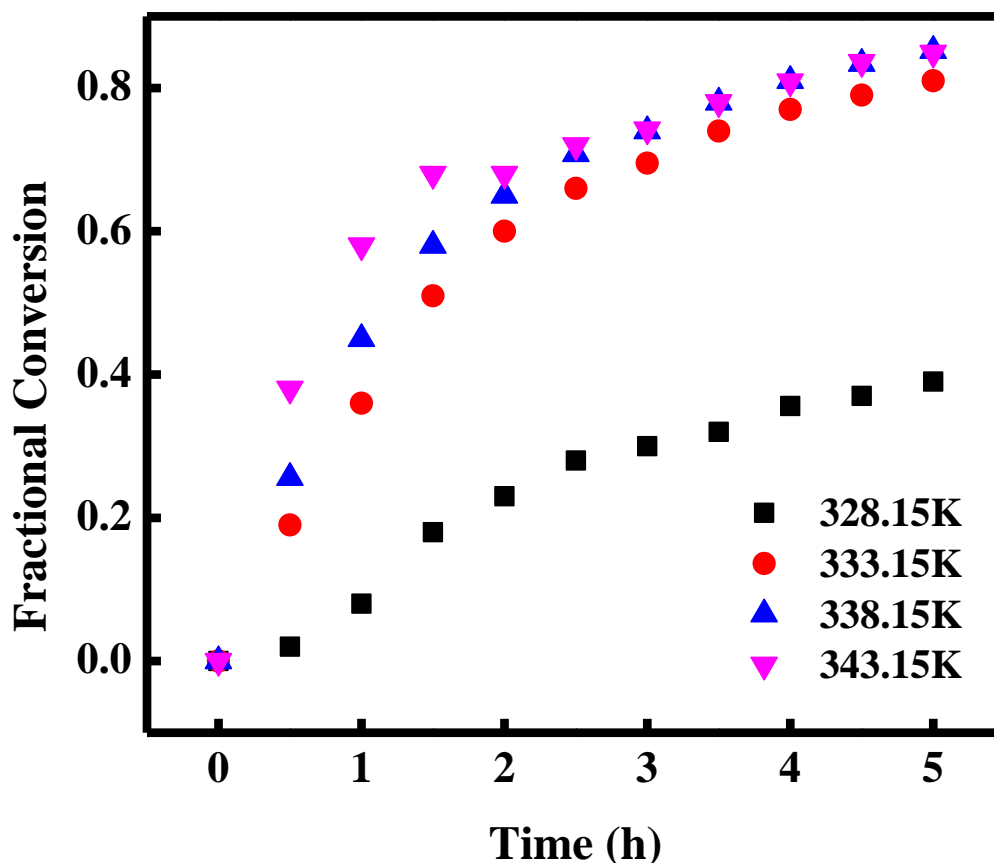


**Figure 4.25:-** Effect of reaction temperature on Karanja oil free fatty acid conversion (R = 1:10 and w = 10 wt. %).

#### 4.2.6.2 Effect of Karanja oil to methanol ratio

Commercial interest always lies in minimizing the use of excess reactants to ease the separation of excess reactants from the product. The reaction conducted at 338 K using 10 wt. % catalyst to study the effect of the molar ratio of Karanja oil to methanol on FFA conversion exhibited a different behavior compared to fatty acids. Scrutinizing Figure 4.26 reveals that, unlike in the case of fatty acids, the molar ratio of reactants has a strong influence on the FFA conversion. Under similar reaction conditions, the amount of methanol required was twice in the case of Karanja oil compared with oleic and palmitic acid. In accordance with Leung et al. [210], more than 1:15 oil to methanol molar ratio is necessary for esterifying oils containing high FFAs. Increasing the molar ratio beyond 1:20 in the present case, does not

change the conversion after 2.5 h, though it affects a bit during an initial period of reaction (0-2.5 h). The primary goal behind using excess methanol is to shift the reaction equilibrium towards the product formation. However, the presence of excessive methanol reduces the catalyst concentration in the total reaction mixture and decreases the possible contact between the reactants and the catalyst. This finding is consistent with Hayyan et al. [205], who reported that molar ratio beyond 1:10 for sludge palm oil esterification does not show any significant change in conversion. Since at 1:20 Karanja oil to methanol molar ratio, there obtained the desired reduction in FFA content (<3 wt. %). Therefore, a 1:20 ratio was chosen as optimum and used in further experiments.

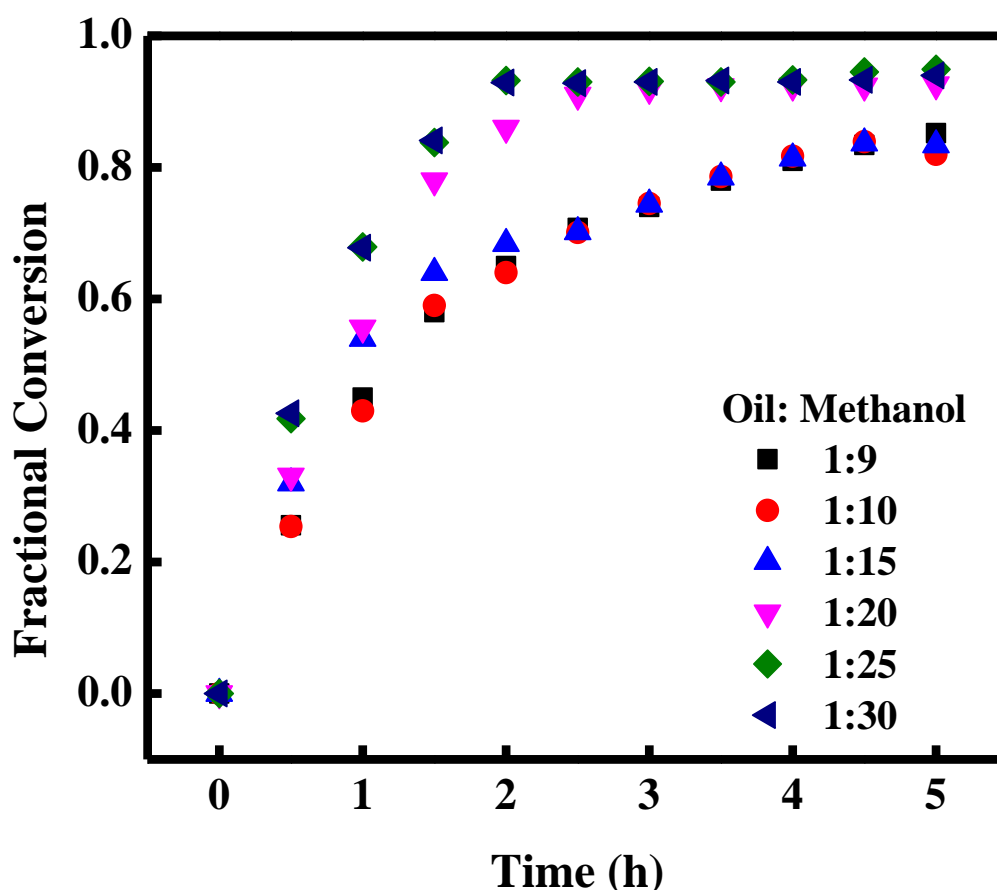


**Figure 4.26:-** Effect of Karanja oil to methanol ratio on free fatty acid conversion (w = 10 wt. % and T = 338 K).

#### 4.2.6.3 Effect of catalyst loading

The amount of solid catalyst determines the amount of surface area and the number of active sites available for the reaction. The optimum catalyst amount required for the FFA conversion evaluated by conducting a reaction using 1:20 molar ratio of Karanja oil to methanol at 338 K shows a similar trend to that of fatty acids. In accordance with Figure 4.27, a maximum of ~50 % FFA conversion observed using a catalyst loading of 5 wt. %.

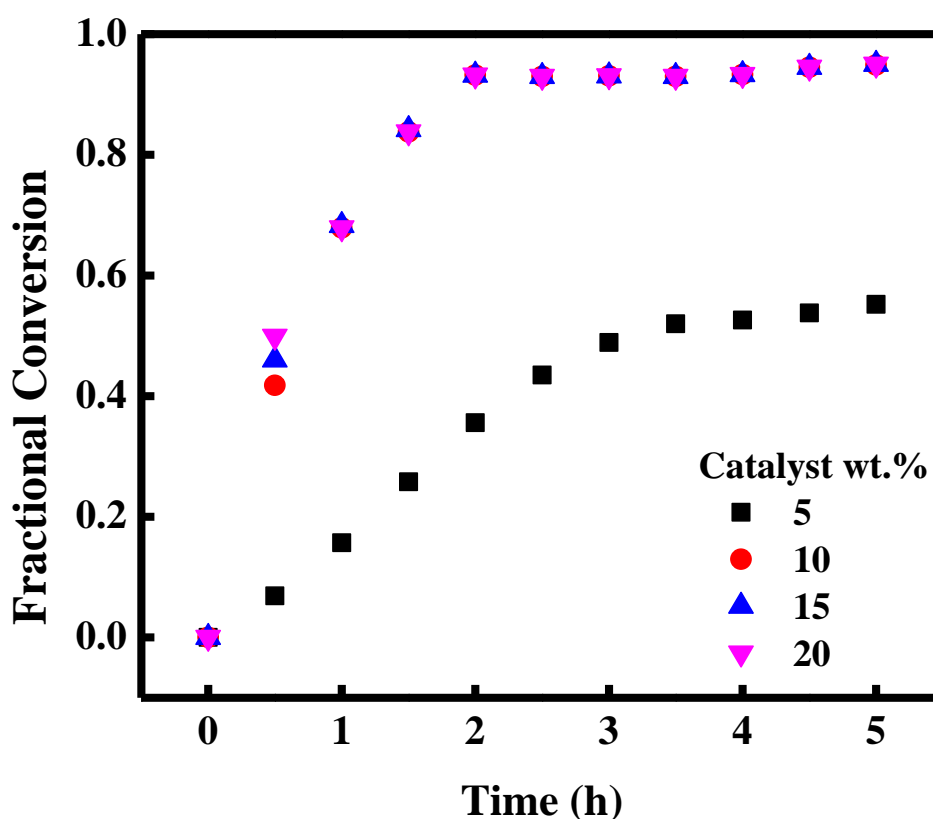


**Figure 4.27:-** Effect of catalyst loading on Karanja oil free fatty acid conversion (R = 1:20 and T = 338 K).

The FFA conversion rises significantly from ~50% to ~93% on increasing the catalyst loading from 5 to 10 wt. %. The increase in the catalyst loading increases the surface area and active sites available for the reaction which enhances the conversion [211]. Further, an increase in the catalyst loading beyond 10 wt. % does not show any significant reduction in

FFA content. Therefore, 10 wt. % catalyst was considered as optimum loading to esterify FFA in Karanja oil.

#### 4.2.7 Reusability of the catalyst

The effectiveness of the catalyst depends on its recoverability and reusability for the biodiesel production. The reusability of the present catalyst was investigated using oleic acid and methanol as a model reaction. The reaction between oleic acid and methanol was conducted at 338 K using a 1:10 molar ratio of oleic acid to methanol and a catalyst loading of 10 wt. %. After completion of the reaction, the reaction mass was withdrawn and filtered through Whatman 40  $\mu\text{m}$  filter paper to recover the catalyst. Then the catalyst was regenerated by washing with 20 ml of solvent (methanol/ ethanol/ n-hexane) and dried at 363 K under vacuum for 3 h. Then the regenerated catalyst was reused in the next cycle of the esterification reaction. The n-hexane was found to be the best regenerating solvent for the present catalyst showing ~90% oleic acid conversion even after the 20th cycle as shown in Figure 4.28.

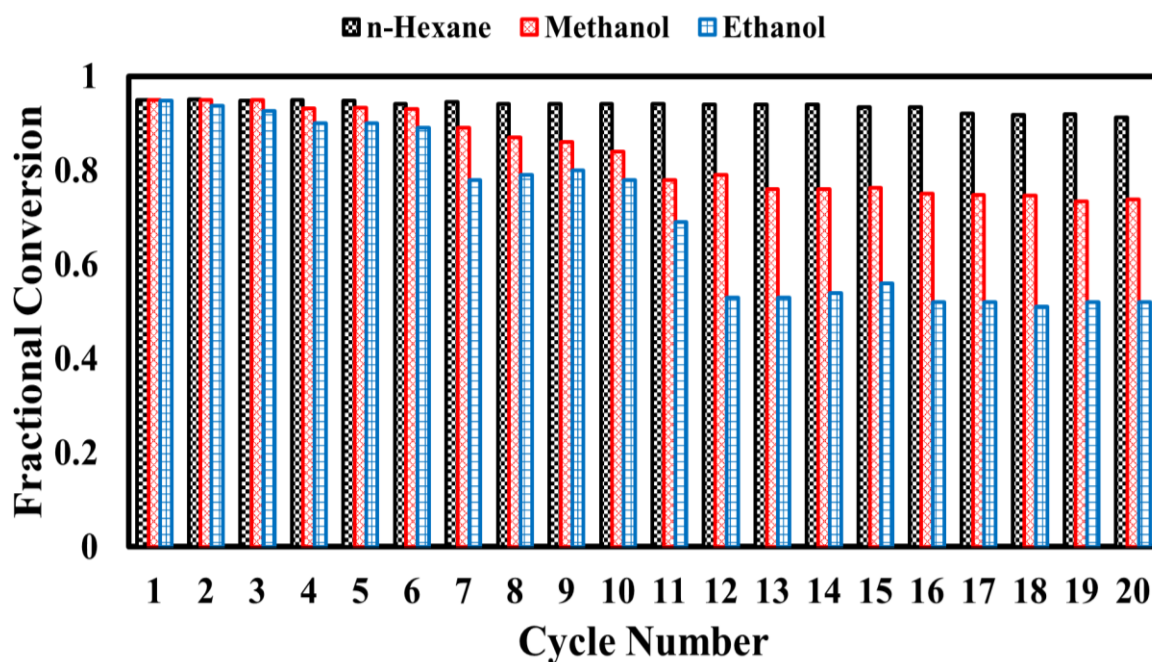


**Figure 4.28:-** Catalyst reusability for oleic acid conversion (R = 1:10, T = 338K and t = 4 h in each cycle).

These findings were consistent with the results reported by Ma et al., [150] for corncob catalyst derived under hydrothermal conditions. The similar performance also observed in case of bagasse-derived solid acid catalyst [133], glucose and starch-derived catalysts [139] and cellulose-derived catalyst [212].

Tables 4.4 and 4.5 shows the estimated acid densities of the spent catalysts washed using various solvents after each esterification cycle. The acid densities of both the spent catalyst (after washing with n-hexane) and the fresh catalyst were found similar as shown in Tables 4.2 and 4.4. Thus, the oleic acid conversion was almost similar in each run. However, washing with methanol and ethanol lowered the acid densities of the spent catalyst as shown in Table 4.5. Consequently, the oleic acid conversion was decreased drastically in each cycle as shown in Figure 4.28. The reduction of the catalyst activity after washing with polar solvents (methanol and ethanol) is due to catalyst poisoning [196]. The poisoning can be attributed to the formation of methyl sulfonate on the carbon surface [212]. This behavior of the catalyst poisoning was also observed by Lou et al. [133] and Aroncon et al. [151]

**Table 4.4:- Acid Densities of the Spent Catalysts Washed with n-Hexane**

Run No.	Acid densities (mmol/g catalyst) of the catalyst: $I_{R=1}^{t=5} - C_{T=723}^{t=8} - S_{T=393}^{t=15}$			
	SO <sub>3</sub> H	COOH	OH	Total
1	3.16	2.22	0.18	5.56
2	3.15	2.22	0.18	5.55
3	3.16	2.22	0.18	5.56
4	3.14	2.22	0.19	5.55
5	3.16	2.22	0.18	5.56
6	3.16	2.22	0.18	5.56
7	3.14	2.22	0.19	5.55
8	3.14	2.22	0.19	5.55
9	3.14	2.22	0.19	5.55
10	3.14	2.22	0.19	5.55
11	3.14	2.22	0.19	5.55
12	3.14	2.22	0.19	5.55
13	3.14	2.22	0.19	5.55
14	3.14	2.22	0.19	5.55
15	3.09	2.18	0.18	5.45
16	3.09	2.18	0.18	5.45
17	3.01	2.16	0.19	5.36
18	2.96	2.16	0.19	5.31
19	2.95	2.15	0.19	5.29
20	2.96	2.15	0.19	5.30

**Table 4.5:- Acid Densities of the Spent Catalysts Washed with Methanol and Ethanol**

Run No.	Acid densities (mmol/g catalyst) of the catalyst: $I_{R=1}^{t=5} - C_{T=723}^{t=8} - S_{T=393}^{t=15}$							
	Methanol washing				Ethanol washing			
	SO <sub>3</sub> H	COOH	OH	Total	SO <sub>3</sub> H	COOH	OH	total
1	3.16	2.22	0.18	5.56	3.16	2.22	0.18	5.56
2	3.14	2.22	0.18	5.54	3.11	2.21	0.18	5.5
3	3.14	2.21	0.18	5.53	3.01	2.19	0.18	5.38
4	2.98	2.22	0.18	5.38	2.98	2.16	0.19	5.33
5	2.98	2.22	0.19	5.39	2.98	2.16	0.19	5.33
6	2.98	2.22	0.21	5.41	2.98	2.16	0.19	5.33
7	2.93	2.22	0.22	5.37	2.63	2.15	0.18	4.96
8	2.91	2.19	0.22	5.32	2.63	2.15	0.18	4.96
9	2.83	2.19	0.22	5.24	2.63	2.15	0.18	4.96
10	2.74	2.16	0.22	5.12	2.63	2.15	0.18	4.96
11	2.69	2.15	0.22	5.06	2.12	2.15	0.19	4.46
12	2.63	2.16	0.22	5.01	1.26	2.12	0.19	3.57
13	2.60	2.14	0.22	4.96	1.26	2.12	0.19	3.57
14	2.60	2.13	0.22	4.95	1.26	2.12	0.19	3.57
15	2.60	2.14	0.22	4.96	1.26	2.12	0.19	3.57
16	2.60	2.14	0.22	4.96	1.26	2.12	0.19	3.57
17	2.60	2.13	0.22	4.95	1.26	2.12	0.19	3.57
18	2.60	2.14	0.22	4.96	1.26	2.12	0.19	3.57
19	2.60	2.14	0.22	4.96	1.26	2.12	0.19	3.57
20	2.60	2.14	0.22	4.96	1.26	2.12	0.19	3.57

#### **4.2.8 Leaching test of the catalyst**

Leaching test of the catalysts was conducted under the specified reaction conditions using the procedure given in the literature [213,214]. The equal amounts of fresh catalyst were added separately into the oleic acid and methanol. Both the reaction mixtures were kept for 4 h at 338 K using the continuous stirring speed of 500 rpm. Then the catalyst from each reaction mixture was separated out by filtration. The obtained reactants were immediately mixed in the reactor and allowed to react at 338 K. At each interval of time (1 h) the reaction mass was withdrawn and analyzed for acid value. No change in the acid value of oleic acid ( $AV_o = 198.6$  mg KOH/g) was observed even after 24 h reaction time. Meanwhile, another reaction without catalyst was conducted for 24 h under the same reaction conditions using fresh reactants and no oleic acid conversion was observed. These results confirm that there is no leaching of the catalyst during the reaction.

#### **4.2.9 Comparison of corncob catalyst with literature**

The performance of the present corncob catalyst with other potential catalysts reported in the literature [26,133,139,150,215–217] for biodiesel production was assessed and presented in Table 4.6. The catalysts listed in Table 4.6 are categorized into three groups. The first group of catalysts is that which showed conversion values below 60% such as niobic acid and amberlyst-15. The second group of the catalysts is that which exhibited 60-90% conversion; corncob-derived (by the hydrothermal process), 20% $H_3PW/ZrO_2$ , 30% $SiW_{12}/H\beta$  and  $TPA_3/H\beta$ . The third group of the catalysts is which exhibited above 90% conversion; concentrated  $H_2SO_4$ , and the catalysts derived from bagasse, kraft lignin, glucose, and starch. The present catalyst synthesized by impregnation-carbonization and sulfonation of corncob showed much higher conversion than the first and second group catalysts. The present I-C-S-corn-cob catalyst showed the high catalytic performance compared to the conventional catalysts in the first group like niobic acid and amberlyst-15. The high-performance was due

to the presence of three different functional groups;  $\text{SO}_3\text{H}$ ,  $\text{COOH}$ , and  $\text{OH}$  [218]. However, the niobic acid and amberlyst-15 contain only one functional group ( $-\text{OH}$ ). During esterification,  $-\text{OH}$  groups allow water (generated during the reaction) to adsorb on the catalyst surface at faster rates than the hydrophobic molecules like oleic acid. This adsorptive competence between hydrophobic oleic acid and hydrophilic water molecules leads to rapid catalyst deactivation and subsequently poisons the catalyst. Thus, niobic acid and amberlyst-15 catalysts display only the marginal acidity in the presence of water and showed lower conversions. In comparison to hydrothermally treated corncob, the catalyst prepared via impregnation technique displayed higher conversion. It is due to the higher  $\text{SO}_3\text{H}$  density (3.16 mmol/g) and total acidic density (5.56 mmol/g) of the present catalyst as compared to hydrothermally treated corncob catalyst (1.54 mmol/g). The present I-C-S-corn-cob catalyst exhibited about the same conversion as obtained by the third group of catalysts. The present catalyst showed a conversion of ~95% in just 2 h reaction time at a mild temperature of 338 K. However, sulfuric acid in homogeneous phase, bagasse-derived, kraft lignin-derived, and glucose-derived catalysts showed similar conversion at a higher temperature (353 K). The concentrated  $\text{H}_2\text{SO}_4$  in homogeneous form impose environmental issues, corrosion problems, and nonrecyclable. Although, the kraft lignin and bagasse derived catalysts are environment-friendly and economical but longer reaction time and higher temperatures are the drawbacks associated with them. The SAC derived from glucose and starch proved their high potential in esterification. However, their use in biodiesel production remains limited due to their higher cost (compared to biomass) and various other prolific applications. Therefore, the present I-C-S-corn-cob catalyst is considered efficient, economical as well as environmentally benign for the biodiesel production.

Recently Endut et al. [140] synthesized the catalyst by sulfonating partially carbonized-coconut shell and evaluated its performance for esterification of FFA in palm oil. Their

catalyst showed a reaction conversion of 88.95% in 6 h at 333 K using 1:30 oil/ methanol ratio, as given in Table 4.7. In comparison to the coconut shell-derived catalyst, the present I-C-S-corncob catalyst is capable to esterify Karanja oil having very high FFA (63.2 mg KOH/g) content. Moreover, I-C-S-corncob catalyst investigated in the current work exhibited higher conversion (>90%) in lesser reaction time (2 h) as compared to the coconut shell-derived catalyst. Furthermore, the present catalyst required a considerably lower amount of methanol (1:20 oil/ methanol) as compared to H<sub>2</sub>SO<sub>4</sub> (1:60 oil/ methanol) and coconut shell-derived catalyst (1:30 oil/ methanol) for FFAs esterification [35].

**Table 4.6:-** Comparison of Present (I-C-S-corncob) Catalyst Performance with Other Catalysts for Oleic Acid Esterification

S. No.	Catalyst	Reaction conditions <sup>a</sup>	Reaction time (h)	Oleic acid conversion (%)	Operational stability (No of runs)	Remarks
1	Without catalyst [150]	10:10:353	24	-	-	No product
2	Corncob-derived [Present work]	10:10:338	2	94.4	>12	Mild temperature, high conversion, shorter reaction time, high stability.
3	Concentrated H <sub>2</sub> SO <sub>4</sub> [150]	10:10:353	2	95.4	-	High conversion, Homogenous, very short reaction time.
4	Corncob-derived [150]	10:10:353	2	89.2	>8	High temperature, good conversion, shorter reaction time, high stability.

**Table 4.6 (continued)**

5	Bagasse-derived [133]	5:10:353	6	95.0	>8	High temperature, high conversion, long reaction time, high stability.
6	Amberlyst-15 [133]	5:10:353	12	60.6	1	High temperature, Low conversion, long reaction time, very low stability.
7	Niobic acid [133]	5:10:353	12	13.7	1	High temperature, Very low conversion, very long reaction time, very low stability.
8	Kraft lignin [217]	5:12:353	5	96.1	-	High temperature, high conversion, short reaction time.
9	Glucose-derived [139]	5:10:353	6	94.8	-	High temperature, high conversion, long reaction time.

**Table 4.6 (continued)**

10	Starch-derived [139]	5:10:353	3	95.2	>50	High temperature, high conversion, very short reaction time, very high stability and reusability.
11	20% H <sub>3</sub> PW <sub>12</sub> O <sub>40</sub> /ZrO <sub>2</sub> [215]	0.2:6:373	4	88	-	Very high temperature, good conversion, short reaction time.
12	30% SiW <sub>12</sub> /H $\beta$ [26]	0.2:20:333	10	86	-	Mild temperature, good conversion, very high reaction time.
13	TPA <sub>3</sub> /H $\beta$ [216]	0.2:20:333	6	84	-	Mild temperature, good conversion, high reaction time.

<sup>a</sup>Reaction conditions:- the amount of catalyst (wt. %): mole ratio of methanol to oleic acid: reaction temperature (K).

**Table 4.7:-** Comparison of Present Catalyst (I-C-S-corncob) Performance with Other Catalysts for Reduction of FFA

S. no.	Catalyst	Oil	Acid value (mg KOH/g oil)	Reaction conditions				Conversion of FFA (%)	Reference
				t	T	w	R		
1	Corncob	Karanja	63.2	2	338	10	1:20	>90	[present]
2	coconut shell	Palm	not reported	6	333	6	1:30	88.95	[140]
3	concentrated H <sub>2</sub> SO <sub>4</sub>	Jatropha	16.1	1	333	10	1:60	>90	[35]

t= reaction time (h); T= reaction temperature (K); w= catalyst loading (wt. %); R= oil to methanol molar ratio.

---

**Kinetic Modeling and Simulation of Novel Corncob-Based  
Catalytic Biodiesel Process**

**5.1 Kinetics of the oleic acid esterification**

After, the detailed experimental study of oleic acid esterification using the novel corncob-based catalyst as presented in Chapter-4, the reaction kinetic modeling and process simulation was studied. The esterification of oleic acid with methanol was represented by a reversible reaction as shown in Equation 5.1;

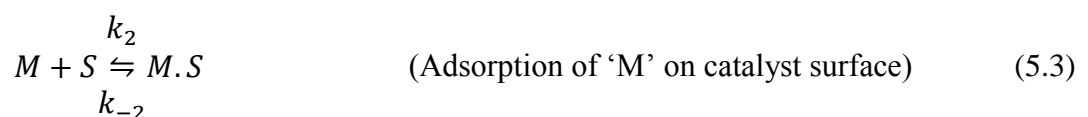
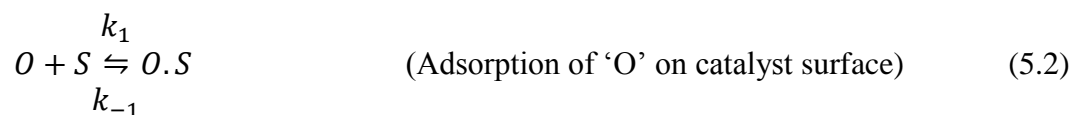


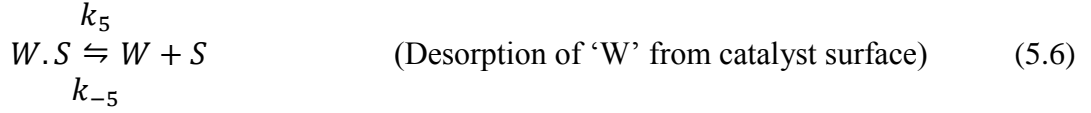
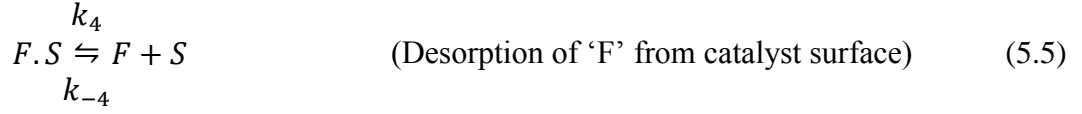
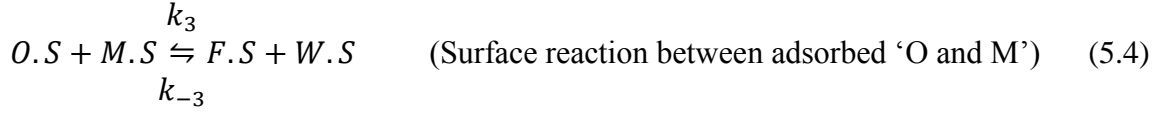
Where,

O, M, F, W represents oleic acid, methanol, fatty acid methyl ester (FAME), and water respectively.

$k_f$  and  $k_{-f}$  represent reaction rate constant for forward and backward directions, respectively.

LHHW approach is most widely used for deriving the rate expression for solid-fluid catalytic reactions. Therefore the following reaction mechanism was considered [219];





Where 'S' denotes the active site of the catalyst

The following assumptions were applied to deduce the rate expression:

1. The adsorption of reactants and desorption of products are fast and at equilibrium.
2. Surface reaction is the rate-limiting step.

Reaction rate at the surface is given by;

$$r = k_3 C_{O.S} C_{M.S} - k_{-3} C_{F.S} C_{W.S} \quad (5.7)$$

At equilibrium,

$$0 = k_3 C_{O.S} C_{M.S} - k_{-3} C_{F.S} C_{W.S} \quad (5.8)$$

$$\Rightarrow \text{Adsorption equilibrium constant for the surface reaction, } K_S = \frac{k_3}{k_{-3}} = \frac{C_{F.S} C_{W.S}}{C_{O.S} C_{M.S}} \quad (5.9)$$

Similarly,

$$\Rightarrow \text{Adsorption equilibrium for oleic acid, } K_O = \frac{k_1}{k_{-1}} = \frac{C_{O.S}}{C_O C_V} \Rightarrow C_{O.S} = K_O C_O C_V \quad (5.10)$$

$$\Rightarrow \text{Adsorption equilibrium constant for methanol, } K_M = \frac{k_2}{k_{-2}} = \frac{C_{M.S}}{C_M C_V} \Rightarrow C_{M.S} = K_M C_M C_V \quad (5.11)$$

$$K_M C_M C_V$$

$$\Rightarrow \text{Adsorption equilibrium constant for FAME, } K_F = \frac{k_{-4}}{k_4} = \frac{C_{F.S}}{C_F C_V} \Rightarrow C_{F.S} = K_F C_F C_V \quad (5.12)$$

$$\Rightarrow \text{Adsorption equilibrium constant for water, } K_W = \frac{k_{-5}}{k_5} = \frac{C_{W.S}}{C_W C_V} \Rightarrow C_{W.S} = K_W C_W C_V \quad (5.13)$$

Substituting Equations 5.10-5.13 in Equation 5.7 gives;

$$r = k_3 K_O C_O C_V K_M C_M C_V - k_{-3} K_F C_F C_V K_W C_W C_V \quad (5.14)$$

$$r = [k_3 K_O C_O K_M C_M - k_{-3} K_F C_F K_W C_W] C_V^2 \quad (5.15)$$

Now, concentration balance for the active sites on the catalyst:

The total concentration of sites= concentration of vacant sites ( $C_V$ ) + concentration of sites occupied by oleic acid ( $C_{O.S}$ ) + concentration of sites occupied by methanol ( $C_{M.S}$ ) + concentration of sites occupied by FAME ( $C_{F.S}$ ) + concentration of sites occupied by water ( $C_{W.S}$ ).

$$C_t = C_v + C_{O.S} + C_{M.S} + C_{F.S} + C_{W.S} \quad (5.16)$$

$$C_t = C_v + K_O C_O C_V + K_M C_M C_V + K_F C_F C_V + K_W C_W C_V \quad (5.17)$$

$$\begin{aligned} \therefore C_v &= \frac{C_t}{1 + K_O C_O + K_M C_M + K_F C_F + K_W C_W} \\ &= \frac{1}{1 + K_O C_O + K_M C_M + K_F C_F + K_W C_W} \end{aligned} \quad (5.18)$$

Substituting Equation 5.18 in Equation 5.15 we get;

$$r = \frac{[k_3 K_O K_M (C_O C_M) - k_{-3} K_F K_W (C_F C_W)]}{[1 + K_O C_O + K_M C_M + K_F C_F + K_W C_W]^2} \quad (5.19)$$

Due to the rapid adsorption of reactants and products the term

$$K_O C_O + K_M C_M + K_F C_F + K_W C_W \gg 1 \quad (5.20)$$

Also, from component balance:

$$\begin{aligned} C_O &= C_{O_o}(1 - X); C_M = C_{M_o}(1 - X_M) = C_{M_o} - C_{O_o}X = C_{O_o} \left( \frac{C_{M_o}}{C_{O_o}} - X \right) \\ &= C_{O_o}(m - X) \end{aligned} \quad (5.21)$$

$$C_F = C_W = C_O - C_{Oo} = C_{Oo}X \quad (5.22)$$

Incorporating all these in Equation 5.19, we get;

$$r = \frac{[k_3K_OK_M C_{Oo}(1-X)C_{Oo}(m-X) - k_{-3}K_FK_W C_{Oo}XC_{Oo}X]}{[K_O C_{Oo}(1-X) + K_M C_{Oo}(m-X) + K_F C_{Oo}X + K_W C_{Oo}X]^2} \quad (5.23)$$

$$r = \frac{[k_3K_OK_M(1-X)(m-X) - k_{-3}K_FK_W X^2]}{[K_O(1-X) + K_M(m-X) + K_F X + K_W X]^2} \quad (5.24)$$

Dividing numerator and denominator with  $K_M^2$  and on rearranging the above expression we get;

$$r = \frac{\frac{[k_3K_OK_M(1-X)(m-X) - k_{-3}K_FK_W X^2]}{K_M^2}}{[K_O(1-X) + K_M(m-X) + K_F X + K_W X]^2} \quad (5.25)$$

$$r = \frac{\frac{\frac{k_3K_O}{K_M}(1-X)(m-X) - \frac{k_{-3}K_FK_W}{K_M^2} X^2}{[K_O(1-X) + K_M(m-X) + K_F X + K_W X]^2}}{K_M^2} \quad (5.26)$$

$$r = \frac{\frac{\frac{k_3K_O}{K_M}(1-X)(m-X) - \frac{k_{-3}K_FK_W}{K_M^2} X^2}{\left[\frac{K_O}{K_M} - \frac{K_O}{K_M} X + m - \frac{K_M}{K_M} X + \frac{K_F}{K_M} X + \frac{K_W}{K_M} X\right]^2}}{K_M^2} \quad (5.27)$$

$$r = \frac{\frac{\frac{k_3K_O}{K_M}(1-X)(m-X) - \frac{k_{-3}K_FK_W}{K_M^2} X^2}{\left[X\left(\frac{K_F + K_W - K_O - K_M}{K_M}\right) + m + \frac{K_O}{K_M}\right]^2}}{K_M^2} \quad (5.28)$$

$$\therefore r = \frac{k_f(1-X)(m-X) - k_{-f}X^2}{[aX + m + b]^2} \quad (5.29)$$

With,

$$a = \frac{K_F + K_W - K_O - K_M}{K_M}$$

$$b = \frac{K_O}{K_M}$$

$$m = \text{Molar ratio of methanol to oil} = \frac{C_{Mo}}{C_{Oo}}$$

$$k_f = \frac{k_3 K_O}{K_M} \quad \text{and} \quad k_{-f} = \frac{k_{-3} K_F K_W}{K_M^2}$$

To evaluate the kinetic parameters it was assumed that there is no conversion of oleic acid before the start of the reaction. Substituting  $X=0$  in Equation 5.29, the initial rate of the reaction could be expressed as;

$$r_o = k_f \frac{m}{(b + m)^2} \quad (5.30)$$

$$\Rightarrow (b + m)^2 = \frac{k_f m}{r_o}$$

$$\therefore \sqrt{\frac{m}{r_o}} = \sqrt{\frac{1}{k_f}} (b + m) \quad (5.31)$$

The relationship between the initial rates of the reaction at various molar ratios of methanol to oleic acid was used to estimate the values of  $k_f$  and  $b$  at each temperature. As given in Equation 5.31, the square root of  $(m/r_o)$  was plotted against  $m$  and the straight line was obtained by linear fit as shown in Figure 5.1. The slope (square root of  $k_f^{-1}$ ) and the intercept ( $b$  times the square root of  $k_f^{-1}$ ) of this plot were used to calculate the values of  $k_f$  and  $b$ . Then these values were incorporated in Equation 5.29, and the other parameters were obtained by non-linear regression of experimental data at each temperature [52]. The obtained kinetic parameters at each temperature have been summarized in Table 5.1. The correlation coefficient ( $R^2$ ) obtained for all the parameters was close to 1, suggesting a very good statistical consistency of the experimental data fitting. The adsorption equilibrium constant for oleic acid ( $K_O$ ) was found in the range of 25.850 to 3.250 for a temperature range

from 333.15 to 343.15 K. This value was much higher than other adsorption equilibrium constants for methanol ( $K_M$ ), methyl oleate ( $K_F$ ) and water ( $K_W$ ), indicating a strong affinity of oleic acid to the catalyst surface. The value of ‘b’ was found to be 325, which implies that the adsorption affinity of oleic acid on the catalyst surface was approximately 325 times higher than that of methanol. This shows the oleophilic property of the catalyst surface, which enhances the rate of the protonation of the carbonyl group to give a carbocation [52,220]. Moreover, the water generated during the esterification reaction desorbs quickly from the active sites of the catalyst surface to make available more active sites for oleic acid molecules to adsorb. Therefore, the rate of esterification was increased by the higher concentration of oleic acid as well as the high turnover of active sites on the catalyst surface [52].

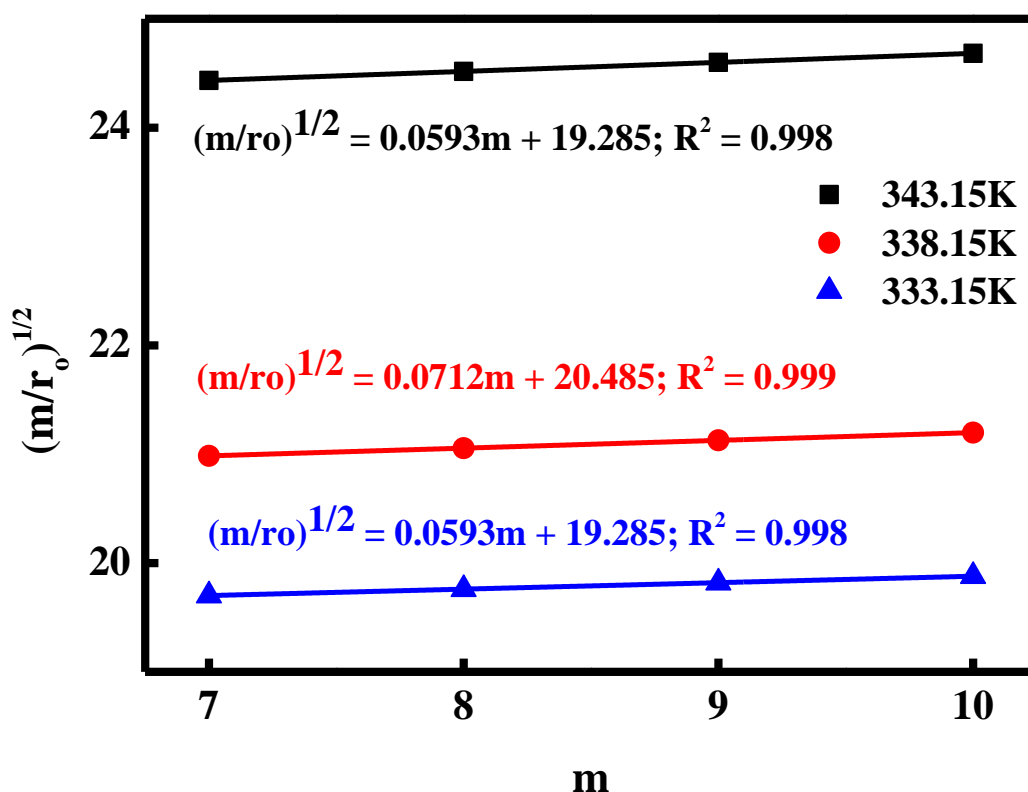


**Figure 5.1:-** Relationship between initial rates ( $r_o$ ) and the molar ratio of methanol to oleic acid ( $m$ ) at various temperatures.

**Table 5.1:- Estimated Kinetic and Arrhenius Parameters**

Parameter	Temperature (K)			Arrhenius parameters		R <sup>2</sup>
	333.15	338.15	343.15	Intercept (A) = lnK <sub>oi</sub>	Slope (B) = - (ΔE <sub>i</sub> /R)	
a	-40.646	-82	-182	-	-	-
b	287.216	287.525	325	-	-	-
k <sub>f</sub> (mol/m <sup>3</sup> .kg <sub>cat</sub> .sec)	4.028E-02	5.472E-02	7.889E-02	19.833	-7.681E+3	0.996
k <sub>-f</sub> (mol/m <sup>3</sup> .kg <sub>cat</sub> .sec)	4.462E-03	5.545E-03	7.253E-03	11.236	-5.549E+3	0.995
K <sub>O</sub> (m <sup>3</sup> /mol)	25.850	8.626	3.250	-67.935	2.371E+4	0.999
K <sub>M</sub> (m <sup>3</sup> /mol)	0.090	0.030	0.010	-77.795	2.511E+4	0.999
K <sub>F</sub> (m <sup>3</sup> /mol)	21.391	5.636	1.060	-99.917	3.432E+4	0.995
K <sub>W</sub> (m <sup>3</sup> /mol)	0.890	0.560	0.380	-29.341	9.732E+3	0.998
R <sup>2</sup>	0.989	0.995	0.995	-	-	-

'i' denotes subscript letter of each parameter; f, -f, O, M, F, W.

## 5.2 Effect of temperature on rate constants and adsorption constants

In irreversible reactions, the reaction rate is usually increased with an increase in the temperature and the magnitude of the increased rate with temperature depends on the activation energy, which can be quantified using the Arrhenius equation. However, in reversible reactions, the effect of temperature is more ambiguous since the temperature has an effect on kinetic coefficients of both forward and backward reactions. Accordingly, in the initial stage of the reaction during which the backward reaction is negligible due to the low concentration of the reaction products, increasing the temperature increases the net reaction rate. As the reaction progresses, the net rate of reaction increases or decreases depends on the magnitude of the variation in the forward and backward kinetic coefficients with temperature. In turn, this variation is a function of the magnitudes of the activation energy of forward and backward reactions [55,221]. Therefore, the influence of temperature on the rate constants (reaction and adsorption) was studied using a linear form of the Arrhenius equation as given in Equation 3.11. The plot between  $\ln k$  vs  $T^{-1}$  for both the rate constants ( $k_f$ ,  $k_r$ ) as shown in Figure 5.2 was obtained by linear fitting. Forward and backward reaction activation energies ( $\Delta E_f$ ,  $\Delta E_r$ ) and forward and backward frequency factors ( $k_o$ ,  $k_r$ ) were evaluated from the slopes and intercepts of the straight lines, respectively. The calculated activation energies and frequency factors were found to be 63.861 kJ/mol and  $4.105E+8$  m<sup>3</sup>/mol.kg<sub>cat</sub>.sec, respectively for the forward reaction and 746.138 kJ/mol and  $7.1581E+4$  m<sup>3</sup>/mol.kg<sub>cat</sub>.sec, respectively, for the backward reaction. The obtained activation energies are consistent with the activation energies observed in the literature [35,222,223]. A Similar procedure was repeated for each adsorption coefficient ( $K_O$ ,  $K_M$ ,  $K_F$ , and  $K_W$ ) as shown in Figure 5.3, whose slopes and intercepts have also been given in Table 5.1. Experimentally observed conversion values were plotted against the model predicted conversions to test the statistical significance

of the data using Student's paired t-test [35,221]. It was found from Figure 5.4 that the proposed model satisfactorily represents all the experimental data.

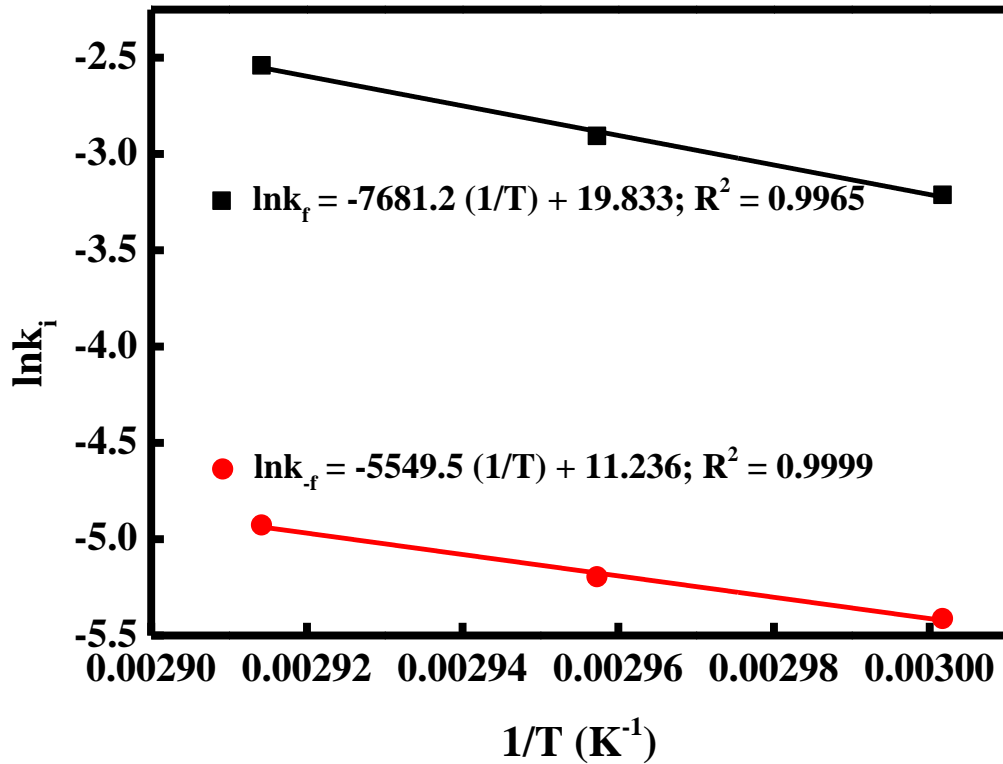


Figure 5.2:- Arrhenius plot for frequency factor.

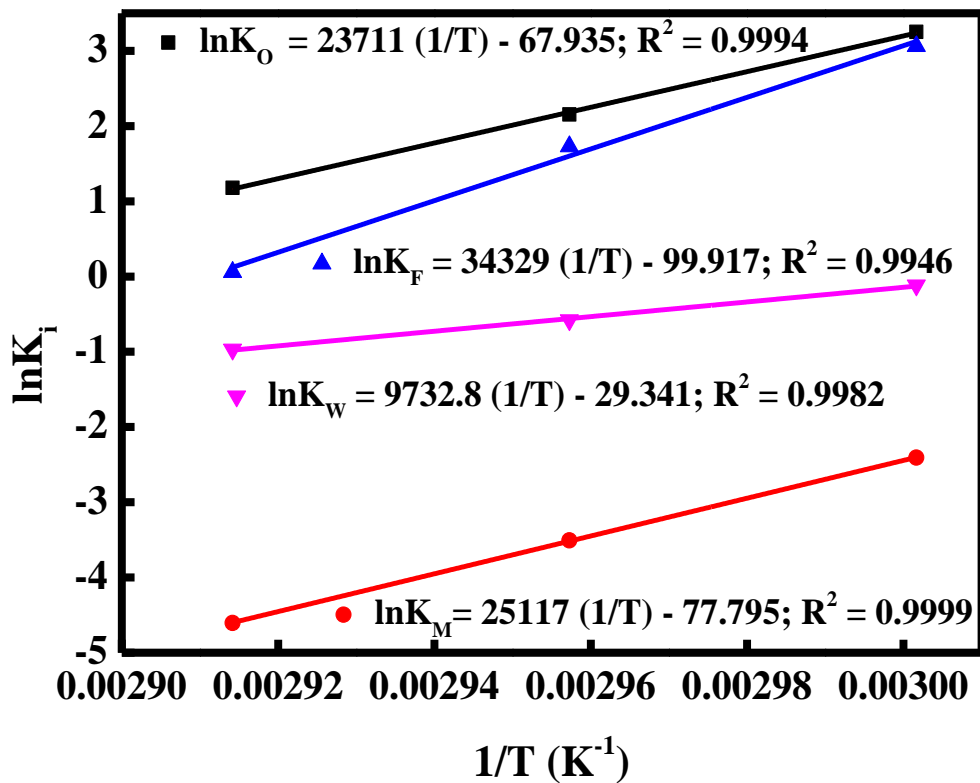


Figure 5.3:- Arrhenius plot for adsorption parameters.

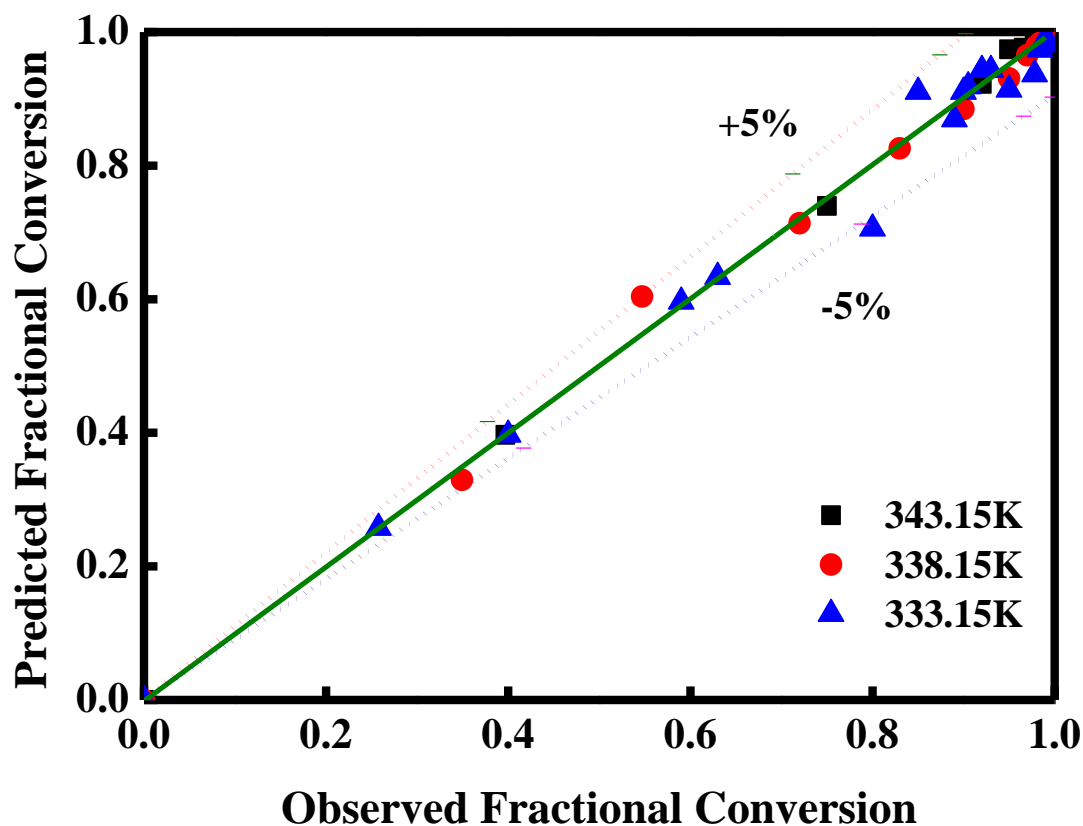


Figure 5.4:- Experimental and model predicted conversions of oleic acid.

### 5.3 Effect of temperature on the reaction equilibrium constant

For a reaction at equilibrium, the basic criteria to be satisfied is that the change in Gibbs free energy must be zero (i.e.,  $\Delta G = 0$ ) at which the equilibrium constant ( $K$ ) can be determined. The equilibrium constant can also be determined using the  $\Delta G^0$  (the difference between the standard Gibbs energy of formation ( $G_f^0$ ) of products and reactants). However, for esterification reaction, this approach has large uncertainty and unreliability due to the high value of  $G_f^0$  of each reacting species and also there is a small difference between the free energies of products and reactants [183]. Therefore, a small inaccuracy in measuring  $G_f^0$  will result in a very large error in the value of  $K$  [224]. In view of this, many researchers usually prefer to determine the  $K$  values from experimental data at equilibrium at various temperatures or from the fitting of experimental rate data to the kinetic models [183]. The

equilibrium constants obtained at various temperatures are presented in Table 5.2 which shows the increase in the equilibrium constant with temperature.

**Table 5.2:- Estimated equilibrium and van't Hoff parameters**

Parameter	Temperature			Van't Hoff parameters		R <sup>2</sup>
	333.15	338.15	343.15	Intercept =( $\Delta S/R$ )	Slope = $\Delta H/R$ (K)	
K= K <sub>f</sub> /K <sub>r</sub>	9.026	9.868	10.877	8.597	-2131.7	0.998
$\Delta G = -RT \ln K$ (kJ/mol)	-6.094	-6.436	-6.809	-	-	-

The magnitude of the variation in the net reaction rate with increasing temperature depends on whether the reaction is endothermic or exothermic, which can be found using the heat of the reaction. The heat of the reaction can be obtained using the difference between the activation energies of forward and backward reaction or can be evaluated from the van't Hoff isochore assuming the standard change in enthalpy is constant for a small temperature range as given in Equation 3.12. The effect of temperature on the equilibrium constant has been shown in Figure 5.5. The slope and intercept of the fitted straight line were used to calculate the change in enthalpy ( $\Delta H$ ) and the change in entropy ( $\Delta S$ ) of the reaction, respectively. The values of  $\Delta H$  and  $\Delta S$  obtained are +17.723 kJ/mol and +0.00714 kJ/mol.K, respectively. The positive sign of  $\Delta H$  indicates the endothermic nature of the reaction. It is consistent with the available literature [52,183,225,226]. To find the spontaneity of the reaction, the change in Gibbs free energy was also calculated at each temperature using Equation 5.33;

$$\Delta G = -RT \ln K \quad (5.33)$$

The calculated Gibb's free energy change ( $\Delta G$ ) was found to be negative at all the temperatures as shown in Table 5.2. It shows that the reaction would be moving in the forward direction (i.e., towards product formation) not in the reverse direction. The positive

values of change in enthalpy ( $\Delta H > 0$ ), change in entropy ( $\Delta S > 0$ ) and negative values of change in Gibbs free energy ( $\Delta G < 0$ ) signify that the reaction is endothermic and spontaneous in the temperature range of 333.15 to 343.15 K.

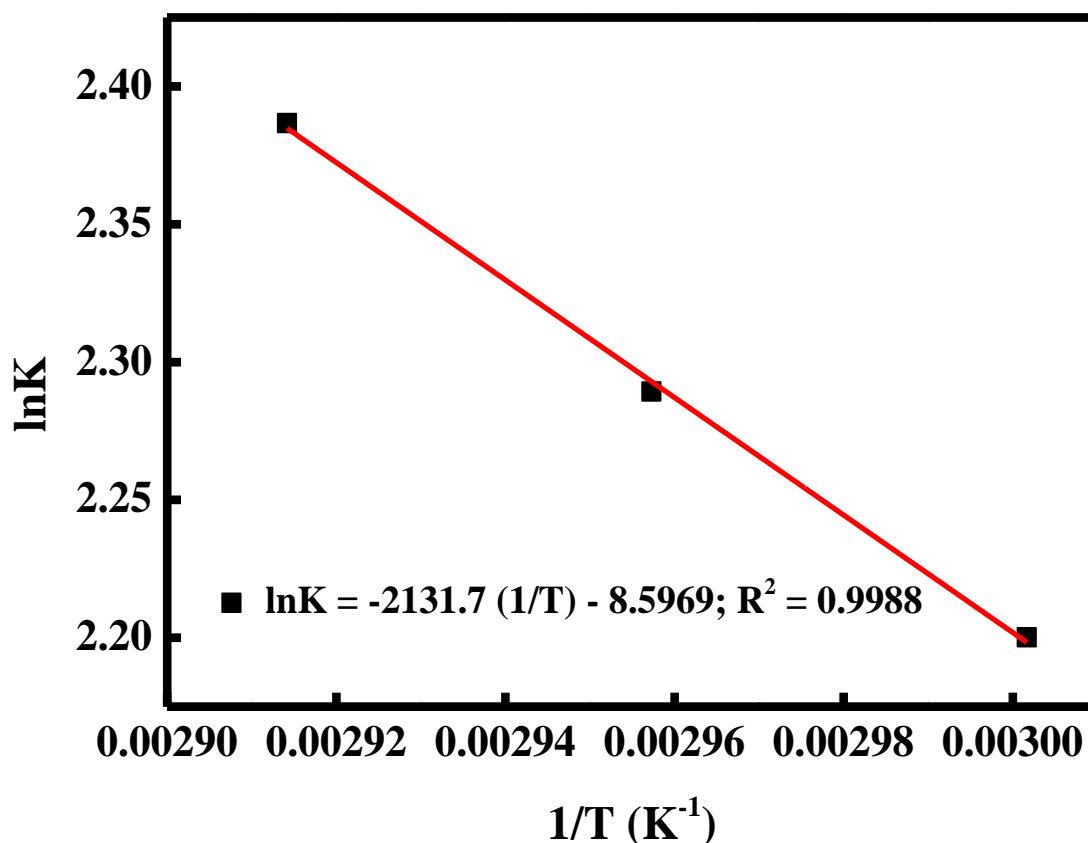


Figure 5.5:- Van't Hoff plot for the esterification process.

## 5.4 Process modeling and simulation

### 5.4.1 Process flow diagram

Process simulation is widely used to obtain valuable information about the operating conditions. In spite of the fact that there are some differences between the real process and simulated process, yet, they provide reliable information due to their extensive component library, comprehensive thermodynamic packages, and diverse computational methods [111,112,155-157]. The oleic acid esterification process was modeled using Aspen Plus simulator (ver.8.6) and the complete process flow diagram (PFD) has been shown in Figure-

5.6. Oleic acid from the mixer (M-100) through the stream; E-101 and methanol from the mixer (M-101) through the stream; E-102 were fed to the reactor (R-100) using feed pumps (P-100 and P-101). After the reaction, the product stream of the reactor was passed through the distillation column (D-100), where FAME and unreacted oleic acid were taken as a bottom product (E-104), and methanol along with water were taken as the top stream (E-105). The stream E-104 was sent to the distillation column (D-102) where pure FAME and unconverted oleic acid were separated. Thereafter, unconverted oleic acid was recycled ( $R_O$ ) back to the mixer (M-100). The stream E-105 was sent to another distillation column (D-103) where the pure methanol was recovered and recycled ( $R_m$ ) to the mixer (M-101). The reactor and distillation columns shown in the flow sheet were modeled using 'RCSTR', and 'RADFRAC' subroutines of the Aspen software, respectively.

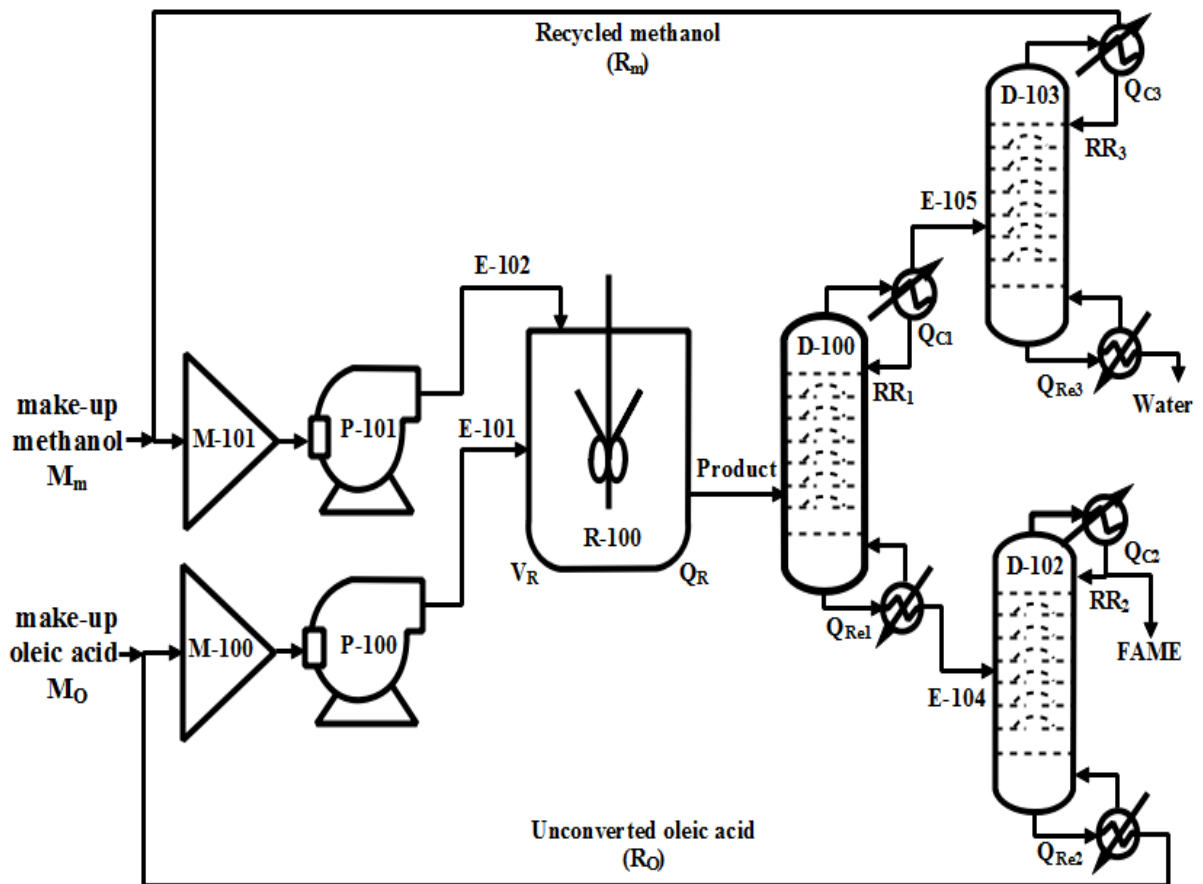


**Figure 5.6:-** Simulated Process flow sheet of the biodiesel production process.

### 5.4.2 Process simulation

The simulation was carried out by importing the required databanks and specifying all the components present in the process (oleic acid, methanol, water, and methyl oleate). Activity coefficient based NRTL thermodynamic model was selected for estimation of properties as well as the calculation of phase equilibrium. The flow rate of oleic acid in the feed stream (E-101) was selected to be 1050 kg/h (or 3.717 kmol/h). Methanol was fed continuously to the reactor (volume,  $V_R = 5.743 \text{ m}^3$ ) at the rate of 1191 kg/h (or 37.189 kmol/h) i.e. at 1:10 oleic acid to methanol molar ratio. The reaction type was defined as the LHHW model as given in Equation 5.34;

$$r = \frac{[k_f C_O C_M - k_{-f} C_F C_W]}{[1 + K_O C_O + K_M C_M + K_F C_F + K_W C_W]^2} = \frac{[\text{Driving force expression}]}{[\text{Adsorption expression}]} \quad (5.34)$$

Where,

$$\ln k_i = A + \frac{B}{T} + C \ln(T) = DT \quad \text{with } i = f, -f, O, M, F, W$$

A = Intercept of  $\ln k_i$  Vs  $T^{-1}$  plot and B = -E/R (slope of the straight line)

The input to define LHHW kinetics in Aspen Plus requires data to be entered in three forms namely kinetic sheet, driving force sheet and adsorption sheet.

#### **Input for Kinetic sheet:**

After defining the stoichiometry of the reaction as given in Equation 5.1, the values of parameters in the kinetic sheet were defined as  $k = 1$ ,  $n$  (order of the reaction) = 0,  $E = 0$ , and reference temperature ( $T_o$ ) = 298.15 K. Rate basis were selected as catalyst weight.

#### **Input for the driving force sheet:**

Term1: The concentration exponents for both the reactants were assigned as '1' and the coefficient for driving force constant ( $k_f$ ) was inserted in the form of intercept and slope as A = intercept of  $\ln k_f$  Vs  $T^{-1} = 19.833$  and B = slope of  $\ln k_f$  Vs  $T^{-1} = -7.681E+03$ .

Term2: Similar to the term 1, the concentration exponents for both the products were assigned as '1' and the coefficient for driving force constant ( $k_f$ ) was inserted in the form of intercept and slope as  $A = \text{intercept of } \ln k_f \text{ Vs } T^{-1} = 11.236$  and  $B = \text{slope of } \ln k_f \text{ Vs } T^{-1} = -5.549E+03$ .

**Input for adsorption sheet:**

The coefficient of adsorption expression ( $[1 + K_O C_O + K_M C_M + K_F C_F + K_W C_W]^2$ ) was assigned as '2' and the concentration exponents for each term were defined in the following form:

Component	Term no. 1	Term no. 2	Term no. 3	Term no. 4	Term no. 5
Oleic acid	0	1	0	0	0
Methanol	0	0	1	0	0
Methyl oleate	0	0	0	1	0
Water	0	0	0	0	1

Then the values of coefficients for each term (A, B) were defined in the form of slopes and intercepts as follows:

Term no.	1	2	3	4	5
A	0	-67.935	-77.795	-99.917	-29.341
B	0	2.371E + 4	2.511E + 4	3.432E + 4	9.732E + 3

All the data defined in the kinetic, driving force and adsorption sheets of the reaction were used in RCSTR subroutine reactor model. The reaction product of oleic acid and methanol was designated as FAME (methyl oleate). In accordance with experimental findings, the temperature and pressure of the reactor were maintained at 338.15 K and 1 bar, respectively. The catalyst (with a particle density of 2.246 g/cc) amount of 116.667 kg i.e. at 10 wt. % of oleic acid was given as input to the reactor. After completion of the reaction, the product was purified using a series of three distillation columns and unconverted oleic acid, as well as excess methanol, was recovered and recycled. Although the boiling point of methanol (approx. 338.15 K at 1.013 bar) is much lower than the boiling point of FAME (617 K at 1.013 bar) or oleic acid (633 K at 1.013 bar), simulation suggested that the desired purity

(99.65 wt. %) of biodiesel as per ASTM standards could not be achieved by a simple flash distillation unit. A similar problem was also observed in the study carried out by Zhang et al. [155]. Therefore, a rigorous distillation method 'Radfrac' subroutine was used to model the distillation columns and the columns were maintained under vacuum to avoid the degradation of FAME at a temperature above 523 K [112]. The required inputs for Radfrac unit were calculated first by DSTWU method. The molar flow rate, composition and stream conditions of 'product', 'E-104' and 'E-105' were given as input to the DSTWU units to obtain the required design variables of D-100, D-102, and D-103 respectively. Also, the light key; water and heavy key; oleic acid for the design of D-100, light key; FAME and heavy key; oleic acid for D-102 design and light key; methanol and heavy key; water for D-103 were given as input in DSTWU models. Finally, the light key and heavy key recoveries were specified in all DSTWU modes as 0.9999 and 0.0001, respectively. DSTWU simulation results obtained for each column are summarized in Table 5.3 which was used as input to the Radfrac subroutine of distillation model in the main flow sheet. The unconverted oleic acid recovered from D-102 was recycled back to the mixer (M-100), where it was mixed with the oleic acid feed stream. Similarly, the recovered methanol (purity = 99.9%) from D-103 was recycled to the mixer (M-101) and mixed with the make-up methanol stream. A product, biodiesel with 99.9% purity was obtained. 'Design specs' tool of the Aspen Plus was used to calculate the flow rate of makeup methanol. Simulation results of the complete flow sheet have been presented in Table 5.4 and the calculated heat duties of each unit are as follows:

**Reactor:-**

Reactor duty ( $Q_R$ ) = 72.538 kW.

**Distillation:-**

**D-100:** Condenser duty ( $Q_{C1}$ ) = -547.028 kW; Reboiler duty ( $Q_{Re1}$ ) = 663.289 kW.

**D-102:** Condenser duty ( $Q_{C2}$ ) = -242.140 kW; Reboiler duty ( $Q_{Re2}$ ) = 451.896 kW.

**D-103:** Condenser duty ( $Q_{C3}$ ) = -819.984 kW; Reboiler duty ( $Q_{Re3}$ ) = 822.411 kW.

The simulation results showed the conversion of oleic acid to be 98.84% which was close to the experimental conversion (98.9%).

**Table 5.3:-** DSTWU Results for Each Distillation Column

<b>Process Parameters</b>	<b>D-100</b>	<b>D-102</b>	<b>D-103</b>
Minimum reflux ratio	3.72E-05	0.941	0.335
Actual reflux ratio	1.5	1.5	1.5
Minimum number of stages	2.331	18.365	12.389
Number of actual stages	3.033	31.878	16.207
Feed stage	2.308	16.587	10.997
Number of actual stages above feed	1.308	15.587	9.997
Reboiler heating required (kW)	853.381	197.618	817.892
Condenser cooling required (kW)	1108.358	191.886	821.976
Distillate temperature (K)	338	504	337
Bottom temperature (K)	615	521	371
Distillate to feed fraction	0.909	0.989	0.900

**Table 5.4:-** Stream Results of the Simulated Flow Sheet

Stream		E-101	E-102	Product	E-104	E-105	FAME	R <sub>o</sub>	Water	R <sub>m</sub>	M <sub>m</sub>	M <sub>o</sub>
T (K)		300.779	333.776	338.15	496.754	338.882	482.295	523.516	370.742	337.358	298.15	298.15
P (bar)		1	1	1	0.06	1	0.04	0.04	1	1	1	1
Molecular Weight		282.467	32.035	54.792	296.130	30.650	296.268	282.468	18.173	32.035	32.042	282.466
m (kg/h)		1050	1191	2242	1101.603	1139.794	1091.071	10.531	67.500	1072.293	119.103	1039.469
n (kmol/h)		3.717	37.189	40.906	3.720	37.187	3.682	0.037	3.714	33.472	3.717	3.680
Mass composition	W	0	2.602E-4	2.967E-2	2.601E-5	5.832E-2	2.626E-5	0	9.802E-1	2.891E-4	0	0
	M	0	0.999	4.789E-1	3.360E-5	9.417E-1	3.393E-5	0	1.983E-2	9.997E-1	1	0
	O	1	0	5.431E-3	1.105E-2	0	1.505E-3	9.999E-1	0	0	0	1
	F	0	0	4.860E-1	9.889E-1	0	9.984E-1	8.545E-5	7.829E-9	0	0	0

### Conclusions and Future Recommendations

#### 6.1 Conclusions

##### 6.1.1 Effect of TMAB Addition on Conventional Process

The effect of TMAB on the conventional biodiesel production process was studied in detail and found to yield positive results.

- The optimum methanol to oil molar ratio was found to be 9:1 when KOH/NaOH was used.
- The decrease in the methanol requirement from 9:1 to 7.5:1 molar ratio was observed when TMAB was added. The decrease in the excess methanol requirement has a positive effect on the purification of the biodiesel.
- Addition of TMAB improves the washability characteristics of the crude biodiesel and lowers the wash water requirement by half of that required in the conventional transesterification process.

##### 6.1.2 Esterification of Free Fatty Acids

- The experimental result shows that the 96.21% FFA conversion can be achieved in 7 hours of reaction time at 220 °C and 1:6 (w/v) oil: methanol ratio.
- The kinetics of the reaction was well modeled using the pseudo first order in the forward direction and second order bimolecular type reaction in the reversible direction.

- The calculated kinetic parameters were found as  $k_f' \text{ (min}^{-1}\text{)} = 0.0106$ ,  $k_r \text{ (g/mg KOH min)} = 6.96\text{E}^{-6}$ . The activation energy for the forward and backward reactions was 48.534 and 18.744 kJ/mol, respectively.
- The values of enthalpy ( $\Delta H > 0$ ), entropy ( $\Delta S > 0$ ) and Gibbs free energy ( $\Delta G < 0$ ) confirm that the reaction is spontaneous only at high temperatures subject to  $T\Delta S > \Delta H$ . Simulation study revealed that 99.85% conversion of oleic acid may be achieved.

### 6.1.3 Synthesis and Characterization of Corncob-Based Solid Acid Catalyst

The highly active and efficient corncob-based solid acid catalysts for esterification of oleic acid, palmitic acid and free fatty acids (FFA) present in Karanja oil were synthesized.

- The optimal catalyst synthesis parameters found to be;  $I_{R=1}^{t=5} - C_{T=723}^{t=8} - S_{T=393}^{t=15}$ .
- The catalyst synthesized at optimum conditions displayed the highest total acid density (5.56 mmol/g catalyst) and exhibited the maximum conversion (94.4%) of oleic acid.
- The FTIR analysis indicated the presence of multiple functional groups (phospho-carbonaceous, hydroxyl and sulfonic) on the surface of the catalyst.
- The specific surface area of the phosphoric acid impregnated catalyst and the sulfonated catalyst was observed to be 1128 m<sup>2</sup>/g and 641m<sup>2</sup>/g, respectively. These catalysts were found to be largely composed of mesoporous structure.
- XRD spectra's indicates the presence of amorphous carbon composed of polycyclic aromatic carbon sheets oriented in a considerably random fashion.

Further, under various reaction conditions, the conversion of both the fatty acids and free fatty acids were assessed.

- A fatty acid (oleic and palmitic) conversion of >90% was achieved in 2 h using 1:10 molar ratio of fatty acid to methanol and a catalyst loading of 10 wt. % at 338 K.

However, the esterification of FFA present in Karanja oil required higher oil/methanol molar ratio (1:20) to achieve >90% conversion under similar reaction conditions.

- The reusability test of the catalyst revealed the crucial role of the solvents in catalyst regeneration. On washing the catalyst using methanol and ethanol considerably reduced the catalytic activity. However, n-hexane was found to be the best regenerating solvent for the present catalyst by showing ~90% conversion of oleic acid even after the 20th cycle of reusability.
- Compared to the other catalyst from the literature the present catalyst was found to produce biodiesel in a short period under the mild reaction temperature. The present catalyst also offers an advantage of lower methanol requirement as compared to other catalysts for the esterification reaction. Moreover, the I-C-S-corncob catalyst synthesized in the current study is biodegradable, economical and environmentally benign.

#### **6.1.4 Kinetic Modeling and Simulation of Corncob-Based Catalytic Process**

- A highly active corncob-based solid acid catalyst was used for esterification of oleic acid. The experimental data were well correlated using a Langmuir-Hinshelwood–Hougen-Watson kinetic model and found to be statistically consistency with an  $R^2$  value close to 1.
- The catalyst surface showed a strong affinity towards the oleic acid due to the higher value of adsorption equilibrium constant of oleic acid ( $K_O$ ) than the other three adsorption equilibrium constants; methanol ( $K_M$ ), methyl oleate ( $K_F$ ) and water ( $K_W$ ).
- The effect of temperature on rate constants and equilibrium constants was studied using Arrhenius and van't Hoff equations. The calculated activation energies and frequency factors were found to be 63.861 kJ/mol and  $4.105E^{+8}$  m<sup>3</sup>/mol.kg<sub>cat</sub>.sec, respectively for the forward reaction and 746.138 kJ/mol and  $7.1581E^{+4}$

$\text{m}^3/\text{mol.kg}_{\text{cat}}.\text{sec}$ , respectively, for the backward reaction. The calculated heat of reaction was 17.723 kJ/mol, indicates the slightly endothermic nature of the reaction. The negative values of change in Gibbs free energy signify that the reaction is spontaneous in the temperature range of 333.15-343.15 K.

- The esterification process was simulated in Aspen Plus and the conversion of oleic acid (98.84%) was found close to experimental conversion (98.9%). The simulation results showed that the biodiesel with 99.9% purity can be obtained after separation of the reaction product in a series of three distillation columns.

## 6.2 Recommendations

- ✓ Biomass has a huge potential in the production of biofuels.
- ✓ Waste biomass can be utilized as the feedstock as well as a catalyst for biodiesel production.
- ✓ Utilization of non-edible oils, as well as waste vegetable oils for biodiesel production, may help us to meet the energy demand of our country.
- ✓ Detailed kinetic modeling and simulation of the process may be useful for scale up the process for industrial application.

## References

- [1] N. Apergis, J.E. Payne, Renewable and non-renewable energy consumption-growth nexus: Evidence from a panel error correction model, *Energy Economics* 34 (2012) 733–738.
- [2] A. Sarin, *Biodiesel: Production and Properties*, 2012. Royal Society of Chemistry. eISBN: 978-1-84973-472-1.
- [3] A.F. Lee, J.A. Bennett, J.C. Manayil, K. Wilson, Heterogeneous catalysis for sustainable biodiesel production via esterification and transesterification, *Chemical Society Reviews* 43 (2014) 7887–7916.
- [4] A. Demirbas, Progress and recent trends in biodiesel fuels, *Energy Conversion and Management* 50 (2009) 14–34.
- [5] J.G. Tamba, D. Njomo, T. Limanond, B. Ntsafack, Causality analysis of diesel consumption and economic growth in Cameroon, *Energy Policy*. 45 (2012) 567–575.
- [6] B. Kavalov, S.D. Peteves, *Impacts of the increasing automotive diesel consumption in the EU*, 2004. European Commission, Directorate General Joint Research Centre, Institute for Energy, Petten, The Netherlands. ISBN 92-894-6088-1.
- [7] S.Salo, O. Tahvonen, Economic growth and transitions between renewable and nonrenewable energy resources, *European Economic Review* 45 (2001) 1379–1398.
- [8] G. Knothe, Biodiesel and renewable diesel: A comparison, *Progress in Energy Combustion Science* 36 (2010) 364–373.
- [9] M. Bhattacharya, S.R. Paramati, I. Ozturk, S. Bhattacharya, The effect of renewable energy consumption on economic growth: Evidence from top 38 countries, *Applied*

- Energy. 162 (2016) 733–741.
- [10] A. Demirbas, Biofuels sources, biofuel policy, biofuel economy and global biofuel projections, *Energy Conversion and Management* 49 (2008) 2106–2116.
- [11] A. Demirbas, Importance of biodiesel as transportation fuel, *Energy Policy*. 35 (2007) 4661–4670.
- [12] M. Sara, S.K. Brar, J.F. Blais, Comparative study between microwave and ultrasonication aided in situ transesterification of microbial lipids, *RSC Advances* 6 (2016) 56009–56017.
- [13] T.D.S. Van, N.P. Trung, V.N. Anh, H.N. Lan, A. T. Kim, Optimization of esterification of fatty acid rubber seed oil for methyl ester synthesis in a plug flow reactor, *International Journal of Green Energy*. 13 (2016) 720–729.
- [14] J. Sebastian, C. Muraleedharan, A. Santhiagu, Enzyme catalyzed biodiesel production from rubber seed oil containing high free fatty acid, *International Journal of Green Energy*. 14 (2017) 687-693.
- [15] S.P. Singh, D. Singh, Biodiesel production through the use of different sources and characterization of oils and their esters as the substitute of diesel: A review, *Renewable and Sustainable Energy Reviews*, 14 (2010) 200–216.
- [16] A. Demirbas, *Biodiesel*, 1<sup>st</sup> edition, Springer-Verlag London, 2008. eISBN: 978-1-84628-995-8.
- [17] F. Ma, M.A. Hanna, Biodiesel production: A review, *Bioresource Technology* 70 (1999) 1–15.
- [18] A.K. Agarwal, Biofuels (alcohols and biodiesel) applications as fuels for internal combustion engines, *Progress in Energy and Combustion Science* 33 (2007) 233–271.

- [19] A. Monyem, J.H. Van Gerpen, The effect of biodiesel oxidation on engine performance and emissions, *Biomass and Bioenergy*. 20 (2001) 317–325.
- [20] J. Xue, T.E. Grift, A.C. Hansen, Effect of biodiesel on engine performances and emissions, *Renewable and Sustainable Energy Reviews* 15 (2011) 1098–1116.
- [21] A.K. Agarwal, L.M. Das, Biodiesel development and characterization for use as a Fuel in compression ignition engines, *Journal of Engineering for Gas Turbines and Power*. 123 (2001) 440–447.
- [22] R.L. McCormick, M.S. Graboski, T.L. Alleman, A.M. Herring, K.S. Tyson, Impact of biodiesel source material and chemical structure on emissions of criteria pollutants from a heavy-duty engine, *Environmental Science and Technology* 35 (2001) 1742–1747.
- [23] M. Farooq, A. Ramli, A. Naeem, Biodiesel production from low FFA waste cooking oil using heterogeneous catalyst derived from chicken bones, *Renewable Energy*. 76 (2015) 362–368.
- [24] E.A. Torres, G.S. Cerqueira, T. M. Ferrer, C.M. Quintella, M. Raboni, V. Torretta, G. Urbini, Recovery of different waste vegetable oils for biodiesel production: A pilot experience in Bahia State, Brazil, *Waste Management* 33 (2013) 2670–2674.
- [25] A.E. Atabani, A.S. Silitonga, I.A. Badruddin, T.M.I. Mahlia, H.H. Masjuki, S. Mekhilef, A comprehensive review on biodiesel as an alternative energy resource and its characteristics, *Renewable and Sustainable Energy Reviews* 16 (2012) 2070–2093.
- [26] N. Narkhede, A. Patel, Biodiesel production by esterification of oleic acid and transesterification of soybean oil using a new solid acid catalyst comprising 12-tungstosilicic acid and zeolite h $\beta$ , *Industrial and Engineering Chemistry Research* 52

- (2013) 13637–13644.
- [27] A.L. Cardoso, S.C.G. Neves, M.J. Da Silva, Esterification of oleic acid for biodiesel production catalyzed by  $\text{SnCl}_2$ : A kinetic investigation, *Energies* 1 (2008) 79–92.
- [28] T. Pinnarat, P.E. Savage, Noncatalytic esterification of oleic acid in ethanol, *Journal of Supercritical Fluids* 53 (2010) 53–59.
- [29] E. de Hoop, Understanding marginal changes in ecosystem services from biodiesel feedstock production: A study of Hassan Bio-Fuel Park, India, *Biomass and Bioenergy* 114 (2018) 55–62.
- [30] K.G. Devi, D. Meghavathu, S. Velluri, C.C. Mehtha, Z. Hussain, Qualitative production of biodiesel using waste vegetable oil, *i-Manager's Journal on Future Engineering and Technology* 10 (2015) 1–11.
- [31] M.I. Al-widyan, A.O. Al-shyoukh, Experimental evaluation of the transesterification of waste palm oil into biodiesel, *Bioresource Technology* 85 (2002) 253–256.
- [32] S.K. Karmee, A. Chadha, Preparation of biodiesel from crude oil of *Pongamia pinnata*, *Bioresource Technology* 96 (2005) 1425–1429.
- [33] R. Sarin, M. Sharma, S. Sinharay, R.K. Malhotra, *Jatropha*-Palm biodiesel blends: An optimum mix for Asia, *Fuel*. 86 (2007) 1365–1371.
- [34] P. Felizardo, M.J.N. Correia, I. Raposo, J.F. Mendes, R. Berkemeier, J.M. Bordado, Production of biodiesel from waste frying oils, *Waste Management* 26 (2006) 487–494.
- [35] K.N.P. Rani, T.P. Kumar, T.S.V.R. Neeharika, B. Satyavathi, R.B.N. Prasad, Kinetic studies on the esterification of free fatty acids in *jatropha* oil, *European Journal of Lipid Science and Technology* 115 (2013) 691–697.

- [36] Y.C. Sharma, B. Singh, Development of biodiesel from Karanja, a tree found in rural India, *Fuel*. 87 (2008) 1740–1742.
- [37] D.A. Kamel, H.A. Farag, N.K. Amin, A.A. Zatout, R.M. Ali, Smart utilization of jatropha (*Jatropha curcas* Linnaeus) seeds for biodiesel production: Optimization and mechanism, *Industrial Crops and Products* 111 (2018) 407–413.
- [38] M. Farooq, A. Ramli, A. Naeem, T. Mahmood, S. Ahmad, M. Humayun, M.G.U. Islam, Biodiesel production from date seed oil (*Phoenix dactylifera* L.) via egg shell derived heterogeneous catalyst, *Chemical Engineering Research and Design* 132 (2018) 644–651.
- [39] M. Mohibbe Azam, A. Waris, N.M. Nahar, Prospects and potential of fatty acid methyl esters of some non-traditional seed oils for use as biodiesel in India, *Biomass and Bioenergy*. 29 (2005) 293–302.
- [40] S.V. Ghadge, H. Raheman, Biodiesel production from mahua (*Madhuca indica*) oil having high free fatty acids, *Biomass and Bioenergy*. 28 (2005) 601–605.
- [41] A.S. Ramadhas, S. Jayaraj, C. Muraleedharan, Biodiesel production from high FFA rubber seed oil, *Fuel*. 84 (2005) 335–340.
- [42] Ayhan Demirbas, M.F. Demirbas, Importance of algae oil as a source of biodiesel, *Energy Conversion and Management* 52 (2011) 163–170.
- [43] I.B. Banković-Ilić, O.S. Stamenković, V.B. Veljković, Biodiesel production from non-edible plant oils, *Renewable and Sustainable Energy Reviews* 16 (2012) 3621–3647.
- [44] Y.C. Sharma, B. Singh, S.N. Upadhyay, Advancements in development and characterization of biodiesel: A review, *Fuel*. 87 (2008) 2355–2373.
- [45] A. Talebian-Kiakalaieh, N.A.S. Amin, Single and two-step homogeneous catalyzed

- transesterification of waste cooking oil: Optimization by response surface methodology, *International Journal of Green Energy*. 12 (2015) 888–899.
- [46] I.M. Atadashi, M.K. Aroua, A.R. Abdul Aziz, N.M.N. Sulaiman, The effects of water on biodiesel production and refining technologies: A review, *Renewable and Sustainable Energy Reviews* 16 (2012) 3456–3470.
- [47] L. Meher, D. Vidyasagar, S. Naik, Technical aspects of biodiesel production by transesterification—a review, *Renewable Sustainable Energy Reviews* 10 (2006) 248–268.
- [48] Y. Wang, S. Ou, P. Liu, Z. Zhang, Preparation of biodiesel from waste cooking oil via two-step catalyzed process, *Energy Conversion and Management* 48 (2007) 184–188.
- [49] E.F. Aransiola, T.V. Ojumu, O.O. Oyekola, T.F. Madzimbamuto, D.I.O. Ikhu-Omoregbe, A review of current technology for biodiesel production: State of the art, *Biomass and Bioenergy*. 61 (2014) 276–297.
- [50] M. Berrios, M.A. Martín, A.F. Chica, A. Martín, Study of esterification and transesterification in biodiesel production from used frying oils in a closed system, *Chemical Engineering Journal* 160 (2010) 473–479.
- [51] J.M. Marchetti, V.U. Miguel, A.F. Errazu, Possible methods for biodiesel production, *Renewable and Sustainable Energy Reviews* 11 (2007) 1300–1311.
- [52] Y.S. Lien, L.S. Hsieh, J.C.S. Wu, Biodiesel synthesis by simultaneous esterification and transesterification using oleophilic acid catalyst, *Industrial and Engineering Chemistry Research* 49 (2010) 2118–2121.
- [53] A. Demirbas, Biodiesel from waste cooking oil via base-catalytic and supercritical methanol transesterification, *Energy Conversion and Management* 50 (2009) 923–927.

- [54] D. Kusdiana, S. Saka, Effects of water on biodiesel fuel production by supercritical methanol treatment, *Bioresource Technology* 91 (2004) 289–295.
- [55] Q. Guan, Y. Li, Y. Chen, Y. Shi, J. Gu, B. Li, R. Miao, Q. Chen, P. Ning, Sulfonated multi-walled carbon nanotubes for biodiesel production through triglycerides transesterification, *RSC Advances* 7 (2017) 7250–7258.
- [56] B. Thangaraj, K.B. Ramachandran, S.P. Raj, Alkaline catalytic transesterification for palm oil biodiesel and characterisation of palm oil biodiesel, *Journal of Biofuels*. 4 (2013) 79–87.
- [57] A. Kovács, C. Ball, Use of colloid chemistry principles to improve efficiency in biodiesel production, *Periodica Polytechnica Chemical Engineering* 56 (2012) 37–48.
- [58] J. Madhusudana Rao, T.B. Rao, Asymmetric synthesis using phase transfer catalysis, *Journal of Indian Institute of Science* 74 (1994) 373–400.
- [59] K.J. Suthar, M.H. Joshipura, A comparative study on predictions of vapor liquid equilibrium of biodiesel systems, *International Conference on Current Trend in Technology* (2011) 1–6.
- [60] Y. Zhang, M. Stanculescu, M. Ikura, Rapid transesterification of soybean oil with phase transfer catalysts, *Applied Catalysis A: General* 366 (2009) 176–183.
- [61] S.M. Hailegiorgis, S. Mahadzir, D. Subbarao, Enhanced in situ ethanolysis of *Jatropha curcas* L. in the presence of cetyltrimethylammonium bromide as a phase transfer catalyst, *Renewable Energy* 36 (2011) 2502–2507.
- [62] Y.Q. Huang, Synthesis of Biodiesel by Phase Transfer Catalysis, *Applied Mechanics and Materials* 291–294 (2013) 355–358.
- [63] S. wei Liu, C. xia Xie, R. Jiang, S. tao Yu, F. sheng Liu, Hydrogenation of biodiesel

- using thermoregulated phase-transfer catalyst for production of fatty alcohols, *Bioresource Technology* 101 (2010) 6278–6280.
- [64] D.G.B. Boocock, Single-phase process for production of fatty acid methyl esters from mixtures of triglycerides and fatty acids, United States Patent (2003). Patent No. US6642399B2.
- [65] D.G.B. Boocock, S.K. Konar, V. Mao, C. Lee, S. Buligan, Fast formation of high-purity methyl esters from vegetable oils, *Journal of American Oil Chemists' Society* 75 (1998) 1167–1172.
- [66] D.G.B. Boocock, S.K. Konar, V. Mao, H. Sidi, Fast one-phase oil-rich processes for the preparation of vegetable oil methyl esters, *Biomass and Bioenergy*. 11 (1996) 43–50.
- [67] S.M. Hailegiorgis, S. Mahadzir, D. Subbarao, Reactive extraction of *Jatropha curcas* l assisted by phase transfer catalyst for the production of biodiesel, National Postgraduate Conference (2011) 1-5.
- [68] Z. Hussain, B. Haider Mohammad, R. Kumar, Usagespecific biodiesel production with and without catalytic booster, *Materials Today Proceedings* (2016) 4115–4120.
- [69] M.L. Pisarello, B. Dalla Costa, G. Mendow, C.A. Querini, Esterification with ethanol to produce biodiesel from high acidity raw materials: Kinetic studies and analysis of secondary reactions, *Fuel Processing Technology* 91 (2010) 1005–1014.
- [70] V. Rathore, S. Tyagi, B. Newalkar, R.P. Badoni, *Jatropha* and *Karanja* oil derived DMC-biodiesel synthesis: A kinetics study, *Fuel*. 140 (2015) 597–608.
- [71] N. Alper Tapan, R. Yıldırım, M.E. Günay, Analysis of past experimental data in literature to determine conditions for high performance in biodiesel production,

- Biofuels, Bioproducts and Biorefining. 10 (2016) 422–434.
- [72] G.W. Gokel, A review of “phase-transfer catalysis fundamentals, applications, and industrial perspectives. C. M. Starks, C. L. Liotta, M. Halper. Chapman and Hall, New York, 1994, 9.25" × 6.25"; xiv + 668 pp. ISBN 0-412-04071-9,” *Supramolecular Chemistry* 5 (1995) 237.
- [73] J. Lifka, B. Ondruschka, Influence of mass transfer on the production of biodiesel, *Chemical Engineering and Technology* 27 (2004) 1156–1159.
- [74] Y. Warabi, D. Kusdiana, S. Saka, Reactivity of triglycerides and fatty acids of rapeseed oil in supercritical alcohols, *Bioresource Technology* 91 (2004) 283–287.
- [75] S. Saka, D. Kusdiana, E. Minami, Non-catalytic biodiesel fuel production with supercritical methanol technologies, *Journal of Scientific and Industrial Research* 65 (2006) 420–425.
- [76] S. Hawash, N. Kamal, F. Zaher, O. Kenawi, G. El Diwani, Biodiesel fuel from *Jatropha* oil via non-catalytic supercritical methanol transesterification, *Fuel*. 88 (2009) 579–582.
- [77] Y. Warabi, D. Kusdiana, S. Saka, biodiesel Fuel from vegetable oil by various supercritical alcohols, *Applied Biochemistry and Biotechnology* 115 (2004) 793–802.
- [78] D. Kumar, G. Kumar, Poonam, C.P. Singh, Fast, easy ethanolysis of coconut oil for biodiesel production assisted by ultrasonication, *Ultrasonics Sonochemistry* 17 (2010) 555–559.
- [79] C. Stavarache, M. Vinatoru, R. Nishimura, Y.M. Maeda, Conversion of vegetable oil to biodiesel using ultrasonic irradiation, *Chemistry Letters* 32 (2003) 716–717.
- [80] S. Saka, D. Kusdiana, Biodiesel fuel from rapeseed oil as prepared in supercritical

- methanol, *Fuel*. 80 (2001) 225–231.
- [81] V. Rathore, G. Madras, Synthesis of biodiesel from edible and non-edible oils in supercritical alcohols and enzymatic synthesis in supercritical carbon dioxide, *Fuel*. 86 (2007) 2650–2659.
- [82] L.K. Doraiswamy, *Organic Synthesis Engineering*, Oxford University Press, New York (2001), eISBN: 9780195096897.
- [83] H. Nouredini, D. Harkey, V. Medikonduru, A continuous process for the conversion of vegetable oils into methyl esters of fatty acids, *Journal of American Oil Chemists' Society* 75 (1998) 1775–1783.
- [84] S. Lim, S.S. Hoong, L.K. Teong, S. Bhatia, Supercritical fluid reactive extraction of *Jatropha curcas* L. seeds with methanol: A novel biodiesel production method, *Bioresource Technology* 101 (2010) 7169–7172.
- [85] Z. Du, Z. Tang, H. Wang, J. Zeng, Y. Chen, E. Min, Research and development of a sub-critical methanol alcoholysis process for producing biodiesel using waste oils and fats, *Chinese Journal of Catalysis* 34 (2013) 101–115.
- [86] C. Tirla, R. Smith, T. Dooling, N. Kingsbury, M. C, R. Panter, A. Van Allen, A study of alternative catalysts and analysis methods for biodiesel production, *Proceedings of 8th International Scientific Forum, ISF 2017, UNCP, USA.* (2017) 124–139.
- [87] H. Han, W. Cao, J. Zhang, Preparation of biodiesel from soybean oil using supercritical methanol and CO<sub>2</sub> as co-solvent, *Process Biochemistry* 40 (2005) 3148–3151.
- [88] D. Zhao, H. Ren, J. Wang, Y. Yang, Y. Zhao, Kinetics and mechanism of quaternary ammonium salts as phase-transfer catalysts in the liquid-liquid phase for oxidation of

- thiopene, *Energy and Fuels*. 21 (2007) 2543–2547.
- [89] C.M. Starks, M. HALPER, Phase transfer catalysis, Springer Netherlands (1994), ISBN: 978-94-011-0687-0.
- [90] C.J. Stacy, C.A. Melick, R.A. Cairncross, Esterification of free fatty acids to fatty acid alkyl esters in a bubble column reactor for use as biodiesel, *Fuel Processing Technology* 124 (2014) 70–77.
- [91] B.S. Gandhi, D.S. Kumaran, The production and optimization of biodiesel from crude *Jatropha curcas* oil by a two step process—An Indian case study using response surface methodology, *International Journal of Green Energy*. 11 (2014) 1084–1096.
- [92] M. Chai, Q. Tu, M. Lu, Y.J. Yang, Esterification pretreatment of free fatty acid in biodiesel production, from laboratory to industry, *Fuel Processing Technology* 125 (2014) 106–113.
- [93] A. Deb, J. Ferdous, K. Ferdous, M.R. Uddin, M.R. Khan, M.W. Rahman, Prospect of castor oil biodiesel in bangladesh: Process development and optimization study, *Internatuional Journal of Green Energy* 14 (2017) 1063-1072.
- [94] M. Kolyaei, G. Zahedi, M.M. Nasef, A. Azarpour, Optimization of biodiesel production from waste cooking oil using ion-exchange resins, *International Journal of Green Energy*. 13 (2016) 28–33.
- [95] K. V. Thiruvengadaravi, J. Nandagopal, P. Baskaralingam, V. Sathya Selva Bala, S. Sivanesan, Acid-catalyzed esterification of karanja (*Pongamia pinnata*) oil with high free fatty acids for biodiesel production, *Fuel*. 98 (2012) 1–4.
- [96] C. Vijaya Lakshmi, K. Viswanath, S. Venkateshwar, B. Satyavathi, Mixing characteristics of the oil-methanol system in the production of biodiesel using edible

- and non-edible oils, *Fuel Processing Technology* 92 (2011) 1411–1417.
- [97] I.M. Atadashi, M.K. Aroua, A.R. Abdul Aziz, N.M.N. Sulaiman, The effects of catalysts in biodiesel production: A review, *Journal of Industrial and Engineering Chemistry* 19 (2013) 14–26.
- [98] I. Nurfitri, G.P. Maniam, N. Hindryawati, M.M. Yusoff, S. Ganesan, Potential of feedstock and catalysts from waste in biodiesel preparation: A review, *Energy Conversion and Management* 74 (2013) 395–402.
- [99] F.I. Gómez-Castro, V. Rico-Ramírez, J.G. Segovia-Hernández, S. Hernández-Castro, Esterification of fatty acids in a thermally coupled reactive distillation column by the two-step supercritical methanol method, *Chemical Engineering Research and Design* 89 (2011) 480–490.
- [100] G. Anitescu, A. Deshpande, L.L. Tavlarides, Integrated technology for supercritical biodiesel production and power cogeneration, *Energy and Fuels* (2008) 1391–1399.
- [101] I. Vieitez, C. da Silva, I. Alckmin, G.R. Borges, F.C. Corazza, J.V. Oliveira, M.A. Grompone, I. Jachmanian, Effect of temperature on the continuous synthesis of soybean esters under supercritical ethanol, *Energy and Fuels*. 23 (2009) 558–563.
- [102] H.Y. Shin, S.H. Lee, J.H. Ryu, S.Y. Bae, Biodiesel production from waste lard using supercritical methanol, *Journal of Supercritical Fluids* 61 (2012) 134–138.
- [103] R. Alenezi, G.A. Leeke, J.M. Winterbottom, R.C.D. Santos, A.R. Khan, Esterification kinetics of free fatty acids with supercritical methanol for biodiesel production, *Energy Conversion and Management* 51 (2010) 1055–1059.
- [104] F.L. Martinovic, F.E. Kiss, R.D. Micic, M. Simikić, M.D. Tomić, Comparative techno-economic analysis of single-step and two-step biodiesel production with supercritical

- methanol based on process simulation, *Chemical Engineering Research and Design* 132 (2018) 751–765.
- [105] H.Y. Shin, S.M. Lim, S.Y. Bae, S.C. Oh, Thermal decomposition and stability of fatty acid methyl esters in supercritical methanol, *Journal of Analytical and Applied Pyrolysis* 92 (2011) 332–338.
- [106] J. Quesada-Medina, P. Olivares-Carrillo, Evidence of thermal decomposition of fatty acid methyl esters during the synthesis of biodiesel with supercritical methanol, *Journal of Supercritical Fluids*. 56 (2011) 56–63.
- [107] E. Minami, S. Saka, Kinetics of hydrolysis and methyl esterification for biodiesel production in two-step supercritical methanol process, *Fuel*. 85 (2006) 2479–2483.
- [108] C.A.R. Melo-Júnior, C.E.R. Albuquerque, M. Fortuny, C. Dariva, S. Egues, A.F. Santos, A.L.D. Ramos, Use of microwave irradiation in the noncatalytic esterification of C18 fatty acids, *Energy and Fuels*. 23 (2009) 580–585.
- [109] K.N.P. Rani, T.S.V.R. Neeharika, T.P. Kumar, B. Satyavathi, S. Chintha, Kinetics of non-catalytic esterification of free fatty acids present in *Jatropha* oil, *Journal of Oleo Science* 65 (2016) 441–445.
- [110] H.J. Cho, S.H. Kim, S.W. Hong, Y.K. Yeo, A single step non-catalytic esterification of palm fatty acid distillate (PFAD) for biodiesel production, *Fuel*. 93 (2012) 373–380.
- [111] M.J. Haas, A.J. McAloon, W.C. Yee, T.A. Foglia, A process model to estimate biodiesel production costs, *Bioresource Technology* 97 (2006) 671–678.
- [112] A.H. West, D. Posarac, N. Ellis, Assessment of four biodiesel production processes using HYSYS. *Plant, Bioresource Technology* 99 (2008) 6587–6601.
- [113] S. Lee, D. Posarac, N. Ellis, Process simulation and economic analysis of biodiesel

- production processes using fresh and waste vegetable oil and supercritical methanol, *Chemical Engineering Research and Design* 89 (2011) 2626–2642.
- [114] M.M. Gui, K.T. Lee, S. Bhatia, Feasibility of edible oil vs. non-edible oil vs. waste edible oil as biodiesel feedstock, *Energy* 33 (2008) 1646–1653.
- [115] M.G. Kulkarni, A.K. Dalai, Waste cooking oil - An economical source for biodiesel: A review, *Industrial and Engineering Chemistry Research* 45 (2006) 2901–2913.
- [116] M. Canakci, The potential of restaurant waste lipids as biodiesel feedstocks, *Bioresource Technology* 98 (2007) 183–190.
- [117] F. Su, Y. Guo, Advancements in solid acid catalysts for biodiesel production, *Green Chemistry* 16 (2014) 2934–2957.
- [118] C.S. Latchubugata, R.V. Kondapaneni, K.K. Patluri, U. Virendra, S. Vedantam, Kinetics and optimization studies using response surface methodology in biodiesel production using heterogeneous catalyst, *Chemical Engineering Research and Design* 135 (2018) 129–139.
- [119] S. Yousefi, M. Haghghi, B. Rahmani Vahid, Facile and efficient microwave combustion fabrication of Mg-spinel as support for MgO nanocatalyst used in biodiesel production from sunflower oil: Fuel type approach, *Chemical Engineering Research and Design* 138 (2018) 506–518.
- [120] X. Liu, H. He, Y. Wang, S. Zhu, Transesterification of soybean oil to biodiesel using SrO as a solid base catalyst, *Catalysis Communications* 8 (2007) 1107–1111.
- [121] M.L. Granados, M.D.Z. Poves, D.M. Alonso, R. Mariscal, F.C. Galisteo, R. Moreno-Tost, J. Santamaría, J.L.G. Fierro, Biodiesel from sunflower oil by using activated calcium oxide, *Applied Catalysis B: Environmental* 73 (2007) 317–326.

- [122] T.K. Mahto, R. Jain, S. Chandra, D. Roy, V. Mahto, S.K. Sahu, Single step synthesis of sulfonic group bearing graphene oxide: A promising carbo-nano material for biodiesel production, *Journal of Environmental Chemical Engineering* 4 (2016) 2933–2940.
- [123] N.A. Negm, G.H. Sayed, O.I. Habib, F.Z. Yehia, E.A. Mohamed, Heterogeneous catalytic transformation of vegetable oils into biodiesel in one-step reaction using super acidic sulfonated modified mica catalyst, *Journal of Molecular Liquids* 237 (2017) 38–45.
- [124] V. SathyaSelvabala, T.K. Varathachary, D.K. Selvaraj, V. Ponnusamy, S. Subramanian, Removal of free fatty acid in *Azadirachta indica* (Neem) seed oil using phosphoric acid modified mordenite for biodiesel production, *Bioresource Technology* 101 (2010) 5897–5902.
- [125] S. Yan, C. Dimaggio, S. Mohan, M. Kim, S.O. Salley, K.Y. Simon Ng, Advancements in heterogeneous catalysis for biodiesel synthesis, *Topics in Catalysis* 53 (2010) 721–736.
- [126] E. Lotero, Y. Liu, D.E. Lopez, K. Suwannakarn, D.A. Bruce, J.G. Goodwin, Synthesis of biodiesel via acid catalysis, *Industrial and Engineering Chemistry Research* 44 (2005) 5353–5363.
- [127] S. Furuta, H. Matsubishi, K. Arata, Biodiesel fuel production with solid superacid catalysis in fixed bed reactor under atmospheric pressure, *Catalysis Communications* 5 (2004) 721–723.
- [128] A.A. Kiss, A.C. Dimian, G. Rothenberg, Solid acid catalysts for biodiesel production - Towards sustainable energy, *Advanced Synthesis and Catalysis* 348 (2006) 75–81.

- [129] K. Srilatha, N. Lingaiah, B.L.A.P. Devi, R.B.N. Prasad, S. Venkateswar, P.S.S. Prasad, Esterification of free fatty acids for biodiesel production over heteropoly tungstate supported on niobia catalysts, *Applied Catalysis A: General* 365 (2009) 28–33.
- [130] N. Yunus, N. Roslan, S. Chin, S. Abidin, Kinetic Studies of Free Fatty Acid Esterification using Cation Exchange Resins as Catalyst, *Indian Journal of Science and Technology* 10 (2017) 1–5.
- [131] K. Saravanan, B. Tyagi, H.C. Bajaj, Sulfated zirconia: an efficient solid acid catalyst for esterification of myristic acid with short chain alcohols, *Catalysis Science and Technology* 2 (2012) 2512-2520.
- [132] A. Rachmat, W. Trisunaryanti, Sutarno, K. Wijaya, Synthesis and characterization of sulfated zirconia mesopore and its application on lauric acid esterification, *Materials for Renewable and Sustainable Energy* 6 (2017) 1–9.
- [133] W.Y. Lou, Q. Guo, W.J. Chen, M.H. Zong, H. Wu, T.J. Smith, A highly active bagasse-derived solid acid catalyst with properties suitable for production of biodiesel, *ChemSusChem* 5 (2012) 1533–1541.
- [134] M.M. Aboelhasan, A.F. Peixoto, C. Freire, Sulfonic acid functionalized silica nanoparticles as catalysts for the esterification of linoleic acid, *New Journal of Chemistry* 41 (2017) 3595-3605.
- [135] C.C. Enweremadu, M.M. Mbarawa, Technical aspects of production and analysis of biodiesel from used cooking oil-A review, *Renewable and Sustainable Energy Reviews* 13 (2009) 2205–2224.
- [136] M.-H. Zong, Z.-Q. Duan, W.-Y. Lou, T.J. Smith, H. Wu, Preparation of a sugar catalyst and its use for highly efficient production of biodiesel, *Green Chemistry* 9

- (2007) 434.
- [137] I.M. Lokman, U. Rashid, Y.H. Taufiq-Yap, R. Yunus, Methyl ester production from palm fatty acid distillate using sulfonated glucose-derived acid catalyst, *Renewable Energy* 81 (2015) 347–354.
- [138] E.T. Lu, S.G. Love, Biodiesel made with sugar catalyst, *Nature*. 438 (2005) 177–178.
- [139] W.Y. Lou, M.H. Zong, Z.Q. Duan, Efficient production of biodiesel from high free fatty acid-containing waste oils using various carbohydrate-derived solid acid catalysts, *Bioresource Technology* 99 (2008) 8752–8758.
- [140] A. Endut, S.H.Y.S. Abdullah, N.H.M. Hanapi, S.H.A. Hamid, F. Lananan, M.K.A. Kamarudin, R. Umar, H. Juahir, H. Khatoon, Optimization of biodiesel production by solid acid catalyst derived from coconut shell via response surface methodology, *International Biodeterioration and Biodegradation* 124 (2017) 250-257.
- [141] A. Hidayat, K. Wijaya, A. Nurdiawati, Esterification of palm fatty acid distillate with high amount of free fatty acids using coconut shell char based catalyst, *Energy Procedia* 75 (2015) 969–974.
- [142] Y. Wu, Z. Fu, D. Yin, Q. Xu, F. Liu, C. Lu, L. Mao, Microwave-assisted hydrolysis of crystalline cellulose catalyzed by biomass char sulfonic acids, *Green Chemistry* 12 (2010) 696-700.
- [143] K. Yan, C. Jarvis, J. Gu, Y. Yan, Production and catalytic transformation of levulinic acid: A platform for speciality chemicals and fuels, *Renewable and Sustainable Energy Reviews* 51 (2015) 986–997.
- [144] K. Yan, Y. Liu, Y. Lu, J. Chai, L. Sun, Catalytic application of layered double hydroxide-derived catalysts for the conversion of biomass-derived molecules,

- Catalysis Science and Technology 7 (2017) 1622–1645.
- [145] Maize in India, India Maize Summit' 14. (2014) 1–32.
- [146] M.M.R. Talukder, J.C. Wu, S.K. Lau, L.C. Cui, G. Shimin, A. Lim, Comparison of novozym 435 and amberlyst 15 as heterogeneous catalyst for production of biodiesel from palm fatty acid distillate, *Energy and Fuels*. 23 (2009) 1–4.
- [147] Y.X. Wang, B.S. Liu, C. Zheng, Preparation and adsorption properties of corncob-derived activated carbon with high surface area, *Journal of Chemical and Engineering Data* 55 (2010) 4669–4676.
- [148] A.S. Franca, C.C.O. Alves, L.S. Oliveira, Production of adsorbents based on food waste ( corn cobs ) for removal of phenylalanine and tyrosine from aqueous solutions, *Biomed Research International* (2013) Article Id. 978256.
- [149] M. Han, K. Jiang, P. Jiao, Y. Ji, J. Zhou, W. Zhuang, Y. Chen, D. Liu, C. Zhu, X. Chen, H. Ying, J. Wu, Bio-butanol sorption performance on novel porous-carbon adsorbents from corncob prepared via hydrothermal carbonization and post-pyrolysis method, *Scientific Reports* 7 (2017) 1–11.
- [150] H. Ma, J. Li, W. Liu, B. Cheng, X. Cao, J. Mao, S. Zhu, Hydrothermal preparation and characterization of novel corncob-derived solid acid catalysts, *Journal of Agricultural and Food Chemistry* 62 (2014) 5345–5353.
- [151] R.A. Arancon, H.R. Barros Jr, A.M. Balu, C. Vargas, R. Luque, Valorisation of corncob residues to functionalised porous carbonaceous materials for the simultaneous esterification/transesterification of waste oils, *Green Chemistry* 13 (2011) 3162-3167.
- [152] N.V. Sych, S.I. Trofymenko, O.I. Poddubnaya, M.M. Tsyba, V.I. Sapsay, D.O. Klymchuk, A.M. Puziy, Porous structure and surface chemistry of phosphoric acid

- activated carbon from corncob, *Applied Surface Science* 261 (2012) 75–82.
- [153] H.-Y. Chen, Z.-W. Cui, A microwave-sensitive solid acid catalyst prepared from sweet potato via a simple method, *Catalysts* 6 (2016) 211.
- [154] I.M. Lokman, U. Rashid, Y.H. Taufiq-Yap, Microwave-assisted methyl ester production from palm fatty acid distillate over a heterogeneous carbon-based solid acid catalyst, *Chemical Engineering and Technology* 38 (2015) 1837–1844.
- [155] Y. Zhang, M.A. Dubé, D.D. McLean, M. Kates, Biodiesel production from waste cooking oil: 1. Process design and technological assessment, *Bioresource Technology* 89 (2003) 1–16.
- [156] Y. Zhang, M.A. Dubé, D.D. McLean, M. Kates, Biodiesel production from waste cooking oil: 2. Economic assessment and sensitivity analysis, *Bioresource Technology* 90 (2003) 229–240.
- [157] A.H. West, D. Posarac, N. Ellis, Simulation, case studies and optimization of a biodiesel process with a solid acid catalyst, *International Journal of Chemical Reactor Engineering* 5 (2007) Article A37.
- [158] ASTM: D6584-08, Test method for determination of free and total glycerin in B100 biodiesel methyl esters by gas chromatography, American Society for Testing Materials, Philadelphia, PA, USA, 2002.
- [159] J.K. Efavi, D. Kanbogtah, V. Apalangya, E. Nyankson, E.K. Tiburu, D. Dodoo-Arhin, B. Onwona-Agyeman, A. Yaya, The Effect of NaOH catalyst concentration and extraction time on the yield and properties of *Citrullus vulgaris* seed oil as a potential biodiesel feed stock, *South African Journal of Chemical Engineering* 25 (2018) 98–102.

- [160] ASTM: D97-969, Book of standard test methods, American Society for Testing Materials, Philadelphia, PA, USA, 1995.
- [161] ASTM: D25100. Book of standard test methods, American Society for Testing Materials. Philadelphia, PA, USA, 1995.
- [162] G. Knothe, Dependence of biodiesel fuel properties on the structure of fatty acid alkyl esters, *Fuel Processing Technology* 86 (2005) 1059–1070.
- [163] G. Knothe, “Designer” Biodiesel: Optimizing Fatty Ester Composition to Improve Fuel Properties, *Energy & Fuels*. 22 (2008) 1358–1364.
- [164] G. Knothe, K.R. Steidley, Kinematic viscosity of biodiesel fuel components and related compounds. Influence of compound structure and comparison to petrodiesel fuel components, *Fuel*. 84 (2005) 1059–1065.
- [165] G. Knothe, R.O. Dunn, Dependence of oil stability index of fatty compounds on their structure and concentration and presence of Metals, *Journal of American Oil Chemists' Society* 80 (2003) 1021–1026.
- [166] O.J. Alamu, M.A. Waheed, S.O. Jekayinfa, Biodiesel production from Nigerian palm kernel oil: Effect of KOH concentration on yield, *Energy for Sustainable Development* 11 (2007) 77–82.
- [167] D.Y.C. Leung, Y. Guo, Transesterification of neat and used frying oil: Optimization for biodiesel production, *Fuel Processing Technology* 87 (2006) 883–890.
- [168] S.S. Chang, E.F. Westrum, Heat capacities and thermodynamic properties of two tetramethylammonium halides, *The Journal of Chemical Physics* 36 (1962) 2420–2423.
- [169] Q. Guan, H. Shang, J. Liu, J. Gu, B. Li, R. Miao, Q. Chen, P. Ning, Biodiesel from

- transesterification at low temperature by  $\text{AlCl}_3$  catalysis in ethanol and carbon dioxide as cosolvent: Process, mechanism and application, *Applied Energy* 164 (2016) 380–386.
- [170] A. Talebian-Kiakalaieh, N.A.S. Amin, H. Mazaheri, A review on novel processes of biodiesel production from waste cooking oil, *Applied Energy*. 104 (2013) 683–710.
- [171] J. Qi, J. Lin, H. Fu, One-step production of biodiesel from waste cooking oil catalysed by  $\text{SO}_3\text{H}$ -functionalized quaternary ammonium ionic liquid, *Current Science* 110 (2016) 2129–2134.
- [172] Manual of methods analysis of foods: Oils & Fats, Lab Manual; Food Safety and Standards Authority of India (Ministry of Health and Family Welfare) Government of India, New Delhi (2015) 24–26.
- [173] A.C.D.A. Abdala, V.A. Dos Santos Garcia, C.P. Trentini, L. Cardozo Filho, E.A. Da Silva, C. Da Silva, Continuous catalyst-free esterification of oleic acid in compressed ethanol, *International Journal of Chemical Engineering* (2014) Article ID 803783.
- [174] H. Nouredini, D. Zhu, Kinetics of transesterification of soybean oil, *Journal of American Oil Chemists' Society* 74 (1997) 1457–1463.
- [175] R. Alcantara, J. Amores, L. Canoira, E. Fidalgo, M.J. Franco, A. Navarro, Catalytic production of biodiesel from soy-bean oil, used frying oil and tallow, *Biomass and Bioenergy*. 18 (2000) 515–527.
- [176] F. Ma, L.D. Clements, M.A. Hanna, The effect of mixing on transesterification of beef tallow, *Bioresource Technology* 69 (1999) 289–293.
- [177] A.H.P. Skelland, J.S. Kanel, Minimum impeller speeds for complete dispersion of non-Newtonian liquid-liquid systems in baffled vessels, *Industrial and Engineering*

- Chemistry Research 29 (1990) 1300–1306.
- [178] A.H.P. Skelland, G.G. Ramsay, Minimum agitator speeds for complete liquid-liquid dispersion, *Industrial and Engineering Chemistry Research* 26 (1987) 77–81.
- [179] K. Neumann, K. Werth, A. Martín, A. Górak, Biodiesel production from waste cooking oils through esterification: Catalyst screening, chemical equilibrium and reaction kinetics, *Chemical Engineering Research and Design* 107 (2016) 52–62.
- [180] R. Rönnback, T. Salmi, A. Vuori, H. Haario, J. Lehtonen, A. Sundqvist, E. Tirronen, Development of a kinetic model for the esterification of acetic acid with methanol in the presence of a homogeneous acid catalyst, *Chemical Engineering Science* 52 (1997) 3369–3381.
- [181] J.T.F. Keurentjes, G.H.R. Janssen, J.J. Gorissen, The esterification of tartaric acid with ethanol: Kinetics and shifting the equilibrium by means of pervaporation, *Chemical Engineering Science* 49 (1994) 4681–4689.
- [182] R. Hernández-Montelongo, J.P. García-Sandoval, E. Aguilar-Garnica, On the non-ideal behavior of the homogeneous esterification reaction: A kinetic model based on activity coefficients, *Reaction Kinetics Mechanism and Catalysis* 115 (2015) 401–419.
- [183] S.Z. Hassan, M. Vinjamur, Analysis of sensitivity of equilibrium constant to reaction conditions for esterification of fatty acids with alcohols, *Industrial and Engineering Chemistry Research* 52 (2013) 1205–1215.
- [184] Y. Liu, H. Lu, C. Liu, B. Liang, Solubility measurement for the reaction systems in pre-esterification of high acid value *Jatropha curcas* L. oil, *Journal of Chemical and Engineering Data* 54 (2009) 1421–1425.
- [185] E. Batista, S. Monnerat, K. Kato, L. Stragevitch, A.J.A. Meirelles, Liquid-liquid

- equilibrium for systems of canola oil, oleic acid, and short-chain alcohols, *Journal of Chemical and Engineering Data* 44 (1999) 1360–1364.
- [186] A.H. West, Process Simulation and catalyst development for biodiesel production, Thesis, University of British Columbia (2006).
- [187] W. Xue, L. Sun, F. Yang, Z. Wang, F. Li, Peanut shell-derived carbon solid acid with large surface area and its application for the catalytic hydrolysis of cyclohexyl acetate, *Materials (Basel)*. 9 (2016) 833.
- [188] S. Li, Z. Gu, B.E. Bjornson, A. Muthukumarappan, Biochar based solid acid catalyst hydrolyze biomass, *Journal of Environmental Chemical Engineering* 1 (2013) 1174–1181.
- [189] K. Nakajima, M. Hara, Amorphous carbon with SO<sub>3</sub>H groups as a solid bronsted acid catalyst, *ACS Catalysis* 2 (2012) 1296-1304.
- [190] E. Fuente, J.A. Menéndez, M.A. Díez, D. Suárez, M.A. Montes-Morán, Infrared spectroscopy of carbon materials: A quantum chemical study of model compounds, *The Journal of Physical Chemistry B* 107 (2003) 6350–6359.
- [191] S. Soltani, U. Rashid, S.I. Al-Resayes, I.A. Nehdi, Mesoporous catalysts for biodiesel production: A new approach, Chapter Sixteen in *Clean Energy for Sustainable Development* (2017) 487–506.
- [192] G. Leofanti, M. Padovan, G. Tozzola, B. Venturelli, Surface area and pore texture of catalysts, *Catalysis Today*. 41 (1998) 207–219.
- [193] H. Sarafraz, A. Minucmehr, G. Alahyarizadeh, Z. Rahimi, Synthesis of enhanced phosphonic functional groups mesoporous silica for uranium selective adsorption from aqueous solutions, *Scientific Reports* 7 (2017) 1–12.

- [194] A. Indrasumunar, P.M. Gresshoff, P.T. Scott, Prospect of the legume tree *Pongamia pinnata* as a clean and sustainable biodiesel feedstock, Chapter Twelve in *Clean Energy for Sustainable Development* (2017) 399–417.
- [195] K. Jacobson, R. Gopinath, L.C. Meher, A.K. Dalai, Solid acid catalyzed biodiesel production from waste cooking oil, *Applied Catalysis B: Environmental* 85 (2008) 86–91.
- [196] Y.M. Sani, W.M.A.W. Daud, A.R. Abdul Aziz, Activity of solid acid catalysts for biodiesel production: A critical review, *Applied Catalysis A: General* 470 (2014) 140–161.
- [197] P.H. Huang, J.W. Jhan, Y.M. Cheng, H.H. Cheng, Effects of carbonization parameters of moso-bamboo-based porous charcoal on capturing carbon dioxide, *The Scientific World Journal* (2014) Article Id. 937867.
- [198] S. Yun, T. Guo, X. Zhu, L. Zhang, J. Zhang, X. Gao, Y. Gao, Effects of carbonization temperature on structure and mechanical properties of monolithic C/SiO<sub>2</sub> aerogels based on ambient pressure dried superhydrophobic resorcinol-formaldehyde/SiO<sub>2</sub>aerogels, *Journal of Porous Materials* 25 (2018) 1825-1830.
- [199] K. Kaneko, Determination of pore size and pore size distribution, *Journal of Membrane Science* 96 (1994) 59–89.
- [200] M. Dong, Z. Wu, M. Lu, Z. Wang, Z. Li, Combining the physical adsorption approach and the covalent attachment method to prepare a bifunctional bioreactor, *International Journal of Molecular Science* 13 (2012) 11443–11454.
- [201] T.F. Dossin, M.F. Reyniers, G.B. Marin, Kinetics of heterogeneously MgO-catalyzed transesterification, *Applied Catalysis B: Environmental* 62 (2006) 35–45.

- [202] I.M. Lokman, U. Rashid, Y.H. Taufiq-Yap, Meso- and macroporous sulfonated starch solid acid catalyst for esterification of palm fatty acid distillate, *Arabian Journal of Chemistry* 9 (2016) 179–189.
- [203] N.M. Haimour, S. Emeish, Utilization of date stones for production of activated carbon using phosphoric acid, *Waste Management* 26 (2006) 651–660.
- [204] C. Samorí, C. Torri, D. Fabbri, G. Falini, C. Faraloni, P. Galletti, S. Spera, E. Tagliavini, G. Torzillo, Unusual catalysts from molasses: Synthesis, properties and application in obtaining biofuels from algae, *ChemSusChem* 5 (2012) 1501–1512.
- [205] A. Hayyan, M.Z. Alam, M.E.S. Mirghani, N.A. Kabbashi, N.I.N.M. Hakimi, Y.M. Siran, S. Tahiruddin, Sludge palm oil as a renewable raw material for biodiesel production by two-step processes, *Bioresource Technology* 101 (2010) 7804–7811.
- [206] Q. Shu, Q. Zhang, G. Xu, J. Wang, Preparation of biodiesel using s-MWCNT catalysts and the coupling of reaction and separation, *Food and Bioproducts Processing* 87 (2009) 164–170.
- [207] A.M. Doyle, T.M. Albayati, A.S. Abbas, Z.T. Alismaeel, Biodiesel production by esterification of oleic acid over zeolite Y prepared from kaolin, *Renewable Energy*. 97 (2016) 19–23.
- [208] Q. Shu, J. Gao, Y. Liao, J. Wang, Reaction kinetics of biodiesel synthesis from waste oil using a carbon-based solid acid catalyst, *Chinese Journal of Chemical Engineering* 19 (2011) 163–168.
- [209] G. Guan, K. Kusakabe, N. Sakurai, K. Moriyama, Transesterification of vegetable oil to biodiesel fuel using acid catalysts in the presence of dimethyl ether, *Fuel*. 88 (2009) 81–86.

- [210] D.Y.C. Leung, X. Wu, M.K.H. Leung, A review on biodiesel production using catalyzed transesterification, *Applied Energy* 87 (2010) 1083–1095.
- [211] P.E. Jagadeeshbabu, K. Sandesh, M.B. Saidutta, Kinetics of esterification of acetic acid with methanol in the presence of ion exchange resin catalysts, *Industrial and Engineering Chemistry Research* 50 (2011) 7155–7160.
- [212] M. Hara, Biomass conversion by a solid acid catalyst, *Energy and Environmental Science* 3 (2010) 601–607.
- [213] D. Zuo, J. Lane, D. Culy, M. Schultz, A. Pullar, M. Waxman, Sulfonic acid functionalized mesoporous SBA-15 catalysts for biodiesel production, *Applied Catalysis B: Environmental* 129 (2013) 342–350.
- [214] M.I.S. Tarakci, O. Ilgen, Esterification of oleic acid with methanol using  $Zr(SO_4)_2$  as heterogeneous catalyst, *Chemical Engineering and Technology* 41 (2018) 845–852.
- [215] C.F. Oliveira, L.M. Dezaneti, F.A.C. Garcia, J.L. de Macedo, J.A. Dias, S.C.L. Dias, K.S.P. Alvim, Esterification of oleic acid with ethanol by 12-tungstophosphoric acid supported on zirconia, *Applied Catalysis A: General* 372 (2010) 153–161.
- [216] A. Patel, N. Narkhede, 12-tungstophosphoric acid anchored to zeolite H $\beta$ : Synthesis, characterization, and biodiesel production by esterification of oleic acid with methanol, *Energy and Fuels*. 26 (2012) 6025–6032.
- [217] F.L. Pua, Z. Fang, S. Zakaria, F. Guo, C.H. Chia, Erratum: Direct production of biodiesel from high-acid value *Jatropha* oil with solid acid catalyst derived from lignin, *Biotechnology for Biofuels*. 4 (2011) 56.
- [218] M. Kitano, K. Arai, A. Kodama, T. Kousaka, K. Nakajima, S. Hayashi, M. Hara, Preparation of a sulfonated porous carbon catalyst with high specific surface area,

- Catalysis Letters. 131 (2009) 242–249.
- [219] H.S. Fogler, Elements of Chemical Reaction Engineering, 4<sup>th</sup> Edition, Pearson Education, Inc., Prentice Hall (2006). ISBN: 978-93-325-4932-6.
- [220] M. Gan, D. Pan, L. Ma, E. Yue, J. Hong, The Kinetics of the Esterification of Free Fatty Acids in Waste Cooking Oil Using  $\text{Fe}_2(\text{SO}_4)_3/\text{C}$  Catalyst, Chinese Journal of Chemical Engineering 17 (2009) 83–87.
- [221] Z. Hussain, R. Kumar, Esterification of free fatty acids: Experiments, kinetic modeling, simulation and optimization, International Journal of Green Energy. 15 (2018) 629–640.
- [222] A. Alegría, J. Cuellar, Esterification of oleic acid for biodiesel production catalyzed by 4-dodecylbenzenesulfonic acid, Applied Catalysis B: Environmental 179 (2015) 530–541.
- [223] J. Chao, F.D. Rossini, Heats of combustion, formation, and isomerization of nineteen alkanols, Journal of Chemical and Engineering Data 10 (1965) 374–379.
- [224] F.A.P. Voll, C. da Silva, C.C.R.S. Rossi, R. Guirardello, F. de Castilhos, J.V. Oliveira, L. Cardozo-Filho, Thermodynamic analysis of fatty acid esterification for fatty acid alkyl esters production, Biomass and Bioenergy. 35 (2011) 781–788.
- [225] M. V.D. Silva, R. Custodio, M.H.M. Reis, Determination of enthalpies of formation of fatty acids and esters by density functional theory calculations with an empirical correction, Industrial and Engineering Chemistry Research 54 (2015) 9545–9549.
- [226] D. Zeng, R. Li, T. Jin, T. Fang, Calculating the thermodynamic characteristics and chemical equilibrium of the stepwise transesterification of triolein using supercritical lower alcohols, Industrial and Engineering Chemistry Research 53 (2014) 7209–7216.

## Appendix

### Sample Calculations

#### A-1: Transesterification of waste vegetable oil (WVO)

##### (1) The molecular weight of waste vegetable oil

- (i) The molecular weight of single fatty acid was calculated using the formula;

$$(MW)_i = 14.027 \times (c) - 2.016 \times (d) + 31.9988$$

Where c = number of carbon atoms

d = number of double bonds

- (ii) The average molecular weight of a mixture of fatty acids was calculated using the values given in Table A1 as follows;

$$(MW_i)_{\text{avg}} = \frac{\sum (wf)_i}{\sum \frac{(wf)_i}{(MW)_i}} = \frac{0.9939}{(3.6894E - 03)}$$

$$(MW_i)_{\text{avg}} = 269.3984 \frac{g}{mol}$$

- (iii) Molecular weight of WVO or triglyceride were calculated using the formula;

$$MW = 3 \times (MW_i)_{\text{avg}} + 38.049 = 3 \times 269.3984 + 38.049$$

$$MW = 846.2442 \text{ g/mol}$$

**Table A1:-** Computation of Molecular Weight of WVO

Fatty acid	(MW) <sub>i</sub>	(wf) <sub>i</sub>	(wf) <sub>i</sub> /(MW) <sub>i</sub>
Caprylic (C8:0)	144.2148	0.0002	1.6642E-06
Capric (C10:0)	172.2688	0.0002	9.2878E-07
Lauric (C12:0)	200.3228	0.0022	1.0783E-05
Myristic (C14:0)	228.3768	0.0079	3.4767E-05
Palmitic (C16:0)	256.4308	0.4410	1.7198E-03
Palmitoleic (C16:1)	254.4148	0.0021	8.1756E-06
Stearic (C18:0)	284.4848	0.0412	1.4486E-04
Oleic (C18:1)	282.4688	0.3900	1.3807E-03
Linoleic (C18:2)	280.4528	0.1052	3.7511E-04
Linolenic (C18:3)	278.4368	0.0013	4.7408E-06
Arachidic (C20:0)	312.5388	0.0015	4.6714E-06
Gadoleic (C20:1)	310.5228	0.0000	0.0000E+00
Behenic (C22:0)	340.5928	0.0006	1.7616E-06
Erusic (C22:1)	338.5768	0.0000	0.0000E+00
Lignoceric (C24:0)	368.6468	0.0005	1.4648E-06
		$\sum (wf)_i = 0.9939$	$\sum \frac{(wf)_i}{(MW)_i} = 3.6894E - 03$

**(2) Acid Value of WVO**

After titration using standard KOH solution of 0.1 N, the volume of KOH required to neutralize FFA present in WVO was found as;

V = 3.2 ml.

$$\text{Acid Value} = \frac{56.1 \times V \times N}{W} = \frac{56.1 \times 3.2 \times 0.1}{10} = 1.8 \text{ mg KOH/g}$$

### (3) Transesterification of WVO at 1:9 molar ratio of methanol to WVO

(i) Waste vegetable oil

The weight of WVO taken = 500 g.

The molecular weight of WVO = 846.244 g/mol.

$$\text{Moles of WVO taken} = \frac{500}{846.244} = 0.5908 \text{ mole.}$$

(ii) Methanol

Molecular weight = 32.04 g/mol.

Density = 0.792 g/cc.

Moles of methanol required =  $9 \times 0.5908 = 5.3172$  mole.

Weight of methanol taken =  $5.3172 \times 32.04 = 170.3630$  g.

$$\text{Volume of methanol taken} = \frac{170.3630}{0.792} = 215.1048 \text{ ml.}$$

(iii) Catalyst (0.5 wt. %)

$$\text{Catalyst, wt. \%} = \frac{\text{Weight of the catalyst}}{\text{Weight of the catalyst} + \text{Weight of WVO taken}}$$

$$\frac{0.5}{100} = \frac{\text{Weight of the catalyst}}{\text{Weight of the catalyst} + 500}$$

Weight of the catalyst = 2.5125 g.

(iv) Biodiesel

The weight of the biodiesel obtained = 495 g.

$$\text{Yield \%} = \frac{\text{Weight of the biodiesel}}{\text{Weight of WVO used}} \times 100 = \frac{495}{500} = 99\%$$

## A-2: Esterification of free fatty acids in Karanja oil through non-catalytic route

(1) The initial acid value of Karanja oil at time  $t=0$

Volume of standard KOH (0.1 N) solution required for titration (V) = 5.597 ml.

$$(\text{Acid Value})_{t=0} = \frac{56.1 \times 5.597 \times 0.1}{0.5} = 62.8010 \text{ mg KOH/g}$$

$$\% \text{ Free fatty acid} = \frac{28.2 \times 5.597 \times 0.1}{0.5} = 31.5670\%$$

(2) Esterified product acid value at  $t = 7$  h

$$(\text{Acid Value})_{t=7 \text{ h}} = \frac{56.1 \times 4.242 \times 0.1}{10} = 2.380 \text{ mg KOH/g}$$

$$\% \text{ Free fatty acid} = \frac{28.2 \times 4.242 \times 0.1}{0.5} = 1.1960\%$$

(3) Conversion of free fatty acids

$$\text{Conversion (\%)} = \frac{(\text{Acid Value})_{t=0} - (\text{Acid Value})_{t=t}}{(\text{Acid Value})_{t=0}} \times 100$$

$$\text{Conversion (\%)} = \frac{62.801 - 2.380}{62.801} \times 100 = 96.21\%$$

## A-3: Esterification of oleic acid using a corncob-based solid acid catalyst

(1) Oleic acid

The weight of oleic acid taken = 28.247 g.

Molecular weight of oleic acid = 282.4688 g/mol.

$$\text{Moles of oleic acid taken} = \frac{28.247}{282.4688} = 0.1 \text{ mole.}$$

(2) Methanol

Moles of methanol taken =  $0.1 \times 10 = 1$  mole.

Weight of methanol taken =  $1 \times 32.04 = 32.04$  g.

$$\text{Volume of methanol taken} = \frac{32.04}{0.792} = 40.4545 \text{ ml.}$$

(3) Catalyst (10 wt. %)

The weight of the catalyst taken = 10 wt. % with respect to oleic acid

$$\frac{10}{100} = \frac{\text{Weight of the catalyst}}{\text{Weight of the catalyst} + \text{Weight of the oleic acid taken}}$$

$$0.1 = \frac{\text{Weight of the catalyst}}{\text{Weight of the catalyst} + 28.247}$$

Weight of the catalyst taken = 3.138 g.

(4) Acid value of the oleic acid (AV)<sub>o</sub>

$$(AV)_o = \frac{56.1 \times 3.54 \times 0.1}{0.1} = 198.6 \text{ mg KOH/g}$$

(5) Acid value of the product (AV)<sub>p</sub>

$$(AV)_p = \frac{56.1 \times 3.894 \times 0.1}{10} = 2.1846 \text{ mg KOH/g}$$

$$\text{Fractional Conversion}(X) = \frac{(AV)_o - (AV)_p}{(AV)_o} = \frac{198.6 - 2.1846}{198.6} = 0.989$$